DISSERTATION

A NANOPARTICULATE-REINFORCED HYALURONAN COPOLYMER HYDROGEL FOR INTERVERTEBRAL DISC REPAIR

Submitted by

Susan S. Yonemura

School of Biomedical Engineering

In partial fulfillment of the requirements

For the Degree of Doctor of Philosophy

Colorado State University

Fort Collins, Colorado

Spring 2011

Doctoral Committee:

Advisor: Susan P. James

Travis S. Bailey
John D. Kisiday
Donna L. Wheeler

ABSTRACT

A NANOPARTICULATE-REINFORCED HYALURONAN COPOLYMER HYDRGEL FOR INTERVERTEBRAL DISC REPAIR

Degenerative disc disease (DDD) is an inevitable consequence of aging, commonly resulting in low back pain (LBP). Current clinical treatment options for disc degeneration exist at two extremes: conservative management or extensive surgical intervention. Given the economic impact of lost productivity and disability associated with low back pain, there is significant interest in earlier, less invasive intervention. Biomimetic disc replacement and regenerative therapies offer an attractive alternative strategy for intervertebral disc repair, but materials employed to date have not exhibited a successful combination of mechanical and biological properties to achieve viable solutions.

The composite material developed and characterized in this work consisted of a novel hyaluronan-*co*-poly(ethylene-*alt*-maleic anhydride) (HA-*co*-PEMA) hydrogel matrix reinforced with nanoparticulate silica; the hydrogel matrix provided a compliant hydrated matrix conducive to integration with the surrounding tissue while the nanoparticulate reinforcement was manipulated to mimic the mechanical performance of healthy ovine nucleus pulposus (NP) tissue. HA-*co*-PEMA was formed via an esterification reaction between a hydrophobically-modified HA complex and PEMA, and candidate formulations were characterized by chemical, thermal, and physical means to select an appropriate base hydrogel for the reinforced composite. Three grades of

commercially-available fumed silica, varying by degree of hydrophobic surface modification, were evaluated as nanoparticulate reinforcement for the composite materials.

Mechanical testing of two reinforced composite formulations (620-R and 720-R) emphasized dynamic shear properties and results were directly compared to ovine nucleus pulposus (NP) tissue. The complex shear modulus (G*) for 620-R ranged from 1.8±0.2 KPa to 2.4±0.3 KPa over the frequency range 0.1 Hz < f < 10 Hz, while G* for 720-R varied from 4.4 ± 0.5 KPa to 6.1 ± 0.6 KPa over the same frequency range. Ovine NP tissue tested using identical methods exhibited G* of 1.7 ± 0.2 KPa at 0.1 Hz up to 3.8 ± 0.5 KPa at 10 Hz. Thus, the complex shear moduli (G*) for 620-R and 720-R effectively bracketed G* for NP over a physiologically-relevant frequency range. Subsequent *in vitro* cytotoxicity and biocompatibility experiments suggest that the 720-R formulation warrants consideration for future *in vivo* modeling.

ACKNOWLEDGMENTS

During the course of my graduate studies at Colorado State University I have had the distinct pleasure to work with two fantastic advisors, Dr. Donna L. Wheeler and Dr. Susan P. James. Dr. Wheeler fostered my interest in pursuing a research-based degree when I first came to CSU, and I feel very fortunate that she agreed to serve on my Ph.D. committee after she left the university. After Dr. Wheeler's departure Dr. James welcomed me into her group as a student in the inaugural School of Biomedical Engineering Ph.D. class. Though initially my research interests did not align particularly well with her lab's research priorities, her confidence in my ability to learn a new discipline exceeded my own, and I thank her for pushing me outside of my comfort zone. As mentors and role models both Dr. Wheeler and Dr. James have been invaluable to me.

I also must extend my deepest thanks to Dr. Travis S. Bailey and Dr. John D. Kisiday for taking time out of their busy schedules to serve on my committee. The work presented in this dissertation truly would not have been possible without their advice and support. In addition to providing polymer chemistry expertise, Dr. Bailey allowed me access to his rheometer for my mechanical testing experiments. I am also grateful to his students Vincent Scalfani and Chen Guo for their assistance in getting me started in the use of this instrument. Dr. John Kisiday provided candid advice regarding the details of cell culture studies, and encouraged taking a more creative, physiologically-relevant approach to biocompatibility testing by suggesting that I pursue an explant tissue

integration study rather than the more typical scaffold seeding study. This pilot study provided some of the most intriguing results of the research described in this dissertation, and I am hopeful that it will be pursued further in the near future.

I am also grateful for the assistance of other faculty and staff members from the School of Biomedical Engineering (SBME) and the Department of Chemistry Central Instruments Facility (CIF). I had the opportunity to work with Dr. Matthew Kipper as part of my first-year SBME lab rotation. The high expectations that he set, the free reign he granted in his lab, and his willingness to review concepts no matter how basic gave me a needed boost in approaching the chemistry involved in my dissertation research. My chemical and thermal characterization work would not have been possible without the well-maintained facilities provided at CIF. Dr. Sandeep Kohli and Don Heyse in particular deserve mention for their training and assistance with Fourier transform infrared spectroscopy (FTIR), Thermogravimetric analysis (TGA), and nuclear magnetic resonance (NMR).

The Orthopaedic Bioengineering Research Laboratory (OBRL) has been my home away from home for the duration of my graduate studies, and I have had the opportunity to work with many good people in this lab over the years. The work of former students Dr. Rachael Oldinski, Ph.D. and Cody Cranson, M.S. provided the starting point for my research. Dr. Marisha Godek graciously trained me in cell culture technique during her post-doctoral fellowship, giving me the confidence to tackle the *in vitro* biocompatibility experiments described herein. I have enjoyed the camaraderie of fellow students in the James group and particularly thank M.S. student Casey Dean and undergraduate Mike Onorato for their specific assistance with my research. I also owe my

thanks to several OBRL and Equine Orthopaedic Research Center (EORC) staff members: Nikki Phillips for her assistance with cell culture techniques, Susan L. James and Bob Zink for histology, and Dr. Christina Lee for serving as a point-of-contact for communication with EORC managing faculty.

The opportunity to mentor talented undergraduate students was as fulfilling to me as any of my graduate school experiences. Ryan Goff from the University of Iowa and Ariane Vartanian from Swarthmore College came to us via the National Science Foundation Research Experience for Undergraduates (NSF REU) program. I am certain I learned as much from them as they learned from me, and I fully expect both Ryan and Ariane to achieve success in their own research careers.

Last but not least, I thank my family and friends for their support and encouragement; I am not sure I would have appreciated the highs or made it through the lows of my graduate school experience without them.

DEDICATION

To my father, Raymond Shoji Yonemura

In memoriam

TABLE OF CONTENTS

Abstract ii

Acknowledgments iv

Dedication vii

Table of Contents viii

List of Tables xii

List of Figures xiii

List of Symbols and Abbreviations xv

Motivation and Significance 1

Literature Review 3

- Intervertebral Disc Anatomy and Physiology 3
  - *Origin and Development* 3
  - *Macroscopic Structure and Matrix Composition* 5
  - *Disc Metabolism* 8
- Degenerative Disc Disease 10
- Clinical Treatment Paradigm 11
  - *Spinal Fusion* 12
  - *Artificial Disc Replacements* 12
  - *Intradiscal Implants* 13
- Regenerative Therapies 14
- Hydrogel-Based Biomaterials 16
  - *Crosslinking Strategies* 17
  - *Particulate-Reinforced Hydrogels* 18
- Methods for Intervertebral Disc Study 19
  - *Mechanical Testing* 19
  - In vitro *Culture Systems* 20

Research Objectives and Specific Aims 24

- Study Rationale 24
- Research Objectives 26
  - *Mechanical Objectives* 26
  - *Biological Objectives* 27
- Hypotheses and Specific Aims 28
  - *Specific Aim 1: Material Formulation* 28
  - *Specific Aim 2: Mechanical Characterization* 28
  - *Specific Aim 3: In vitro Modeling* 29

Dissertation Research 30

Introduction 30
Specific Aim 1: Hydrogel Synthesis and Characterization 33
Materials and Methods *33*
Results *37*
Discussion *41*
Specific Aim 2: Mechanical Properties of Reinforced Hydrogels 47
Materials and Methods *47*
Results *51*
Discussion *55*
Specific Aim 3: *In vitro* Biocompatibility 59
Materials and Methods *60*
Results *63*
Discussion *67*
Conclusions 71

Intellectual Merit and Future Work 74

References 77

Appendix A: Protocols A-1

1 Polymer Development A-2
1.1 Hydrogel Synthesis A-2
1.1.1 HA-CTA Complexation A-2
1.1.2 HA-*co*-PEMA Hydrogel Synthesis A-4
1.1.3 Copolymer Crosslinking A-7
1.1.4 Copolymer Washing A-8
1.1.5 Gel Casting and Reinforcement A-9
1.2 Characterization A-12
1.2.1 Identifying Hyaluronan with Toluidine Blue O A-12
1.2.2 Swell Testing A-13
1.2.3 Fourier Transform Infrared Spectroscopy A-15
1.2.4 Thermogravimetric Analysis A-17
2 Mechanical Testing A-19
2.1 Shear Rheometry A-19
3 Biological Response A-22
3.1 *In vitro* Cell Culture A-22
3.1.1 Cell Culture Basics A-22
3.1.2 Cell Line Information A-27
3.2 Biocompatibility A-28
3.2.1 Cytotoxicity Assay A-28
3.2.2 alamarBlue® Cell Viability Assay A-30
3.3 Tissue Culture A-32
3.3.1 Ovine Disc Tissue Harvest A-32
3.3.2 Ovine Nucleus Pulposus Tissue Culture A-35

Appendix B: Characterization Reference Data B-1

Chemicals Used in Research B-1
Fourier Transform Infrared Spectroscopy (FTIR) B-3
Hyaluronan (HA) *B-3*
Cetyl trimethylammonium bromide (CTAB) *B-4*
Hyaluronan-cetyl trimethylammonium complex (HA-CTA) *B-5*

*Poly(ethylene-*alt*-maleic anhydride) (PEMA)* *B-6*
Thermogravimetric Analysis (TGA) B-7
^{1}H Nuclear Magnetic Resonance (NMR) B-8
*Poly(ethylene-*alt*-maleic anhydride)* *B-8*
Cetyl trimethylammonium bromide (CTAB) *B-9*

Appendix C: Copolymer Design C-1

Basic Design Parameters and Nomenclature C-3
Weight Ratio *C-3*
Network Ratio *C-4*
Reactive Ratio *C-4*
Hydrogel Design Concepts C-5
References C-7

Appendix D: REU Program Research Report D-1

Appendix E: Demineralized Bone Matrix-Reinforced Gels E-1

Materials and Methods E-1
Gel Synthesis *E-1*
Rheometry *E-2*
Results E-3
Gel Synthesis *E-3*
Swell Testing *E-3*
Rheometry *E-4*
Discussion E-5
References E-7

Appendix F: Rheometry Method Validation F-1

Appendix G: Reinforcement Level And Air-Free Chemistry G-1

Appendix H: Statistical Analyses H-1

Specific Aim 1: Swell Test Parameters for LD and HD Gel Formulations H-1
Swell Ratio (Q) *H-1*
Percent Hydration (H) *H-1*
Specific Aim 2: Reinforced Gel Characterization H-2
Swell Testing: Q in Deionized Water (DI) *H-2*
Swell Testing: Q in Phosphate-Buffered Saline (PBS) *H-2*
Swell Testing: H in DI *H-3*
Swell Testing: H in PBS *H-3*
Rheometry: Complex Modulus (G) at 0.1 Hz* *H-4*
Rheometry: G at 1 Hz* *H-4*
Rheometry: G at 10 Hz* *H-5*
Rheometry: Storage Modulus (G′) at 0.1 Hz *H-5*
Rheometry: G′ at 1 Hz *H-6*
Rheometry: G′ at 10 Hz *H-6*
Rheometry: Loss Modulus (G″) at 0.1 Hz *H-7*
Rheometry: G″ at 1 Hz *H-7*
Rheometry: G″ at 10 Hz *H-8*
Rheometry: Loss Factor (G″/G′) at 0.1 Hz *H-8*
Rheometry: G″/G′ at 1 Hz *H-9*

Rheometry: G″/G′ at 10 Hz *H-9*
Swell Testing: Q for Air-Cast and Air-Free Cast Gels *H-10*
Rheometry: Air-Cast vs. Air-Free Cast 620-R Gel *H-10*
Specific Aim 3: Cytotoxicity H-11
Cytotoxicity Elution Assay *H-11*
Cytotoxicity Titration Assay *H-14*
Appendix I: Patent Application I-1

LIST OF TABLES

Table 1: Material properties for intervertebral disc tissue 21
Table 2: Design parameters for hydrogel variations 34
Table 3: FTIR peak identification and location comparison 38
Table 4: Summary of TGA transitions and dTG peaks for hydrogels and reactants 40
Table 5: Swell test parameters (mean ± SEM, n=3 per group) 41
Table 6: Fumed silica specifications 47
Table 7: Cast gel constituents 48
Table 8: Swell ratio and hydration for reinforced gels 52
Table 9: Summary of PBS swell test parameters determined for different gel synthesis methods 57
Table B1: Chemical structures and molecular formulae B-1
Table B2: FTIR peak identification for hyaluronan B-3
Table B3: FTIR peak identification for CTAB B-4
Table B4: FTIR peak identification for HA-CTA B-5
Table B5: FTIR peak identification for PEMA B-6
Table E1: DBM-reinforced gel formulations E-1
Table E2: Swell test parameters for DBM-reinforced gels E-3
Table F1: Comparison of measured G* to values reported in the literature F-3
Table G1: Comparison of gel formulations for in-air and air-free casting G-2
Table G2: Swell test parameters after 72 hours in PBS G-5

LIST OF FIGURES

Figure 1: Changes in structure and composition of the intervertebral disc with age and development 4
Figure 2: Age-related changes to the extra-cellular matrix of the nucleus pulposus 7
Figure 3: Potential microstructures based upon constituent molecular weight, weight ratio and degree of reaction 27
Figure 4: Hypothesized chemical structure for HA-*co*-HDPE 30
Figure 5: Chemical structures for (a) poly(ethylene-*alt*-maleic anhydride) and (b) maleic anhydride-grafted polyethylene 31
Figure 6: HA-*co*-PEMA hydrogel reaction scheme 32
Figure 7: Result of reaction between HA-CTA and PEMA 37
Figure 8: FTIR spectra for high- and low-network density HA-*co*-PEMA hydrogels 38
Figure 9: TGA results for LD and HD gel formulations compared to their respective control blends 39
Figure 10: Swell test parameters for LD and HD HA-*co*-PEMA formulations 40
Figure 11: Difference spectrum highlighting changes in peak intensities between HA-*co*-PEMA and an equivalent control blend of HA and PEMA 43
Figure 12: Ester bond linkage between HA and PEMA 43
Figure 13: The "rule of 3" for identifying ester bonds in FTIR spectra 44
Figure 14: Hydrogel sample loaded on the rheometer 50
Figure 15: Reinforced gels produced through the gel casting method 51
Figure 16: Strain sweep traces for reinforced gels and ovine nucleus pulposus 52
Figure 17: Frequency sweep results for complex modulus 53
Figure 18: Statistical comparisons of all dynamic shear parameters at 0.1, 1, and 10 Hz 54
Figure 19: Effect of synthesis conditions (air vs. air-free) on the mechanical properties of 620-R gels 58
Figure 20: alamarBlue® readings for overall cytotoxicity and eluant titration 64
Figure 21: Histological sections for tissue integration study, 200x magnification 66
Figure 22: 600x image of the interface between NP and 720-R 66
Figure 23: ^{1}H NMR spectra for HD gel eluant compared to PEMA and CTAB 68
Figure 24: FTIR spectra for AF-620-R gel after wash cycles 69
Figure 25: Measured pH values for conditioned media used in the cytotoxicity study 70
Figure B1: FTIR reference spectrum for hyaluronan B-3
Figure B2: FTIR reference spectrum for CTAB B-4
Figure B3: FTIR reference spectrum for HA-CTA B-5
Figure B4: FTIR reference spectrum for PEMA B-6
Figure B5: TG and dTG traces for HA and PEMA B-7
Figure B6: ^{1}H NMR reference spectrum and peak identification for PEMA B-8
Figure B7: ^{1}H NMR reference spectrum and peak identification for CTAB B-9
Figure C1: FTIR spectrum for "tripoly" C-7
Figure E1: DBM-reinforced gels E-3
Figure E2: Example swell test samples E-3

Figure E3: Effect of particulate reinforcement with native DBM E-4
Figure E4: Strengthening effect of denatured DBM..... E-4
Figure E5: DBM reinforcement combined with HMDI Crosslinking..... E-5
Figure F1: Agarose shear modulus results figure reprinted from Chen et. al. F-2
Figure F2: Comparison of complex shear modulus (G*) measured with and without sandpaper F-3
Figure F3: Effect of axial stress relaxation on measured G* values F-3
Figure F4: Repeatability of measurements over 10 identical frequency sweeps..... F-4
Figure G1: Comparison of dynamic shear properties between air-free cast gels and ovine NP tissue.....G-4

LIST OF SYMBOLS AND ABBREVIATIONS

α	Type I error rate; statistical significance level.
δ	Phase lag angle; the angle by which the response lags the applied load in dynamic mechanical tests
ACUC	Animal Care and Use Committee
AF	Annulus fibrosus
ANOVA	Analysis of variance
BMP	Bone morphogenetic protein; a class of growth factors
copoly	Hyaluronan-*co*-high density polyethylene
CS	Chondroitin sulfate
CTAB	Hexadecyltrimethylammonium bromide
Da	Dalton; unit for molecular weight (g/mol)
DBM	Demineralized bone matrix
DDD	Degenerative disc disease
DMEM	Dulbecco's modified Eagle's medium
DMEM/F12	Dulbecco's modified Eagle medium and Ham's F-12 medium
DMMB	Dimethylmethylene blue dye; used for sulfated GAG assay
DMSO	Dimethyl sulfoxide
ECM	Extra-cellular matrix
EDC	1-ethyl-3-(3-dimethylaminopropyl)carbodiimide
FBS	Fetal bovine serum
FSU	Functional spinal unit; vertebra-disc-vertebra fundamental spinal motion segment (see SMS)
FTIR	Fourier transform infrared spectroscopy
G*	Dynamic shear complex modulus
G'	Dynamic shear storage modulus; real portion of G*
G"	Dynamic shear loss modulus; imaginary portion of G*
GAG	Glycosaminoglycan
GDF	Growth differentiation factor
HA	Hyaluronan, hyaluronic acid
HA-*co*-HDPE	Copolymer of hyaluronan and high-density polyethylene
HA-*co*-PEMA	Copolymer of hyaluronan and poly(ethylene-*alt*-maleic anhydride)
HA-CTA	Hyaluronan complexed with hexadecyltrimethylammonium ion; hydrophobically-modified hyaluronan
HDPE	High-density polyethylene
H&E	Hematoxylin and eosin; histology stain
HMDI	Hexamethylene diisocyanate
IGF	Insulin-like growth factor
IL	Interleukin; class of cytokines

IVD	Intervertebral disc
KS	Keratin sulfate
LBP	Low back pain
LP	Link protein
LVR	Linear viscoelastic region
MA	Maleic anhydride
MA-*g*-HDPE	Maleated high-density polyethylene
MMP	Matrix metalloproteinase
MSC	Mesenchymal stem cell or marrow stromal cell
M_w	Weight-average molecular weight
NP	Nucleus pulposus; central gelatinous portion of the intervertebral disc
PBS	Phosphate buffered saline
PE	Polyethylene
PEMA	Poly(ethylene-*alt*-maleic anhydride); alternating copolymer of polyethylene and maleic anhydride
PG	Proteoglycan
SEM	Scanning electron microscopy
SMS	Spinal motion segment; vertebra-disc-vertebra unit (see FSU)
tanδ	Loss factor; the ratio of G''/G'
TCPS	Tissue-culture polystyrene
TDA	Total disc arthroplasty
T_g	Glass transition temperature
TGA	Thermogravimetric analysis
TGF-β	Transforming growth factor beta
THA	Total hip arthroplasty
TIMP	Tissue inhibitor of metalloproteinase production
TNF	Tumor necrosis factor
WSC	Water-soluble carbodiimide

MOTIVATION AND SIGNIFICANCE

Low back pain (LBP) is nearly ubiquitous in industrial societies. Estimates of the lifetime incidence of back pain range up to 80% [1]. In working populations LBP has been reported to affect as many as 35% of sedentary workers and 45% of heavy handlers during the course of their careers, and ranks second only to respiratory infections such as the common cold in lost productivity [2]. Furthermore, disorders of the spine are the leading cause of chronic disability for those under the age of 45 [2, 3]. Costs associated with this lost productivity and disability have been estimated to be as much as $50 billion per year in the United States [4]. Given the economic loss as well as the morbidity associated with low back pain, there is considerable research interest in preventing and treating lumbar degenerative disc disease.

Current clinical options for treatment of back pain exist at two extremes: non-invasive conservative management or surgery. The current "gold standard" for the surgical treatment of low back pain is fusion of one or more spinal motion segments (SMS), though total disc arthroplasty (TDA) is becoming more available. These are invasive surgical procedures with risks of serious complications and poor clinical outcomes. Thus, those suffering from symptomatic degenerative disc disease often attempt to manage the pain conservatively until they have no option but to undergo surgery.

The risk of certain iatrogenic complications associated with arthrodesis has promoted the development of less invasive interventions and non-fusion treatment strategies. Advances in instrumentation have enabled the development of minimally-invasive discectomy procedures; these advances may also be leveraged for disc augmentation via nucleus replacement. Nucleus replacement technologies replace the desiccated, dysfunctional nucleus pulposus (NP) tissue while maintaining a healthy annulus fibrosus (AF). The AF works in conjunction with the implant to restore normal loading and kinematics and, it is hoped, alleviate pain [5]. Nucleus replacements can be targeted for mechanical reinforcement, delivery of biologic agents, or a combination of both mechanical and biological effects [6].

To our knowledge, there is no published literature on nucleus replacement therapies that adequately address both the mechanical and biological requirements for the IVD. Thus, the vision for this research endeavor is to mechanically reinforce while also restoring the biochemical composition and water content of the disc, elevating the nuclear hydrostatic pressure and thus slowing or halting the progression of disc degeneration.

LITERATURE REVIEW

Intervertebral Disc Anatomy and Physiology

The intervertebral discs (IVD) are an integral component of the spinal column, which is among the most intricate structures within the skeletal system [3]. The spinal column provides axial rigidity to support the trunk and protect the spinal cord, yet affords enough flexibility to allow motion in six degrees of freedom at each vertebral element. While the spine is very mobile overall, motion is limited in a vertebra-disc-vertebra functional spinal unit (FSU). The discs primarily resist compression, but also assist the facet joints in constraining rotation, flexion, extension, lateral bending, and shear.

The human spine contains 23 intervertebral discs separating the vertebrae. They increase in size from cranial to caudal, and the lumbar intervertebral discs are the largest avascular structures in the human body [3]. The disc is not a homogenous tissue; rather, it includes a fibrous outer annulus encapsulating a central, gelatinous nucleus. These structures are capped by vertebral endplates consisting of hyaline cartilage. Disc health and normal biomechanical function require the integrity of all three of these structures.

Origin and Development

The structure and composition of the IVD change radically with age (Figure 1). Developmentally, the NP arises from the central notochord while the AF derives from the surrounding mesenchyme [7]. The notochord is a transitional structure that regulates spinal development by secreting ECM molecules and growth factors and by modifying

the behavior of other cell types through cell-cell contact [8]. In the embryo, the fluid-like nucleus is rich in notochordal cells and proteoglycan, while the annulus is composed primarily of fibroblast-like cells and collagen. Vascularization of the end plates and AF persists through juvenile growth and development, providing a rich nutrient supply to allow for the rapid accumulation of extra-cellular matrix (ECM) in all disc tissues. As the blood vessels recede the notochordal cells slowly decline, such that by age ten in the human they are essentially absent. They are replaced by chondrocyte-like cells of mesenchymal origin. The texture of the nucleus pulposus becomes firmer with the appearance of these cells due to the accumulation of collagen.

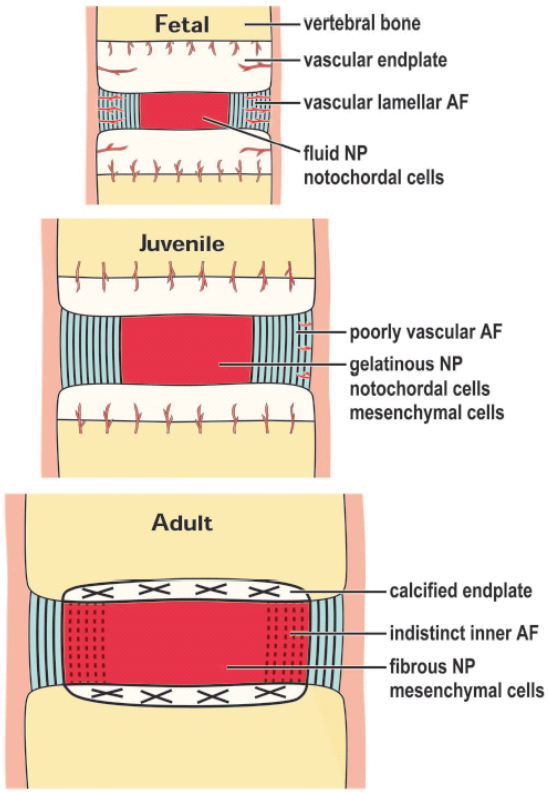

Reprinted with permission from Roughley, P.J., *Biology of intervertebral disc aging and degeneration - Involvement of the extracellular matrix.* Spine, 2004. 29(23): p. 2691-2699.

Figure 1: Changes in structure and composition of the intervertebral disc with age and development. The vertebral endplates and annulus fibrosus are vascularized in the fetus, but the blood vessels recede and eventually disappear during juvenile development. The nucleus pulposus has a fluid-like form in the fetus, but becomes more gelatinous as mesenchymal cells replace notochordal cells and collagen begins to accumulate in the juvenile. By adulthood the demarcation between nucleus and inner annulus becomes indistinct.

At maturity, the cell density of the NP is on the order of 4×10^6 cells/cm^3; this is much less than even hyaline cartilage (typical cell density of 1.4×10^7 cells/cm^3), making the NP one of the least cellular tissues in the human body [7]. The cells of the IVD exist

in a complex physicochemical environment; the unique properties of this environment are a function of the avascular nature of the adult intervertebral disc, the composition of the ECM, and the mechanical loading experienced over a diurnal cycle [9].

All the cells of the mature human disc are mesenchymal in origin, and no unique phenotypic markers have been identified to differentiate disc cells from chondrocytes [10]. However, the ECM produced by the different cells is distinct. Both nucleus pulposus and annulus fibrosus cells produce macromolecules similar to those found in hyaline cartilage – namely collagen and proteoglycans (PG) – but the ratio of PG to collagen varies by an order of magnitude. Mwale et. al. [10] found a glycosaminoglycan (GAG):hydroxyproline ratio, indicative of the PG to collagen ratio, of 27:1 in the NP and 2:1 in the AF. The differences in ECM production are maintained *in vitro*, suggesting distinct phenotypes rather than environmentally-induced differences [7].

Macroscopic Structure and Matrix Composition

Collagen and proteoglycan are the chief components of the extra-cellular matrix in the disc, but the organization of these components differs greatly among the different structural components. In the AF, the primarily Type I collagen fibrils are parallel and arranged in up to 25 concentric laminae of alternating lay-up, an arrangement optimized to resist tensile forces caused by bending and twisting of the spine. Type II collagen is most abundant in the NP, with a randomly-oriented collagen fibril meshwork interspersed with PG-rich matrix. This PG matrix can also be found between lamellae of the inner AF. These regions enriched with proteoglycans are responsible for resistance to compression [7].

The role of the vertebral endplates in the structure and function of the disc should not be overlooked. Nutrients to the inner annulus and nucleus are supplied by a capillary network originating from the vertebral arteries and terminating in loops at the bone-cartilage endplate junction. The capillaries are protected by the dense hyaline cartilage endplate. The cartilage of the endplate is lower in hydration than that of articular cartilage, so it limits transport of large molecules into and out of the disc [11]. Studies tracking the infiltration of contrast medium into the disc have shown that transport characteristics vary appreciably with age and degeneration, but the status of the endplate zone was the principal factor influencing rate of diffusion to the center of the disc [11, 12].

The intervertebral disc contains more types of collagen than any other connective tissue [13]. Varieties found in the disc include Types I, II, III, V, VI, IX, X, XI, XII, and XIV, but Types I and II are most abundant [7, 13]. Collagen Types I and II are found in opposing gradients, with Type I most abundant in the outer AF and Type II most concentrated in the NP. The most prevalent PG in the disc resembles the bottlebrush-structured aggrecan of articular cartilage. At birth, the aggrecan variant in the disc consists primarily of GAGs rich in chondroitin sulfate (CS) bound by a link protein (LP) to a hyaluronan core, but as an individual ages the proportion of keratin sulfate (KS)-based GAGs increases (Figure 2).

The GAG side chains of the aggrecan molecule are negatively charged, giving the matrix a high fixed negative charge density. Intramolecular repulsion forces among the negatively charged GAGs in this proteoglycan are responsible for resistance to

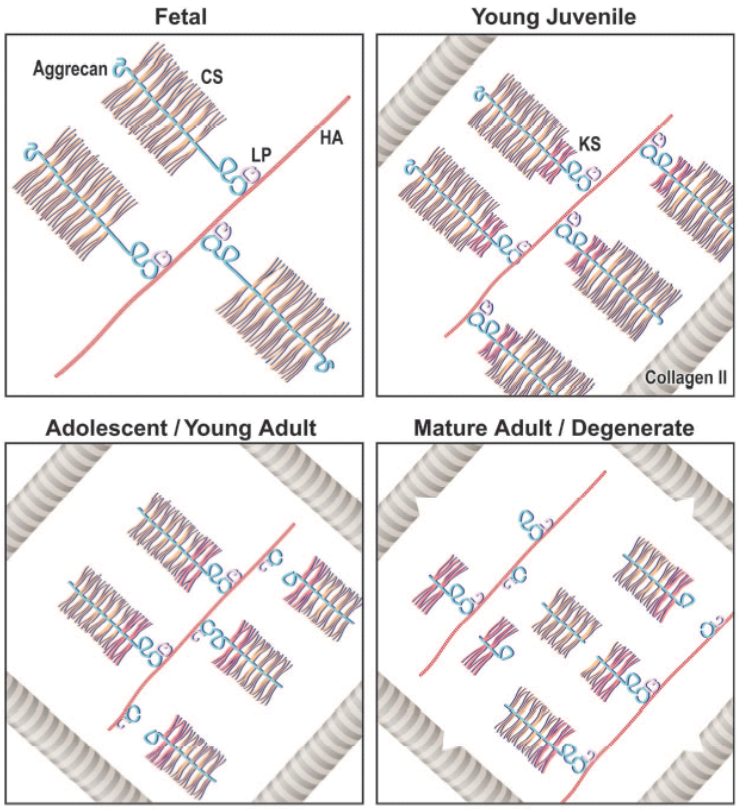

Reprinted with permission from Roughley, P.J., *Biology of intervertebral disc aging and degeneration - Involvement of the extracellular matrix.* Spine, 2004. 29(23): p. 2691-2699.

Figure 2: Age-related changes to the extra-cellular matrix of the nucleus pulposus. In the fetus all side chains for the aggrecan molecule are based upon chondroitin sulfate. Substitution with keratin sulfate begins in the juvenile, and collagen accumulation begins. With age, proteolytic cleavage of the side chains begins, resulting in an increased proportion of non-aggregating proteoglycan in the mature adult.

compression [7]. The high concentration of aggrecan in the disc matrix also affects the extracellular ionic composition and osmolarity. In order to maintain charge equilibrium, the concentration of cations and anions in the disc are higher and lower, respectively, than those found in other surrounding fluids [9]. Since the osmolarity of the disc is higher than that of surrounding tissues, the disc tends to imbibe fluid. This helps maintain hydration and swelling pressure within the disc, enabling its function as a hydrodynamic cushion.

Disc Metabolism

Cell Nutrition

As with all cells, nutrients are required to sustain disc cells and to fulfill their cellular functions. Nutrient flow into the disc is supplied from its margins. The outer annulus is supplied by blood vessels surrounding its periphery, while the nucleus is nourished by the vasculature of the vertebrae via diffusion through the endplates. Diffusion distances may be as large as 6-8 mm distant from the blood supply. The balance between the rate of cellular demand and the rate of transport results in steep concentration gradients of both glucose and oxygen from disc margin to the center of the disc [11]. Metabolic waste products including lactic acid are cleared through the reverse pathway, resulting in concentration gradients in the opposite direction.

Maintenance of the ECM is also heavily influenced by extracellular pH. The local acidity is one factor that affects the rate at which disc cells metabolize glucose. Extracellular pH is driven by concentrations of both GAG and lactic acid, while intracellular pH can be maintained by specialized transporters until extracellular pH falls below 6.8 [9]. Below this pH level synthesis of ECM components falls steeply, and at acidic pH levels on the order of 6.0 cell viability is reduced. Production of catabolic factors such as matrix metalloproteinase (MMP) is less sensitive to pH, leading to a further accelerated degeneration cascade under acidic ECM conditions.

In addition to reducing production of ECM, nutritional stresses can adversely affect the disc cell population. Reduction in nutrients may inhibit cell division, thus accounting for the age-related reduction in cell density. Furthermore, loss of glucose appears to be the driving factor for cell death; while they produced no matrix at 0% O_2,

disc cells have survived for up to 13 days under completely anaerobic conditions [9]. In contrast, disc cells begin to die within 24 hours when the glucose concentration falls below 0.2 mM. It is not clear whether cell death occurs by apoptosis or necrosis [11].

Mechanical Factors

In vivo discs are always under the influence of mechanical loads, whether by the effects of body weight, muscular forces, or a combination of both. When resting and lying down, hydrostatic pressures in the disc are on the order of 0.1 to 0.2 MPa; they increase 5 to 10-fold with normal daily activity [9]. The load history plays a role in determining the physicochemical environment of the disc. The pattern of mechanical loading over the course of a diurnal cycle significantly alters the water content of the disc; disc hydration is approximately 25% lower in the evening than in the morning. Mechanically, loss of hydration reduces the compliance of the disc, thus leading to differences in the load-induced hydrostatic pressure experienced by the disc cells [9]. Disc height loss during the course of a day reduces the diffusional transport distances and thus may affect oxygen, glucose, and pH gradients; however, these effects may be offset by changes in matrix permeability.

Matrix loading is recognized as an important disc metabolism signaling pathway, in that it results in deformation of the matrix and cells, an increase in hydrostatic pressure, and exudation of interstitial fluid. Both unloaded and static loading states have been found to inhibit ECM generation, while intermittent cyclic loading enhances ECM production [7, 9]. The cyclic application of hydrostatic pressure within a physiologic range upregulates synthesis of proteoglycans and production of tissue inhibitors of metalloproteinase production (TIMPs), whereas pressures outside the physiologic range

reduce proteoglycan synthesis or increase production of catabolic factors such as MMPs. The level of hydration based upon whether fluid is imbibed or expressed appears to play a role in this effect; hydration-induced changes in osmolarity lead to changes in disc cell volume and behavior [9].

Degenerative Disc Disease

The susceptibility of the disc to degeneration is a function of its unique physiology. The avascular nature of IVD tissue presents a physiological milieu in which the precarious balance between anabolic and catabolic processes is easily disrupted. Disruption of this environment, whether by injury or the inevitable consequences of aging, initiates a degenerative cascade.

Disc health requires good transport properties from the blood supply, across the endplates, and through the ECM [7, 12]. With endochondral ossification and invasion of calcified cartilage, the permeability of the endplates is reduced and severe calcification acts as a barrier to solute transport [9, 11]. Even further upstream, atherosclerosis of the arteries supplying the vertebral bodies can restrict blood supply and thus the nutrients available to the disc [11, 12].

When the nutrient supply is disrupted the disc cells are unable to maintain the extracellular matrix; notably, the large aggregating proteoglycans begin to break down. The proportion of aggregates relative to the total PG content of the disc decreases [14]; analyzed spatially, aggregation decreases gradually from the outer annulus to the inner annulus and nucleus of the mature disc [15]. Interestingly, when studying the structure of newly-synthesized disc proteoglycan *in vitro* a single proteoglycan morphology of high molecular weight is the main product no matter the age, the type of disc cell or the

pathologic status of the disc. This suggests that the increasing proportion of non-aggregating proteoglycan in the disc is the consequence of proteolytic cleavage and an accumulation of degradation products resulting from a long diffusion pathway and poor transport properties due to size rather than age-related or pathologic changes in the ability of the disc cell to produce the desired aggregating proteoglycans [7, 15].

The water content decreases with the loss of PG and with it the turgor of the disc [16]. Macroscopic characteristics of disc degeneration include progressive dehydration of the NP, formation of tears in the annulus fibrosus, and in severe cases disruption of the endplates [14, 17]. Endplate fissures can also lead to loss of hydration, further altering the permeability of the disc matrix proper [18].

As this degenerative cascade progresses the disc loses its ability to fulfill its structural function – to serve as a hydrodynamic cushion. This loss of function adversely affects other structural components of the spinal motion segment (SMS), notably the facet joints. Overloading of the facet joints can lead to osteoarthritis, one potential source for chronic LBP. Degenerative changes to the SMS can also lead to neuropathic pain, as when narrowing of the intervertebral foramina due to loss of disc height causes impingement of spinal nerves.

Clinical Treatment Paradigm

Degenerative conditions of the lumbar spine span a pathophysiologic continuum from the asymptomatic to the chronically disabling; diagnosis of the root cause of low back pain is imprecise and often an exercise of exclusion [19]. Given the uncertain etiology, conservative treatments are often prescribed first. In cases where conservative treatment proves ineffective clinicians turn to major surgical procedures such as

decompression, fusion, or disc arthroplasty. Success rates vary, as psychosocial factors tend to have a large influence on outcomes.

While some disc injuries can be managed conservatively, the altered biomechanics of the injured disc can initiate a biochemical cascade leading to disc degeneration; e.g. Melrose et. al. demonstrated in an ovine model that rim lesions can lead to progressive degeneration of the nucleus and inner annulus, even when the outer annulus heals [20]. Matrix loading is recognized as an important disc metabolism signaling pathway, and the cyclic application of hydrostatic pressure outside of the normal physiologic range can reduce proteoglycan synthesis and/or increase production of catabolic factors [9].

Spinal Fusion

The current "gold standard" surgical treatment is discectomy and fusion of two or more adjacent vertebrae. IVD disorders now account for 51% of patients requiring lumbar fusion procedures [21]. In 2001 more than 300,000 spinal fusion operations were performed, putting the number of procedures on par with that of hip replacement surgery [22]. Spine fusion is considered to be one of the most challenging bone grafting applications, as even autograft has a relatively high failure rate [23]. The rate of nonunion has been reported to be on the order of 15% of all primary procedures [24].

Artificial Disc Replacements

A more recent innovation for the treatment of back pain is the artificial disc. Currently, two lumbar disc replacement devices and one cervical disc replacement device have FDA approval. Given the few approved indications and many contraindications for lumbar disc replacement, only about 5% of current lumbar surgical patients are

considered total disc arthroplasty (TDA) candidates. Based upon numerous case series published on lumbar TDA, clinical success rates are on par with fusion. However, no Class I (prospective, randomized) evidence has been published, nor have long-term results. The effects of device wear observed for TDA mirror what is seen for total hip arthroplasty (THA). For metal-on-metal devices serum chromium levels slightly exceed THA, and devices with polyethylene inserts have exhibited wear-debris mediated inflammation and osteolysis. Other complications observed include subsidence, expulsion, loosening, migration, fracture, and adjacent segment disease.

While total disc replacement preserves spinal motion, it is a complicated surgical procedure similar in invasiveness to fusion. Replacement of the nucleus pulposus is a potentially less invasive prosthetic strategy, in that the AF is spared. By replacing the nucleus, disc height can be restored, thus restoring annulus tension, stabilizing spinal ligamentous structures, and restoring segmental biomechanics.

Intradiscal Implants

Given the high complication rate associated with fusion procedures, there is considerable interest in the development of non-fusion treatment strategies and less-invasive interventions. Mechanical characteristics of an effective nucleus replacement include a similar stiffness to the native disc to avoid stress shielding, a modulus compatible with the vertebral endplates to minimize implant subsidence, and high wear resistance and fatigue life to endure up to 100 million cycles over 40 years [25].

The traditional medical device companies have taken an intradiscal implant approach to nucleus replacement. The intradiscal implant with the longest clinical track record is the Prosthetic Disc Nucleus (Raymedica, Inc., Bloomington, MN), a polyacrylamide and

polyacrylonitrile copolymer hydrogel pellet encased in an inelastic polyethylene jacket that has performed favorably in biocompatibility and biomechanical tests. Similar hydrogel-based intradiscal implants include Aquarelle (Stryker Spine, Allendale, NJ), NeuDisc (Replication Medical Inc., New Brunswick, NJ), and the Newcleus (Zimmer Spine) [25]. The premise of many of these systems for nucleus pulposus replacement is that restoring mechanical function is of utmost importance; thus, intradiscal implants still require open surgical procedures. Furthermore, these relatively stiff implants do not conform to the intra-annular space, thus they do not benefit from load sharing from the annulus and implant subsidence remains a significant complication [5].

Regenerative Therapies

Current research interest in inducing biologic repair via methods including tissue engineering, gene therapy, and cellular therapies is high [6]. Generally, the aim is to prevent, arrest, or reverse degeneration by increasing accumulation of ECM either by upregulating synthesis or by downregulating degradation. This strategy can be implemented directly by providing appropriate growth factors and cytokine inhibitors or by altering gene expression [26].

Although the cytokine-mediated catabolic cascade is not yet well-understood, some growth factors have been investigated as regenerative treatments for degenerative disc disease (DDD). Growth factors known to stimulate matrix production include bone BMP-2, BMP-7 (also known as osteogenic protein or OP-1), GDF-5, TGF-β, and IGF-1, whereas the cytokines IL-1 and TNF are known to inhibit matrix synthesis. Protein "cocktails" may be more effective; e.g. combinations of TGF-β, BMP-2, and IGF-1 have been shown to act collaboratively to stimulate proteoglycan synthesis [26]. These small-

molecule biologics are amenable to percutateous injection, opening up the possibility of a non-invasive IVD therapy. However, a significant drawback to the use of recombinant proteins is their price; e.g. a single dose of BMP-2 can cost $5,000. Furthermore, such approaches focus solely upon regeneration of the extracellular matrix (ECM) and do not account for the physiological processes that initiated disc degeneration in the first place. It is unclear whether the exogenous signalling molecules will be able to induce production of new ECM without removal of the existing pathologic tissue.

More recently, tissue-engineering principles have been incorporated as a means to stimulate a repair response in the IVD -- therapies might include cells, a scaffold, signaling molecules or any combination thereof [27]. Numerous research groups have based their regenerative therapies upon injectable natural biopolymers including forms of HA [28-30], collagen derivatives [31-33], or combinations of these with proteoglycans [27]. These ECM mimics, either stand-alone or seeded with cells, have been shown to provide a favorable, bioactive environment for endogenous ECM synthesis. However, these systems still lack the mechanical strength required for IVD function. Other biopolymers such as chitosan [34] and a silk-elastin copolymer [35] have been investigated to better match the mechanical properties of native nucleus pulposus, but these systems are not injectable.

Most tissue engineering approaches involve a combination of cells, scaffold, and signaling molecules, but drawing from results seen in viscosupplementation of osteoarthritic diarthroidal joints it appears that the bioactivity of the repair material itself may be of greater importance. Supplementation of diarthroidal joints with hyaluronan was initially seen as a means to restore the viscoelastic properties of the synovial fluid,

but the beneficial effects of the injections far outlast the expected residence time of the exogenous hyaluronan [36]. The beneficial effect of viscosupplementation is likely multi-factorial, but broadly four mechanisms are described in the literature: (1) restoration of viscoelastic properties of the synovial fluid, (2) upregulation of biosynthetic processes resulting in chondrogenesis, (3) anti-inflammatory effects slowing or preventing degradation, and (4) analgesia resulting from desensitization of stretch-activated ion channels to mechanical stimuli [36, 37]. These effects are also desirable in treating low back pain, thus hyaluronan and other bioactive molecules are good candidates for systems to repair the nucleus pulposus.

Hydrogel-Based Biomaterials

Revell *et al* [28] evaluated two HA-based materials, one acellular (HYAFF®) and the other (HYADD®) seeded with mesenchymal stem cells (MSC), in a porcine nucleotomy model. After six weeks *in vivo*, they found that injected discs retained a central nucleus pulposus-like region and a relatively normal biconvex morphology, though the biconvex region was smaller than control discs. Interestingly, discs injected with the acellular gel retained relatively normal disc space while those injected with the MSC-seeded gel showed some signs of disc narrowing. Histologic examination of discs injected with the acellular gel showed cellular tissue with chondrocytes producing matrix in the center of the disc while the MSC-treated discs exhibited a heterogeneous cell population and areas of loose matrix relatively lacking in cells. The authors suggest that the cells in the HYAFF® were recruited from the inner annulus region, which has been shown to be the main site of cell proliferation in the normal IVD. Thus, while the acellular HYAFF® showed promise, the inability to retain biconvexity comparable to

control discs may be attributed to the inferior mechanical properties of HYAFF® relative to NP tissue.

This *in vivo* study demonstrates the promise of injectable HA-containing biomaterials as a DDD treatment, but the inability of the injected materials to withstand physiological loads compromised outcomes. The study focused on the regenerative capability of the gels without regard for the mechanical characteristics. *In vitro* mechanical testing of similar ECM mimics [27, 29, 34] achieved aggregate moduli on the order of one-third to one-half that of healthy human NP tissue.

Crosslinking Strategies

Other research groups have focused upon developing materials that are mechanically comparable to the NP based upon the hypothesis that maintaining physiologic biomechanical loading is sufficient to prevent the degenerative cascade. One means of achieving this mechanical integrity is by further crosslinking the hydrogel. Numerous crosslinking chemistries for hyaluronan have been studied. One relatively non-toxic scheme involves the use of 1-ethyl-3-(3-dimethylaminopropyl)carbodiimide (EDC), also known as water-soluble carbodiimide (WSC), which is known to crosslink HA and other polysaccharides [38]. The byproduct of the crosslinking reaction, a urea derivative, displays a very low degree of cytotoxicity. However, the pH dependence of this crosslinking scheme disqualifies it for *in situ* use; an optimal pH range from 3.5 to 4.5 has been reported.

Cloyd et al [30] have reported on a mechanical characterization of three HA-based hydrogel systems. While some of the gels were able to match or exceed elastic properties of NP tissue, they did not mimic the viscoelastic behavior of the NP tissue.

The gels that had comparable unconfined compression moduli to NP tissue showed significantly less stress relaxation. This lack of stress relaxation is likely due to the crosslinking used in the gels to increase modulus. Natural NP tissue has a relatively compliant, proteoglycan-rich matrix that is reinforced with collagen fibers to increase its compressive modulus. The natural tissue's more compliant matrix reinforced with collagen affects the health and migration of cells [39]; furthermore, as described above cell proliferation is dependent upon diffusion of nutrients and waste products through the matrix.

Particulate-Reinforced Hydrogels

The idea of reinforcing hydrogels with particulates to increase compressive properties has also been explored. Usta *et al* [40] studied the behavior of gelatins reinforced with alumina particulates. In this case, the alumina was meant to model hydroxyapatite filler and it was employed for ease of handling and reduced cost. The small particles were very effective at increasing the compressive modulus of the gelatin: volume fractions of alumina as low as 7% in the hydrated gelatin doubled the compressive modulus, while volume fractions of 14% resulted in a 5-fold increase in compressive modulus. These results far exceeded the 1.2x and 1.4x modulus increases predicted by rule of mixtures for those volume fractions of reinforcement in a typical thermoplastic polymer/ceramic particulate composite.

Giordano *et al* [33] found similar results studying hydroxyapatite-reinforced HYAFF 11. HYAFF 11 is a benzyl ester of hyaluronic acid that exhibits poor mechanical properties. Large amounts of reinforcement (14/86 weight ratio of hydroxyapatite/HYAFF) were employed in an effort to raise the compressive mechanical

properties of the HYAFF to those of spongy bone. The reinforcement increased the elastic compressive modulus of the HYAFF 7-fold.

Methods for Intervertebral Disc Study

Mechanical Testing

Classically, the NP has been considered to be an incompressible fluid; as such most of the early mechanical testing of NP tissue focused upon measuring hydrostatic pressure *in situ* or swelling pressure *in vitro*. However, as computational modeling has become more prevalent it has become clear that the incompressible fluid assumption is flawed. The need for better characterization of the deformational behavior of the NP under load for more accurate spinal finite element models led to a resurgence in the experimental measurement of NP material properties.

One such study strove to assess the solid and fluid characteristics of the NP in torsional shear. Iatridis *et al* [41] used parallel plate rheometry to study the behavior of healthy NP tissue under both dynamic oscillatory shear and transient stress relaxation test conditions. At a strain amplitude of 0.01 rad over the frequency range 1 rad/s $\leq \omega \leq$ 100 rad/s mean values for the complex modulus ($|G^*|$) ranged from 7-21 kPa and $\tan\delta$ increased from 23° to 31° indicating that the NP became more dissipative with frequency. In the stress relaxation tests, rapid relaxation immediately following the peak shear stress followed by more gradual relaxation to near-equilibrium values at the 600 s duration of the test indicated fluid-like transient behavior.

While dynamic shear testing provides useful information on the viscoelastic nature of materials, confined compression testing accounts for the biphasic and viscoelastic nature of NP tissue while also better mimicking the actual stress state of the

native NP. The specific aggregate modulus derived from confined compression depends upon the constitutive model used, but all have been shown to characterize the viscoelastic nature of the native NP tissue and to delineate the state of degeneration in the tissue [42-46]. For example, Johannessen et al found the isometric swelling pressure measured during confined compression decreased by 73% comparing healthy to degenerated human NP tissue [44]. Perie et al found that confined compression aggregate moduli (H_a and H_{ao}) for NP tissue tend to vary from about 0.31 to 1.0 MPa depending on the species tested and constitutive models used [42, 43].

There continues to be great variation in the methodologies used to mechanically characterize NP tissue. However, the increasing body of literature (Table 1) will provide useful points of comparison for potential NP mimics tested by the same or similar methodology.

In vitro *Culture Systems*

In vitro cell culture is a useful tool for the study of biological responses in a particular system. In cases where specific functions of a particular cell type is not under consideration, transformed cell lines provide well-characterized, robust models for experimentation. As an example, generalized cytotoxicity assays are typically run on cell lines derived from target tissues, e.g. fibroblasts.

In vitro systems specifically for the study of the IVD include the use of primary cell culture, tissue culture, and whole-disc (including end plates) organ culture. Appropriate culture conditions depend upon the question under study; e.g., to study the physiology of degenerative disc disease the pH, oxygen tension, and nutrient supply should be altered to mimic a catabolic microenvironment [47].

Table 1: **Material properties for intervertebral disc tissue**

Species	Material Properties	Methodology	Reference
Compressive Modulus			
Ovine	41.2 ± 5.1 Pa (NP) 64.6 ± 5.3 kPa (AF)	Stress relaxation under confined compression	Mizuno *et al.* [48]
	3 kPa	Unconfined compression	Johannsessen *et al* [44]
Bovine	H_{A0}= 0.31 ± 0.04 MPa (NP), 0.74 ± 0.13 MPa (AF)	Stress relaxation under confined compression	Perie *et al* [42]
Human	5.39 ± 2.56 kPa (linear region), Poisson's ratio 0.62 ± 0.15	Stress relaxation under unconfined compression	Cloyd *et al* [30]
	H_A^{eff} = 1.01 ± 0.43 Mpa (normal) H_A^{eff} = 0.44 ± 0.19 MPa (degen)	Stress relaxation under confined compression	Johannsessen *et al* [44]
	6 ± 0.05 kPa	Indentation	Umehara *et al* [49]
Dynamic Properties			
Ovine	Fresh: E' = 64 ± 28 KPa E'' = 23 ± 13 KPa tanδ = 0.34 ± 0.08 Frozen: E' = 83 ± 20 KPa E'' = 26 ± 8 KPa tanδ = 0.33 ± 0.05	Sinusoidal cyclic compression w/ 10 μm displacement applied at 8 frequencies (1Hz reported)	Leahy and Dukins [50]
Porcine	G' ~ 300 Pa at 1 Hz, G" ~80-90 Pa, tanδ ~0.24–0.4	Small amplitude oscillatory shear tests	Causa *et al* [51]
Human	|G*|and ω @ 1, 10, 100 rad/s 1: 7.4 ± 11.6 kPa, 23 ± 5˚ 10: 11.3 ± 17.9 kPa, 24 ± 5˚ 100: 19.8 ± 31.4 kPa, 30 ± 6˚	Dynamic shear	Iatridis *et al* [52]
Hydraulic Permeability			
Ovine	$2.1 \pm 1.8 \times 10^{-14}$ m^2/Pa s (AF) $6.2 \pm 1.5 \times 10^{-14}$ m^2/Pa s (NP)		Mizuno *et al* [48]
Bovine	$0.67 \pm 0.09 \times 10^{-15}$ m^4/N s (AF) $0.23 \pm 0.19 \times 10^{-15}$ m^4/N s (NP)		Perie *et al* [42]
Water Content			
Ovine	80 ± 2%		Leahy and Hukins [50]
Bovine	86.5 ± 0.7% (confined swelling) 92.3 ± 0.6% (free swelling)		Perie *et al* [42]
	86 ± 3%		Antoniou *et al* [53]
Human	88 ± 3.5% to 92 ± 7.1% (cultured NP cells)		Sakai *et al* [54]
	78-80%		Antoniou *et al* [53]

Cell culture techniques for disc cells have benefited from a deep body of literature on articular cartilage chondrocyte cell culture. Fibrochondrocyte-like cells of mesenchymal origin are found in both the annulus fibrosus and nucleus pulposus in the adult human; cells of notochordal origin are also found in the nucleus pulposus of young humans and some animal models. As with articular chondrocytes, these mesenchymal-derived disc cells have been found to de-differentiate in monolayer culture. They take on a "spindle-shaped" cell morphology and alter gene expression for aggrecan and collagen I and II [55, 56].

While monolayer culture may be appropriate for expansion of primary disc cells, three-dimensional culture systems better preserve the chondrocytic phenotype [57]. As with articular cartilage chondrocytes, common three dimensional culture systems include agarose, alginate, and collagen sponges [54, 58-60]; more exotic scaffolds under recent investigation include chitosan derivatives [61, 62] and bioactive glass [63].

Common assays for cell viability, metabolic activity, gene expression, ECM synthesis, etc. have also been adapted from the extensive cartilage cell culture literature. Fluorescence assays such as LIVE/DEAD™ (Molecular Probes) and AlamarBlue (Invitrogen) have been used to assess cell viability [64, 65] and relative metabolic activity [65], respectively. Radiolabeling techniques such as [^{3}H]-thymidine uptake into newly-synthesized DNA can be used as a marker for cellular proliferation [54]. Similarly, [^{35}S]-sulfate uptake can be used to monitor proteoglycan synthesis [54, 66] and release into media [67]. The dimethylmethylene blue (DMMB) assay is also commonly used to measure sulfated GAG content and thus proteoglycan accumulation [48, 54, 64, 67]. Collagen synthesis can be determined by measuring the hydroxyproline content using the

Chloramine T assay (VWR) [68] or can be inferred by evaluating gene expression levels via RT-PCR [65].

Traditional histology methodologies should not be overlooked; they remain a useful tool for the assessment of tissue and organ culture systems. Hematoxylin and eosin (H&E) is an effective stain for collagen [54] while Toluidine blue [54, 69] or Safranin O with a Fast Green counterstain [64, 68] have been used for GAG and PG.

Often, a range of *in vitro* techniques will be used to probe different aspects of the biologic response before moving on to more resource-intensive *in vivo* studies. While cytotoxicity studies can be used to screen a wide range of test articles with relatively little investment of resources, their results do not always translate directly to the response *in vivo*. Rather than taking any one assay as a sole measure of the biological response, multiple assays taken together can paint a broader, more well-rounded picture of the biologic response.

RESEARCH OBJECTIVES AND SPECIFIC AIMS

Study Rationale

The avascular nature of IVD tissue presents a physiological milieu in which the balance between anabolic and catabolic processes is easily disrupted, making intervertebral disc degeneration a natural consequence of aging. Current clinical treatment options for disc degeneration exist at two extremes: conservative management or surgical intervention. Given the economic impact of lost productivity and disability associated with low back pain, there is significant interest in earlier, less invasive interventions.

Numerous research groups are investigating polymer systems as tissue engineering scaffolds for the nucleus pulposus. Nucleus replacement systems open-up the possibility of less invasive procedures that maintain the existing annulus structure. The premise of many of these systems for nucleus pulposus repair is that restoring mechanical function is of utmost importance; hence, the chosen material must duplicate native nucleus pulposus mechanical properties. However, drawing from results seen in viscosupplementation of osteoarthritic diarthroidal joints, the bioactivity of the repair material may be of greater importance. Thus, the overall goal of this work is to establish a nucleus pulposus replacement that (a) sufficiently restores mechanical function and (b) induces tissue regeneration via cell migration from the inner annulus fibrosus and upregulation of extracellular matrix synthesis.

The ubiquity of low back pain in industrialized societies makes the intervertebral disc an attractive target for regenerative medicine research. Its avascular nature, while on the one hand a causal factor in the development of degenerative changes, on the other allows for immunogenic isolation. As such, current research interest in inducing biologic repair via methods including tissue engineering, gene therapy, and cellular therapies is high. However, it must be noted that in comparison to other orthopaedic tissues, relatively little is known about disc biology. The extent to which the mechanisms linking load, the chemical milieu, and cellular activity in the disc have been characterized does not approach that of chondrocytic activity in cartilage or osteoblastic and osteoclastic behavior in bone.

We propose that taking a materials-based approach is a more logical first step in developing a minimally-invasive implantable treatment for degenerative disc disease. A reinforced hydrogel based upon the natural polysaccharides found in the disc ECM could be used to restore the mechanical function of the disc. While such a hydrogel could be seeded with cells as part of a regenerative strategy, the materials-only approach is not affected by nutritional limitations of the degenerated disc and how these limitations will affect the viability of implanted cells *in vivo*. We expect that the reinforcing phase of the composite will provide immediate mechanical support while the polysaccharide hydrogel phase will restore the biochemical composition and water content of the disc, elevating the nuclear hydrostatic pressure and thus slowing or halting the progression of disc degeneration.

Research Objectives

The **long term goal** of this research is to develop an implantable polysaccharide-based hydrogel as a less invasive alternative to fusion or disc arthroplasty for the preventative or therapeutic treatment of degenerative disc disease. The **immediate objective** is to take a materials-based approach to develop a bioactive hydrogel that will restore the swelling behavior and mechanical properties of the NP. Thus, it is proposed that particulate-reinforced hydrogels can be used for an NP replacement, providing a compliant matrix for cell migration from the inner annulus. This composite biomaterial will also mimic the mechanical performance of healthy NP tissue in order to maintain structural support of the functional spinal unit and to provide an appropriate mechanical signaling environment to resident cells.

The foundation of this work is a hyaluronan-*co*-high density polyethylene (HA-*co*-HDPE) copolymer that was recently developed in the James Laboratory. The amphiphilic nature of this copolymer allows for the engineering of unique microstructures and properties appropriate for different applications by adjusting the raw material molecular weights, constituent ratios, and extent of reaction (Figure 3). Additionally, the compressive properties of hydrogels have been improved with relatively small volume fractions of particulate reinforcement [40]; fumed silica is used as a model system to evaluate the effect of such reinforcement.

Mechanical Objectives

Mechanically, the NP serves as a hydrodynamic cushion in the spinal column. It is viscoelastic in nature, allowing for an elastic solid-like response to impact loading (as during locomotion) as well as a viscous fluid-like response to static loads (exuding or

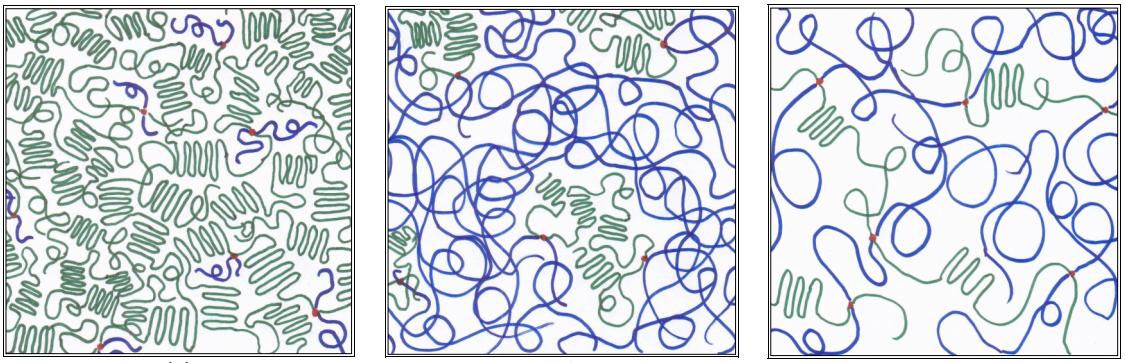

Figure 3: Potential microstructures based upon constituent molecular weight, weight ratio and degree of reaction. (a) suggests a microstructure for an HA-*co*-HDPE copolymer with a low molecular-weight HA (blue) covalently bonded (red) to high molecular-weight PE (green). The PE is primarily crystalline with HA grafted in the amorphous regions. Such a microstructure would behave as a lubricious solid. (b) illustrates a copolymer with a sub-critical proportion of PE. The PE grafts to single HA chains, forming an amphiphilic molecule. Depending upon the size of the PE phase compact crystalline regions may form or the PE will collapse into a micelle with a hydrophobic PE core surrounded by the hydrophilic HA phase. The resulting structured fluid will have unique rheologic properties. (c) shows an intermediate structure in which a the critical extent of reaction has been reached such that a gel network forms. A copolymer with this structure will still be very hydrophilic while having some solid-like behavior.

imbibing fluid during the diurnal cycle). In order to effectively mimic the function of a healthy NP, we aim to tune the hydrogel system to closely match the properties of native nucleus pulposus in terms of dynamic shear parameters and water-carrying capacity.

Biological Objectives

The core component of they hydrogel system is hyaluronan, a highly conserved natural biopolymer that is found throughout the body. Given the ubiquity of hyaluronan, we expect that the gel will be biocompatible. Furthermore, it has been seen in other tissues that an appropriately-bioactive implanted substrate can initiate a regenerative healing response, as is seen in viscosupplementation of diarthroidal joints. We expect that a hyaluronan-based hydrogel serve as a substrate for a similar healing response.

Hypotheses and Specific Aims

We hypothesize that an HA-based copolymer hydrogel can be developed for use following nucleotomy as a less invasive implantable treatment to restore the swelling behavior, mechanical properties, and biochemical signaling environment of a moderately degenerated nucleus pulposus.

We further hypothesize that though the structure will differ, the viscoelastic properties of the large aggregating proteoglycans found in healthy intervertebral discs can be mimicked. We will use rheometry to evaluate the mechanical properties of particulate-reinforced hydrogels based upon two hydrogel formulations.

Lastly, since HA is abundant in the healthy disc and silica has a history of use in pharmaceuticals and as a biomaterial we hypothesize that the hydrogel will be biocompatible; further, it will provide a compliant matrix for the infiltration of disc cells and integration with remaining disc tissue.

To explore the hypotheses described above, three specific aims were formulated:

Specific Aim 1: Material Formulation

Two variations on a HA-based copolymer will be explored for use as a particulate-reinforced hydrogel. The design goal for this copolymer is to achieve a persistent network structure while retaining a high degree of water-binding ability as demonstrated through swell testing.

Specific Aim 2: Mechanical Characterization

The mechanical behavior of the copolymers developed in Specific Aim 1 will be characterized, including the effect of particulate reinforcement with fumed silica. The

target formulation will have dynamic shear properties similar to healthy nucleus pulposus (NP) tissue.

Specific Aim 3: In vitro Modeling

Cytotoxicity will be assessed according to an ISO standard assay appropriate for implanted devices. The *in vitro* response of a transformed cell line exposed to leachable substances from the HA-based composite hydrogels will be assessed. An explant tissue culture study will evaluate the integration of the hydrogel with the tissue as a further measure of biocompatibility.

DISSERTATION RESEARCH

THE SYNTHESIS AND CHARACTERIZATION OF A HYALURONAN-CO-POLY(ETHYLENE-ALT-MALEIC ANHYDRIDE) HYDROGEL COMPOSITE

Introduction

Previous work in the James Laboratory [70, 71] has focused upon randomly bonding high-density polyethylene (HDPE) chains onto hyaluronan (HA) molecules. An interfacial polymerization was used to react HA and maleic anhydride-grafted HDPE (MA-*g*-HDPE) under inert synthesis conditions, resulting in the amphiphilic copolymer HA-*co*-HDPE (Figure 4). This unique copolymer retained hydrophilic qualities from the HA while gaining some desirable characteristics from the HDPE, such as mechanical strength and melt-processability.

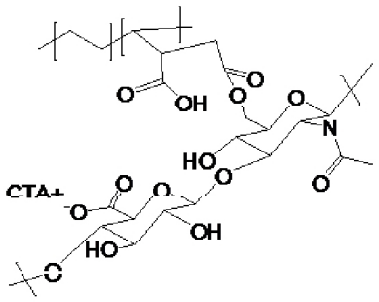

Figure 4: Hypothesized chemical structure for HA-co-HDPE.

HA-*co*-HDPE has been investigated for use in a number of orthopaedic applications. To date, the formulations that have been explored include lubricious solids for diarthroidal joint repair [72], scaffolds for cartilage tissue engineering [73], and viscous fluids to bind demineralized bone matrix (DBM) into malleable putties [74]. For treatment of the intervertebral disc a hydrogel formulation is most desirable in order to mimic the "hydrodynamic cushion" functionality of the disc. Broadly speaking, a hydrogel is a 3-dimensional network comprised of hydrophilic polymers that are

crosslinked such that they remain insoluble in water. Relative to the previous incarnations of HA-*co*-HDPE, a hydrogel requires a greater capacity to imbibe water and a denser crosslinked network. While still useful, the mechanical strength and hydrophobic interactions afforded by the crystalline polyethylene domains of HA-*co*-HDPE are less critical in this application.

The development of such a hydrogel is the focus of the work described herein. Another synthetic polymer, poly(ethylene-*alt*-maleic anhydride) (PEMA), was identified for use in place of the MA-*g*-HDPE in order to achieve the necessary crosslink density. PEMA differs from the graft copolymer in that rather than hanging pendant, the maleic anhydride (MA) groups are directly incorporated into the polyethylene backbone (Figure 5). The strictly alternating monomer sequence results in a substantially greater proportion of the reactive MA groups: PEMA is 77.8% MA by weight, whereas currently commercially-available MA-*g*-HDPE is at most 3% MA by weight. The greater availability of anhydride reactive groups enables the required crosslink density for hydrogel formation via a reaction scheme similar to that for HA-*co*-HDPE (Figure 6). The design requirement for this new copolymer, HA-*co*-PEMA, was to achieve a persistent, covalently bound network while retaining a high degree of hydrophilicity.

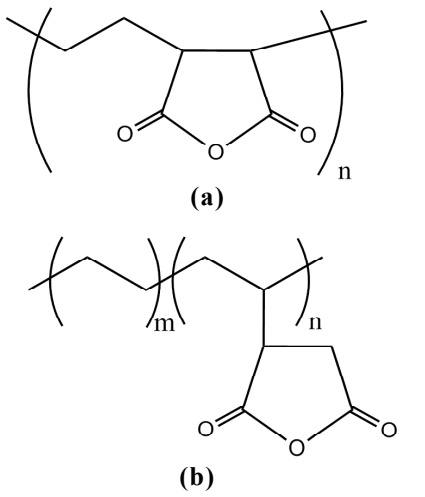

Figure 5: Chemical structures for (a) poly(ethylene-*alt*-maleic anhydride) and (b) maleic anhydride-grafted polyethylene.

While substituting PEMA for MA-*g*-HDPE was necessary to achieve the desired hydrogel network, it also sacrificed the mechanical strength provided by the crystalline

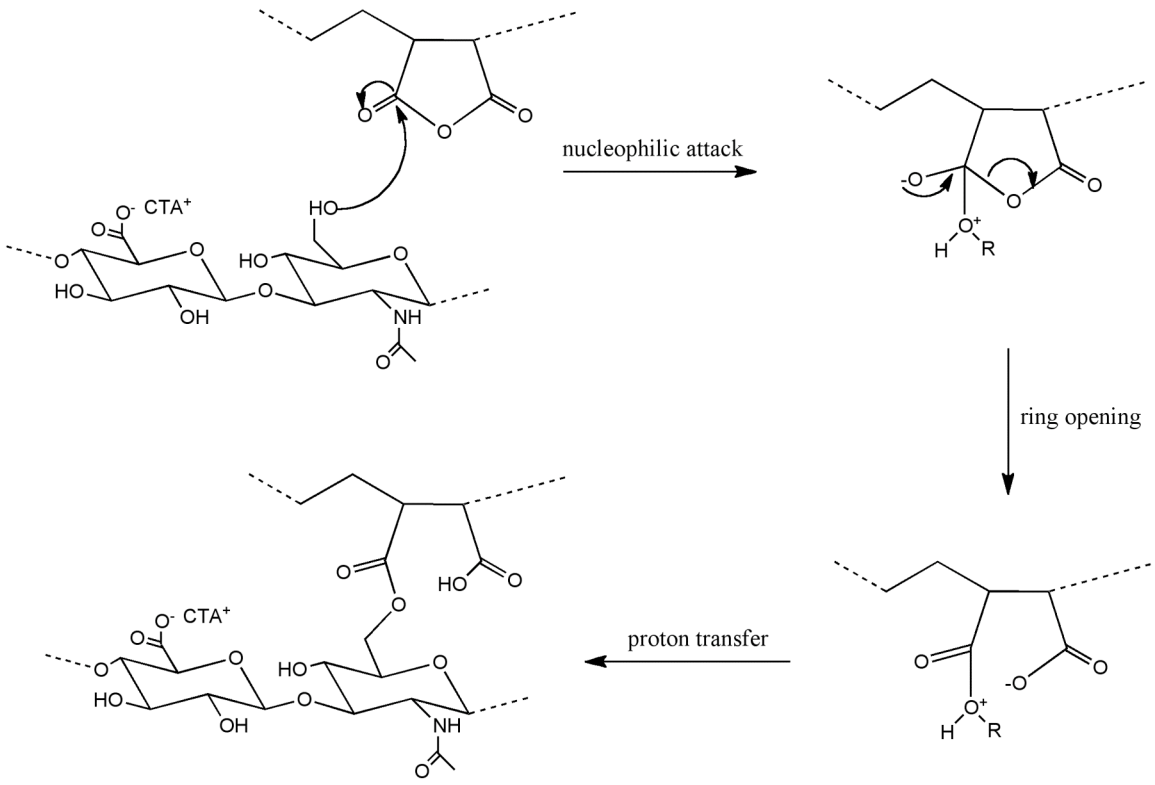

Figure 6: HA-*co*-PEMA hydrogel reaction scheme. Maleic anhydride groups are subject to nucleophilic attack by alcohols, resulting in a ring-opening reaction and formation of an ester linkage to the hyaluronan molecule.

domains of the HDPE. The mechanical integrity required for an intervertebral disc application would be approached by a different strategy, namely that of a particulate-reinforced composite system. Much recent research interest has focused upon the use of inorganic nanoparticles in composite hydrogels; the unique physical properties of the nanoparticles and the possibility of chemical or physical interactions with the hydrogel polymer provide a rich set of tools for the design of improved soft materials [75]. Fumed silica was chosen as the model system to study the effect of reinforcement. It is a common additive used for rheology modification in a wide range of commercial products and industrial applications, including cosmetics, pharmaceuticals, and packaged foods. It is commercially available in many forms, including some with different surface treatments to allow for varying degrees of hydrophobicity. Incorporating different

surface chemistries into the particulate reinforcement model system can provide insight into the strengthening effect of non-covalent interactions, i.e. hydrogen bonding or hydrophobic interactions. Three such surface treatments on otherwise identically-sized and shaped fumed silica were investigated in this work.

Lastly, though the intervertebral disc can be thought of as an immunologically privileged compartment owing to its avascular nature, biocompatibility testing is required of any material destined for use in the human body. While hyaluronan, the main constituent of the HA-*co*-PEMA hydrogel is a natural biomacromolecule with a long history of use in medical treatments, less is known about PEMA. Further, reaction intermediates or degradation products can influence biocompatibility. As an initial step toward demonstrating biocompatibility, a cytotoxicity assay modeled after ISO standard 10993 was performed [76]. Finally, based upon preliminary cytotoxicity screens two materials were carried forward into a pilot tissue culture experiment in which the integration between nucleus pulposus (NP) tissue and the hydrogels was explored as a second test of biocompatibility.

Specific Aim 1: Hydrogel Synthesis and Characterization

Materials and Methods

Sodium hyaluronate (Na-HA, 720-780 kDa) was purchased from Lifecore Biomedical (Chaska, MN) and stored at -20°C until use. Cetyltrimethylammonium bromide (CTAB), poly(ethylene-*alt*-maleic anhydride) (PEMA), and dimethyl sulfoxide (DMSO, anhydrous, 99.9+%) were obtained from Sigma-Aldrich (Milwaukee, WI). Acetone and sodium chloride were supplied by Mallinckrodt Chemicals (Phillipsburg,

NJ). Potassium bromide (99+%, for spectroscopy, IR grade) came from Acros Organics (Morris Plains, NJ). All chemicals were used as received unless otherwise specified.

Hydrogel Synthesis

Hydrophobic modification of hyaluronan (HA) by complexation with a cationic surfactant has been described previously [77, 78]. Briefly, Na-HA was dissolved in deionized water to a concentration of approximately 0.5% (w/v). An aqueous solution of CTAB was titrated into the HA solution until a precipitate was observed. The precipitate was centrifuged and washed in several changes of deionized water to remove residual CTAB, then was vacuum dried at 50°C and -25" Hg until no change in weight was observed. Once dry, the precipitate was ground to a fine powder using a freezer mill (SPEX Sample Prep, Metuchen NJ). The resulting hyaluronan ammonium salt (HA-CTA) is soluble in DMSO, a polar solvent that is miscible with a wide range of organic solvents as well as water.

While the PEMA was used as received from the supplier, care was taken to ensure dry copolymer synthesis conditions since the reactivity of the anhydride moieties is sensitive to water. Both the PEMA and HA-CTA powders were vacuum dried at 50°C for a minimum of 24 hours prior to use, and the 99.9+ anhydrous DMSO solvent was handled assiduously to prevent the absorption of water from the environment. Table 2 summarizes two preliminary hydrogel formulations that

Table 2: Design parameters for hydrogel variations

	LD	**HD**
HA M_w	750 – 780 KDa	
HA-CTA:PEMA (w/w)	36:1	7:1
[HA-CTA] Solution (w/v)	0.5%	1.5%
[PEMA] Solution (w/v)	0.5%	1%
Reactive Ratio [MA]:[OH]	1:46	1:9
Network Ratio mol MA:mol HA chain	164:1	852:1

were evaluated; they differed primarily in PEMA content and solution concentration. With four OH groups per disaccharide, one covalent bond for roughly every ten HA disaccharide pairs was possible for the low crosslink-density (LD) formulation given the 1:46 reactive ratio; for the high density (HD) formulation one covalent bond was possible for approximately every other disaccharide unit. While it was unlikely that every MA would form a covalent bond with the HA, theoretically just one crosslink per HA chain was required to form an infinite network [79]. Thus, MA was available in sufficient excess that both formulations were expected to form gels. Details of these stoichiometric design ratios are discussed in further detail in Appendix C.

To synthesize the gels, concentrated solutions of HA-CTA and PEMA were prepared in separate round-bottomed flasks by solvation in DMSO at 80°C under an N_2 blanket. Once the reactants were fully dissolved, they were combined into a single flask via cannula under dry N_2 flow. The temperature was raised to 90°C and the reaction was allowed to proceed under magnetic stirring for 12 hours. Upon completion of the reaction, the contents of the reaction chamber were allowed to swell in a copious volume of acetone. Since PEMA is soluble in acetone while HA-CTA is not, this step was intended to remove unbound PEMA. Swollen gels were separated from the solvents and then were hydrolyzed to remove complexed -CTA by ion exchange in a 0.2M aqueous NaCl solution with gentle agitation overnight. Following hydrolysis the gels were vacuum dried at 50°C for 24 hours or until no change in weight was observed.

Characterization

The chemical structures of the synthesized hydrogels were investigated by means of Fourier transform infrared spectroscopy (FTIR). Dry powdered samples were mixed

with potassium bromide (KBr) salt at approximately 2% (w/w) and pressed into pellets for analysis. Spectra were collected using a Nicolet Magna-IR 760 spectrometer (Thermo-Nicolet, Madison WI). Absorption spectra were averaged over 128 scans spanning the mid-IR range (4000-400 cm^{-1}) at a resolution of 4 cm^{-1}. Peak locations were automatically identified using the OMNIC software suite (Thermo-Nicolet, Madison WI).

Thermal stability and bulk composition were investigated using thermogravimetric analysis (TGA). Dry powdered samples of 3-7 mg were loaded in open aluminum pans under an inert He atmosphere using a TA Instruments TGA-2950 (TA Instruments, New Castle DE). A heating rate of 10°C/min was used from ambient temperature to 110°C, at which point the temperature was held for 15 minutes to evaporate residual water. The 10°C/min heating rate was then resumed up to 600°C. Thermogravimetric (TG) and derivative thermogravimetric (dTG) curves were collected for compositional analysis per ASTM E1131-08 [80].

Swell tests were used to investigate the water-carrying capacity of the hydrogels. Dry hydrogel samples (n=3 per group) were immersed in deionized water (DI) or phosphate buffered saline (PBS) and allowed to swell at room temperature. The weight of the swollen hydrogels was monitored until equilibrium swelling was achieved. Equilibrium was determined by three consecutive measurements with no further weight gain. The swelling ratio was determined as follows:

$$Q = \frac{(W_s - W_d)}{W_d}$$

where Q is the swelling ratio, W_s is the swollen weight, and W_d is the dry weight. For

comparison to the hydration levels of natural tissues, the weight percentage of solvent was also determined:

$$H = \frac{(W_s - W_d)}{W_s}$$

Q and H for the LD and HD formulations were statistically compared using a pair-wise Student's t-test. Statistical significance was set at α=0.05. All statistical analyses were conducted using the statistical tools built into the SigmaPlot® 11.2 software package (Systat Software Incorporated, San Jose CA).

Results

Upon completion of the 12-hour reaction a golden-hued, viscous product remained in the round-bottomed flask as seen in Figure 7. The consistency of the putative HA-*co*-PEMA reaction product ranged from jelly-like for the LD formulation to a firm gel with the HD formulation. The gels lost color as hydrolysis in 0.2M NaCl solution proceeded, eventually becoming completely transparent and colorless when fully hydrolyzed.

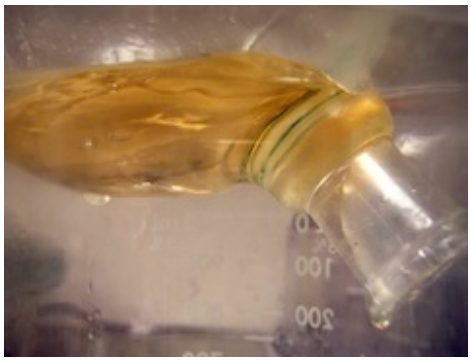

Figure 7: Result of reaction between HA-CTA and PEMA (LD formulation) in DMSO after 12 hours at 90°C.

FTIR spectra for the original reactants and the two HA-*co*-PEMA gel formulations are shown in Figure 8. The spectra for both gels exhibit the characteristic peaks seen in the HA spectra, but key peaks in the PEMA spectra associated with the maleic anhydrides are not apparent. The carboxylic acid peak at roughly 1600 cm^{-1} in the HD spectra is blunted in comparison to the same peak in the HA and LD spectra. A

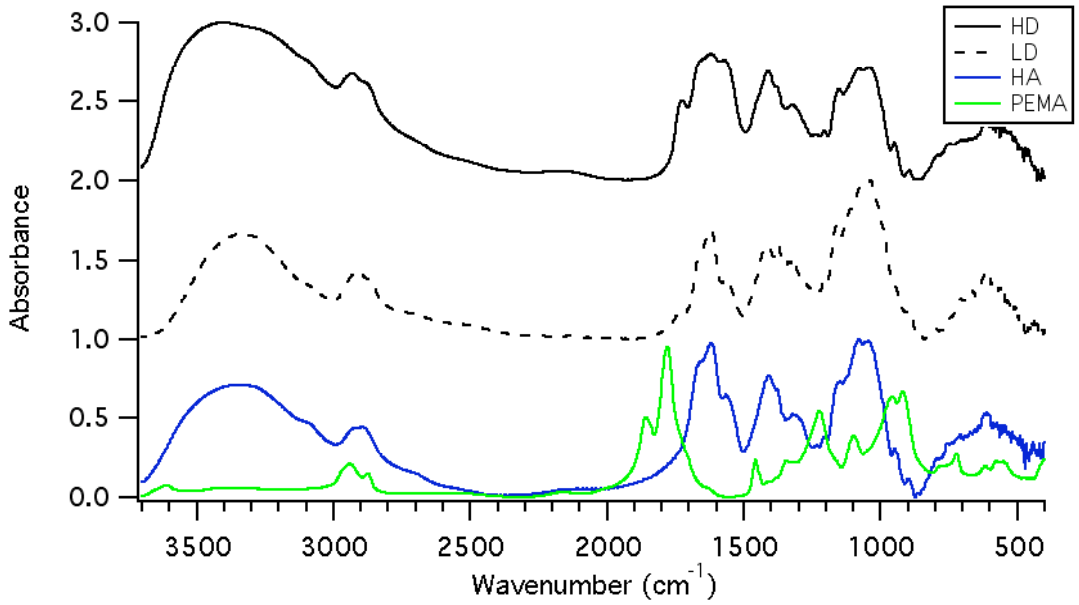

Figure 8: FTIR spectra for high- (HD) and low-network density (LD) HA-*co*-PEMA hydrogels. Spectra for the base constituents of the hydrogels, hyaluronan (HA) and poly(ethylene-*alt*-maleic anhydride) (PEMA), are provided for comparison.

Table 3: FTIR peak identification and location comparison

Vibration Identification	HD Peak (cm^{-1})	LD Peak (cm^{-1})	HA Peak (cm^{-1})	PEMA Peak (cm^{-1})
Bonded OH				3609.43
OH stretch	3406	3336.92	3353.68	
CH_2 asymmetric	2930	2921.97		2939.01
CH_2 symmetric				
CH_3 symmetric			2897.05	
Cyclic anhydride C=O (sym)				1857.95
Cyc. Anhydride C=O (asym)				1778.29
Ester C=O stretch	1725.15			
$-COO^-$	1619.55	1621.50	1618.99	
C-CH_3 asymmetric bend	1466.82			
C-CH_2 scissors				1457.21
-COOH	1411.24	1408.69	1407.42	
C-CH_3 umbrella bend		1374.22		
Secondary amide	1317.82	1318.06	1318.77	
Cyc. Anhydride C-C stretch				1222.87
Ester C-C-O stretch	1205.45	1160.25		
Cyc. Anhydride C-C stretch				1097.97
Ester O-C-C stretch	1042.89	1035.85		
Cyc. Anhydride C-O stretch				956.45
Cyc. Anhydride C-O stretch	911.72			918.24
C-CH_2 rocking	721.39			720.81
	610.99	617.67		612.22

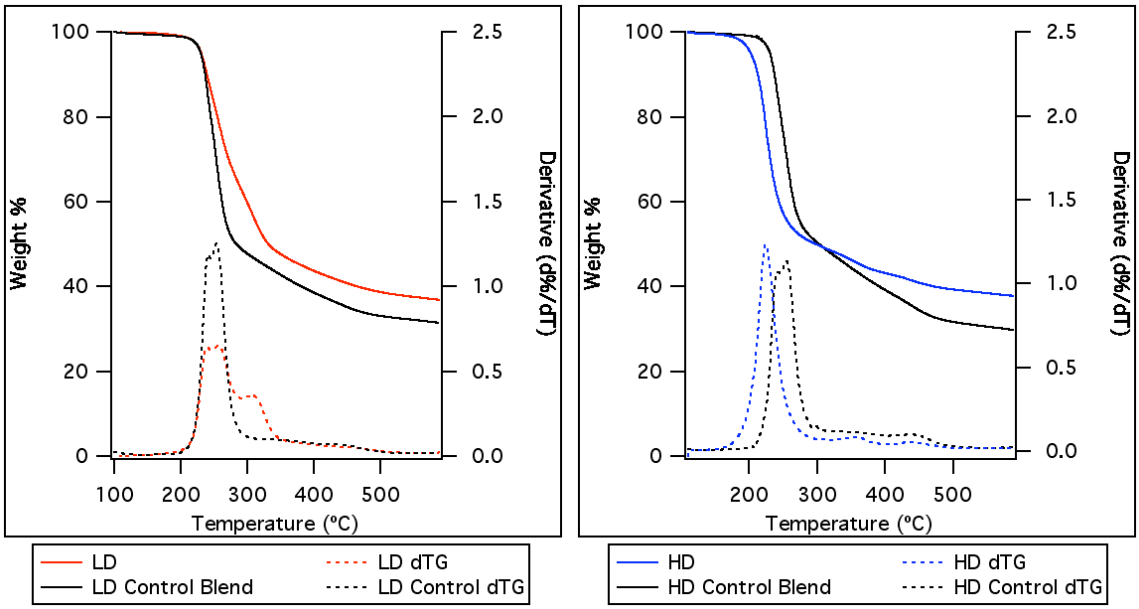

Figure 9: TGA results for LD and HD gel formulations compared to their respective control blends (HA and PEMA blended in the same weight ratio as for the gel formulation). TG traces show the change in mass as a function of temperature, while dTG scans highlight the rate of mass loss.

prominent new peak is seen in the HD gel at 1742 cm^{-1}. In the LD gel a shoulder has appeared at 1741 cm^{-1}, but otherwise new peaks are not as readily apparent as in HD. Peak locations and functional group identification are summarized in Table 3.

Thermogram (TG) and derivative thermogram (dTG) traces for the LD and HD hydrogels compared to their respective control blends of HA and PEMA are shown in Figure 9, while Table 4 summarizes decomposition temperature intervals and peak mass loss temperatures. For both control blends, thermal degradation begins at 230°C, consistent with the decomposition behavior of neat hyaluronan. Roughly 40% of the mass was lost for both control blends in this first decomposition interval.

Thermal decomposition initiates at 5°C lower for the LD gel and proceeds at a slower rate over a wider interval than the control blend. An additional maximum in the dTG curve for the LD gel is seen at 313°C. For the HD gel the initiation temperature was

Table 4: Summary of TGA transitions and dTG peaks for hydrogels and reactants

Sample	Mass Loss (%)	Decomposition Interval (°C)	dTG Peak Temp (°C)	Residue at 600°C (% mass)
HA (780 KDa)	42.62	230.43 – 268.20	253.53	39.04[1]
PEMA[2]	n/a	290.9 – n/a	296.41	n/a
LD control blend	41.26 19.69	230.87 – 271.23 271.23 – 475.35	241.26 254.05	31.46
LD	49.47	225.1 – 352.22	239.69 260.42 313.07	36.88
HD control blend	39.06 23.50	230.09 – 272.44 272.44 – 473.44	254.32	29.77
HD	32.68 16.13	207.31 – 243.39 375.39 – 470.02	222.97	37.90

[1] Residue at 400°C
[2] PEMA TGA scan stopped at 300°C due to rapid weight gain

depressed even further, to 207°C. Decomposition proceeded rapidly over the interval up to 243°C, then flattened out to a non-zero decomposition rate up to 470°C. Both gel formulations left a larger residue at 600°C than their respective control blends.

Swell test results for the two hydrogel formulations are shown in Figure 10. The data illustrated in this figure represent equilibrium swelling in PBS; a complete dataset for swelling in DI could not be collected since the LD hydrogel samples partially dissolved or broke apart.

The swell ratio (Q) and percent hydration (H) are related parameters, in that Q describes the weight ratio of absorbed solvent to dry polymer whereas H considers the percentage

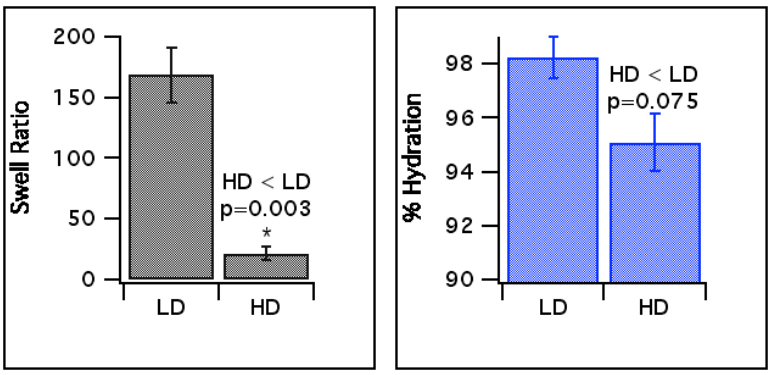

Figure 10: Swell test parameters for LD and HD HA-*co*-PEMA formulations, swollen to equilibrium in phosphate buffered saline. Mean ± SEM, n=3 per group.

of solvent in the swollen gel. Both parameters indicate HD < LD but Q is the more sensitive measure, achieving statistical significance (p=0.003). Mean values and standard errors for both parameters are tabulated in Table 5.

Table 5: Swell test parameters (mean ± SEM, n=3 per group)

Group	Q (DI)	H (DB)	Q (PBS)	H (PBS)
LD	n/a	n/a	168.37 ± 22.44	98.23 ± 0.78
HD	75.70 ± 25.22	98.58 ± 0.52	21.67 ± 5.46	95.09 ± 1.05

Discussion

In this specific aim two hydrogel formulations were explored, varying primarily in the density of the network that forms via the reaction of MA functional groups provided by the PEMA with OH groups on the HA. The density of the hydrogel network was adjusted by varying the ratio of reactants and the solution concentrations. Network polymer theory states that the gel point at which an infinite network first appears is given by the critical extent of reaction, p_c:

$$p_c = \frac{1}{\sum_{i=1}^{\infty} w_i(N_i - 1)} \approx \frac{1}{\sum_{i=1}^{\infty} w_i N_i} = \frac{1}{N_w}$$

where N_i is the degree of polymerization of the i^{th} chain, w_i is the weight fraction of N_i-mers, and N_w is the weight-average degree of polymerization [79]. HA with a molecular weight of 750 KDa averages 1870 disaccharide units, so the gel point p_c= 0.0005. For the formulations explored here, MA functional groups are available in orders of magnitude excess for gelation; multiplying p_c by the network ratios given in Table 2 indicates that if every MA formed a covalent bond with the HA p=0.0877 for formulation LD and p=0.0456 for HD. In addition to the availability of the reactive groups, the solution concentrations come into play in determining the density of the crosslinked network. In dilute solutions the polymer chains have the freedom to adopt more extended

conformations and the reactive functional groups are less likely to encounter one another, resulting in greater distances between crosslinks and thus a looser network structure. At higher solution concentrations one would expect to see more entanglement among polymer chains in addition to increased interaction between reactive groups, thus increasing network density.

Upon completion of the synthesis procedure, a single swollen mass was left in the flask for both formulations. These reaction products were insoluble at room temperature in DMSO, acetone, 0.2M aqueous NaCl solution, and ethanol suggesting that an infinite polymer network had indeed formed. The synthesis method employed here was similar to that described previously for the synthesis of HA-*co*-HDPE, in that maleic anhydride (MA) is the key functional group that enables the reaction. However, while HA-*co*-HDPE was based upon a graft copolymer of MA and PE, the hydrogel utilized the alternating copolymer, poly(ethylene-*alt*-maleic anhydride) or PEMA, allowing for significantly more linkages between the HA and the synthetic polymer.

The PEMA had the further advantage of being soluble in polar solvents including DMSO, thus allowing for a simplified reaction scheme compared to HA-*co*-HDPE. Synthesizing HA-*co*-HDPE involved a reaction at the interface of two immiscible solvents: the MA-*g*-HDPE in a xylenes phase and the HA-CTA in a dimethyl sulfoxide (DMSO) phase. Reaction efficiency was dependent upon the emulsification of the two solvents, a variable that was difficult to control. In contrast, since both the PEMA and HA-CTA are soluble in DMSO a single-phase reaction was possible for the HA-*co*-PEMA hydrogel. Furthermore, dissolving PEMA in DMSO can be accomplished with

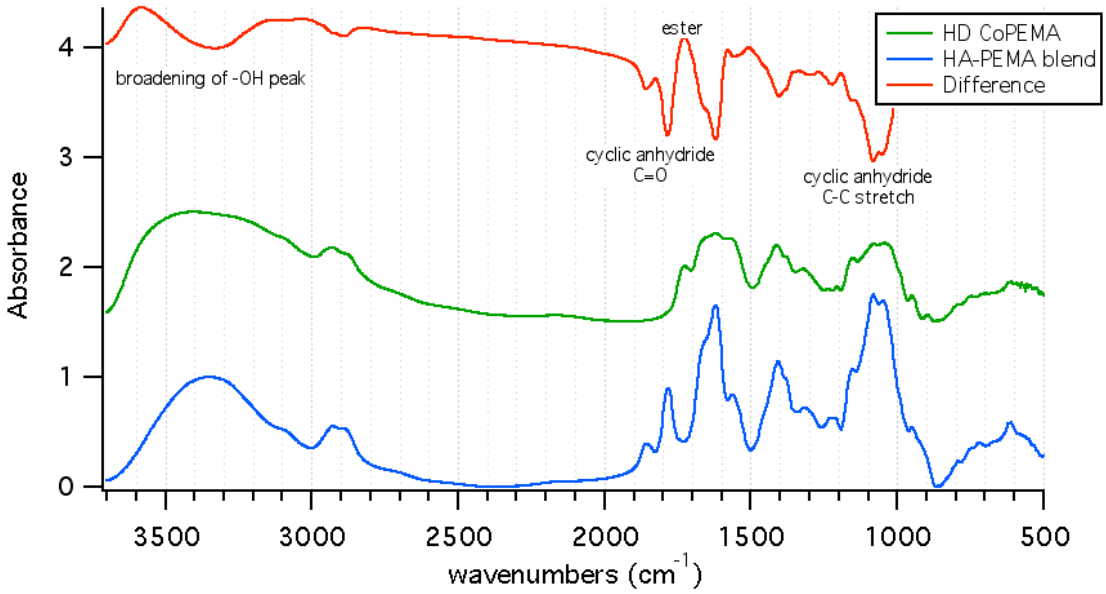

Figure 11: Difference spectrum highlighting changes in peak intensities between HA-*co*-PEMA and an equivalent control blend of HA and PEMA

lower temperatures than is required for solvating MA-*g*-HDPE in xylenes, thus reducing the risk of degrading the HA when the two solutions are mixed.

Evidence of the proposed reaction is readily seen when the FTIR spectrum for a control blend of HA and PEMA is subtracted from the HA-*co*-PEMA spectrum (Figure 11). The intensities of the peaks related to cyclic anhydrides are reduced, as would be expected since the reaction mechanism involves the opening of the anhydride rings. Once open half of the anhydride is used the formation of the ester bond to the HA chain and the other half forms a carboxylic acid, as seen in Figure 12. Ester bonds exhibit strong infrared bands corresponding to the

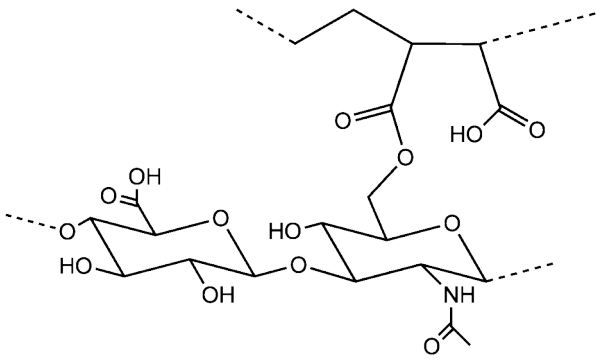

Figure 12: Ester bond linkage between HA and PEMA

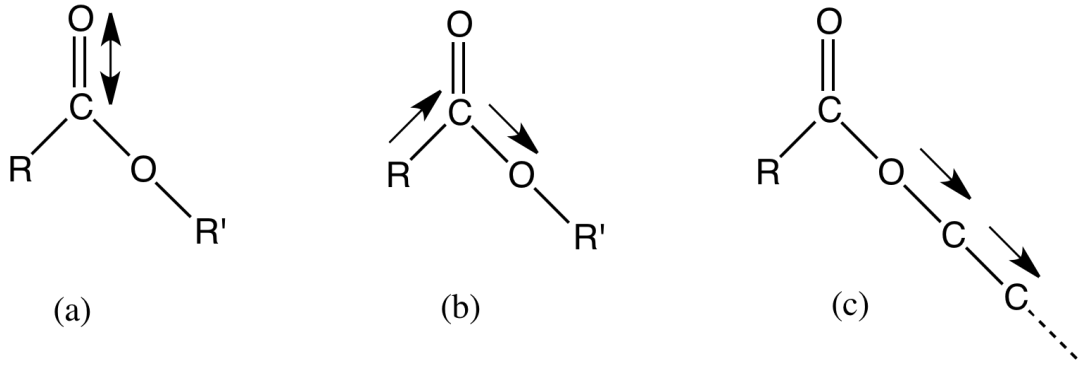

Figure 13: The "rule of 3" for identifying ester bonds in FTIR spectra is based upon strong IR bands due to (a) vibration of the carbon-oxygen double bond, (b) asymmetric stretching across the carbonyl carbon, and (c) stretching of the first two carbons in the reactive species bonded to the ester oxygen.

C=O vibration, asymmetric C-C-O stretching, and the O-C-C stretch (Figure 13); thus they are identified by the "rule of three" in FTIR spectra, with prominent peaks at roughly 1700, 1200, and 1100 cm^{-1} [81]. Taken together, these three peaks provide strong evidence for the presence of ester bonds. All three characteristic peaks are clearly seen in the FTIR spectra for the HD gel formulation. For the LD formulation, peaks at 1160 cm^{-1} and 1035 cm^{-1} were detected and a shoulder in the vicinity of 1700 cm^{-1} is apparent.

TGA was employed to investigate changes in thermal degradation behavior of the hydrogels compared to blends of the starting materials. Both the LD and HD hydrogel formulations began losing mass at lower temperatures than their respective control blends. Chemical alteration to the hyaluronan structure inevitably affects its physico-chemical properties; in this case the formation of ester bonds with the PEMA likely interrupted the normal, most stable arrangement of hydrogen bonding within and among HA molecules, thus resulting in a reduction in thermal stability [82]. The reduction in thermal stability appears to be concentration-dependent, in that the degradation

temperature for the HD formulation is depressed by 23°C while that for the LD formulation is only 5°C lower.

For the LD formulation, there is a second, smaller dTG peak at 313°C, perhaps due to the PEMA phase. The degradation behavior of the PEMA is difficult to ascertain in the control blend, but TGA analysis of PEMA alone (Appendix B) shows that it is thermally stable up to 290°C and that just beyond this temperature it rapidly loses the entirety of its mass. Given this sharp stair-step behavior when analyzed alone, it is surprising not to see a distinct PEMA degradation step in the control blend. However, it is possible that during the TGA temperature ramp the PEMA reacts with the HA even when simply blended; vapor-phase solventless attachment of long-chain molecules to PEMA films have been described in the literature [83]. When linked into the LD hydrogel network, conformational constraints may limit further reaction with the HA, allowing for the PEMA degradation peak to be observed. The PEMA degradation peak in the LD hydrogel occurs at a higher temperature than in neat PEMA, suggesting that it is more thermally stable when covalently bound to HA.

Interestingly, the HD hydrogel formulation does not exhibit the dTG peak attributed to PEMA in the LD formulation. Over the temperature range studied HD degrades in nearly a single stair-step fashion, more similar to neat HA than to LD. In fact, HD degrades at a higher peak mass loss rate over a narrower temperature range than HA, suggesting a relatively homogenous underlying chemical structure. In contrast, the two-step degradation profile of the LD formulation may be an indication of inhomogeneity due to phase separation or incomplete mixing.

The consistency or lack thereof of the hydrogel structure suggested by TGA results was borne out in the swelling behavior. The swell ratios measured among different samples of the LD gel formulation were highly variable in comparison to those for HD samples; furthermore, LD samples partially dissolved or otherwise began to lose weight with time in the swelling media, suggesting domains of incomplete polymer networking. While somewhat delicate, the HD gels remained intact when handled carefully. The HD formulation swelled significantly less than the LD gel, but still achieved a 95% hydration level when swollen in PBS.

The goal for Specific Aim 1 was to develop a hydrogel that could serve as an appropriate matrix for a particulate-reinforced composite nucleus pulposus replacement. Briefly defined, a hydrogel is a hydrophilic polymer that is crosslinked to the extent that it retains its shape and is insoluble in water. The strategy pursued involved an esterification reaction between HA and PEMA, where the PEMA served the role of a long-chain, multifunctional crosslinking agent. FTIR confirmed the presence of ester bonds in the reaction products for the two formulations investigated. TGA suggested that the HD formulation was more homogenous than LD, a result that was confirmed with swell testing. Swell testing further demonstrated a 95% hydration level in PBS for the HD formulation, still above the typical water content for healthy NP tissue. For these reasons the HD formulation was selected as the base formulation for the particulate-reinforced hydrogels investigated in Specific Aim 2.

Specific Aim 2: Mechanical Properties of Reinforced Hydrogels

Materials and Methods

In addition to materials described for Specific Aim 1 above, fumed silica was used as a particulate reinforcing agent. Three grades of fumed silica were generously donated by Cabot Corporation (Boston, MA): CAB-O-SIL® M-5, CAB-O-SIL® TS-620, and CAB-O-SIL® TS-720. All three grades are of similar particle size and density, but while the untreated M-5 grade has a hydrophilic surface the TS-620 and TS-720 grades have been hydrophobically modified with dimethyl-dichlorosilane and polydimethylsiloxane, respectively. Specifications for the three grades of fumed silica are summarized in Table 6.

Table 6: **Fumed silica specifications**

	M-5	**TS-620**	**TS-720**
Density	2.2 g/cm^3 @ 20°C	2.0 g/ cm^3 @ 20°C	2.2 g/cm^3 @ 20°C
pH	3.6-4.5	4.0-5.0	Not determined
Melting temperature	1700°C	1700°C	1700°C
Thermal stability (decomposition T)	n/a	> 300°C	> 150°C
Water solubility	Insoluble	Insoluble	Insoluble
Surface treatment	None -- hydrophilic	Moderately hydrophobic	Hydrophobic
Surface chemistry	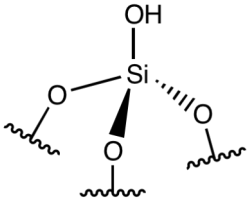	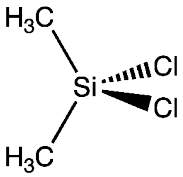	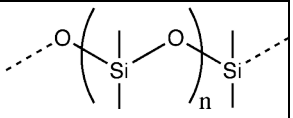

Gel Casting

A concentrated, 2.5% w/v stock solution of hyaluronan (HA, 720-780 kDa, Lifecore Biomedical, Chaska, MN) complexed with an ammonium salt (CTAB, Sigma-Aldrich, Milwaukee, WI) (HA-CTA) was prepared by dissolving HA-CTA in dimethyl sulfoxide (DMSO, anhydrous, 99.9+%, Sigma-Aldrich) at 80°C in an inert environment.

The solution was stored at room temperature in a flask charged with N_2 gas. Similarly, a 10% w/v solution of poly(ethylene-*alt*-maleic anhydride) (PEMA, Sigma-Aldrich) in DMSO was prepared using identical methods and stored under the same conditions.

Table 7: Cast gel constituents

Formulation*	HA-CTA (ml)	PEMA (ml)	Silica (g)
HD-GC	16.5	0.6	-
M5-R	16.5	0.6	0.8
620-R	16.5	0.6	0.8
720-R	16.5	0.6	0.8

* The HD gel cast without silica reinforcement is distinguished from the ge in Specific Aim 1 by the "GC" designation. M5-R, 620-R, and 720-R are reinforced with CAB-O-SIL M-5, TS-620, and TS-720, respectively.

The composition of gels used for mechanical testing are summarized in Table 7. Silica reinforcement levels were chosen empirically after formulating trial gels with 0.1 g, 0.4 g, and 0.8 g reinforcement. It was observed that 0.8 g was approaching the maxmum amount of fumed silica that could be incorporated into the concentrated stock solution of HA-CTA in DMSO, and the resulting reinforced gels were observed to be qualitatively similar to NP tissue. Reinforced gels were stained with Toluidine Blue O to confirm the presence of HA.

The HD gel described in Specific Aim 1 was used as the base gel, but rather than carrying out the reaction in a sealed round-bottomed flask the reactants were cast as a slab to enable samples for mechanical testing to be punched. The concentrated HA-CTA and PEMA solutions were mixed in a 70x50 mm crystallizing dish, forming a layer approximately 2 mm in thickness. The crystallizing dish was then sealed in a vacuum bag, charged with N_2 gas, and left to cure in an oven at 75°C for 24 hours. To synthesize reinforced gels, fumed silica was mixed into the concentrated HA-CTA solution prior to the addition of the PEMA solution. The reinforced gels were then cast and cured by the same method employed for the gel without reinforcement. Following curing, excess reactants and reaction intermediates were washed from the gel by sequentially swelling in

acetone, 0.2M NaCl solution, and ethanol. Washed gels were vacuum dried (-25" Hg, 25°C) for a minimum of 24 hours. Gels were characterized by swell tests (n=3 per group) as described in Specific Aim 1.

Rheometry Sample Preparation

In preparation for mechanical testing, the cast gels were swollen in Dulbecco's phosphate-buffered saline (DPBS, Thermo Scientific HyClone, Logan UT) a minimum of 72 hours. Test samples were punched from the swollen gels using an 8 mm biopsy punch and were maintained in a copious volume of DPBS until testing.

To allow for direct comparison to physiologic tissue, intervertebral disc tissue was harvested from a sheep euthanized in conjunction with an Animal Care and Use Committee (ACUC)-approved research study. The lumbar spine was removed *en bloc* and endplate-disc-endplate units were isolated using a bone saw (Exakt Technologies, Inc., Oklahoma City, OK). Extracted tissue was wrapped in saline-soaked gauze until use. Immediately prior to testing, the disc was dissected from the endplate using a scalpel, and an 8 mm sample was taken from the nucleus pulposus with a biopsy punch. A total of six samples suitable for rheometry were obtained.

Rheometry

Dynamic shear testing was performed on an Advanced Rheometric Expansion System (ARES, TA Instruments, New Castle, DE) equipped with a 2K FRTN1 transducer (measurement range from 0.02 to 2000 g•cm torque, 2 to 2000 gmf normal force). An 8mm parallel plate geometry was used for testing, where a bath chamber with a serrated surface was used as the bottom plate for improved sample grip. A 150-grit sandpaper disc was adhered with ethyl-2-cyanoacrylate to the 8mm top plate for the same

reason. Temperature was held at 25°C via a Julabo recirculating fluid bath (Julabo Labortechnik GmbH, Seelbach, Germany). A humid atmosphere was maintained by placing a saline-soaked tissue inside the bath chamber and installing the bath cover.

Samples were loaded by placing the test specimen on the bath chamber surface and manually lowering the top platen until approximately one gram force was indicated by the axial load cell (Figure 14). The gap displacement value was taken to be the sample thickness. The instrument's software control was then used to set the gap to a 10% compressive strain to ensure planar contact and gripping of the sample.

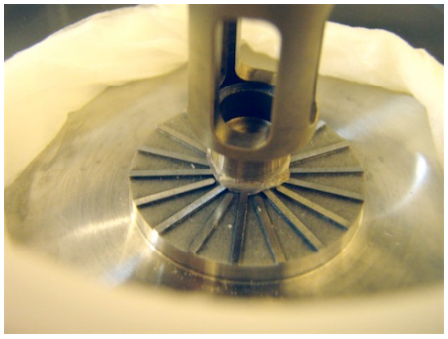

Figure 14: Hydrogel sample loaded on the rheometer. This image also shows the serrated surface of the bath chamber and a moistened tissue that was used to maintain humidity within the chamber.

Test methods employed included an oscillatory strain sweep and a dynamic frequency sweep. The strain sweep was run over the strain amplitude range from 0.005% to 10% at a frequency of 1 Hz. The strain sweep was conducted on at least one sample from each group in order to determine the linear viscoelastic region (LVR) for that material type. Within the linear viscoelastic region the moduli are independent of stress amplitude and are thus become a function of only oscillation frequency; this allows for selection of an appropriate strain amplitude for subsequent frequency sweeps. The chosen strain amplitude for the dynamic frequency sweep experiments was within the LVR for all testable sample groups, and frequency sweeps were run from 0.05 Hz to 20 Hz to cover a physiologically relevant range. Dynamic shear modulus parameters for the 620-R and 720-R gels (n=7 per group) were compared to NP (n=6) at 0.1, 1, and 10 Hz.

Statistical analysis made use of a one-way ANOVA with multiple comparisons adjustment by the Holm-Sidak method for multiple comparisons against a control group. The overall significance level was set to $\alpha=0.05$.

Results

Gel Casting

High-network density gel-cast (HD-GC) HA-*co*-PEMA hydrogels were successfully cast using the weight ratio and solution concentrations for the HD gel described in Specific Aim 1. Reinforcement with the two grades of hydrophobically-modified fumed silica also produced intact gels (620-R and 720-R), but the casting incorporating the un-treated hydrophilic fumed silica crumbled apart during the wash and hydrolysis procedure. Staining with Toluidine Blue-O verified that the 620-R and 720-R gels were held together by a hyaluronan-based matrix (Figure 15). The water content of the equilibrium-swollen reinforced gels was characterized by swell tests as described previously, using both deionized water and PBS as swelling media. No significant differences were detected for Q in either DI or PBS for the two reinforced gels ($p > 0.7$), but both reinforced gels had a significantly smaller Q than HD-GC ($p < 0.007$). Swell test results are summarized in Table 8.

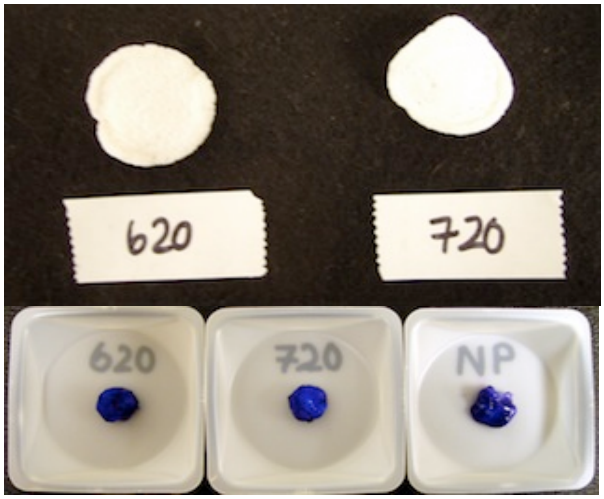

Figure 15: Reinforced gels produced through the gel casting method (top). Toluidine Blue-O staining of reinforced gel samples compared to a tissue sample from ovine nucleus pulposus (bottom).

Table 8: Swell ratio and hydration for reinforced gels

Media	Group	Q	H (%)
DI	HD-GC	175.25 ± 43	99.40 ± 0.15
	620-R	22.75 ± 1.54	95.78 ± 0.26
	720-R	25.59 ± 13.54	95.10 ± 3.94
PBS	HD-GC	46.77 ± 4.23	97.89 ± 0.19
	620-R	6.92 ± 0.72	87.31 ± 1.35
	720-R	4.44 ± 0.63	81.47± 2.55

Rheometry

During the strain sweep experiments it was found that the HD-GC gels were too compliant to be tested with the 8 mm parallel plate geometry; even at very large strains, torque measurements fell below the detection capability of the instrument. Based on the strain sweep data for the 620-R, 720-R, and NP groups a 2% strain amplitude was selected for the dynamic frequency sweep experiments. As with the HD-GC gels, shear measurements could not be reliably made at small strain amplitudes, but the measurement stabilized by roughly 0.3% strain. Torque measurements for all groups were within the specification of the load cell by 2% strain; 2% strain also appeared to be near the upper limit of the LVR for two of the three groups (Figure 16).

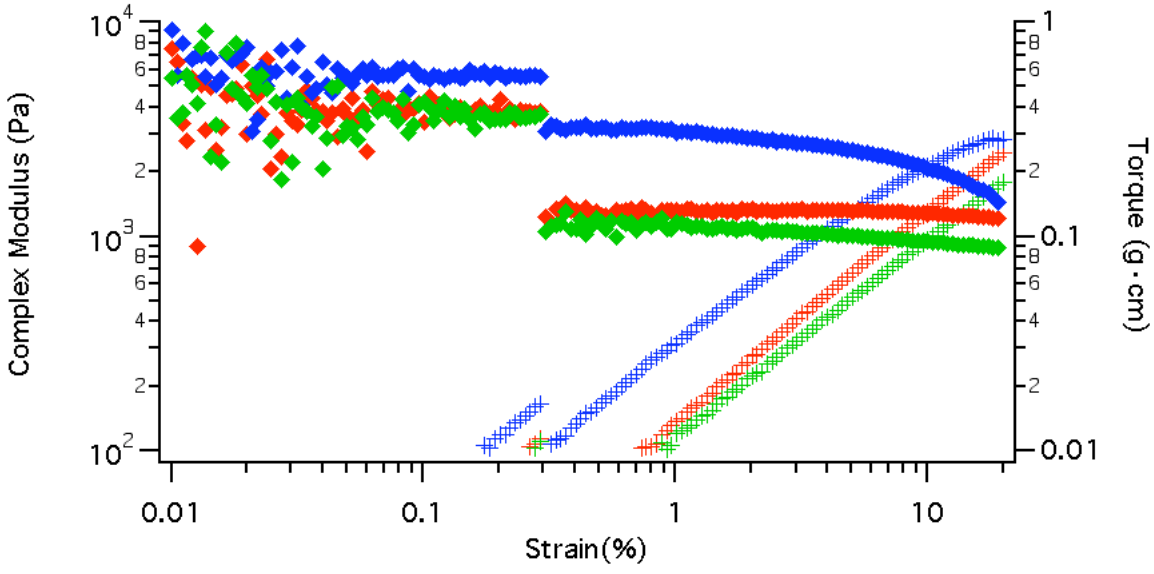

Figure 16: Strain sweep traces for reinforced gels and ovine nucleus pulposus. The strain sweep data was used to assess the linear viscoelastic region and to select a strain amplitude for subsequent frequency sweep esperiments.

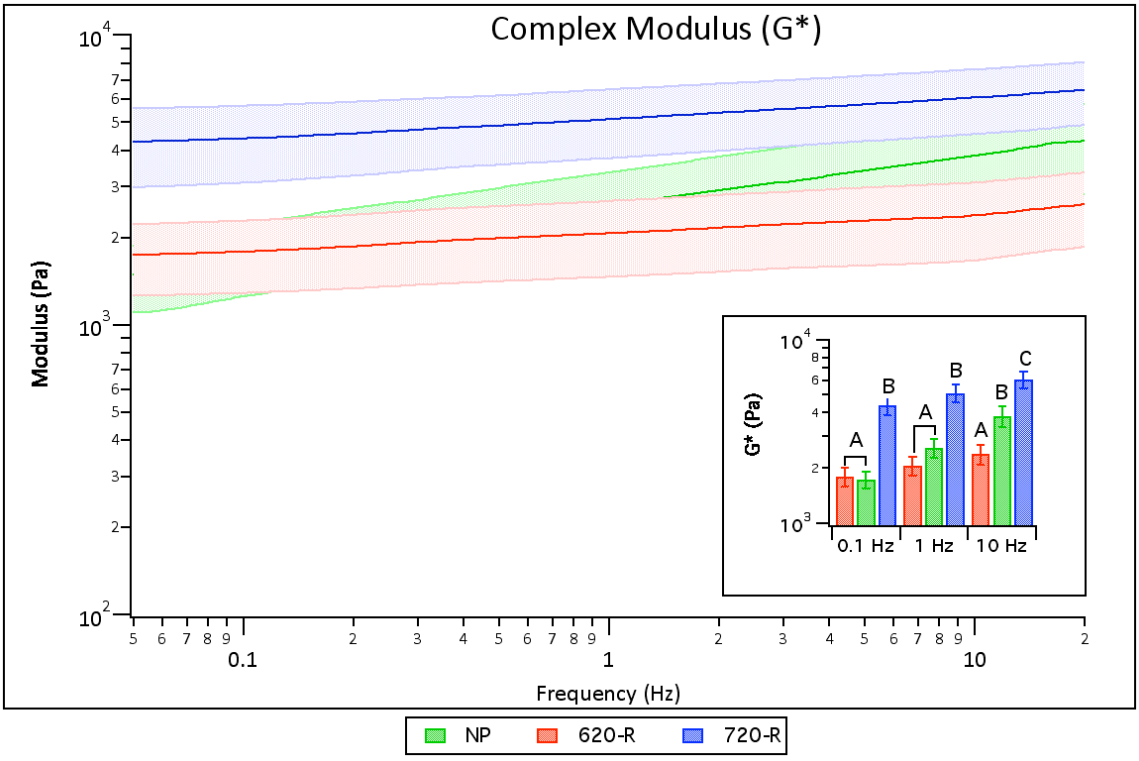

Figure 17: Frequency sweep results for complex modulus. Lines represent mean values, and shaded areas are ± 95% confidence intervals. Synthesized gels were statistically compared to NP at 0.1, 1, and 10 Hz (inset)

Figure 17 illustrates the complex modulus, G*, across the entire frequency spectrum studied. The complex modulus is a phasor describing the dynamic shear properties of a material, accounting for both elastic and dissipative effects. Data shown in the main figure represent mean values ± 95% confidence interval. Over the range studied, NP is effectively bound on the low end by 620-R and capped by 720-R. When statistically compared at discrete frequencies (Figure 17 inset), no significant difference is detected between 620-R and NP at 0.1 and 1 Hz ($p>0.147$). At 10 Hz, there is a statistically significant difference among all groups (620-R<NP, $p=0.005$; NP<720-R, $p<0.001$).

G* can be broken into storage (G') and loss (G") components where G' describes the in-phase elastic response and G" represents the 90° out-of-phase dissipative behavior. The loss factor, also known as tan(δ), is the ratio of G" to G'. A comparison of these dynamic shear parameters at 0.1, 1, and 10 Hz is shown in Figure 18. While G* for NP is effectively bound by 620-R and 720-R, the loss factor for NP is significantly higher than for the other two groups ($p<0.001$). G' tracks trends seen in G*, in that NP is bound by 620-R and 720-R with no significant differences between NP and 620-R at 0.1 and 1 Hz ($p>0.226$). A different trend is seen for G"; mean values for the synthetic gels trend

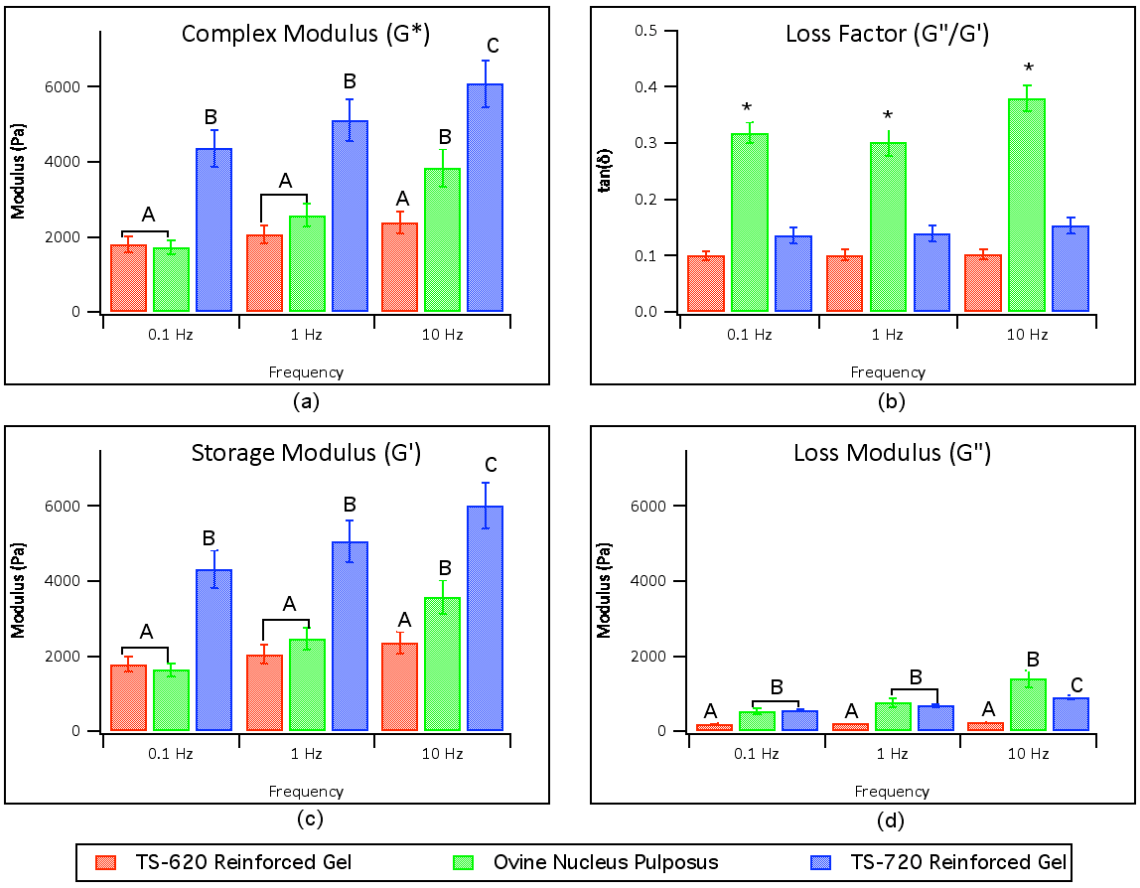

Figure 18: Statistical comparisons of all dynamic shear parameters at 0.1, 1, and 10 Hz: (a) complex modulus G*; (b) loss factor or tan(δ), where δ is the phase angle by which the material response lags the sinusoidal stimulus; (c) storage modulus G'; (d) loss modulus G".

lower than that for NP, with no significant differences detected between 720-R and NP at 0.1 Hz ($p=0.758$) and 1 Hz ($p=0.076$).

Discussion

In order to improve the mechanical properties of the hydrogel developed in this research, fumed silica was used as a particulate reinforcement. Fumed silica is a rheology modifier, so mixing it into the already-viscous concentrated HA-CTA solution was not possible with magnetic stirring. Furthermore, since these gels would be subject to mechanical testing, shape control was needed in order to enable the desired sample geometry. Both of these factors led to the decision to formulate the samples using a gel casting process.

Initially, the environment for gel casting was not controlled. Fumed silica was mixed with the gel reactants by hand while exposed to air. It was recognized that this air exposure could cause a reduction in the MA reactivity, particularly when the air is humid. However, since MA moieties were available in excess, it was expected that gels would form even with exposure to air. Indeed, HD-GC gels and gels reinforced with hydrophobically-modified fumed silica were successfully produced. M5-R gels reinforced with untreated silica disintegrated during the hydrolysis process. Two mechanisms can explain this failure. Firstly, the hydrophilic surface chemistry of the untreated silica likely introduced a greater amount of water into the reaction during the air-exposed mixing process, reducing the overall reactivity of the PEMA. Further, the silanol surface chemistry (Table 6, page 47 above) provides OH functional groups that can react with the PEMA in competition with the OH groups on the HA. Either factor can explain a reduction in the HA crosslinking density to below p_c.

Another consequence of the methods used to produce reinforced gels was the introduction of bubbles into the cast gels. Larger bubbles formed due to the vigorous mixing of the concentrated reactant solutions could be manually dissipated, but the smaller bubbles resulting from trapped gases introduced when the dry, low-density fumed silica was added were not addressed. For future processing refinements, a centrifugation step or degassing procedure prior to the overnight cure should be considered to eliminate this potential source of variability.

Swell test parameters measured for the HD-GC gel were higher than those for HD determined in Specific Aim 1, suggesting that a looser network formed. In order to investigate the effect of air exposure on the HD-GC and reinforced gel properties, a follow-up experiment was conducted in which HD-GC and 620-R gels were re-cast using a disposable glove bag to eliminate air exposure during casting. Swell test parameters for the HD gel produced in Specific Aim 1, the HD-GC, 620-R and 720-R gels synthesized for mechanical testing in Specific Aim 2, and the replicate HD-GC and 620-R gels cast in an air-free environment (AF-HD-GC and AF-620-R) are summarized in Table 9. Casting in an air-free environment reduced the swell ratio for both the HD-GC

Table 9: Summary of PBS swell test parameters determined for different gel synthesis methods

Formulation (experiment)	Synthesis Method	Q	H (%)
HD (Specific Aim 1)	Air-free glassware, 12h @ 90°C	21.67 ± 5.46	95.09 ± 1.05
HD-GC (current)	Air-exposed casting, 24h @ 75°C	46.77 ± 4.23	97.89 ± 0.19
620-R (current)	Air-exposed casting, 24h @ 75°C	6.92 ± 0.72	87.31 ± 1.35
720-R (current)	Air-exposed casting, 24h @ 75°C	4.44 ± 0.63	81.47± 2.55
AF-HD-GC (follow-up)	Air-free casting, 24h @ 75°C	22.55 ± 0.66	95.75 ± 0.11
AF-620-R (follow-up)	Air-free casting, 24h @ 75°C	3.57 ± 0.16	78.07 ± 0.79

(AF-HD-GC < HD-GC, $p < 0.001$) and 620-R formulation by a factor of 2. The AF-HD-GC gels cast using the air-free glove bag method had similar swell characteristics to the HD gels produced using air-free glassware as in Specific Aim 1 (AF-HD-GC = HD, $p=0.831$).

On the basis of G*, the measured value for NP is effectively bound by 620-R on the low end and 720-R on the high end across the frequency range of interest. However, when broken down into storage and loss components it is apparent that the bounding behavior is driven by G'. G" is for the most part lower for both 620-R and 720-R compared to NP across the frequency range studied. Physically, this suggests that the reinforced gels behave less dissipatively, suggesting less shock absorbing capability than the healthy natural tissue. The dynamic shear properties of the reinforced gels are less variable with frequency than the NP tissue, indicating less variation in viscoelastic behavior with loading rate. In particular, the natural tissue behaves most elastically at frequencies associated with locomotion, while at semi-static (standing) and high (vibration, e.g. riding in a car) frequencies more viscous behavior is seen [84].

While dynamic shear testing is a suitable methodology for probing the viscoelastic characteristics of materials, compression testing is more reflective of the primary physiologic loading state of NP tissue. Further, the properties of biphasic materials are better probed using a confined compression apparatus equipped with a porous platen to allow for exudation of the liquid phase. Confined compression tests were not performed in these experiments due to a scarcity of materials in that larger, thicker sample geometries were required to achieve loads within the detection limits of the test systems that were available for use.

As previously discussed, the reinforced gels evaluated by shear rheometry were synthesized under non-ideal conditions. The practicalities of mixing the fumed silica reinforcement into viscous solutions and the need for shape control drove the development of a gel casting methodology. Initial trials of the gel casting process included a step where the reactants were briefly exposed to air, potentially altering the reactivity of MA functional groups. The resulting lower crosslink density in turn can affect the physical properties of the gels.

To determine the effect of air-exposure during casting on mechanical properties of the gel, rheometry was repeated on gels synthesized using the air-free glove box method in the follow-up experiment described previously. As with the gels tested in Specific Aim 2, gels cast in an air-free environment (AF-620-R) were swollen in PBS and samples (n=3) were punched for evaluation by rheometry. The G* results for the AF-HD-GC gel are compared to the HD-GC gel in Figure 19.

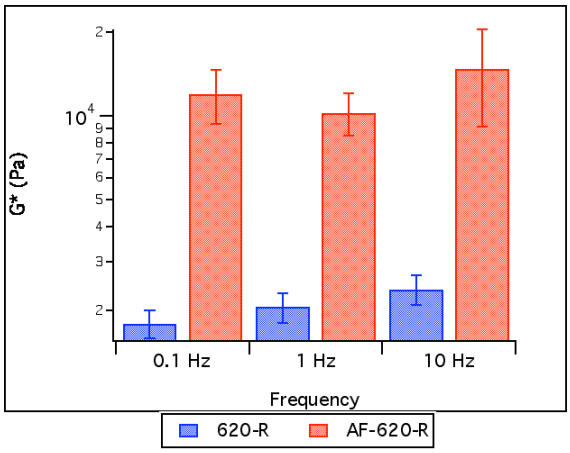

Figure 19: Effect of synthesis conditions (air vs. air-free) on the mechanical properties of 620-R gels. 620-R < AF-620-R ($p < 0.007$).

The AF-620-R gel exhibited nearly an order of magnitude increase in G* compared to the gel cast in air. These results suggest the possibility of achieving mechanical properties appropriate to the intervertebral disc application with a reduced fraction of silica reinforcement when the synthesis environment is well-controlled. Reducing the volume fraction of silica reinforcement may also increase the dissipative

behavior of the gel, in that the viscoelastic behavior of the crosslinked hyaluronan matrix may play a more prominent role in the overall mechanical behavior of the composite. Preliminary results from a follow-on experiment exploring the effect of reinforcement level on air-free cast gels is detailed in Appendix G.

In this specific aim two particulate-reinforced hydrogels were produced and mechanically evaluated against ovine NP tissue. Despite non-ideal synthesis conditions, the 620-R and 720-R hydrogels bracketed G* and G' of the NP over the frequency range of interest. This is a significant result, in that other hyaluronan-based hydrogels described in the literature [85, 86] have lacked the mechanical strength required for load-bearing tissues. While these reinforced gels were found to be a good match for the elastic aspects of NP mechanical behavior, they are not as well matched for the shock-absorbing, dissipative properties described by G". However, the results of the follow-up experiments in which reinforced gels were cast under better controlled synthesis conditions demonstrate that a wide range for tuning of mechanical properties exists.

Specific Aim 3: *In vitro* Biocompatibility

The final aim was to assess the biocompatibility of the materials developed and characterized in the previous two aims. Two *in vitro* experiments were conducted to probe their interaction with biological systems. The first was a cytotoxicity elution assay modeled after ISO standard 10933; this assay evaluates the cytotoxic effects of leachable substances from implanted or otherwise tissue-contacting materials and has found utility in the testing of other hydrogel-based medical devices such as contact lenses [76, 87]. Following the cytotoxicity experiment, a tissue culture pilot experiment was conducted. This experiment aimed to assess the integration between ovine nucleus pulposus tissue

and the materials developed in this research when cultured in direct contact with each other.

Materials and Methods

Media Conditioning

HD-GC, 620-R, and 720-R hydrogels synthesized as described in Specific Aim 2 were used to condition a 10:1 volume of Dulbecco's Modified Eagle Medium (DMEM) buffered with 1% HEPES and were allowed to elute for 72 hours at 37°C. Two reference materials were similarly eluted: biologically inert high-density polyethylene (HDPE) and biologically active latex rubber. A solution control, medium absent test or reference materials, was incubated in the same manner. Conditioned solutions were sterile filtered and stored at 4°C until use.

Cell Lines and Culture

HEK-293 human embryonic kidney cells, a common cell line known for ease of culture, were used for the cytotoxicity assay. Cells were taken from liquid nitrogen storage and expanded in monolayer culture under standard conditions (5% CO_2, 37°C) using a propagation medium of DMEM supplemented with 10% fetal bovine serum and 1% penicillin-streptomycin. At approximately 90% confluence adherent cells were detached from the cell culture flask using Trypsin-EDTA, resuspended in a minimal medium of DMEM with 1% FBS, and seeded into 48-well plates. 36 test wells were seeded at a density of $6x10^4$ cells/well, and the remaining 12 wells were used as a concentration ladder, with cell densities ranging from $1x10^4$ to $10x10^4$ cells/well. Seeded plates were maintained in culture for 24 hours to allow the cells to attach into a sub-confluent monolayer.

Cytotoxicity Assay

Seeding medium was aspirated from the prepared well plates prior to application of the test solutions. 400 µl of conditioned DMEM was aliquoted in six replicates for each test article, reference material, and the solution control. DMEM supplemented with 1% HEPES was used for the concentration ladder wells. Plates were incubated for 24 hours, then cell viability was assessed using the alamarBlue® (Invitrogen, Carlsbad CA) assay.

AlamarBlue® is based upon resazurin, a non-toxic cell-permeable compound that, upon reduction due to cellular metabolism, is converted to the highly fluorescent red compound resorufin. Viable cells continuously perform this reduction, resulting in increased fluorescence with viable cell count and incubation time. Test solutions were aspirated from all wells and replaced with 500µl of a 10% solution of alamarBlue in DMEM. Plates were incubated for 3 hours, then fluorescence was read using a SpectraMax Gemini XS (Molecular Devices, Sunnyvale CA) microplate reader with fluorescence and emission wavelengths of 344 nm and 390 nm, respectively.

A test plate was prepared as previously described for the test article found to be cytotoxic (620-R) in order to conduct a titration study. Dilutions to 75%, 50%, and 25% (v/v) concentrations of the conditioned medium in DMEM were prepared. The dilutions, HDPE and Latex reference solutions, and a solution control were applied to seeded well plates and assessed in the same manner as that just described for the 100% neat solutions.

Fluorescence intensity data for both of the alamarBlue® assays was statisitcally analyzed using ANOVA methods with multiple-comparisons adjustments appropriate for comparisons made against a control.

Ovine Nucleus Pulposus Tissue Harvest

Ovine spinal tissue was obtained from an Animal Care and Use Committee (ACUC)-approved study unrelated to the spine. The lumbar spine was harvested *en bloc* at necropsy within four hours of euthanasia. Musculature and connective tissue was stripped, then the skeletonized lumbar spine was sprayed with 70% ethanol. Intervertebral discs were dissected from the vertebrae as aseptically as possible, using a new scalpel blade for each slice into the tissue. Outer annulus tissue was dissected from each disc, and the remaining tissue was placed into a sterile tissue-culture polystyrene (TCPS) Petri dish and incubated in a 1:1 mixture of Dulbecco's Modified Eagle Medium and Ham's F-12 Nutrient Mixture (DMEM/F-12) supplemented with 1% penicillin-streptomycin under standard culture conditions. After 24 hours the tissue explants were examined to ensure that no contamination occurred during harvest.

Tissue Culture

Hydrogel formulations HD-GC and 720-R were carried forward into the tissue culture experiment based upon indications of biocompatibility from preliminary cytotoxicity testing. Following quarantine, NP samples were cut from explanted tissue using a sterile 8 mm biopsy punch and placed into individual wells of a 24-well plate. NP samples were overlaid with an 8 mm hydrogel discs that had previously been swollen in sterile Dulbecco's Phosphate Buffered Saline (DPBS). The NP-hydrogel samples were then sealed in apposition to each other with 2% (w/v) agarose. Samples were maintained in culture a total of 3 weeks in DMEM/F-12 supplemented with 10% FBS, 1% HEPES, 1% non-essential amino acids, and 1% pen/strep under standard culture conditions with media changes every three days.

Histology

After three weeks in culture, samples were fixed in 10% neutral buffered formalin for 2 days and processed for histology using standard techniques. Samples were sliced axially to allow sections to be taken across the NP-gel interface, then were embedded in paraffin using standard procedures. Sections were stained with Toludine Blue, a cationic blue dye commonly used to stain cartilaginous tissues for anionic proteoglycans [88]. Slides were imaged on an Olympus IX70 inverted system microscope (Olympus Americas, Center Valley PA).

Results

Media Conditioning

Following 72 hours of incubation several of the conditioned media were observed to have changed color. Standard DMEM contains phenol red, a pH indicator that shifts from yellow at or below pH 6.8 to fuchsia above pH 8.2. Between pH 6.8 and 8.2 it exhibits a gradual transition through shades of orange to red. The medium conditioned with 620-R gels turned yellow, while the solution control and HDPE-conditioned reference media turned pink. The 720-R conditioned medium, HD-GC conditioned medium, and latex reference medium all exhibited varying degrees of an orange-red color.

Cytotoxicity Assay

Upon measuring the alamarBlue® fluorescence by plate reader for the cytotoxicity assay, an anomalous pattern of attenuated signals in the wells around the periphery of the plate was noted. Studentized residuals were calculated for a statistical outlier analysis; data points having a studentized residual with absolute value greater than

3.5 were considered outliers and eliminated from the statistical analysis. The remaining data set did not meet the normality assumption for a parametric ANOVA, so a Kruskal-Wallis one-way ANOVA on ranks was performed while using Dunn's method to adjust for multiple comparisons against a control group. In this analysis, the median value for 620-R was found to be significantly lower than the solution control ($p < 0.05$), but otherwise no significant differences were detected.

Figure 20(a) illustrates the data with all of the observed anomalous data points removed. This data set passed the normality test, allowing a parametric one-way ANOVA to be computed. The Holm-Sidak method was used for multiple comparisons adjustments. In this analysis, 620-R was found to be significantly lower ($p < 0.001$) than all other groups, indicating a profound cytotoxic effect. A trend was observed comparing latex < solution control, but with multiple comparisons adjustments the computed p=0.04 did not meet the critical level for statistical significance. HD-GC and 720-R were found to be significantly greater than the latex reference ($p < 0.005$) and trended for better

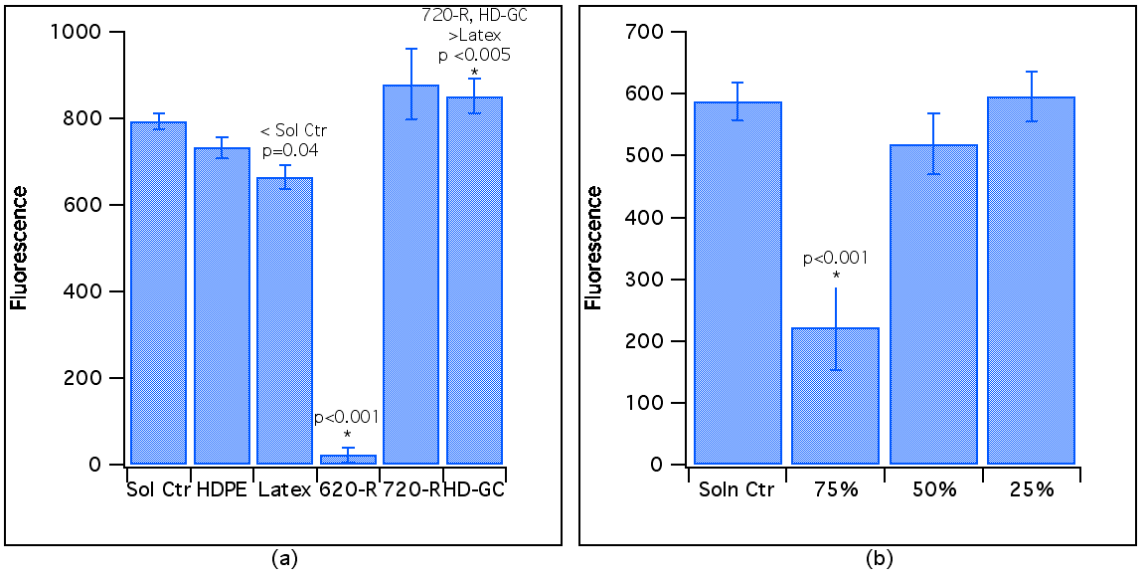

Figure 20: alamarBlue® readings for (a) overall cytotoxicity test and (b) eluant titration for 620-R conditioned medium.

biocompatibility than HDPE ($p < 0.057$), but were not significantly different from the solution control ($p > 0.159$).

The same anomaly of peripheral attenuated signals was observed for the 620-R titration, so the statistical analysis was treated identically. When median values were compared using the Kruskal-Wallis ANOVA on ranks, no statistically significant differences were detected ($p=0.166$). The data again fit a normal distribution when the anomalous data points from the peripheral wells was removed, so that filtered data set was used to compute a parametric one-way ANOVA. In this case the mean value for the 75% concentration of 620-R conditioned medium was found to be significantly lower than all other groups ($p < 0.001$) but otherwise no significant differences were detected.

Tissue Culture Pilot

Toluidine Blue-stained sections from the tissue integration pilot study are shown in Figure 21. The bulk of the HD-GC and 720-R gels were inadvertently separated from the NP tissue during processing for histology, but areas where the gel remained in the vicinity of the tissue were located and imaged. HD-GC exhibits little evidence of integration with NP tissue in that large gaps are visible between the gel and the tissue. Pieces of the 720-R gel remain in apposition to the NP tissue despite the difficulties encountered in handling the specimen for histological processing. This suggests that the gel tore some distance away from the interface from the tissue, implying adhesion between the gel and the tissue.

A higher magnification image of the interface is shown Figure 22. Although cell nuclei are not visible with the Toludine Blue staining, cells in the NP tissue can be identified by staining of the pericellular matrix. Based upon size homology, it appears

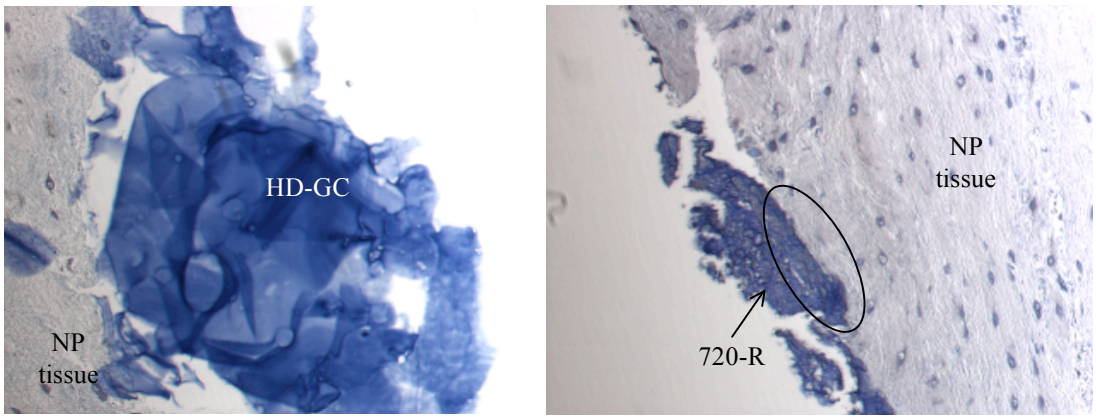

Figure 21: Histological sections for tissue integration study, 200x magnification. Interface of HD-GC (left) and 720-R (right) materials with NP tissue. Toluidine Blue-O staining.

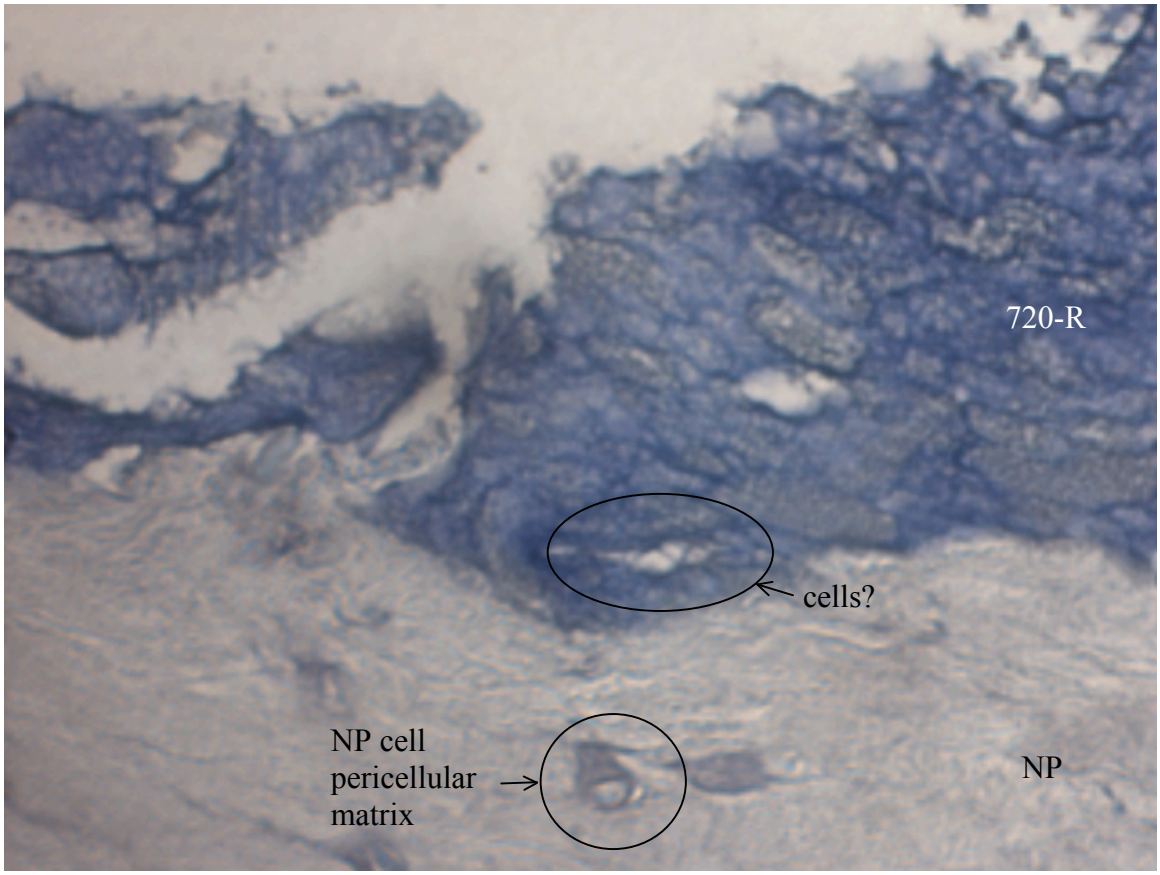

Figure 22: 600x image of the interface between NP and 720-R. The presence of cells can be inferred from the Toludine Blue staining of GAGs in the pericellular matrix; one such cell is highlighted in the NP tissue. Based upon size and similarity of appearance to the cell identified in NP tissue, an area of possible infiltration of 3 cells into the 720-R gel is indicated by the oval.

that there is a cluster of three cells that have infiltrated the 720-R gel a short distance from the NP tissue interface.

Discussion

A number of technical difficulties were encountered in the implementation of the cytotoxicity assay. Most noticeable was the anomaly involving attenuated signals, and thus dead cells, in the peripheral cells around the well plates. A plausible explanation for this is a perturbation in the culture environment, e.g. a drop in incubator humidity levels leading to dehydration of the wells on the edge of the well plate, or perhaps toxic effects of chemical disinfectants or other contaminants in the incubator. Cell seeding technique or pipetting errors could also explain some variability in results, but do not account for the distinct pattern seen since these sorts of errors would be random. Repeating the cytotoxicity assay for the 720-R and HD-GC gels in a different incubator would give stronger support to the conclusion that these materials are not cytotoxic.

The other main issue encountered in the cytotoxicity assay was that the cytotoxic reference material did not behave as a true positive control. The use of latex as a positive control has been described for a contact lens cytotoxicity elution assay [87], but the specific standard latex reference material cited was not purchased for this work. In a study looking specifically at the cytotoxicity of latex rubber gloves, Baek et. al. [89] evaluated different elution solutions (DI, saline, DMEM, DMEM supplemented with FBS) and different incubation protocols varying in time (24 hours or 72 hours) and temperature (37°C or 50°). They found that the most cytotoxic results were obtained when MEM with or without 10% FBS was incubated at 37°C for 72 hours. The notable

difference between the optimal media conditioning protocol described by Baek and collaborators and the one used here was the additon of 1% HEPES to the DMEM.

The decision to add HEPES to the conditioning medium was made after a pilot experiment in which slight changes in pH and correspondingly slight cytotoxic effects were noted for all materials at shorter incubation times. To better understand the cytotoxic effect, an HD-GC gel was conditioned in deuterium oxide for 72 hours and the eluant was examined by ^{1}H nuclear magnetic resonance (NMR). The collected NMR spectrum was compared to spectra for possible excess reactants and was found to match the PEMA spectrum (Figure 23). When PEMA is exposed to water, the maleic anhydride rings open to become carboxylic acids. Carboxylic acids exist in a number of biomacromolecules including hyaluronan and other GAGs, and physiologically the body has some capacity to buffer these acids. Thus, HEPES was added to the conditioning

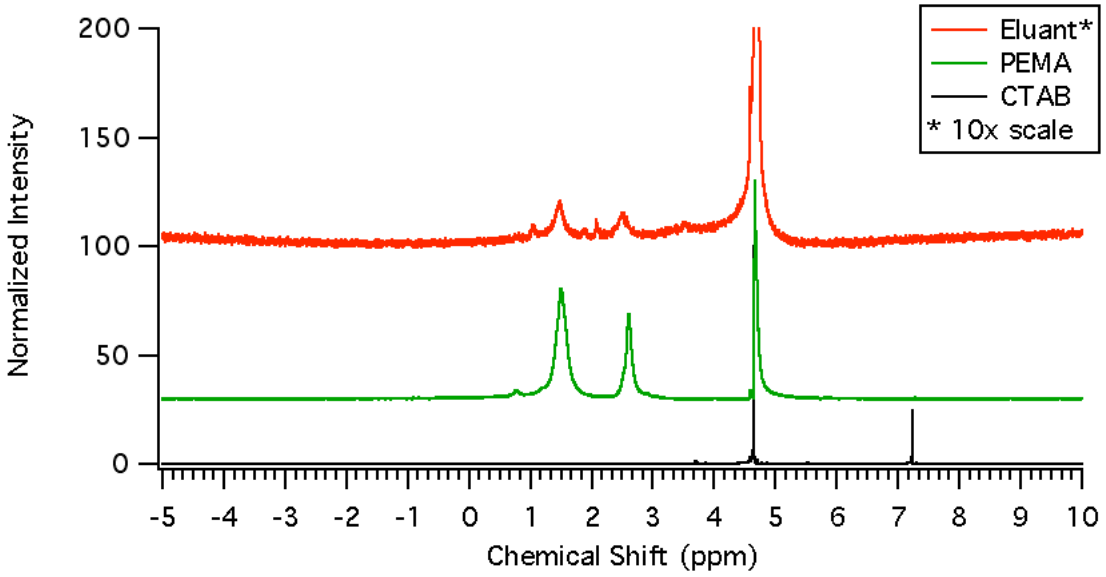

Figure 23: ^{1}H NMR spectra for HD gel eluant compared to PEMA and CTAB. Eluant sample taken after 72 hours of swelling in deuterium oxide (D_2O). Note that all spectra were normalized to the D_2O peak, then the scale for the eluant spectra was expanded by 10x.

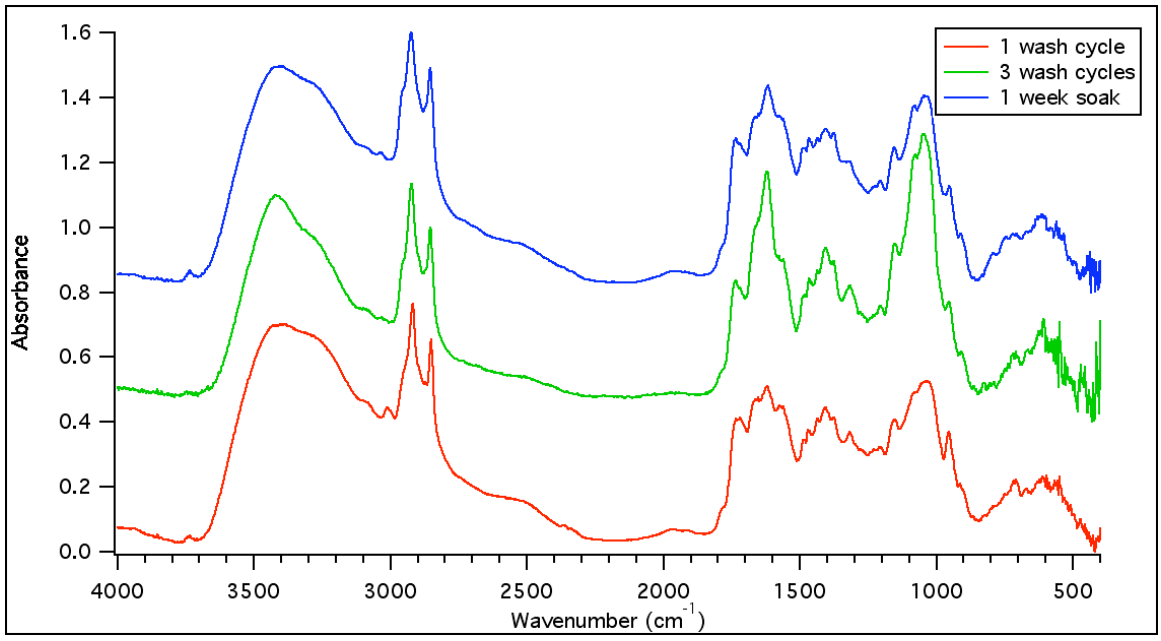

Figure 24: FTIR spectra for AF-620-R gel after wash cycles. The aliphatic carbon peaks at approximately 2900 and 2800 cm^{-1} suggest –CTA entrapped in the hydrogel.

solution to account for this buffering ability, but it may have had the unintended effect of masking the cytotoxicity of the latex positive reference material as well.

During the course of this initial cytotoxicity investigation, FTIR spectra of the reinforced gels were also collected. It became apparent that residual -CTA is present in the 620-R gel, as evidenced by the strong aliphatic hydrocarbon peaks at approximately 2900 and 2800 cm^{-1}. The intensity of the hydrocarbon peaks was even stronger in the air-free casting of the 620-R gel. Attempts to remove the -CTA with further wash and hydrolysis cycles consisting of an hour of sonication in DI water followed by a further hour of sonication in dilute saline solution were not successful (Figure 24). Given that the -CTA groups are thoroughly entrapped in the gel they are unlikely to be responsible for any observed cytotoxic effects.

The presence of excess reactants and reaction intermediates in the hydrogels is an issue that bears further investigation, but thus far cannot explain the vast difference in

cytotoxicity due to the 620-R gel. While changes in the pH indicator color were noted during media conditioning, pH measurements were not taken until the conclusion of the cytotoxicity assay. The pH measurements for conditioned media ranged from 5.3 for the 620-R media to 8.6 for the HD-GC media and solution control (Figure 25). Note that these pH measurements are slightly higher than they would be under normal culture conditions since they were taken on chilled media samples, and the pK_a for HEPES is temperature sensitive. The measured pH for the dilutions of 620-R media used in the titration assay and for AF-620-R media conditioned by the same process are also included in Figure 25 for comparison. Given the extreme acidity of the 620-R conditioned media, the cytotoxicity result is not surprising; extremes of pH are known to kill cells.

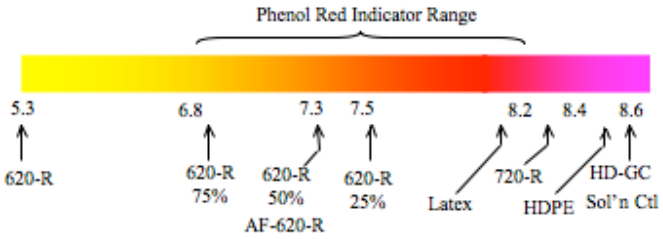

Figure 25: Measured pH values for conditioned media used in the cytotoxicity study. Values for diluted 620-R and AF-620-R media conditioned by the same process included for comparison.

1% (v/v) HEPES added to the conditioning medium was able to buffer the mild acidity of the 720-R and HD-GC gels, but was overwhelmed by the 620-R acidity. This points to the reinforcing agent rather than the gel as the main contributor to the cytotoxic effects seen in 620-R. The two grades of hydrophobically-modified silica are identical save for the specific hydrophobic surface treatment. The non-toxic TS-720 grade silica is treated with polydimethylsiloxane (PDMS), while the toxic TS-620 grade silica has

dimethyldichlorosilane bound to its surface. Dimethyldichlorosilane is a precursor to PDMS; it polymerizes by hydrolytic polycondensation [90]:

$$n\ (CH_3)_2SiCl_2 + n\ H_2O \rightarrow [(CH_3)_2SiO]_n + 2n\ HCl$$

HEPES is a relatively weak buffer, so the production of HCl in this hydrolysis process can certainly explain the drastic drop in pH and the associated cytotoxicity seen in the 620-R conditioned media.

Despite technical difficulties encountered with the cytotoxicity assay, it did provide reasonable indications for the biocompatibility of the HD-GC and 720-R gel formulations while the 620-R hydrogel formulation was found to be clearly cytotoxic. The results of the tissue culture pilot are even more encouraging. The 720-R gel appears to have started to integrate with the NP tissue after 3 weeks in culture, with possible infiltration of nucleus pulposus cells.

This level of integration was not seen with the HD-GC gel. This follows from a mechanical sense, in that the modulus mismatch between the two materials would make for a poor physical interface. It is also possible that evidence of interaction (e.g. cells in the HD-GC gel) was lost during handling for histological processing.

Conclusions

In this work, we set out to accomplish three specific aims: (1) to synthesize and characterize a hyaluronan-based hydrogel leveraging chemistry previously explored in our lab, (2) to reinforce the hydrogel for mechanical properties suitable for an intervertebral disc repair application, and (3) to assess the biocompatibility of the reinforced gel system. Each of these specific aims was achieved.

A hydrogel was created through the reaction of hyaluronan with poly(ethylene-*alt*-maleic anhydride). Two variations of this HA-*co*-PEMA were characterized by chemical, thermal, and physical means. These characterization methods demonstrated that the reaction scheme did indeed produce covalently-bound copolymers. One of the formulations, HD, was seen to behave as a homogenous material, displaying a single TGA decomposition step and maintaining its shape when swollen in good solvents. It was capable of swelling to a 95% hydration level in PBS, leaving it some headroom compared to the hydration level for natural NP tissue for losing swelling ability while gaining strength from particulate reinforcement.

Fumed silica was used as a model system to investigate the effect of nanoparticulate reinforcement on the mechanical properties of the gel. Fumed silica was chosen since it is considered bio-inert and is available widely with different surface treatments on silica with otherwise identical size and morphology. Reinforced gels were successfully synthesized with two grades of hydrophobically-modified silica, even under non-ideal reaction conditions. The resulting 620-R and 720-R gels were found to bracket the complex shear modulus and shear storage modulus of ovine nucleus pulposus. Maintaining an air-free synthesis environment will allow for further tuning of the mechanical properties. Utilizing a lower volume fraction of reinforcement should allow the viscoelastic properties of the hyaluronan matrix to play a greater role in the bulk material, perhaps even allowing for better alignment to the shear loss modulus and tanδ of NP tissue.

While mechanical results for the two reinforced gels were extremely promising, the *in vitro* cytotoxicity assay highlighted a severe biocompatibility issue for the 620-R

gel – acidity resulting from the hydrolysis of the silica surface treatment. This result highlights the need for understanding the properties of the reinforcing agent, particularly its behavior in water. In contrast, the *in vitro* work with the 720-R gel provides some exciting glimpses of its utility for intervertebral disc applications. The cytotoxicity assay, flawed as it was, showed no cytotoxic effects attributable to 720-R. Even more tantalizing, the tissue integration pilot experiment suggests that 720-R can integrate with native nucleus pulposus tissue. Follow-up experiments to verify these results are needed.

INTELLECTUAL MERIT AND FUTURE WORK

This dissertation describes the significant progress made in transforming the "copoly" technology previously developed in the James Laboratory into a material suitable for intervertebral disc applications. Conceptually the same reaction scheme was leveraged – i.e. the hydrogel is made via ester bond formation between a maleic anhydride and a hydroxyl, yet a more efficient reaction at gentler temperatures was enabled by identifying a different, more reactive maleic anhydride copolymer, poly(ethylene-*alt*-maleic anhydride) (PEMA). The synthesis method and properties of this newly-developed polymer differed from copoly enough to merit filing a new patent (Appendix I).

While the progress made thus far in developing this material is exciting, one's work can always use refinement. Short-term priorities should focus upon purification methods to ensure that excess reactants are removed to the extent possible. The existing hydrolysis and washing protocols may be sufficient, but need monitoring steps (e.g. using pH measurements and FTIR spectra to track the elimination of excess reactants and reaction intermediaries). Other approaches such as Soxhlet extraction should also be considered.

Further tuning the mechanical properties of the reinforced gel system to better match those of native nucleus pulposus tissue may also be worthwhile. Upon observing an order of magnitude increase in G* for a heavily-reinforced gel synthesized under an

inert atmosphere compared to one synthesized in air, we speculated that the desired elastic properties could be maintained while the dissipative properties could be enhanced to better match the G' and tanδ for NP tissue by stepping-down the amount of PDMS-treated silica and maintaining an air-free synthesis environment. Preliminary experiments (Appendix G) demonstrate that the dynamic shear properties are indeed altered with differing reinforcement levels, but the dissipative properties do not scale in as straightforward a manner as originally hypothesized.

The reinforced gel is a complex system consisting of the covalently-crosslinked hydrogel, hydrophobically-treated silica nanoparticles that can form mechanically-strong aggregates based upon their concentration within the gel, and water interacting with both the hydrophilic and hydrophobic phases of the composite. The dynamic shear analysis performed over a physiologically-relevant range of frequencies is but a small slice of the data needed to fully characterize the system. Tests for transient viscoelastic parameters, i.e. creep or stress relaxation, would still be physiologically-relevant while providing insight into the competing effects of water attraction and repulsion due to the hydrophilic and hydrophobic fractions of the material. Understanding the phase transition behavior of the composite from a more fundamental polymer characterization perspective will require further testing over much wider ranging frequencies and temperatures.

Hydrophobically-modified silica was used as a model system for particulate reinforcement, but other strengthening mechanisms such as ionic bonding could also be explored. Further, using biologically-active reinforcement such as demineralized bone matrix (DBM) or chitosan may be worth considering, especially as interest in the regenerative potential of materials grows. Some early work with DBM reinforcement

yielded a remarkable improvement in mechanical properties with a very low level of reinforcement with denatured DBM (Appendix E). We suspect that the denaturing DBM either adsorbed to the hydrogel or formed quinone-based crosslinks with the PEMA phase of the gel. Unfortunately, the effect was not repeatable and the relevance of denatured DBM to the desired biologic function was in question, so this avenue of reinforcement was not pursued further.

While the fumed silica was intended to be a model for particulate reinforcement, the biocompatibility results do suggest that it may be a feasible implant material in itself. Fumed silica does have a history of use in biomaterials for pharmaceuticals and cosmetics; furthermore, in an intervertebral disc application it would be used in a relatively isolated immunologic site, owing to the avascular nature of the disc. To confirm the suitability of the silica-reinforced gel as a biomaterial, repeating the tissue integration experiment should be a priority. To be meaningful, this study should include more samples, tissue from multiple animals, and longer time-points than the pilot experiment. A change in how the samples are prepared should be considered. The tissue-disc "stack" approach required the sample to be cut axially in order to take sections that would expose the tissue-gel interface. Adopting a "jelly donut" approach in which a disc of tissue is punched from the whole disc and the resulting hole filled with gel would allow histological sections to be taken through the tissue-disc interface without requiring manipulation of the processed tissue. Histology could also be improved with the use of differential staining. Further out, *in vivo* modeling will be an important step to demonstrate biocompatibility.

REFERENCES

1. Long, D.M., et al., *Persistent Back Pain and Sciatica in the United States: Patient Characteristics.* Journal Of Spinal Disorders, 1996. **9**(1): p. 40-58.

2. Kelsey, J.L. and White, A.A., *Epidemiology and Impact of Low-Back-Pain.* Spine, 1980. **5**(2): p. 133-142.

3. Ashton-Miller, J.A. and Schultz, A.B., *Biomechanics of the Human Spine*, in *Basic Orthopaedic Biomechanics*, Mow, V.C. and Hayes, W.C., Editors. 1997, Lippincott-Raven: Philadelphia.

4. Panjabi, M.M., *Clinical spinal instability and low back pain.* J Electromyogr Kinesiol, 2003. **13**(4): p. 371-9.

5. Dahl, M.C., et al., *The Restoration of Lumbar Intervertebral Disc Load Distribution A Comparison of Three Nucleus Replacement Technologies.* Spine. **35**(15): p. 1445-1453.

6. Gruber, H.E. and Hanley, E.N., *Biologic strategies for the therapy of intervertebral disc degeneration.* Expert Opinion On Biological Therapy, 2003. **3**(8): p. 1209-1214.

7. Roughley, P.J., *Biology of intervertebral disc aging and degeneration - Involvement of the extracellular matrix.* Spine, 2004. **29**(23): p. 2691-2699.

8. Oegema, T.R., *The role of disc cell heterogeneity in determining disc biochemistry: a speculation.* Biochemical Society Transactions, 2002. **30**: p. 839-844.

9. Urban, J.P.G., *The role of the physicochemical environment in determining disc cell behaviour.* Biochemical Society Transactions, 2002. **30**: p. 858-864.

10. Mwale, F., et al., *Distinction between the extracellular matrix of the nucleus pulposus and hyaline cartilage: A requisite for tissue engineering of intervertebral disc.* European Cells & Materials, 2004. **8**: p. 58.

11. Grunhagen, T., et al., *Nutrient supply and intervertebral disc metabolism.* Journal Of Bone And Joint Surgery-American Volume, 2006. **88A**: p. 30-35.

12. Kauppila, L.I., et al., *Disc degeneration/back pain and calcification of the abdominal aorta. A 25-year follow-up study in Framingham.* Spine, 1997. **22**: p. 1642 - 1647.

13. Eyre, D.R.;Matsui, Y. and Wu, J.J., *Collagen polymorphisms of the intervertebral*

disc. Biochemical Society Transactions, 2002. **30**: p. 844-848.

14. Roughley, P.J.;Alini, M. and Antoniou, J., *The role of proteoglycans in aging, degeneration and repair of the intervertebral disc.* Biochemical Society Transactions, 2002. **30**: p. 869-874.

15. Johnstone, B. and Bayliss, M.T., *The Large Proteoglycans Of The Human Intervertebral Disc - Changes In Their Biosynthesis And Structure With Age, Topography, And Pathology.* Spine, 1995. **20**(6): p. 674-684.

16. Shchuenke, M.;Schulte, E. and Schumacher, U., *General Anatomy and Muskuloskeletal System*. Atlas of Anatomy. 2006, Stuttgart: Thieme.

17. Osti, O.L.;Vernonroberts, B. and Fraser, R.D., *Anulus Tears and Intervertebral-Disk Degeneration - an Experimental-Study Using an Animal-Model.* Spine, 1990. **15**(8): p. 762-767.

18. Gruber, H.E. and Hanley, E.N., *Recent advances in disc cell biology.* Spine, 2003. **28**(2): p. 186-193.

19. Truumees, E., *The Role of Fusion in Degenerative Lumbar Disease.* Seminars in Spine Surgery, 2003. **15**(4): p. 430-459.

20. Melrose, J., et al., *Topographical variation in the catabolism of aggrecan in an ovine annular lesion model of experimental disc degeneration.* Journal Of Spinal Disorders, 1997. **10**(1): p. 55-67.

21. Katz, J.N., *Lumbar spinal fusion: Surgical rates, costs, and complications.* Spine, 1995. **20**(24 SUPPL.).

22. Deyo, R.A.;Nachemson, A. and Mirza, S.K., *Spinal-Fusion Surgery -- The Case for Restraint.* N Engl J Med, 2004. **350**(7): p. 722-726.

23. Kruyt, M.C., et al., *Bone tissue engineering and spinal fusion: the potential of hybrid constructs by combining osteoprogenitor cells and scaffolds.* Biomaterials, 2004. **25**(9): p. 1463.

24. Etminan, M., et al., *Revision strategies for lumbar pseudarthrosis.* Orthopedic Clinics Of North America, 2002. **33**(2): p. 381-+.

25. Di Martino, A., et al., *Nucleus pulposus replacement - Basic science and indications for clinical use.* Spine, 2005. **30**(16): p. S16-S22.

26. Evans, C., *Potential biologic therapies for the intervertebral disc.* Journal Of Bone And Joint Surgery-American Volume, 2006. **88A**: p. 95-98.

27. O'Halloran, D.M. and Pandit, A.S., *Tissue-engineering approach to regenerating the intervertebral disc.* Tissue Engineering, 2007. **13**(8): p. 1927-1954.

28. Revell, P.A., et al., *Tissue engineered intervertebral disc repair in the pig using injectable polymers.* Journal Of Materials Science-Materials In Medicine, 2007. **18**(2): p. 303-308.

29. Moss, I.L., et al. *Nucleus pulposus tissue repair in intervertebral disc degeneration: biochemical and mechanical evaluation of a novel human disc cell-hyaluronan/elastin polypeptide scaffold composite.* in *54th Annual Meeting of the Orthopaedic Research Society*. 2008. San Francisco, CA.

30. Cloyd, J.M., et al., *Material properties in unconfined compression of human nucleus pulposus, injectable hyaluronic acid-based hydrogels and tissue engineering scaffolds.* European Spine Journal, 2007. **16**(11): p. 1892-1898.

31. O'Halloran, D., et al. *Injectable atelocollagen type II scaffold for intervertebral disc regeneration*. in *Tissue Engineering and Regenerative Medicine International Society-Europe*. 2007. London UK.

32. Nagae, M., et al., *Intervertebral disc regeneration using platelet-rich plasma and biodegradable gelatin hydrogel microspheres.* Tissue Engineering, 2007. **13**(1): p. 147-158.

33. Giordano, C., et al., *Chemical-physical characterization and in vitro preliminary biological assessment of hyaluronic acid benzyl ester-hydroxyapatite composite.* Journal Of Biomaterials Applications, 2006. **20**(3): p. 237-252.

34. Halloran, D.O., et al., *An injectable cross-linked scaffold for nucleus pulposus regeneration.* Biomaterials, 2008. **29**(4): p. 438-447.

35. Boyd, L.M. and Carter, A.J., *Injectable biomaterials and vertebral endplate treatment for repair and regeneration of the intervertebral disc.* European Spine Journal, 2006. **15**(Suppl. 3): p. S414-S421.

36. Moreland, L.W., *Intra-articular hyaluronan (hyaluronic acid) and hylans for the treatment of osteoarthritis: mechanisms of action.* Arthritis Res Ther, 2003. **5**: p. 54-67.

37. Greenberg, D.D., et al., *Biochemical effects of two different hyaluronic acid products in a co-culture model of osteoarthritis.* Osteoarthritis And Cartilage, 2006(14): p. 814-822.

38. Sannino, A., et al., *Crosslinking of cellulose derivatives and hyaluronic acid with water-soluble carbodiimide.* Polymer, 2005. **46**: p. 11206-11212.

39. Ghosh, K., et al., *Cell adaptation to a physiologically relevant ECM mimic with different viscoelastic properties.* Biomaterials, 2007. **28**(4): p. 671-679.

40. Usta, M., et al., *Behavior and properties of neat and filled gelatins.* Biomaterials, 2003. **24**(1): p. 165-172.

41. Iatridis, J.C., et al., *Is the nucleus pulposus a solid or a fluid? Mechanical behaviors of the nucleus pulposus of the human intervertebral disc.* Spine, 1996. **21**(10): p. 1174-1184.

42. Perie, D.;Korda, D. and Iatridis, J.C., *Confined compression experiments on bovine nucleus pulposus and annulus fibrosus: sensitivity of the experiment in the determination of compressive modulus and hydraulic permeability.* Journal Of Biomechanics, 2005. **38**(11): p. 2164-2171.

43. Perie, D.S., et al., *Correlating material properties with tissue composition in enzymatically digested bovine annulus fibrosus and nucleus pulposus tissue.* Annals Of Biomedical Engineering, 2006. **34**(5): p. 769-777.

44. Johannessen, W. and Elliott, D.M., *Effects of degeneration on the biphasic material properties of human nucleus pulposus in confined compression.* Spine, 2005. **30**(24): p. E724-E729.

45. Ateshian, G.A., et al., *The correspondence between equilibrium biphasic and triphasic material properties in mixture models of articular cartilage.* Journal Of Biomechanics, 2004. **37**(3): p. 391-400.

46. Ateshian, G.A., et al., *Finite deformation biphasic material properties of bovine articular cartilage from confined compression experiments.* Journal Of Biomechanics, 1997. **30**(11-12): p. 1157-1164.

47. An, H.S. and Masuda, K., *Relevance of in vitro and in vivo models for intervertebral disc degeneration.* Journal Of Bone And Joint Surgery-American Volume, 2006. **88A**: p. 88-94.

48. Mizuno, H., et al., *Tissue-engineered composites of anulus fibrosus and nucleus pulposus for intervertebral disc replacement.* Spine, 2004. **29**(12): p. 1290-7.

49. Umehara, S., et al., *Effects of degeneration on the elastic modulus distribution in the lumbar intervertebral disc.* Spine, 1996. **21**: p. 811-9.

50. Leahy, J.C. and Hukins, D.W.L., *Viscoelastic properties of the nucleus pulposus of the intervertebral disk in compression.* Journal Of Materials Science-Materials In Medicine, 2001. **12**(8): p. 689-692.

51. Causa, F., et al., *Spatial and structural dependence of mechanical properties of porcine intervertebral disc.* Journal Of Materials Science-Materials In Medicine, 2002. **13**(12): p. 1277-1280.

52. Iatridis, J.C., et al., *The viscoelastic behavior of the non-degenerate human lumbar nucleus pulposus in shear.* Journal Of Biomechanics, 1997. **30**(10): p. 1005-1013.

53. Antoniou, J., et al., *The human lumbar intervertebral disc: evidence for changes in the biosynthesis and denaturation of the extracellular matrix with growth,*

maturation, ageing, and degeneration. Journal of Clinical Investigation, 1996. **98**: p. 996-1003.

54. Sakai, D., et al., *Atelocollagen for culture of human nucleus pulposus cells forming nucleus pulposus-like tissue in vitro: Influence on the proliferation and proteoglycan production of HNPSV-1 cells.* Biomaterials, 2006. **27**(3): p. 346-353.

55. Kluba, T., et al., *Human anulus fibrosis and nucleus pulposus cells of the intervertebral disc - Effect of degeneration and culture system on cell phenotype.* Spine, 2005. **30**(24): p. 2743-2748.

56. Wang, J.Y., et al., *Intervertebral disc cells exhibit differences in gene expression in alginate and monolayer culture.* Spine, 2001. **26**(16): p. 1747-1751.

57. Chou, A.I., et al., *The effect of serial monolayer passaging on the collagen expression profile of outer and inner anulus fibrosus cells.* Spine, 2006. **31**(17): p. 1875-1881.

58. Le Maitre, C.L.;Hoyland, J.A. and Freemont, A.J., *Studies of human intervertebral disc cell function in a constrained in vitro tissue culture system.* Spine, 2004. **29**(11): p. 1187-1195.

59. Gruber, H.E., et al., *Three-dimensional culture of human disc cells within agarose or a collagen sponge: assessment of proteoglycan production.* Biomaterials, 2006. **27**(3): p. 371-376.

60. Gruber, H.E., et al., *Human intervertebral disc cells from the annulus: Three-dimensional culture in agarose or alginate and responsiveness to TGF-beta 1.* Experimental Cell Research, 1997. **235**(1): p. 13-21.

61. Mwale, F., et al., *Biological evaluation of chitosan salts cross-linked to genipin as a cell scaffold for disk tissue engineering.* Tissue Engineering, 2005. **11**(1-2): p. 130.

62. Di Martino, A.;Sittinger, M. and Risbud, M.V., *Chitosan: A versatile biopolymer for orthopaedic tissue-engineering.* Biomaterials, 2005. **26**(30): p. 5983-90.

63. Gan, J.C., et al., *Bioactive glass serves as a substrate for maintenance of phenotype of nucleus pulposus cells of the intervertebral disc.* Journal of Biomedical Materials Research, 2000. **51**(4): p. 596-604.

64. Roughley, P., et al., *The potential of chitosan-based gels containing intervertebral disc cells for nucleus pulposus supplementation.* Biomaterials, 2006. **27**: p. 388-396.

65. Brown, R.Q.;Mount, A. and Burg, K.J.L., *Evaluation of polymer scaffolds to be used in a composite injectable system for intervertebral disc tissue engineering.*

Journal Of Biomedical Materials Research Part A, 2005. **74A**: p. 32-39.

66. Poiraudeau, S., et al., *Phenotypic characteristics of rabbit intervertebral disc cells - Comparison with cartilage cells from the same animals.* Spine, 1999. **24**(9): p. 837-844.

67. Maeda, S. and Kokubun, S., *Changes with age in proteoglycan synthesis in cells cultured in vitro from the inner and outer rabbit annulus fibrosus - Responses to interleukin-1 and interleukin-1 receptor antagonist protein.* Spine, 2000. **25**(2): p. 166-169.

68. Mizuno, H., et al., *Biomechanical and biochemical characterization of composite tissue-engineered intervertebral discs.* Biomaterials, 2006. **27**(3): p. 362-370.

69. So, K., et al., *Antidegenerative effects of partial disc replacement in an animal surgery model.* Spine, 2007. **32**(15): p. 1586-1591.

70. James, S.P. and Kurkowski, R., inventors. *Copolymer synthesized from modified glycosaminoglycan, GAG, and an anhydride functionalized hydrophobic polymer*. USA patent PCT/US08/05054. April 18, 2008.

71. Kurkowski, R., *The chemical crosslinking, compatibilization, and direct molding of ultra high molecular weight polyethylene and hyaluronic acid microcomposites* [M.S. Thesis]. Fort Collins, CO: Colorado State University (Mechanical Engineering); 2007.

72. Oldinski, R.A., *Development of a hyaluronan-polyethylene copolymer for use in articular cartilage repair* [Ph.D. Dissertation]. Fort Collins, CO: Colorado State University (Mechanical Engineering); 2008.

73. Harris, J., *Hyaluronan grafted high density polyethylene copolymer for articular cartilage tissue engineering* [M.S. Thesis]. Fort Collins, CO: Colorado State University (Mechanical Engineering); 2009.

74. Cranson, C.N., *A Novel Hyaluronan-Polyethylene Graft Copolymer as a Carrier for Demineralized Bone Matrix* [M.S. Thesis]. Fort Collins, CO: Colorado State University (Mechanical Engineering); 2008.

75. Schexnailder, P. and Schmidt, G., *Nanocomposite polymer hydrogels.* Colloid and Polymer Science, 2009. **287**(1): p. 1-11.

76. *Biological evaluation of medical devices Evaluation biologique des dispositifs m√©dicaux. Partie 1, Evaluation et essais Evaluation and testing* =. Evaluation and testing. 2003, Geneva, Switzerland: ISO.

77. Zhang, M. and James, S.P., *Synthesis and properties of melt-processable hyaluronan esters.* Journal Of Materials Science, 2005. **40**(11): p. 2937-2943.

78. Zhang, M. and James, S.P., *Silylation of hyaluronan to improve hydrophobicity and reactivity for improved processing and derivatization.* Polymer, 2005. **46**(11): p. 3639-3648.

79. Hiemenz, P.Z. and Lodge, T.P., *Polymer Chemistry*. Second ed. 2007, Boca Raton, FL: CRC Press.

80. ASTM E1131-08, *Standard Test Method for Compositional Analysis by Thermogravimetry*. West Conshohocken, PA: ASTM International.

81. Smith, B., *Infrared Spectral Interpretation: A Systematic Approach*. 1999, Boca Raton, FL: CRC Press. 265.

82. Benesova, K., et al., *Stability evaluation of n-alkyl hyaluronic acid derivates by DSC and TG measurement.* Journal of Thermal Analysis and Calorimetry, 2006. **83**(2): p. 341-348.

83. Evenson, S.A. and Badyal, J.P.S., *Solventless attachment of long-chain molecules to poly(ethylene-alt-maleic anhydride) copolymer surfaces.* Journal of Physical Chemistry B, 1998. **102**(28): p. 5500-5502.

84. Wainwright, S.A., *Mechanical design in organisms*. 1976, New York: Wiley.

85. Ghosh, K., et al., *Rheological characterization of in situ cross-linkable hyaluronan hydrogels.* Biomacromolecules, 2005. **6**(5): p. 2857-2865.

86. Shu, X.Z., et al., *Synthesis and evaluation of injectable, in situ crosslinkable synthetic extracellular matrices for tissue engineering.* Journal Of Biomedical Materials Research Part A, 2006. **79A**(4): p. 902-912.

87. Lehmann, D.M. and Richardson, M.E., *Impact of assay selection and study design on the outcome of cytotoxicity testing of medical devices: The case of multi-purpose vision care solutions.* Toxicology in Vitro. **24**(4): p. 1306-1313.

88. Melrose, J., et al., *Aggrecan, versican and type VI collagen are components of annular translamellar crossbridges in the intervertebral disc.* European Spine Journal, 2008. **17**(2): p. 314-324.

89. Baek, H.S., et al., *Evaluation of the Extraction Method for the Cytotoxicity Testing of Latex Gloves.* Yonsei Med J, 2005. **46**(4): p. 579-583.

90. Chernyshev, E.A.;Ivanov, P.V. and Golubykh, D.N., *Intermediates of chemical assembling of oligoorganosiloxanes in hydrolysis of organochlorosilanes.* Russian Chemical Bulletin, 2001. **50**(11): p. 1998-2009.

APPENDIX A: PROTOCOLS

1 POLYMER DEVELOPMENT

1.1 HYDROGEL SYNTHESIS

1.1.1 HA-CTA Complexation
1.1.2 HA-*co*-PEMA Synthesis
1.1.3 Copolymer Crosslinking
1.1.4 Copolymer Washing
1.1.5 Gel Casting and Reinforcement

1.2 CHARACTERIZATION

1.2.1 Identifying Hyaluronan with Toluidine Blue O
1.2.2 Swell Testing
1.2.3 Fourier Transform Infrared Spectroscopy
1.2.4 Thermogravimetric Analysis

2 MECHANICAL TESTING

2.1 SHEAR RHEOMETRY

3 BIOLOGICAL RESPONSE

3.1 *IN VITRO* CELL CULTURE

3.1.1 Cell Culture Basics
3.1.2 Cell Line Information

3.2 BIOCOMPATIBILITY

3.2.1 Cytotoxicity Assay
3.2.2 Alamar Blue Cell Viability Assay

3.3 TISSUE CULTURE

3.3.1 Ovine Disc Tissue Harvest
3.3.2 Ovine Nucleus Pulposus Tissue Culture

1 POLYMER DEVELOPMENT

1.1 HYDROGEL SYNTHESIS

1.1.1 HA-CTA Complexation

Objective

Hydrophobic modification of hyaluronan for reaction in anhydrous solvents

Materials & Equipment

- Sodium hyaluronate (HA)
- Cetyltrimethylammonium bromide (CTAB)
- Distilled deionized water
- 1000 ml beaker or flask
- 500 ml beaker or flask
- magnetic stir bars
- stir plates
- Freezer mill
- Liquid nitrogen

Procedure

- Prepare a 0.25% w/v solution of sodium hyaluronate in DI H_2O (e.g. 1.5g HA in 600 ml DI H_2O). Allow to stir at room temperature until completely dissolved. This can take several hours depending upon the molecular weight of the HA.
- Prepare a 0.50% w/v solution of CTAB in DI H_2O (e.g. 1.5g CTAB in 300 ml DI H_2O); CTAB should fully dissolve in a few minutes.
- Slowly add the CTAB solution to the HA solution under magnetic stirring. The mixture will become increasingly opaque as CTAB solution is added, until at the reaction end point a white precipitate forms and the supernatant becomes clear.
- Collect the precipitate by centrifugation.
- Wash the precipitate by rinsing with DI H_2O and re-centrifuging several times to remove CTAB residue. The CTAB residue will have a “soapy” character, so rinse until no soapy bubbles form.
- Dry HA-CTA in a vacuum oven (-25 mm Hg, 50°C) 24 hours or until no weight change is observed.
- Grind dried HA-CTA to a powder using the freezer mill.
- HA-CTA should be sealed in vials and stored in a dessicator.

Note: Concentrations and volumes suggested are to control viscosity based upon sodium hyaluronate with a molecular weight > $1x10^6$ Da; higher concentrations can be used for smaller sodium hyaluronate.

References

Zhang, M. and James, S.P., (2005). *Silylation of hyaluronan to improve hydrophobicity and reactivity for improved processing and derivatization*. Polymer, **46**(11):3639-3648.

1.1.2 HA-*co*-PEMA Hydrogel Synthesis

Objective

Formation of a 3-D hydrogel by the reaction of HA with PEMA

Materials & Equipment

- Poly(ethylene-*alt*-maleic anhydride) (PEMA)
- HA-CTA
- Dimethyl Sulfoxide (DMSO), anhydrous, 99.9+% (*Sigma*)
- 250 ml 3-neck round bottom flask (RBF)
- 500 ml 3-neck RBF
- 2 stir bars
- Rubber serum stoppers
- Vacuum grease
- Copper wire
- Parafilm
- 2 condensers
- Vaccum grease or teflon sleeves (sized to glassware)
- Plastic Keck glassware clips
- 2 16-gauge stainless steel cannulas
- 2 hot plate stirrers with temperature control (*VWR International*)
- 2 mineral oil baths

Procedure

Preparation

- Determine the dry weight of reactants (HA-CTA and PEMA) required for desired end product HA:PE ratio (based upon 1g HA & PE in end product):

Weight Ratio (HA:PE)	Mass HA-CTA (g)	Mass PEMA (g)
99:1	1.635	0.045
95:5	1.569	0.225
70:30	1.156	1.349
5:95	0.083	4.271

For ratios not listed in the table above, the masses can be calculated as follows:

$$(desired\,mass)(proportion\,HA)\left(\frac{662.8\,g/mol\,HA-CTA}{401.3\,g/mol\,HA}\right) = mass\,HA-CTA$$

$$(desired\,mass)(proportion\,PE)\left(\frac{126.1\,g/mol\,PEMA}{28.1\,g/mol\,PE}\right) = mass\,PEMA$$

- Weigh a slight excess of reactants (to allow for weight loss due to the evaporation of water) and place into separate labeled containers.
- Vacuum-dry reactants at 50°C and -25 inches Hg for a minimum of 24 hours.

Note: Exposure to water will hydrolyze the maleic anhydride and reduce the reactivity of the PEMA. Vacuum drying will close the anhydride rings and reactivate the MA functional groups.

- Place glassware to be used for the reaction in a 100°C oven

Copolymerization Reaction

- Place HA-CTA in 500 ml RBF along with an appropriate stir bar. Spread vacuum grease on two rubber serum stoppers and place stoppers in side necks of the flask. Secure stoppers with copper wire and parafilm.
- Attach condenser to middle neck of RBF, using vacuum grease or teflon sleeve to seal. Wrap connection with parafilm and secure with Keck clip.
- Add DMSO via cannula under dry nitrogen gas flow, forming ~0.5 – 1.0% w/v solution (lower concentrations for HA M_w on the order of MDa; higher concentrations can be used for smaller HA). Continue to flush the system for a few minutes after the appropriate volume of DMSO has been added, closing off the system with a slight positive pressure of N_2.
- Heat to 80°C in an oil bath and stir vigorously for four hours to dissolve all HA-CTA.
- Place PEMA and appropriate stir bar in 250 ml RBF. Seal flask and add DMSO as described above for HA-CTA to form ~1-5% w/v concentration. Heat to 80°C under vigorous stirring in an oil bath until PEMA goes into solution, approximately two hours.
- Once the HA-CTA and PEMA have completely dissolved, transfer the PEMA-DMSO solution to the 500 ml RBF via cannula under N_2 flow. Mix the two solutions, stirring vigorously, for 12 hours at 80°C.

  Note: Solution concentrations are primarily a matter of controlling the solution viscosity to allow transfer via canula.

Copolymer Processing

- Process reaction product per "Copolymer Crosslinking," or "Copolymer Washing" protocols.

References

Cranson, C. *HA-co-HDPE synthesis methods for DBM carrier*. Standard operating protocol, James Laboratory, Colorado State University, Fort Collins, CO (2007).

Kurkowski, R., *The chemical crosslinking, compatibilization, and direct molding of ultra high molecular weight polyethylene and hyaluronic acid microcomposites* [M.S. Thesis]. Fort Collins, CO: Colorado State University (Mechanical Engineering); 2007.

Revision History

08-11-2009	SY	Adapted from HA-*co*-HDPE Synthesis Methods SOP
10-15-2009	SY	Modified concentrations and reaction temperature
10-19-2009	SY	Added weight ratio variations

1.1.3 Copolymer Crosslinking

Materials

- Copolymer suspension (reaction product)
- Large beaker or flask
- Acetone or xylenes (acetone for high HA content; xylenes for mid to high PEMA content)
- Büchner funnel
- Filter paper
- Vacuum flask
- Dimethyl sulfoxide (DMSO)
- Vortexer
- Poly(hexamethyldiisocyanate) (HMDI)
- Sodium chloride
- Distilled, deionized water

Procedure

- Combine the copolymer reaction product and an excess volume (3-4x) of acetone or xylenes in the large beaker to form a "gel" precipitate. Cover and soak for a minimum of 4 hours.
- Filter solvents from the gel using the Büchner funnel and vacuum flask. Wash and filter gel precipitate with acetone three times (may be increased).
- Resuspend the copolymer in a small volume of DMSO; mix vigorously using a vortexer. Add HMDI for a final concentration of up to 5% v/v with the DMSO and cast the suspension into a vial or petri dish as appropriate for desired shape. Allow the suspension to cure at room temperature for a minimum of 24 hours.
- Soak the crosslinked gel in several changes of acetone to remove excess HMDI.
- Prepare a 0.2M NaCl aqueous hydrolyzing solution. Immerse the crosslinked gel in the hydrolyzing solution and gently agitate (e.g. in shaker oven) at room temperature overnight.

References

Kurkowski, R., *The chemical crosslinking, compatibilization, and direct molding of ultra high molecular weight polyethylene and hyaluronic acid microcomposites* [M.S. Thesis]. Fort Collins, CO: Colorado State University (Mechanical Engineering); 2007.

Revision History

10-15-2009 SY Adapted protocol from Kurkowski thesis

1.1.4 Copolymer Washing

Materials

- Copolymer (HA-*co*-HDPE, HA-*co*-PEMA, tripolymer) suspension
- Large (1000 ml+) beaker or flask
- NaCl
- Deionized water
- Ethanol (EtOH)
- Isopropyl alcohol
- Ceramic filter
- Vacuum flask

Procedure

- Prepare a 0.2M NaCl aqueous hydrolyzing solution (volume greater than the reaction volume) in the large beaker or flask. Add the copolymer suspension to the hydrolyzing solution and mix at room temperature overnight.
- Add an excess of chilled EtOH and mix for a minimum of four hours to precipitate the copolymer. Allow to stand at room temperature; copolymer will begin to settle at the bottom of the beaker/flask.
- Centrifuge for 10 minutes to begin separating precipitate from supernatant. Filter supernatant using a ceramic filter and vacuum flask; soak precipitate pellets in isopropyl alcohol. Wash and filter precipitate with isopropyl alcohol three times (may be increased).
- Resuspend the copolymer in a small volume of distilled H_2O; mix at room temperature for four hours. Re-precipitate with an excess of isopropyl alcohol, mixing again at room temperature for four hours. Allow the solution to stand at room temperature; filter and wash as described above.
- Vacuum dry the HA-*co*-PEMA at -25 inches Hg overnight or until there is no change in weight.

References

Cranson, C. *HA-co-HDPE synthesis methods for DBM carrier.* Standard operating protocol, Colorado State University Orthopaedic Bioengineering Research Laboratory, Fort Collins, CO (2007).

Kurkowski, R., *The chemical crosslinking, compatibilization, and direct molding of ultra high molecular weight polyethylene and hyaluronic acid microcomposites* [M.S. Thesis]. Fort Collins, CO: Colorado State University (Mechanical Engineering); 2007.

Revision History

08-12-2009 SY Adapted from HA-*co*-HDPE Synthesis Methods SOP

1.1.5 Gel Casting and Reinforcement

Materials & Equipment

- Hyaluronan-cetyl trimethylammonium complex (HA-CTA)
- Poly(ethylene-*alt*-maleic anhydride) (PEMA)
- Dimethyl sulfoxide (DMSO)
- Qty. 2 two-necked round-bottomed flasks (RBF)
- Serum stoppers
- Copper wire
- Keck clips
- Condensers
- N_2 (dry) gas
- Oil bath
- Weigh boat(s)
- Analytical scale
- Magnetic stir bar(s)
- Stir plate(s)
- 70x50 crystallizing dish
- Reinforcing agents (optional)
  - Cab-o-Sil fumed silica, TS-620/TS-720 (Cabot, Boston, MA)
  - Chitosan nanofibers
- Disposable pipettes, 25 ml and 1 ml
- Forceps
- Pipette aid or bulb pipetter
- Vacuum bags and sealer
- Disposable glove box (Sigma Aldrich)
- Temperature-controlled oven, e.g. Shake ‘n Bake Hybridization Oven
- Ultrasonic bath
- Acetone
- NaCl
- Deionized water
- Ethanol (EtOH)
- Vacuum oven

Procedure

<u>Stock Solutions</u>

Note: Allow a minimum of 1 day prior to gel casting for preparation of stock solutions. Precautions for air/water-sensitive chemistry should be observed, i.e. HA-CTA and PEMA powders should be vacuum dried a minimum of 24 hours prior to

use, glassware should be stored at 100℃ to ensure it is completely dry, stir bars should be rinsed with acetone before use.

- Prepare a concentrated solution of HA-CTA in DMSO, aiming for a viscosity similar to honey. A 2.5% w/v concentration is appropriate for HA-CTA prepared from HA in the 450-500 kDa size range.
    - Weigh HA-CTA and place along with stir bar in an appropriately-sized RBF.
    - Seal side neck of RBF with a serum stopper secured with copper wire.
    - Attach RBF to condenser with a Keck clip, lower into oil bath, set temperature to 80°C and begin stirring
    - Insert vent needle and transfer canula into rubber serum stopper. Transfer appropriate volume of DMSO (100 ml for every 2.5g HA-CTA) into flask via canula under N_2 flow.
    - Flush flask with N_2 by plugging vent, allowing slight positive pressure to build, and releasing plug a total of 3 times; plug vent and remove along with canula, leaving slight positive pressure of N_2 in the flask.
    - When HA-CTA is fully dissolved (can take 12+ hours) remove from heat and allow to come to room temperature.
- Prepare a 10% w/v concentrated solution of PEMA in DMSO, following procedure described above for HA-CTA solution. The PEMA will go into solution much more readily than the HA-CTA and thus will not need to be on heat for as long.

Gel Casting

Note: This reaction is air/water sensitive. If available, work inside a glove box filled w/ dry nitrogen, sealing the cast gel into a vacuum bag prior to removal from the glove box. If a glove box is not available, air/water contact can be minimized by working with sealed vacuum bags as described below.

- Base formulation: 16.5 ml 2.5% (w/v) HA-CTA in DMSO
  0.6 ml 10% (w/v) PEMA in DMSO
- Reinforcement (optional): 0.8g treated silica (Cabot TS-620 or TS-720) max or fibrous reinforcement (e.g. carbon nanotubes, chitosan nanofibers)
- Measure PEMA solution into a vial and seal with a serum stopper and copper wire. Flush vial with N_2 gas.

- Measure HA-CTA solution into 70x50 crystallizing dish using 25 ml serological pipette. If reinforcement is to be used, add and stir by hand at this time. Place appropriately-sized stir bar into dish, then place dish and a pair of forceps into a large vacuum bag modified with a serum-stopper "port"; remove air with vacuum and flush with N_2 gas three times.
  Omit vacuum bag if working in glove box
- Place crystallizing dish on stir plate; turn-on stir plate to start mixing. Slowly add PEMA solution to the stirring HA-CTA solution via canula and low N_2 flow (if using vacuum bag) or dropwise using a pipette (if working in a glove box). The HA-CTA and PEMA solutions should complex, becoming more viscous. This may necessitate moving the dish around on the plate and adjusting the stir plate r.p.m. to get good mixing.
  - Remove the stir bar from the dish using the forceps. If working in a glove box, place the cast gel into a vacuum bag and seal immediately upon removal from glove box. Otherwise, push the forceps and stir bar to one end of the vacuum bag and re-seal the vacuum bag around the forceps and stir bar; cut bag to remove.
- Place sealed dish into 75°C oven to cure for 24 hours.
- After curing, remove excess PEMA by sonication with acetone for 30 minutes. Flip gel and repeat.
- Prepare a 0.2M NaCl aqueous hydrolyzing solution in a large beaker or flask. Add the hydrolyzing solution to the crystallizing dish and sonicate for 30 minutes. Repeat sonication if gel retains golden hue (indicative of PEMA in DMSO)
- Replace hydrolyzing solution with deionized water and repeat sonication for 30 minutes. The gel will swell to a greater extent in deionized water, allowing trapped NaCTA to be removed. Repeat the sonication if the solution appears to be "soapy."
- Dehydrate gel by soaking in ethanol a few hours or overnight; drain ethanol and completely dry in a vacuum oven at equipped with a solvent trap at -25 inches Hg until there is negligible change in weight..

References

Cranson, C. *HA-co-HDPE synthesis methods for DBM carrier.* Standard operating protocol, Colorado State University Orthopaedic Bioengineering Research Laboratory, Fort Collins, CO (2007).

Kurkowski, R. *The chemical crosslinking, compatibilization, and direct molding of ultra high molecular weight polyethylene and hyaluronic acid microcomposites*, M.S. thesis, Colorado State University Department of Mechanical Engineering, Fort Collins, CO (2007).

Revision History

09-10-2010 SY updated for particulate reinforcement
10-15-2010 Updated to include use of glove bag

1.2 CHARACTERIZATION

1.2.1 Identifying Hyaluronan with Toluidine Blue O

Materials

- Toluidine Blue O (TBO, dye content 84%, Sigma-Aldrich)
- Urea (99+%, ACS reagent, Sigma-Aldrich)
- Distilled water
- Glass beaker
- Glass petri dish

Procedure

- Prepare an 8M aqueous urea solution (60.06 g/mol); allow to mix at room temperature for 30 minutes.
- Add TBO powder to the urea solution at an 0.1% w/v concentration
- Submerge sample in TBO solution for 10 minutes at room temperature, then rinse copiously with distilled water to leave behind only bound TBO.
- Take pictures of at least three samples from each treatment group.

References

Kurkowski, R., *The chemical crosslinking, compatibilization, and direct molding of ultra high molecular weight polyethylene and hyaluronic acid microcomposites* [M.S. Thesis]. Fort Collins, CO: Colorado State University (Mechanical Engineering); 2007.

Revision History

10-15-2009	SY	Added molecular weight for urea
01-18-2007	RK	

1.2.2 Swell Testing

Materials

- Hydrogel samples (n=3 per hydrogel type)
- Swelling media (distilled deionized water, phosphate-buffered saline, etc.)
- Vials
- Weigh dishes
- Kimwipes
- Analytical scale (mg resolution or better)

Procedure

- Tare and label a weigh dish for each hydrogel sample.
- Measure and record the dry weight (W_d) of each hydrogel.
- Immerse hydrogel samples in individual labeled vials filled with swelling media and allow to swell at room temperature or other specified temperature.
- At regular time intervals, remove hydrogels from the vials and blot excess solution on the surface with a Kimwipe. Weigh using the appropriate tared weigh dish and record the swolen weight for that timepoint (W_t).
- Continue soaking and weighing gels until weight equilibrium has been reached, i.e. no weight gain is seen for three consecutive measurements (W_s).
- Calculate swell test parameters as follows:

$$\text{Equilibrium swelling ratio}: \quad q = \frac{W_s}{W_d}$$

$$\text{Equilibrium hydration}: \quad H = \left(\frac{W_s - W_d}{W_s} \right) \times 100$$

- Note: Swell kinetics can also be mapped by calculating hydration at each timepoint, i.e. substituting W_t for W_s in the numerator of the hydration equation.
- At study completion, rinse hydrogels thoroughly with deionized water to remove any buffer salts.
- Dry hydrogels in a vacuum oven overnight or until no change in weight is observed. Reweigh dry hydrogel and note any differences with previous dry measurement.
- Repeat for other solutions of interest.

Swell Test Data Table

Date/Time		Sample 1	Sample 2	Sample 3
	Weigh Dish Tare			
	Dry Hydrogel (W_d+tare)			
	Sol'n: Temp:			

References

ASTM D2765-01(2006), *Standard Test Methods for Determination of Gel Content and Swell Ratio of Crosslinked Ethylene Plastics*. West Conshohocken, PA: ASTM International.

Dinerman A.A. et. al. *Swelling behavior of a genetically engineered silk-elastinlike protein polymer hydrogel*. Biomaterials 23 (2002) 4203–4210.

Chang C et. al. *Superabsorbent hydrogels based on cellulose for smart swelling and controllable delivery*. European Polymer Journal 46(2010) 92-100.

Revision History

11-24-2009 SY Originated protocol

1.2.3 Fourier Transform Infrared Spectroscopy

Materials

- Sample for analysis
- Potassium Bromide (KBr), spectroscopy grade
- Sample pellet press
- Sample holder
- Spectrometer

Procedure

- Prepare samples by vacuum drying and grinding into a powder, either using a mortar and pestle or cryogrinding. This preparatory step should be completed prior to going to the Central Instruments Facility

  Note: cryoground powders generally press into better, more transparent samples for spectroscopy, but for the small sample mass (~mg) needed cryogrinding is impractical. However, FTIR samples should be saved when materials are cryoground for other reasons.

- Collect spectra using the following generalized procedure:
- Set-up instrument data collection. Typical parameters that can be modified include the range, the number of scans collected, and the resolution.
- Press a plain KBr pellet using the sample press supplied with the instrument. The KBr should just coat the bottom of the sample press insert and should not require excessive force to press into a transparent sample.
- Place the pellet into the sample holder and load the sample into the instrument. Open the nitrogen gas valve and observe the spectrum displayed while the instrument is autogaining, watching for water peaks. Wait for the water peaks to disappear before collecting the sample (typically around 5 minutes for KBr that has been kept dry).
- Save the spectrum and set-up the instrument to use it as the background for subsequent samples
- Press a sample pellet following the same procedure described for the KBr background pellet, but adding a small amount (approximately 2% w/w) of the sample powder to the KBr.
- Load the sample into the instrument as previously described for the background. In addition to watching for the water peaks to disappear, examine the quality of the spectrum, e.g. looking for an extremely sloped baseline, presence of peaks, noise, etc.

- Problems with the spectrum (sloped baseline, no/noisy peaks) are generally due to sample pellets that are too opaque, as when they are pressed too thick or the sample is clumped. Sometimes the spectrum can be improved by rotating the sample in the sample holder, otherwise a new pellet should be pressed.
- Collect and save the sample spectrum, then process using the analysis software provided with the instrument. Typical analysis functions include baseline correction, normalization, and peak location labeling.
- Interpret spectra by identifying functional groups associated with peaks; some understanding of the underlying chemistry of the sample is helpful.
- Assign common intense bands first, e.g. O-H, C-H, C=O, etc. Identify other intense bands using spectral atlases, textbooks, the literature, etc.
- Look for secondary peaks based upon your knowledge of the reactants, reaction intermediates, and other chemical processes
- Identify differences among spectra (e.g. a control blend of reactants compared to the reaction products) to gain an understanding of reaction processes.

References

Smith, B., Infrared Spectral Interpretation: A Systematic Approach. 1999, Boca Raton, FL: CRC Press. 265.

1.2.4 Thermogravimetric Analysis

Materials

- Sample for analysis
  - 5-10 mg for dry samples
- Aluminum pans
- Forceps
- TGA platinum loading pan ("basket-like" pan with handle)
- TA Instruments 2950 Thermogravimetric Analyzer

Procedure

- The TGA is programmatically controlled by TA Advantage software. Start the software and set-up control program.
- Typical program settings for bulk compositional analysis and thermal stability testing: temperature range from ambient to 600°C, 10°C/min ramp rate.

  Note: Do note exceed 600°C when using aluminum pans. Sample should be placed directly on the TGA platinum pan if higher temperatures are required.
- For hygroscopic samples, temperature may be held isothermally for 15 minutes at 110°C to evaporate unbound water (will need to adjust for lost water weight during analysis).
- Include external trigger if concurrent mass spectrometry will be used.
- Set the instrument end-of-test condition to air-cool.
- Using forceps, place an empty aluminum pan on the TGA loading tray. Tare by pressing the "tare" button on the TGA instrument control panel and allowing the robotic stage to load the pan on the balance.
- If the pan mis-loads, DO NOT attempt to place the loading pan on the balance wire manually (the balance is a precision instrument, and "dropping" a sample on the balance wire can damage the instrument).
- Wait for the robotic stage to return to its start position, then rotate the TGA loading pan to reposition its "basket" handle.
- Push the tare button again and observe the position of the handle relative to the balance wire. If it looks like the pan will mis-load again, gently guide the balance wire by pushing and holding it in proximity to the pan handle with forceps. Allow the instrument to load pan on to the balance wire.
- The pan will be loaded into the furnace, then the instrument will automatically tare the pan. Wait for the instrument to return the pan to the start position.

- Prepare samples for analysis. Generally, for dry samples the most consistent results will be obtained from samples with high surface area, e.g. powders.
- Pack powder into tared aluminum pan and place on TGA loading pan with forceps. Load the sample by pushing the "load" button on the TGA control panel. Observe the same precautions as described for taring the pan if the sample mis-loads
- Observe the sample weight measured by the instrument – powdered samples should be in the 5-10 mg range. If sample weight is not in the right range, unload the sample by pushing "unload" on the instrument panel. Adjust sample and repeat load process.
- Note: the sample will not be loaded into the TGA furnace until the TGA program is started
- Click "run" in the TA Advantage software to load the sample and run the control program.
- Analyze collected data using TA Universal Analysis software. Plot the weight% and derivative weight% as a function of temperature. Typical analysis parameters to identify include start and end temperatures for degradation steps, peak degradation rate temperatures, % mass loss over a degradation step, and sample residues.

References

ASTM E1131-08, *Standard Test Method for Compositional Analysis by Thermogravimetry*. West Conshohocken, PA: ASTM International.

2 MECHANICAL TESTING

2.1 Shear Rheometry

Objective

Dynamic characterization of hydrogels in shear

Materials

Samples

- Swollen HA-*co*-PEMA hydrogel samples
- Deionized Water (DI) or Phosphate Buffered Saline (PBS)

Apparatus and Consumables

- Rheometer (TA Instruments ARES)
- 8 mm parallel plate
- Acetone
- Sandpaper (150 grit)
- Ethyl-2-cyanoacrylate (Krazy Glue or Super Glue)
- Fluid bath, serrated surface
- 8mm biopsy punch
- Razor blades
- Kimwipes

Procedure

Sample Preparation

- Swell hydrogels to equilibrium in DI or PBS
    - Immerse hydrolyzed, cast gel in DI or PBS
    - Sonicate 30 minutes at room temperature (sonication will raise temperature)
    - Replace solution and allow to swell overnight
- Cut samples using an 8 mm biopsy punch
- Prepare n=6 samples per experimental group

Rheometer Set-up

- Adhere sandpaper to top platen
    - Cut an 8mm sandpaper disc with a new biopsy punch

- Clean surface of 8mm top plate with acetone
- Apply a layer of ethyl-2-cyanoacrylate to the cleaned 8mm plate
- Align sandpaper disc to 8mm plate and apply pressure for 30 seconds or until well-adhered

- Install appropriate thermocouple, recirculating fluid peltier, bath chamber and 8mm parallel top plate following instructions in the instrument manual
- Auto-zero the rheometer force and displacement, then raise upper platen to allow sample to be loaded
- Ensure that the appropriate motor (dynamic or steady) is turned on and that there is enough air pressure (typically 60 psi) for proper air bearing operation
- Load hydrogel
  - Place gel onto bath chamber surface
  - Manually lower upper plate to just above sample surface
  - Ensure that the sample is flush with the outer diameter of the parallel plates
  - Continue lowering upper plate until a slight force is read by the axial load cell; note the gap displacement value and take this to be the sample thickness
  - Using the system's software control set the gap to a 10% compressive strain to ensure planar contact and gripping of the sample
- Create a "humidity chamber" by placing a moistened Kimwipe into the bath chamber and installing the bath cover

Experiments

- Strain sweep
  - The purpose of the strain sweep is to verify the linear viscoelastic region (LVR) of the test samples. The strain amplitude for further experiments should be within the LVR, preferably at the upper-end to ensure a good signal-to-noise ratio
  - Test parameters: 0.005 – 10% strain amplitude at 1.0 Hz
  - Perform strain sweep experiments on at least one sample from all groups in order to select a consistent strain amplitude for the dynamic frequency sweep experiment
- Dynamic frequency sweep
  - Evaluate G', G", and tanδ over a range of conditions
  - Test parameters: 0.1 – 10 Hz frequency range at strain amplitude as determined by strain sweep experiments (use 0.01 rad if it is in LVR to be consistent with literature)

References

Anseth, K.S., C.N. Bowman, and L. BrannonPeppas, *Mechanical properties of hydrogels and their experimental determination.* Biomaterials, 1996. **17**(17): p. 1647-1657.

Cranson, C.N., *A Novel Hyaluronan-Polyethylene Graft Copolymer as a Carrier for Demineralized Bone Matrix* [M.S. Thesis]. Fort Collins, CO: Colorado State University (Mechanical Engineering); 2008.

Iatridis, J.C., et al., *Alterations in the mechanical behavior of the human lumbar nucleus pulposus with degeneration and aging.* Journal Of Orthopaedic Research, 1997. **15**(2): p. 318-322.

Revision History

07-23-2009	SY	Initial methods adapted from Cody Cranson's thesis
03-17-2010	SY	Methods modified based upon validation experiments

3 BIOLOGICAL RESPONSE

3.1 *IN VITRO* CELL CULTURE

3.1.1 Cell Culture Basics

Background

Cell culture procedures should be performed in a biosafety cabinet (BSC). All materials introduced into the BSC should be sterilized using an autoclave or disinfected with 70% ethanol prior to transfer into the BSC, or opened using sterile technique in the BSC. Any fluids that may come into contact with cells need to be equilibrated at 37°C prior to use.

Operating within Biosafety Cabinet

- Start-up the BSC.
  - Turn-on blower (leave on for duration of BSC use)
  - Turn-on UV light, expose for ~10 min.
- Spray the BSC with 70% ethanol and wipe, working from the back to the front of the cabinet. Always wipe from the most sterile to the least sterile area (generally, top-to-bottom, back-to-front).
- Transfer supplies to the cabinet and arrange to minimize clutter (air flow disruption and to prevent from moving hands above open containers)

Sterile Technique

- Avoid double-dipping into any reagents or medium containers. Use a new pipette/tip for each "dip" into the container.
- Avoid adding bubbles to the fresh medium as you aliquot. Keep the tip of the pipette away from the lip of the flask, and try not to let any medium get on the lip or neck of the flask.
- Avoid tilting the flasks so that medium approaches the cap. Keep the flask tilted such that the medium flows to the opposite end of the container. Be especially careful when placing the flasks in the incubator and lifting them out.
- Avoid splashes of medium on the outside of the container. If you get medium on the outside of dishes or flasks clean it off with ethanol and a Kimwipe.
- Do not leave medium or cells out at room temperature for longer than is absolutely necessary.
- If cells are suspect or appear contaminated remove them from the incubator immediately and bleach them before disposal.

- Remove incubator shelves/water pan and autoclave them.
- Remove all reagents from the BSC and re-filter or dispose of suspect medium.
- Replace the aspirator hose; this is often a contamination source.
- Re-autoclave Pasteur pipets.
- Typically, contamination from sub-culturing arises within 24 hours.

Viability and Cell Count

- Add an equal volume (50 µl) of trypan blue dye to the cell suspension (50 µl) to be counted.
- Mix gently in Eppendorf tube by inverting or gentle flicking of tube. Do NOT use pipet to mix solution; the shear from the pipet tip will destroy cells.
- Load 9 µl of counting solution in a hemocytometer.
- Using a microscope, count all the live cells within a square and average the totals for the 4 squares
  - Live cells will only have a blue outline and will retain normal morphology.
  - Dead cells will appear a solid dark blue and will have an odd shape.
  - Calculate cell count
  - Multiply by dilution factor (for equilivent amounts of dye and cell suspension, the dilution factor is two).
  - Multiply by 10^4 cell/ml to calculate cell density (cells/ml)
  - Multiply the cell density by the total volume to determine the total number of cells
- Centrifuge cells again at 260 x g and resuspend to prepare desired cell concentration solution

Thawing Cells

Rule: THAW QUICKLY

- Cells should be brought up in medium that contains 20% FBS. To make medium you will need:
  - DMEM or RPMI* stored at 4°C (refrigerated) in 500 ml bottles
  - FBS stored at -20°C (frozen) in 50 ml aliquots
  - Penicillin/Streptomycin
  - Steri-Cup vacuum filtration system
- Prepare medium

- Thaw sufficient FBS in a 37°C water bath for the volume of medium you wish to prepare (e.g. 100 ml total FBS in 500 ml V_T or 200 ml for 1000 ml V_T).
- Attach Steri-Cup to vacuum pump and engage vacuum.
- Filter medium components, allowing DMEM and pen-strep (if used) to completely filter before adding FBS (so FBS does not foul filter).
- Label as "20% FBS in DMEM (with Pen-Strep)", the date and your initials.
- Warm medium to 37°C prior to use. Treat as sterile. Do not leave medium out for extended periods of time.

- Prepare culture flask(s). Directions below apply to T25 flasks; adjust volumes according to table for larger flasks.
  - Add 9 ml of medium, and place in the incubator to allow medium to adjust to its proper pH (~30 minutes).
  - Remove cells from liquid nitrogen storage (or from the -70°C freezer) and immediately place vial in 37°C water bath, taking care to avoid direct contact of the cap area with the water. Allow the sample to thaw.
  - Spray vial with 70% ethanol, transfer to the BSC and immediately transfer (using a 5 or 10 ml pipet and sterile technique) to the flask.
  - Alternatively, you may spin down the cells at no more than 1,000 x g for 5 minutes to remove dimethyl sulfoxide (DMSO) and resuspend in medium before adding cells to the flask/plate.
  - Place in the incubator (37°C, 5% CO_2, 98% humidity). Cells should be 90% confluent in 2-5 days. Change the medium after 12-24 hours if you did not spin out the DMSO.

Flask working volume	Cell Media	Trypsin EDTA (.25%)
T-25	10 ml	1 ml
T-75	25 ml	4 ml
T-175	45ml	5 ml

Changing the media in a cell culture

- Before beginning make sure to place the media into a 37^0C water bath for at least 30 min.
- When the media is up to temperature place it in a disinfected BSC and transfer the cell culture flask(s) into the BSC.
- Open the lids on all flasks but leave them on the flask. Using sterile technique and a new pipette per flask carefully aspirate all media out of the flasks. Do not touch the outside of the flask(s) with the pipette(s).

- Add media of the appropriate volume back into the flasks and put them back into the incubator.
- While this should be done in accordance with the recommended media turnover time as per the ATCC, it will also depend on cell density within the flask.

Sub-culturing cells

Rules: NEVER work with more than one cell type in the BSC at the same time -- this invites cross-contamination. Use sterile technique at all times -- if you are unsure about whether you might have contaminated something, assume you did and treat appropriately.

- Determine "% confluence" of the culture by examining the flask/plate using an inverted microscope and a 10x objective. Cells should not be allowed to progress beyond 90% confluence.
- Set medium out to warm in a water bath (37°C).
- Disinfect the work area (pay special attention to the aspirator tube) and any reagent bottles to be opened using 70% ethanol. Wipe bottles from the top down and reapply ethanol before transferring to the BSC.
- Work with the BSC blower on, using sterile techniques at all times. Wear gloves and spray your hands regularly with ethanol to protect the cells from contamination. Do not wipe your hands with a towel. If you leave the BSC to do other work, change gloves before returning to cell culture work.
- Prepare (label) new flasks for cells. Be sure to label the flasks with cell identification, the sub-culture number, the date and your initials.
- Remove cells from the incubator, transfer to the BSC and aspirate old medium from the flask using sterile technique (preferably using a Pasteur pipet with vacuum). Use one sterile Pasteur pipet per flask or plate.
- Add enough 1x (sterile) HBSS or PBS without divalent cations (Ca^{2+} and Mg^{2+} free) to cover the bottom of the flask (14 ml for a large flask). If the cells are very close to 90% confluence, rock the flask and aspirate this HBSS/PBS as a rinse. Then add a second volume of HBSS/PBS. Place the cells back in the incubator. Allow them to sit 10 minutes before checking for cell lifting (never longer than 30 minutes). For stubborn cells, successive treatments of HBSS/PBS can be employed.
- Check the progress of cell lifting by examining the flask with an inverted microscope.
- Tap the flask hard against the back of your hand and check for loosening. Smacking the flask too lightly will result in liberation of too few cells. Smacking the flask too hard will result in damaging the flask and leaking.
- Most of the cells should be free from the surface after 10 minutes. If cells are not coming off return them to the incubator and check again in five minutes.

- As the cells age (usually upwards of 50 passages) they will become more resistant to removal.
- Remove a small aliquot of cells (10-100 ml) to count using Trypan blue if so desired.
- Remove a small amount of cells and transfer to a new flask containing fresh medium. Plate cells at the desired density (usually 5 x 10^5 cells for experimental 15 x 100 mm plates, 1-2 x 10^6 for cryo vials, and 1 x 10^5 cells for passage flasks). Return flasks to the incubator.

Freezing Cells

Rule: FREEZE SLOWLY

- Thaw an aliquot of FBS/DMSO (90% FBS should be aliquoted with 10% cell culture grade DMSO and stored frozen in sterile 15 ml Falcon tubes).
- Remove cells using the procedure outlined in the sub-culturing section.
- Remove a small amount (10-100 ml) of the cells and count using Trypan blue dye and a hemacytometer (see cell counting section).
- Transfer the cell suspension into centrifuge tubes and spin for 5 minutes at 1,000 x g or less.
- Decant the supernatant and resuspend the cell pellet in the desired amount of 10% DMSO/FBS solution. (Calculate from desired amount of cells per vial as noted above, typically 1-2 x 10^6 cells/ml).
- Aliquot 1 ml of cell suspension per cryo tube using a 10 ml pipet. Place into a cell freezer container containing ethanol (or Styrofoam container) to provide some insulation.
- Freeze at -20°C for several hours. Move to -80°C for 24 hours. (Viable for 6 months if left here).
- Transfer cryotubes to liquid nitrogen storage. They should be viable for 12 months. Update the frozen cell storage records.

References

Godek, M.L., *Molecular characterization of macrophage response to model biomaterial surfaces in vitro* [Ph.D. Dissertation]. Fort Collins, CO: Colorado State University (Chemistry); 2006.

Revision History

03-25-2008 SY Adapted from Godek protocol

3.1.2 Cell Line Information

Description

Cell Type: HEK-293

Biosafety Level: 2 (contain adenovirus)

Origin: Human Embryonic Kidney

Morphology: Epithelial

Overview: HEK-293 cells are very easy to grow and are commonly used in biomedical research. As an experimentally-transformed cell line they are not a good model for normal kidney cell function but are useful in experiments in which the functional behavior of the cell itself is not of interest.

Culture and Maintenance: The base medium for this cell line is Eagle's Minimal Essential Medium supplemented with 10% fetal bovine serum. Standard culture conditions are a 95% air/5% CO_2 atmosphere at 37°C. Although this is an adherent cell line, it may take several days in culture for cells to attach when brought up from liquid N_2 storage. Medium should be changed every 2-3 days. Subculture at approximately 90% confluence (cell density 6 to $7x10^4$ cells/cm^2). A split ratio between 1:10 and 1:20 is recommended.

Cell Culture Information Sources

- Information on commercially-available cell lines is available online from the American Type Culture Collection (ATCC): www.atcc.org
- Biosafety information is available online from the Centers for Disease Control (CDC): http://www.cdc.gov/od/ohs/biosfty/bmbl4/bmbl4toc.htm.
- Biohazard level definitions are available at: http://bmbl.od.nih.gov/sect3bsl2.htm.

References

Godek, M.L., *Molecular characterization of macrophage response to model biomaterial surfaces in vitro* [Ph.D. Dissertation]. Fort Collins, CO: Colorado State University (Chemistry); 2006.

3.2 BIOCOMPATIBILITY

3.2.1 Cytotoxicity Assay

Objective

To assess the detrimental effects (cell death and/or inhibition of cell growth) of exposure to leachable substances eluted from candidate materials

Materials

- Minimal Essential Medium (e.g. DMEM, α-MEM, etc.)
- Fetal bovine serum
- Test materials
- Reference materials (e.g. high density polyethylene, latex rubber)
- 50 ml conical Falcon™ tubes
- 0.22 μm sterile filter unit
- Cell culture well plate
- Primary cells or cell line (e.g. HEK-293)
- Cell seeding supplies (e.g. pipetters, pipette tips, etc.)

Procedure

Except where noted, all procedures are to be performed using sterile technique in a biosafety cabinet (BSC) under aseptic conditions. All materials should be sterilized via autoclave or disinfected with 70% ethanol prior to introduction into the BSC. Sterile packaged materials are to be opened using sterile technique in the BSC.

Media Conditioning

- Disinfect test articles and reference materials by rinsing in ethanol and washing with sterile PBS.

  Note: It is extremely important to ensure all ethanol is rinsed from the materials since ethanol itself is cytotoxic. For materials that swell significantly allow sufficient time (hours) and use a minimum of 3 wash solution changes. For hyaluronan-based hydrogels, Milli-Q water was used for the first two rinses for better diffusion through the gels while PBS was used for the last rinse to shrink the gels to the expected physiological configuration. The 3 rinse steps were conducted over the course of 24 hours.

- Prepare conditioning medium:
  - 500 ml DMEM
  - 1% 4-(2-Hydroxyethyl)piperazine-1-ethanesulfonic acid (HEPES)

- 1% fetal bovine serum

- Add equal volumes of test articles and reference materials to separate Falcon™ tubes (i.e. to 5 ml mark). Fill tubes to 50 ml mark with medium. Fill an additional Falcon™ tube with 50 ml medium to serve as a solution control.
- Incubate Falcon™ tubes at 37°C for 12-72 hours. Adjust elution time based upon device contact time for intended application (e.g. temporary, prolonged, implant)
- Sterilize conditioned media by filtration through 0.22 μm sterile filter.

Preparation of Cell Layer

- Bring-up and expand frozen HEK cells to 90% confluence in T75 flask as described in General Cell Culture Practices protocol (5-7 days).
- Prepare cell suspension of known concentration (see "Subculturing Cells" in General Cell Culture Practices protocol).
- Seed cell culture well plate with cells aiming for a sub-confluent (70-80%) monolayer for each test well. Select well plate size to allow for a minimum of 3 replicates for each test solution and duplicate concentration ladders if quantitative measurements are desired.
- Allow seeded cells a minimum of 12 hours to attach to the well plate surface. Examine wells by microscope and reject any wells that are not of the correct confluency or that show signs of poor health (e.g. dead/sloughing cells).

Cytotoxicity Assay

- Aspirate the seeding medium, then aliquot test solutions into test wells. Use solution control medium for control wells and concentration ladder.
- Incubate well plate for defined exposure period (24 hours) under standard conditions (37°C, 95% air/5% CO_2, 95% humidity).
- Assess cell viability per the alamarBlue® assay (protocol 3.2.2) or by counting live and dead cells.

References

Biological evaluation of medical devices Evaluation biologique des dispositifs medicaux. Partie 1, Evaluation et essais Evaluation and testing. 2003, Geneva, Switzerland: ISO.

Lehmann, D.M. and Richardson, M.E., Impact of assay selection and study design on the outcome of cytotoxicity testing of medical devices: The case of multi-purpose vision care solutions. Toxicology in Vitro. **24**(4): p. 1306-1313.

3.2.2 alamarBlue® Cell Viability Assay

Objective

Quantitative or semi-quantitative assessment of cell viability

Materials

- Cell culture sample plate
- Cell culture medium (same composition as used to maintain sample plate in culture)
- Pasteur pipettes and vacuum source
- Pipette aid
- Serological pipettes
- μ-pipetters and pipette tips
- alamarBlue® reagent (Invitrogen, Carlsbad CA)
- Plate reader
- 0.25% w/v trypsin-EDTA
- Hemocytometer

Procedure

All procedures are to be performed using sterile technique in a biosafety cabinet (BSC) under aseptic conditions. All materials should be sterilized via autoclave or disinfected with 70% ethanol prior to introduction into the BSC. Sterile packaged materials are to be opened using sterile technique in the BSC.

Prepare alamarBlue® Solution

- Determine volume of alamarBlue® solution needed for assay; e.g. for a 48-well plate with 500 μl volume added to each well 24 ml will be required. Round-up to allow for pipetting errors.
- Prepare a 10% (v/v) solution of alamarBlue® reagent in cell culture medium in an appropriately-sized falcon tube. Example: for 25 ml, add 2.5 ml reagent to 22.5 ml medium. Mix by gently pipetting up and down a few times.

  Note: alamarBlue® is light-sensitive, so should be prepared immediately prior to use. If not used immediately, wrap the falcon tube in aluminum foil to limit light exposure

Conduct Assay

- Asipirate existing medium from each well of the well plate. Replace with an appropriate volume of prepared alamarBlue® solution, e.g. 0.5 ml per well for a 48-well plate.
- Incubate cell culture plate 1-4 hours.

Note: Preliminary experiments to determine optimal incubation for a particular cell line and plating density can be conducted. Seed a well plate with a minimum of two replicates of a concentration ladder spanning the range of cell densities you expect to encounter in your assay. Add alamarBlue® solution to wells and incubate. Read plate at 30-minute intervals and plot response. Select an incubation time that provides a linear response over the range of interest.

- Read plate on plate reader. Either fluorescence or colorimetric readings can be made, but the most accurate results will be achieved with fluorescence measurements.
- Fluorescence settings: excitation at 540-570 nm (peak=570 nm), emission at 580-610 nm (peak=585 nm)
- Colorimetric settings: absorbance at 570 nm normalized to 600 nm reference
- (Optional) For quantitative measurements, detach cells from concentration ladder wells with trypsin-EDTA and count with hemocytometer (refer to protocol 3.1.1, Cell Culture Basics, for counting procedure)

References

alamarBlue® Cell Viability Assay Protocol, Invitrogen™ Protocols, http://www.invitrogen.com

3.3 TISSUE CULTURE

3.3.1 Ovine Disc Tissue Harvest

Objective

Aseptic harvest of ovine lumbar intervertebral discs for isolation of nucleus pulposus and annulus fibrosus tissue/cells.

Materials

Chemicals and Reagents

- Sterile Dulbecco's Phosphate Buffered Saline (DPBS) with divalent cations
- Sterile Dulbecco's Modified Eagle Medium (DMEM)
- Penicillin-streptomycin
- 4-(2-Hydroxyethyl)piperazine-1-ethanesulfonic acid (HEPES), buffer

Biological Materials

- Fetal Bovine Serum (FBS)
- Ovine lumbar spine

Apparatus and Consumables

- Nitrile exam gloves
- 70% ethanol spray bottle
- Pipette aid
- Sterile serological pipettes
- Sterile disposable 0.22 µm vacuum filter unit
- Aluminum foil
- Scalpel blades (#10 and #60 blades, individually packaged)
- Scalpel handles
- Forceps
- Hemostats
- Osteotome
- Sterile tared Tissue Culture Polystyrene (TCPS) petri dishes
- Sterile pipette tips

Procedure

All procedures are to be performed using sterile technique in a biosafety cabinet (BSC) under aseptic conditions. All materials should be sterilized via autoclave or disinfected with 70% ethanol prior to introduction into the BSC. Sterile packaged materials are to be opened using sterile technique in the BSC.

Prepare Incubation Medium

- Set-up disposable vacuum filter in the BSC and attach vacuum line. While pulling vacuum, add the following to the filter funnel:
  - 1% HEPES
  - 1% penicillin-streptomycin
  - 78% DMEM
  - 20% FBS (most likely to clog filter, so always filter last)
- Label the medium container with the date, medium base and supplements, and initials.
- Bring medium up to 37°C prior to use, either in a water bath or small amounts may be aliquoted into an appropriate dish or plate and placed in the incubator to equilibrate to the appropriate temperature and pH.

Gross Dissection

- For ease of clean-up cover BSC work surface with a layer of aluminum foil; spray with 70% ethanol.
- Remove spine from packaging and spray exterior musculature with ethanol; if spine is already skeletonized avoid spraying discs.
- Using sterile forceps and scalpel begin gross dissection of musculature to expose spinal column.
  - Remove ventral musculature first (the ventral side w/o musculature is more stable than the dorsal side, making removal of muscle on the other side easier)
  - Replace scalpel blades often, especially after scraping bone
  - An osteotome can be used to remove tissue from the vertebral bodies and dorsal column.
  - Ensure removal/disruption of all ligaments between transverse processes, spinous processes, and around facet joints.

Tissue Harvest

- Dispose of foil from gross dissection and re-cover work surface with new foil sprayed with ethanol and wiped-down.
- Place covered TCPS Petri dishes (two per disc if separating NP and AF tissue) with sterile DPBS in safe location in hood.
- Use new scalpel blades to harvest disc tissue.
- Cut through the caudal-most disc axially and disarticulate the motion segment.
  - Remove sections of disc tissue from both the cranial and caudal vertebrae.
  - Separate nucleus pulposus (NP) from annulus fibrosus (AF) tissue.

  - Take care that the harvested tissues do not come into contact with other tissues.
  - Place harvested tissues into DPBS; use separate petri dishes for NP and AF.
  - Label dishes with disc level (e.g. L5-L6 for disc between L5 & L6 vertebrae)
- Continue harvest with new scalpel blade for next caudal-most disc until all lumbar discs are harvested.
- Clean out hood and disinfect with ethanol.

Weighing Tissue

- Using sterile forceps or hemostats, rinse tissue thoroughly with sterile room temperature DPBS with divalent cations.
- Transfer the harvested tissue to tared sterile TCPS petri dish.
- Weigh and record the weight change to determine the wet weight of disc tissue collected.

Tissue Quarantine

- Add 10 ml sterile incubation medium to each dish.
- Incubate under standard conditions (37˚C, 5% CO_2, 98% humidity) for 2 days to confirm no contamination occurred during harvest.
- Proceed to tissue culture if no contamination observed.

References

Chou, A.I., et al., *The effect of serial monolayer passaging on the collagen expression profile of outer and inner anulus fibrosus cells*. Spine, 2006. **31**(17): p. 1875-1881.

3.3.2 Ovine Nucleus Pulposus Tissue Culture

Objective

Maintenance of tissue *in vitro* for tissue integration study

Materials

- Nitrile exam gloves
- Disposable vacuum filter flask unit
- Pipet aid, e.g. Eppendorf Easypet®
    - Individually-packaged serological pipets (25, 10, 5 ml)
- 4-(2-Hydroxyethyl)piperazine-1-ethanesulfonic acid (HEPES)
- Fetal bovine serum (FBS)
- Ascorbic acid, cell culture tested
- Penicillin/Streptomycin
- Dulbecco's Modified Eagle's Medium/Nutrient Mixture (DMEM/F-12)
- Harvested ovine nucleus pulposus tissue (per protocol 3.3.1)
- Test materials (e.g. hydrogels)
- Agarose, 2% (w/v) in Milli-Q water
- 8 mm biopsy punch
- 24-well culture plate

Unless otherwise noted, all procedures are to be performed using aseptic techniques in a biosafety cabinet (BSC) under sterile conditions. All materials should be sterilized via autoclave or disinfected with 70% ethanol prior to introduction into the BSC. Packaged materials are to be opened using sterile technique in the BSC.

Prepare Incubation Medium

- Set-up disposable vacuum filter in the BSC and attach vacuum line. While pulling vacuum, add the following to the filter funnel:
    - 1% HEPES
    - 1% penicillin-streptomycin
    - 78% DMEM
    - 20% FBS (most likely to clog filter, so always filter last)
- Label the medium container with the date, medium base and supplements, and initials.
- Bring medium up to 37°C prior to use, either in a water bath or small amounts may be aliquoted into an appropriate dish or plate and placed in the incubator to equilibrate to the appropriate temperature and pH.

Prepare Tissue Culture Plates

- Punch 8 mm disc of NP tissue using biopsy punch. Place NP discs into individual wells of 24-well plate
- Punch 8 mm discs of test material. Test materials should have been disinfected by rinsing in ethanol and swelling in a minimum of three changes of sterile PBS over a 24-hour period.
- Layer test material over NP tissue in well plate. Seal tissue and test material in apposition to each other with agarose.
- Add incubation media to each well, filling to approximately 75% of the well height.

Incubation

- Place prepared well plate into incubator maintained at 37°C, 95% air/5% CO_2 atmosphere, 95% humidity
- Change media every 2-3 days until experimental end point

References

Harris, J., *Hyaluronan grafted high density polyethylene copolymer for articular cartilage tissue engineering* [M.S. Thesis]. Fort Collins, CO: Colorado State University (Mechanical Engineering); 2009.

APPENDIX B: CHARACTERIZATION REFERENCE DATA

Chemicals Used in Research

Table B1: Chemical structures and molecular formulae

CoPEMA *Hyaluronan*-co-*poly(ethylene*-alt-*maleic anhydride)*	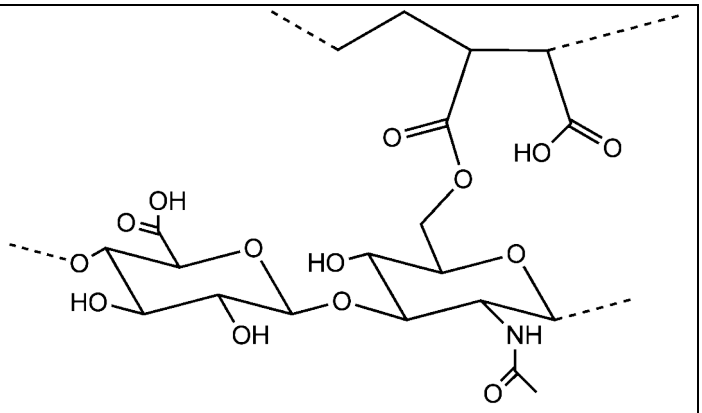
Copoly *Hyaluronan*-co-*polyethylene*	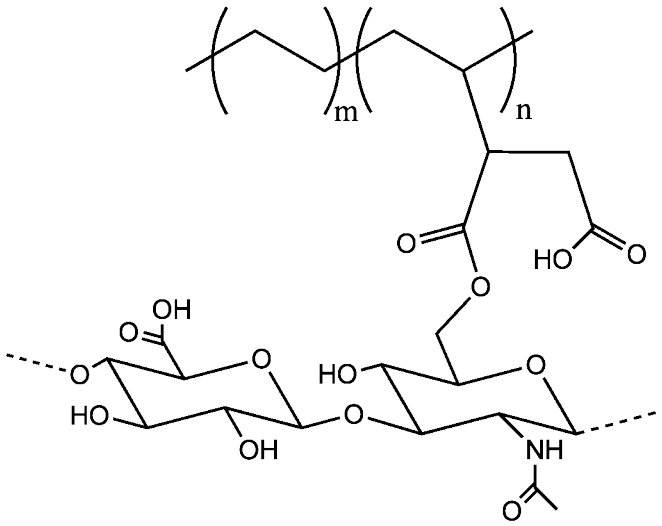
CTAB *Cetyl trimethylammonium bromide* $(C_{16}H_{33})N(CH_3)_3Br$	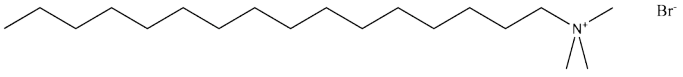
Dimethyldichlorosilane $(CH_3)_2Cl_2Si$	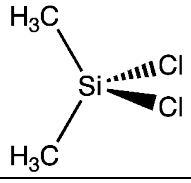

DMSO *Dimethyl sulfoxide* $(CH_3)_2SO$	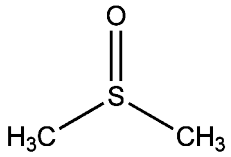
HA *Hyaluronan, hyaluronic acid* $(C_{14}H_{21}NO_{11})_n$	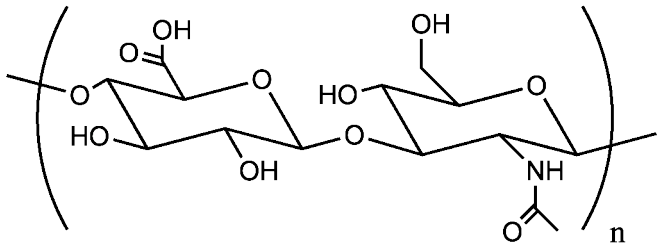
HA-CTA *Hyaluronan-cetyl trimethylammonium complex*	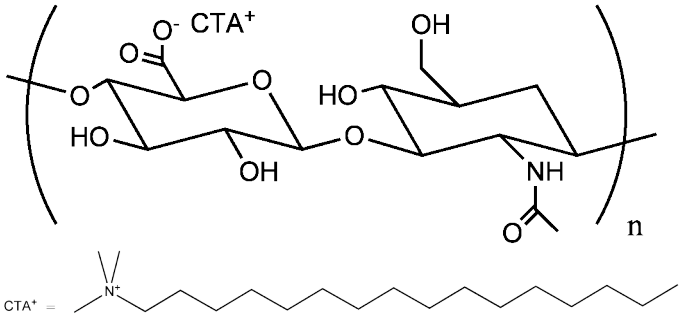
PE-*g*-MA *Polyethylene*-graft-*maleic anhydride*	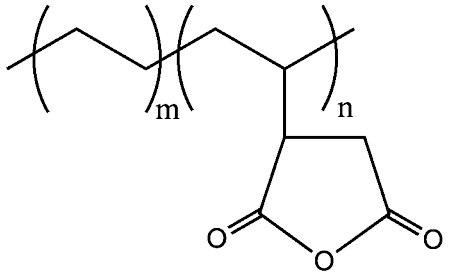
PEMA *Poly(ethylene*-alt-*maleic anhydride)*	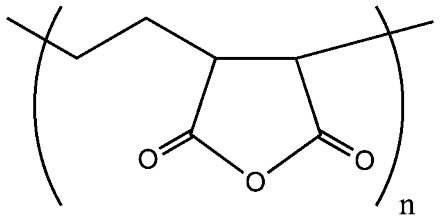
PDMS *Polydimethylsiloxane* $(C_2H_6OSi)_n$	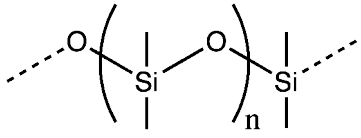

Fourier Transform Infrared Spectroscopy (FTIR)

Hyaluronan (HA)

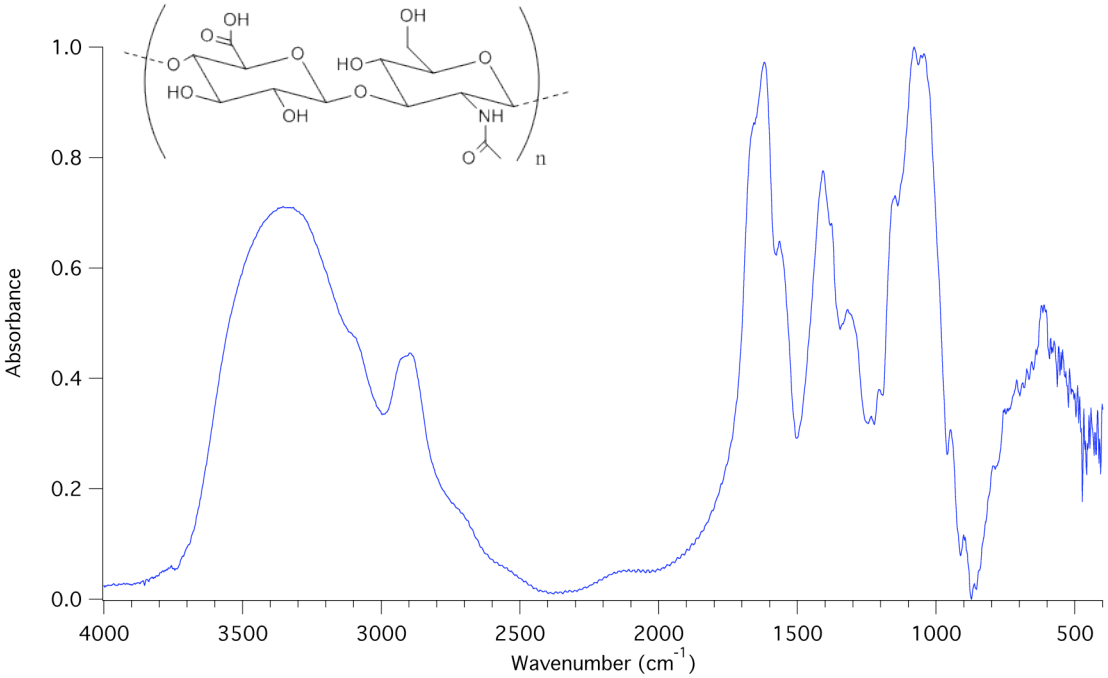

Figure B1: FTIR reference spectrum for hyaluronan

Table B2: FTIR peak identification for hyaluronan

Peak Location (cm^{-1})	Functional Group	Comments
3340	-OH	Broad peak due to intermolecular interaction (hydrogen bonding)
2890	-OH	Bonded OH in carboxlic acid
1622	$-COO^-$	
1405	-COOH	
1313	secondary amide	
1040	CH_2OH	

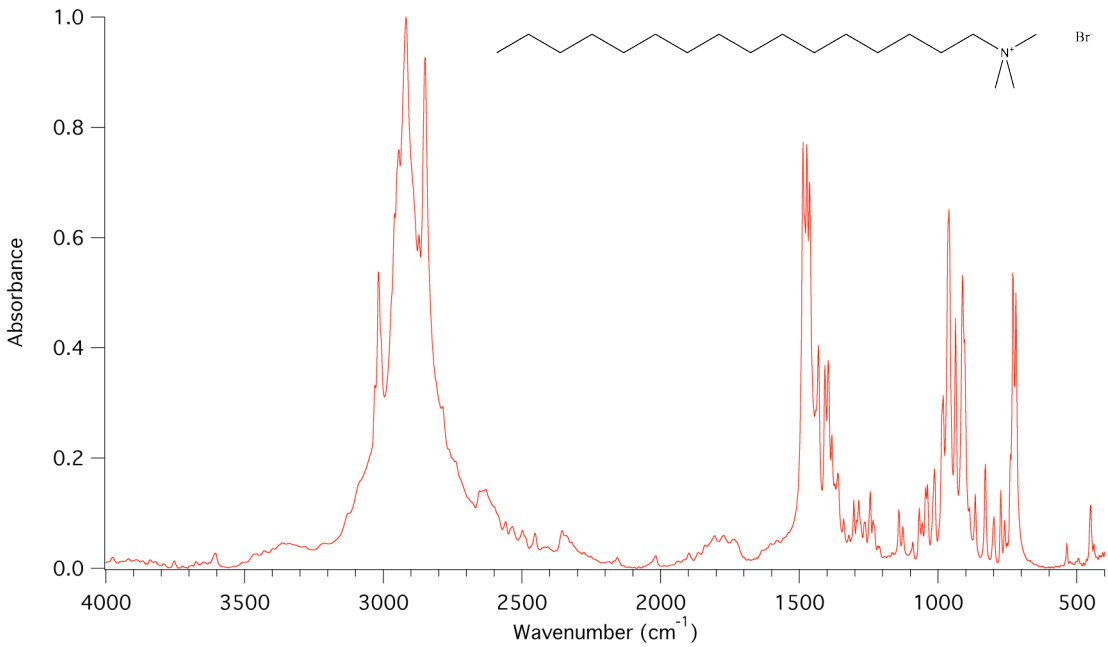

Figure B2: FTIR reference spectrum for CTAB

Cetyl trimethylammonium bromide (CTAB)

Table B3: FTIR peak identification for CTAB

Peak Location (cm^{-1})	Functional Group	Comments
3017.19	C-H	
2917.61	CH_2, CH_3	Asymmetric vibration
2849.19	CH_2	Symmetric vibration
1462.93	C-CH_2, C-CH_3	Scissors, asymmetric bend
1430-1390	C-N	
960.91, 911.73	CH_2=CH_2	

Hyaluronan-cetyl trimethylammonium complex (HA-CTA)

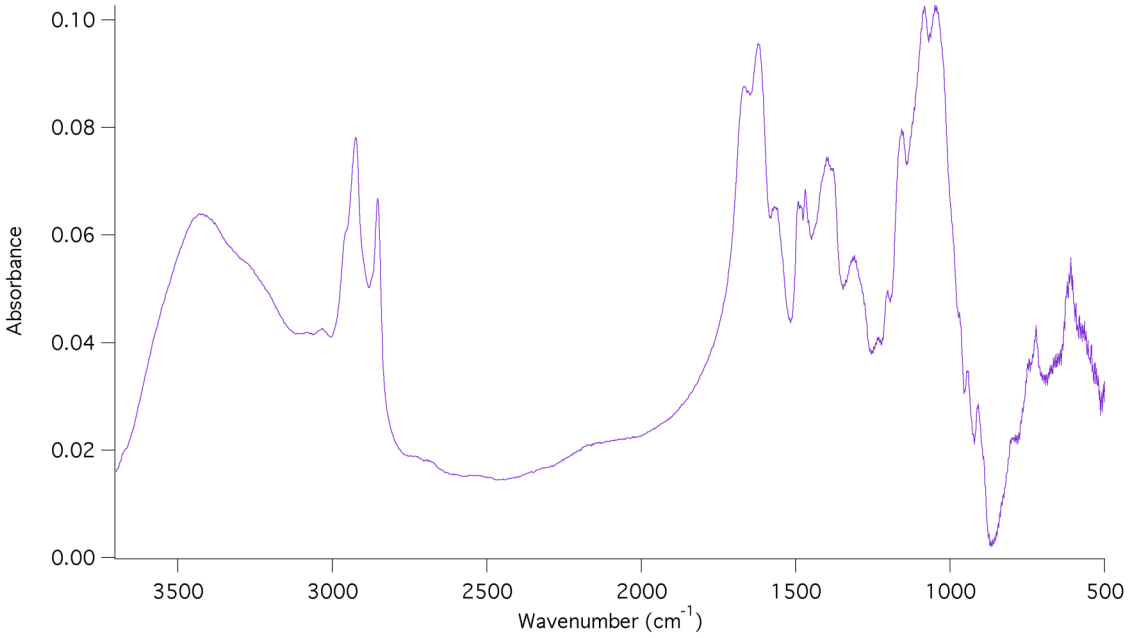

Figure B3: FTIR reference spectrum for HA-CTA

Table B4: FTIR peak identification for HA-CTA

Peak Location (cm^{-1})	Functional Group	Comments
3430.34	-OH	
2924.25	CH_2, CH_3	Asymmetric vibration
2853.21	CH_2	Symmetric vibration
1621.4	-COO	
1468.42	C-CH_2, C-CH_3	Scissors, asymmetric bend
1399.88	-COOH	
1309.67	secondary amide	
1048.84	CH_2OH	

Poly(ethylene*-alt-*maleic anhydride) (PEMA)

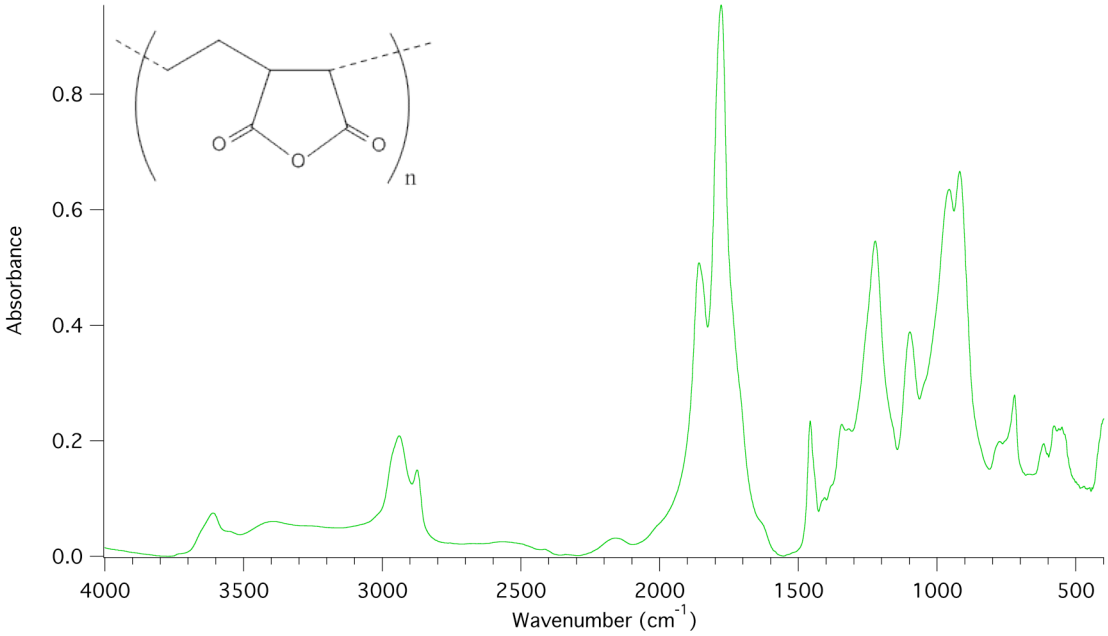

Figure B4: FTIR reference spectrum for PEMA

Table B5: FTIR peak identification for PEMA

Peak Location (cm^{-1})	Functional Group	Comments
3609.43	Bonded OH	
2939.01	CH_2	Symmetric vibration
1857.95	C=O	Cyclic anhydride symmetric
1778.29	C=O	Cyclic anhydride asymmetric
1457.21	C-CH_2	Scissors vibration
1222.87, 1097.97	C-C	Cyclic anhydride stretch
956.45, 918.24	C-O	Cyclic anhydride stretch

Thermogravimetric Analysis (TGA)

Hyaluronan

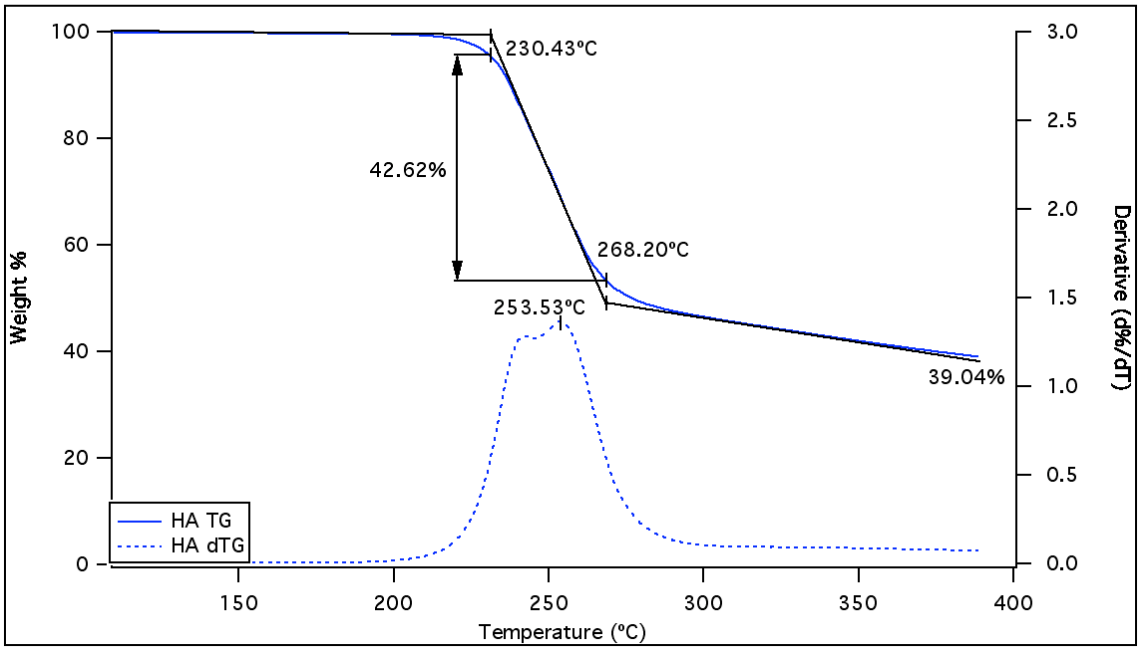

*Poly(ethylene-**alt**-maleic anhydride)*

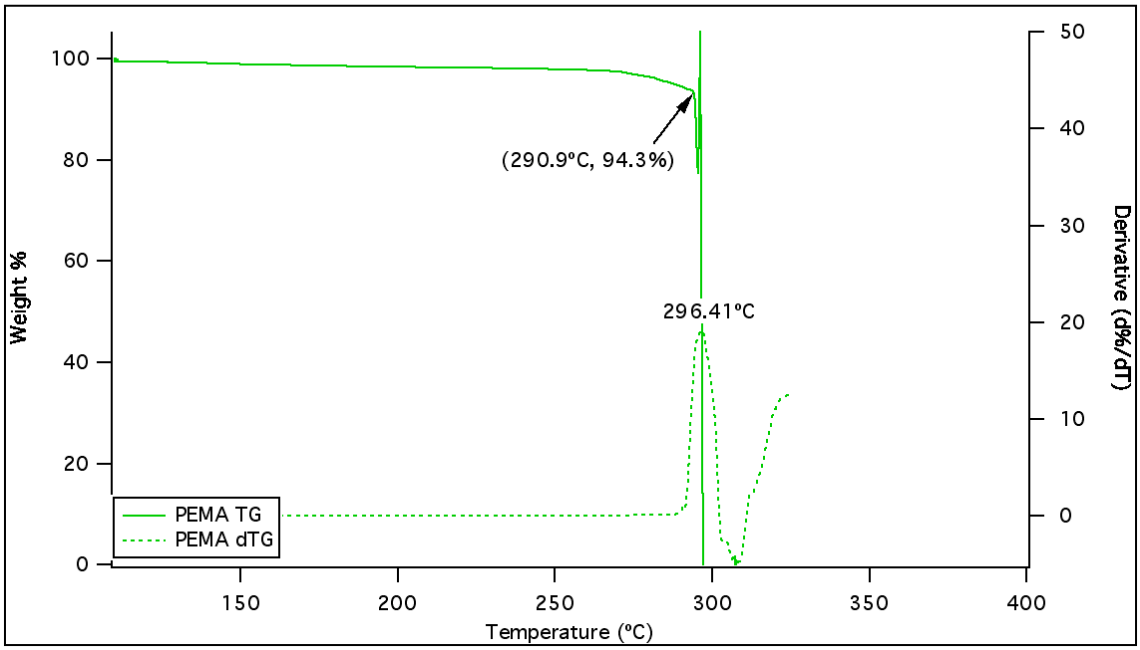

Figure B5: TG and dTG traces for HA and PEMA

^{1}H Nuclear Magnetic Resonance (NMR)

Poly(ethylene*-alt-*maleic anhydride)

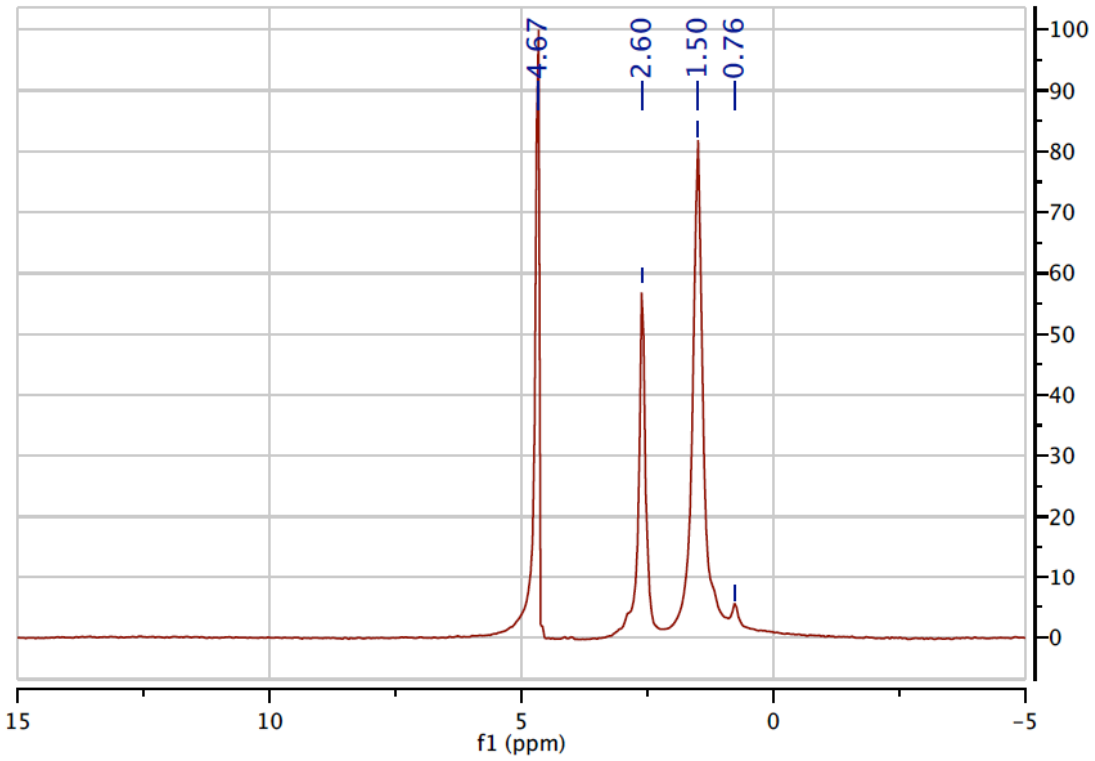

	ppm	Intensity	Width	Type
1	4.67	107.2	25.02	Compound
2	2.60	58.1	35.66	Compound
3	1.50	82.0	59.31	Compound
4	0.76	5.7	63.51	Compound

Figure B6: ^{1}H NMR reference spectrum and peak identification for PEMA

Cetyl trimethylammonium bromide (CTAB)

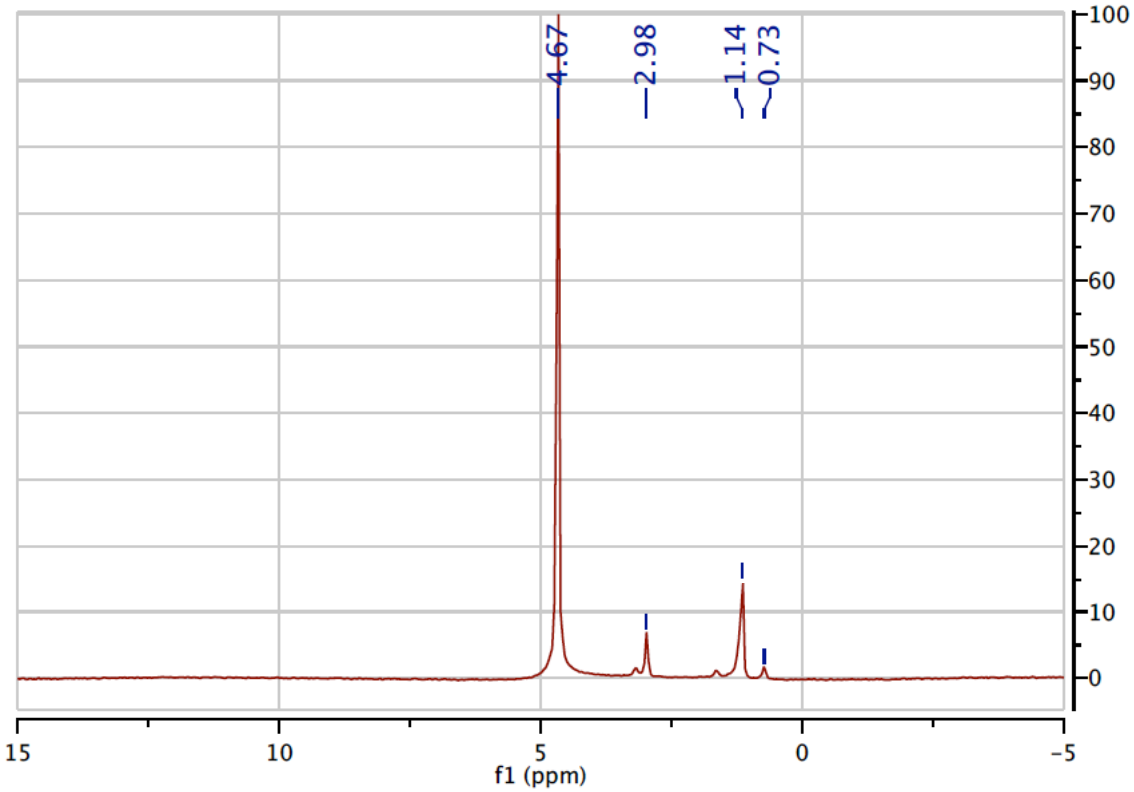

	ppm	Intensity	Width	Type
1	4.67	101.4	18.18	Compound
2	2.98	7.0	18.26	Compound
3	1.14	14.8	25.52	Compound
4	0.73	1.8	20.57	Compound

Figure B7: ^{1}H NMR reference spectrum and peak identification for CTAB

APPENDIX C: COPOLYMER DESIGN

In previous work conducted in the James Laboratory [1-5], HA-*co*-HDPE copolymer design came down to a matter of choosing the HA molecular weight, the PE molecular weight, and the relative ratio of HA to PE. For example, in lubricious solids for load bearing applications a high PE content was chosen since mechanical strength is derived from the crystalline microstructure in the polyethylene phase. On the other hand, the polyethylene phase was a minor component in the viscous fluid for DBM putties; its role was to alter the rheologic behavior of a concentrated HA solution and to bind to the DBM proteins through hydrophobic interactions. In these cases the HA:PE weight ratio was used to describe the formulation, e.g. 10:90 for the lubricious solid and 99:1 for the viscous fluid.

Commercial HA is either purified from biological sources (e.g. rooster comb) or synthesized via microbial fermentation and is available in a wide range of molecular weights (5×10^3 Da – 2.6×10^6 Da, Lifecore Biomedical; 0.5×10^6 Da – 4.0×10^6 Da, Genzyme). While physiologic HA is on the order of 4-5 MDa, other factors must be considered in selecting an appropriate molecular weight for copolymerization. Chiefly, since the copolymer is synthesized via bulk polymerization, reaction efficiency can be expected to decrease as HA chain length increases since entanglement of the chains will inhibit mixing of the polymers and limit the sites available for interaction with the

reactive groups of the synthetic polyolefin phase. Thus, an HA of moderate size was chosen for this work.

The constituent ratios for different copolymer formulations have previously been described as end-product weight ratios, but it is in fact the maleic anhydride (MA) to HA ratio that drives the extent of reaction. In the case where a hydrogel network structure is desired, the poly(ethylene-*alt*-maleic anhydride) (PEMA) acts as a linking agent between HA chains , noting that a minimum of two ester bonds are required to form a link. An infinite network first appears at the "gel point," or critical extent of reaction (p_c) which is given by

$$p_c = \frac{1}{\sum_{i=1}^{\infty} w_i (N_i - 1)} \approx \frac{1}{\sum_{i=1}^{\infty} w_i N_i} = \frac{1}{N_w}$$

where N_i describes the degree of polymerization of the i^{th} chain, w_i is the weight fraction of N_i-mers, and N_w is the weight-average degree of polymerization [6]. Assuming a perfectly efficient reaction, Equation 1 suggests that a network can form with a minimum of one crosslink (two ester bonds) per HA chain. Knowing the minimum number of bonds desired, it became apparent that commercially-available maleic anhydride-grafted polyethylenes (MA-*g*-PE) were not suitable for this application. In the commercial products the PE molecular weight decreases as MA graft content increases, resulting on average in the same number of MA groups per PE chain.

The following equations illustrate how to calculate some basic design parameters for the HA-*co*-PEMA copolymer given the reactant masses and molecular weights. The simplest design specification is the weight ratio of the reactants. Further, two types of

molar ratios are considered: (1) a "network" ratio that enumerates an average number of MA reactive groups per HA chain and (2) a "reactive" ratio that quantifies the reactive groups. The former can be related to a theoretical maximum link density, where a minimum of two (2) ester bonds are required to form a PEMA link between HA molecules. The latter is the more traditional molar ratio used in synthetic polymer chemistry.

Basic Design Parameters and Nomenclature

The following parameters are assumed to be known, either by manufacturer specification, calculation, or laboratory measurement:

- Mass of reactants (HA-CTA and PEMA)
- Formula weights
  - HA (401.3 g/mol)
  - HA-CTA (662.8 g/mol)
  - MA (98.06 g/mol)
  - PEMA (126.11 g/mol)
- Molecular weight (M_w) of HA used to synthesize HA-CTA

The following parameters are also useful, but not often provided in manufacturer specifications:

- Number-average molecular weight (M_n) for reactants
- Polydispersity Index (PDI) for reactants

Weight Ratio

The weight ratio is the simplest of the design parameters, but can be viewed in a number of ways, e.g. the weight ratio of the reactants (HA-CTA and MA-*g*-HDPE) or the intended weight ratio of the primary product constituents (HA and PE). For consistency with previous work, the weight ratio here is defined as the intended weight ratio of the product.

$$mass\ HA = \left(mass\ HA - CTA\right)\left(\frac{formula\ weight\ HA}{formula\ weight\ HA - CTA}\right)$$

$$mass\ PE = \left(mass\ PEMA\right)\left(\frac{formula\ weight\ PE}{formula\ weight\ PEMA}\right)$$

$$mass\ fraction\ HA = \frac{mass\ HA}{mass\ HA + mass\ PE}$$

$$mass\ fraction\ PE = \frac{mass\ PE}{mass\ HA + mass\ PE}$$

$$weight\ ratio = mass\ fraction\ HA \times 100 : mass\ fraction\ PE \times 100$$

Network Ratio

The network ratio is defined as the moles of reactive maleic anhydride groups to the number of hyaluronan chains. Note that molecular weights as specified by commercial manufacturers are typically weight average (M_w) molecular weights rather than number average (M_n); as a result the number of HA chains will be under-estimated. A correction can be incorporated if the polydispersity index (PDI) is known.

$$mass\ MA = \left(mass\ PEMA\right)\left(\frac{formula\ weight\ MA}{formula\ weight\ PEMA}\right)$$

$$mol\ MA = \frac{mass\ MA\ (g)}{molar\ mass\ MA\ (g/mol)}$$

$$mol\ HA\ chains = \frac{mass\ HA\ (g)}{(PDI)\left[M_w\ HA\ (g/mol)\right]}$$

$$Network\ ratio = \frac{mol\ MA}{mol\ HA\ chains} : 1$$

Reactive Ratio

The reaction mechanism theorized for HA-*co*-HDPE is a ring-opening esterification of the maleic anhydride by nucleophilic attack from an HA hydroxyl group. Thus, the reactive ratio compares the concentration of MA to OH, where four (4) OH

groups are available per HA repeat unit. For the purposes of this calculation it is assumed that all groups are equally reactive, though steric hinderances will likely affect the relative reactivity of OH groups.

$$mol\ OH = \left(\frac{mass\ HA(g)}{molar\ mass\ HA(g/mol\ r.u.)} \right) \left(\frac{4\ OH}{HA\ r.u.} \right)$$

$$mol\ MA\ calculated\ as\ in\ network\ ratio$$

$$reactive\ ratio = 1 : \frac{mol\ OH}{mol\ MA}$$

Hydrogel Design Concepts

The initial design concepts for the copolymer developed in this work were based upon modifications to HA-*co*-HDPE. PEMA was identified as a commercially-available polymer that could potentially be used to increase the maleic anhydride content of the reactants.

To increase the maleic anhydride moieties available in the reaction, PEMA could be added to the original copoly reaction ("Tripoly") or it could completely replace the MA-*g*-HDPE ("Copoly Gel"). By adding the PEMA to the original copoly, the crystalline polyethylene domains contributed by the HDPE would be preserved. These domains were considered desirable in that they would contribute some mechanical strength as well as large hydrophobic domains potentially allowing for physical interactions with hydrophobic domains on other molecules, e.g. proteins. Substituting PEMA for MA-*g*-HDPE would lose these crystalline polyethylene regions, but would simplify the reaction scheme to a single phase since both PEMA and HA-CTA are soluble in DMSO. In the original copoly reaction scheme, MA-*g*-HDPE is dissolved in

xylenes and the reaction with HA-CTA in DMSO requires an interfacial emulsion polymerization process since xylenes and DMSO are immiscible.

Since emulsion polymerization processes are difficult to control, 1,2,4-trichlorobenzene (1,2,4-TCB) was evaluated as a substitute for xylenes in the tripoly reaction. While still capable of solvating MA-*g*-HDPE, 1,2,4-TCB exhibits better miscibility with DMSO. While different tripoly constituent ratios were explored, the general synthesis method included solvating MA-*g*-HDPE in 1,2,4-TCB, adding PEMA dissolved in DMSO, then allowing the two solutions to mix thoroughly in hopes that the PEMA and MA-*g*-HDPE would become entangled. Once thoroughly mixed, the PEMA/MA-*g*-HDPE solution was reacted with HA-CTA in DMSO.

Figure C1 shows an FTIR spectrum for tripoly. The appearance of a broad ester bond peak around 1700 cm^{-1} seemed to be a promising indication of a successful reaction; this ester peak had not been seen previously in FTIR spectra for the various copoly formulations. However, after subsequent washing in acetone and analysis of the wash residue, it became clear that the MA-*g*-HDPE was not covalently bound into the polymer network to a substantial degree. In this one-step reaction the PEMA evidently out-competed the MA-*g*-HDPE for reaction sites on the HA-CTA. Synthesizing a true "tripolymer" would require a two-step reaction, i.e. a "copoly" reaction (in either xylenes or 1,2,4-TCB) followed immediately by a reaction with PEMA and the unhydrolyzed copoly reaction product.

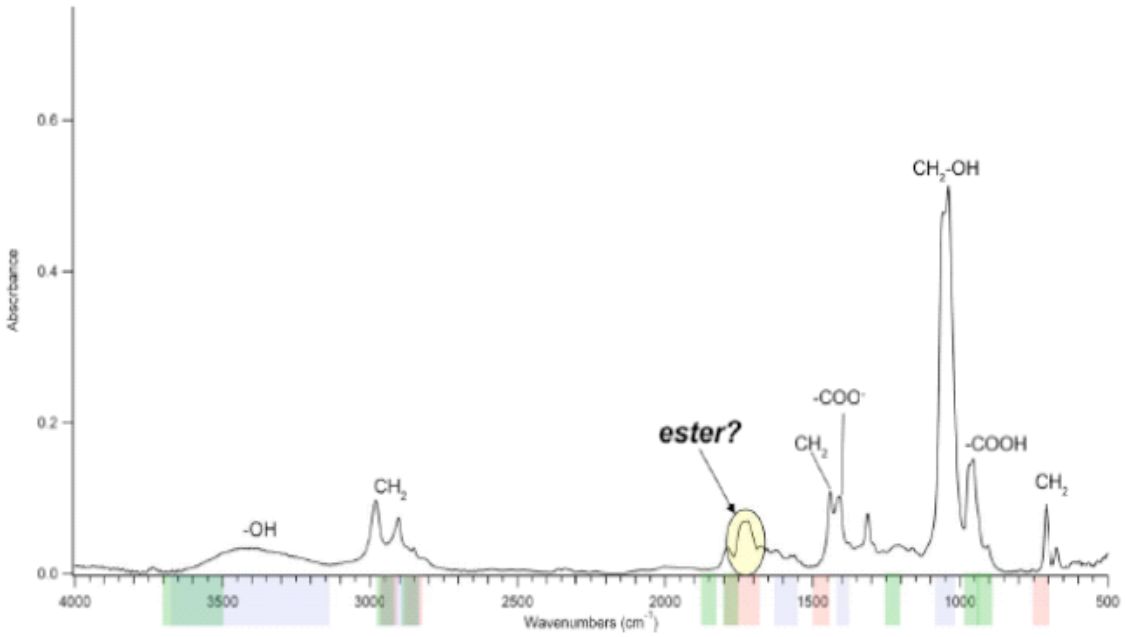

Figure C1: FTIR spectrum for "tripoly." The appearance of a probable ester peak was taken as an indication of a successful reaction; subsequent analysis revealed that the ester bonding was primarily due to PEMA and that the MA-g-HDPE was not substantially bound into the network.

Given that the efforts to synthesize a "tripoly" was not bearing fruit, focus was placed upon the reaction of HA-CTA with PEMA alone. Replacing the MA-*g*-HDPE with PEMA proved to be a more consistent route to producing hydrogels. A single-phase reaction was possible, since both PEMA and HA-CTA are soluble in DMSO. A further advantage is that both reactants can be solvated in DMSO at 80-90°C, a relatively low temperature well below the degradation temperature for HA-CTA. The consistency of the resultant gels varied with solution concentration as well as the relative ratio of reactants. The highest practical concentrations for HA-CTA and PEMA were determined empirically and carried forward to the research described in the body of this dissertation.

References

1. Cranson, C.N., *A Novel Hyaluronan-Polyethylene Graft Copolymer as a Carrier for Demineralized Bone Matrix* [M.S. Thesis]. Fort Collins, CO: Colorado State University (Mechanical Engineering); 2008.

2. Harris, J., *Hyaluronan grafted high density polyethylene copolymer for articular cartilage tissue engineering* [M.S. Thesis]. Fort Collins, CO: Colorado State University (Mechanical Engineering); 2009.

3. James, S.P. and Kurkowski, R., inventors. *Copolymer synthesized from modified glycosaminoglycan, GAG, and an anhydride functionalized hydrophobic polymer*. USA patent PCT/US08/05054. April 18, 2008.

4. Kurkowski, R., *The chemical crosslinking, compatibilization, and direct molding of ultra high molecular weight polyethylene and hyaluronic acid microcomposites* [M.S. Thesis]. Fort Collins, CO: Colorado State University (Mechanical Engineering); 2007.

5. Oldinski, R.A., *Development of a hyaluronan-polyethylene copolymer for use in articular cartilage repair* [Ph.D. Dissertation]. Fort Collins, CO: Colorado State University (Mechanical Engineering); 2008.

6. Hiemenz, P.Z. and Lodge, T.P., *Polymer Chemistry*. Second ed. 2007, Boca Raton, FL: CRC Press.

APPENDIX D: REU PROGRAM RESEARCH REPORT

A significant portion of the chemistry experiments leading to the development of the HA-*co*-PEMA hydrogel were performed by Ariane Vartanian. Ariane came to us through the Department of Chemistry's National Science Foundation-sponsored Research Experience for Undergraduates (NSF REU) program during the summer of 2009. Ariane's final research report is contained here in its entirety.

Synthesis of a hyaluronan-polyethylene copolymer hydrogel for orthopedic repair

Ariane Vartanian*†
Susan Yonemura and Susan P. James‡

Abstract

Hyaluronan-high density polyethylene graft copolymer (HA-*co*-HDPE, or Copoly) has previously been synthesized from hyaluronan (HA), a glycosaminoglycan, and high density polyethylene (HDPE), a synthetic plastic. HA-*co*-HDPE combines the mechanical properties of polyethylene with the lubricating benefits of hyaluronan; due to its biocompatibility, it may be a promising material for meniscal cartilage replacement or injectable nucleus pulposus repair. The following study attempts to improve upon the chemistry of the original reaction in order to synthesize a hyaluronan-polyethylene copolymer that behaves as a true hydrogel.

Introduction

Biocompatible hydrogels serve as practical materials in orthopedic medicine. A true hydrogel network will swell and preserve structural integrity in a water or saline environment, which are advantageous properties for materials used in orthopedic replacements or repair. An ideal hydrogel for such applications would feature both the mechanical strength of polyethylene (PE), a plastic used in artificial joints, and the lubricating character of hyaluronan (HA), the "gooey" glycosaminoglycan found throughout the body. Previous studies[1] synthesized an HA-PE copolymer (HA-*co*-PE) from ammonium cation-complexed HA and maleated PE, via esterification reactions between the primary hydroxyls of the HA chain and maleic anhydride (MA) groups grafted onto the polyethylene backbone. However, this original HA-*co*-PE lacked mechanical integrity when swollen in water. The objective of this research was to synthesize a hyaluronan-polyethylene copolymer that behaves as a true hydrogel.

Several approaches are described here. The original copolymer reaction was repeated, replacing 1,2,4-trichlorobenzene for xylenes as a more DMSO-miscible

* *Permanent* 116 Arcadia Avenue, Santa Clara, CA 95051; ariane.vartanian@gmail.com; *School* 500 College Avenue, Swarthmore, PA 19081; avartani@swarthmore.edu
†Department of Chemistry and Biochemistry, Swarthmore College, Swarthmore PA
‡School of Biomedical Engineering, Departments of Mechanical Engineering and Chemistry, Colorado State University, Fort Collins CO

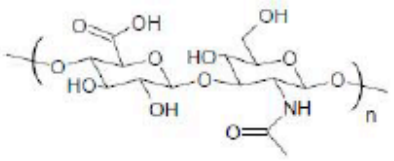

Figure 1 Hyaluronan is a hydrophilic glycosaminoglycan found in synovial fluid and coating articular cartilage, known for its lubricating properties.

Figure 2 Polyethylene is a hydrophobic durable thermoplastic often used in artificial joints.

solvent in order to increase the reactive interface. An HA amide reduction experiment was also conducted in an attempt to functionalize HA with crosslinker-compatible primary amine reactive groups. Finally and most promisingly, a collection of copolymers with varying ratios of PE-*g*-MA, HA-CTA, and a new functionalized polyethylene were synthesized, crosslinked, and characterized by swell tests and FTIR.

Hyaluronan Amine Functionalization

The glycosaminoglycan hyaluronan contains one glucuronic acid residue, a carboxylic acid structurally similar to glucose, and one acetylglucosamine residue, an amide linking glucosamine and acetic acid. Although it boasts several reactive functional groups including a primary alcohol, an secondary amide, and a carboxylic acid, it is noticeably missing a primary amine. A primary amine is a useful functional group for such crosslinking methods as genipin, a natural and non-toxic molecule that has previously been used to crosslink amine-containing proteins and polysaccharides, and reductive alkylation crosslinking with polyaldehydes synthesized from natural molecules. Since the desired HA-*co*-PE product is projected for biomedical applications, these low-toxicity crosslinkers are preferable to the current cytotoxic array of HA crosslinkers.

Genipin is already safely used as an injectable *in vivo* crosslinker and is both widely-available and convenient. It uses two reaction schemes, one for each linked compound. In the first, the amine nucleophilically attacks the genipin di-

hydropyran ring, opening and reforming it as a nitrogen-containing heterocyclic compound. The second scheme is an S_N2 nucleophilic substitution as the amine attacks the ester[2]. A genipin-compatible material would be especially useful in nucleus pulposus repair, since the copolymer could ideally be injected into the disc as a liquid and crosslinked and gelled *in vivo*.

Reductive alkylation is a lesser-known but promising biocompatible crosslinking method[3,4]. The polyaldehyde crosslinker is simply a periodate-oxidized macromolecule, such as sucrose, starch, or cellulose, and thus is likely to be biocompatible, inexpensive, and environment-friendly. The primary amine nucleophilically attacks an aldehyde, forming an imine; addition of a reducing agent such as $NaBH_4$ will achieve the final crosslinked product.

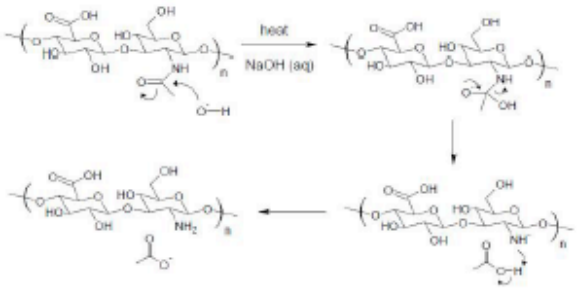

Figure 3 Base-catalyzed hydrolysis of the secondary amide of hyaluronan to a primary amine.

This experiment attempts to functionalize hyaluronan with a primary amine group. The available 2° amide may serve as a convenient starting point if the acetylglucosamine can be reduced to a glucosamine by deacetylation. In order to lose a degree of substitution (2° amide to 1° amine), a simple reduction with $LiAlH_4$ or a Hofmann degradation will not work. Chemical hydrolysis was explored in this study. HA is known to degrade in acid or alkaline conditions, and because hydrolysis is a random process, it is likely to result in monosaccharide or oligosaccharide units and byproducts that may or may not behave like native HA[5]. Base-catalyzed hydrolysis is known to prefer the acetylglucosamine residue, the residue of interest, due to the electrophilic nature of the basic reaction; acids prefer to catalyze the glucuronic acid. Unfortunately, the amide is not the only hydrolytically active site on the acetylglucosamine; hydrolysis will also target the ring oxygen and the C1 atom, the latter of which may result in glycosidic bond cleavage and chain scission[6]. However, under mild enough conditions hydrolysis may be effective in reducing the amide group without severely degrading the HA. Because the acetylglucosamine also features

a reactive 1° hydroxyl, which reacts with the maleic acid in the copolymer esterification reaction, it is possible that hydrolyzing HA-*co*-HDPE rather than HA may reduce undesirable reactions since the hydroxyl will have been already consumed.

This study merely attempted to reduce the amide group, and future work can focus on limiting degradation by altering pH, reaction time, and temperature. 0.1M NaOH(aq) solution was added to either HA or HA-*co*-HDPE powder and heated to 50°C for 12 hours while being stirred vigorously. Base-catalyzed hydrolysis reactions are typically carried under reflux temperatures[7], but the temperature was set conservatively due to HA's lability.

The dried product was analyzed with FTIR and compared to a control to determine any change in amide, amine, or potential byproduct stretches. An FTIR subtraction analysis clearly demonstrated positive change in the primary amine and carboxylate ion (byproduct) stretches, which is indicative that hydrolysis did indeed occur. However, a qualitative viscosity test between the HA control and the hydrolyzed HA suggested that the hydrolyzed HA degraded; milder conditions should be used in the future.

HA-co-HDPE reaction in 1,2,4-TCB and DMSO

The original Copoly reaction was performed with PE-*g*-MA in xylenes and HA-CTA in DMSO; no known solvent exists that can solvate both reactants. Since xylenes and DMSO are fairly immiscible, it is likely that the esterification occurs at a single reaction interface, a "surface" between the two solvents at which the two reactants can interact. Replacing xylenes with a more DMSO-miscible solvent, such as 1,2,4-trichlorobenzene (TCB), may increase the space into which both reactants can venture and come into contact.

A miscibility test comparing TCB/DMSO and xylenes/DMSO was performed in order to confirm the improved miscibility of TCB. The Copoly protocol was followed with TCB replacing xylenes. As hoped, a product with new properties was formed: unlike Copoly, the final product was fibrous and tough. In water, however, it disintegrated and did not appear to swell.

CopolyGel: Functionalized PE and HA-CTA

The maleic anhydride to hydroxyl (MA:OH) reactive ratio of the Copoly reaction is 1:185; that is, the hydroxyl is in extreme excess. (The "perfect" ratio is 1:4, since HA contains four hydroxyl groups, only one of which is primary and thus reactive.) In order to optimize the molar ratio, a polyethylene incorporating more reactive functional groups is ideal. For this purpose a new functionalized polyethylene (Functionalized PE)[1] was chosen to replace polyethylene-*graft*-maleic anhydride, which featured only 3% maleic anhydride by weight. Functionalized PE shifts the reactive ratio in favor of the new functional group.

[1]The results of this research are currently pending patent protection, so some information cannot be disclosed.

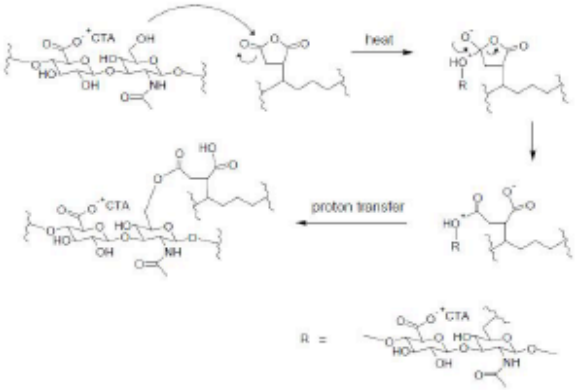

Figure 4 The esterification reaction between maleated polyethylene and HA-CTA.

However, the structure of Functionalized PE, unlike the maleic anhydride-grafted PE, does not contain a polyethylene backbone, so it may not behave like true polyethylene. In fact, it cannot form the random crystalline segments that provide polyethylene its characteristic strength, and any network it forms with HA could potentially lack necessary mechanical integrity.

CopolyGel was synthesized in two formulations, a 85:15 or 70:30 HA:PE final product ratio, so that it could be compared to Copoly materials of similar product composition. Functionalized PE and HA-CTA were dissolved in DMSO separately, then reacted together at 90°C for 12 hours. (A single solvent flask reaction yielded similar results, but separate solvent flasks are recommended to ensure homogeneity.) Hydrolysis, precipitation, washing, hydration, and drying steps were followed as according to the Copoly protocol, although isopropanol replaced ethanol as a washing agent but *not* as a precipitating agent as salt solutions are insoluble in isopropanol.

Both CopolyGel products behaved as hydrogels. 70:30 was stronger than 85:15 as expected by the relative amount of modified polyethylene present, but both swelled significantly in PBS, a saline solution that mimics physiological salt concentration (95.08% water after one hour for 70:30, 93.53% for 85:15) without falling apart. Still, they lacked the desired mechanical strength; the lubricated outer surface easily separated from the rest of the network, and too much agitation or pressure could cause the network to break apart entirely.

HMDI-Crosslinked CopolyGel

The diisocyanate crosslinker HMDI was explored as a potential avenue for increasing networking in CopolyGel. HMDI, or hexamethylenediisocyanate, crosslinks via an alcohol group on hyaluronan, so it can link together stray chains of HA that disrupt the mechanical integrity of the network. It is less toxic than the commonly used HA crosslinker gluteraldehyde, but due to its water sensitivity it cannot be used as an injectable *in vivo* crosslinker and requires toxic non-aqueous solvents. An ideal crosslinked gel strikes a balance between strength and swelling ability; a more crosslinked network will hold together tightly but may not be able to absorb much water.

Dry CopolyGel networks were soaked in excess 5% (v/v) HMDI/DMSO solution for approximately 20 hours under nitrogen. The samples were transferred to the vacuum oven at 50-70°C for 2 hours in order to cure the crosslinker, then washed with acetone and dried. The 70:30 CopolyGel swelled significantly in the HMDI solution, while 85:15 did not swell at all; this may be attributable to the possible excess of Functionalized PE in 70:30. It is likely that the crosslinking solution could not saturate the network and access loose HA strands, which is reflected in the swell tests (85.39% for 70:30 crosslinked, but 95.31% for 85:15 crosslinked, an increase). However, both crosslinked CopolyGels appeared qualitatively more resistant to stress; 70:30 was hardly lubricious and held together incredibly well in PBS. In order to improve crosslinking, a different CopolyGel- and HMDI-soluble solvent should be tested, and to optimize swelling ability, future work can use a more dilute HMDI solution and shorten the reaction time. This study utilized aggressive conditions to test the effectiveness of crosslinking.

TripolymerGel: Functionalized PE, PE-g-MA, and HA-CTA

While CopolyGel swelled significantly and maintained a network in water, it lacked mechanical strength and cohesion, breaking apart fairly easily under stress. Meanwhile, Copoly featured the might of polyethylene but never successfully behaved as a hydrogel. Thus a new polymer material, TripolymerGel, was synthesized to unite both features and create a sturdy, resilient hydrogel. Functionalized PE in DMSO and PE-*g*-MA in TCB were tangled together, effectively saturating the graft polyethylene with an abundance of functional groups and creating a reactive polyethylene backbone. This new functionalized polyethylene was reacted with HA-CTA; subsequent steps adhered to the Copoly protocol.

Two TripolymerGel compositions (85:10:5 and 70:15:15) were synthesized according to the amount of final HA to PE provided by each reactant, in the ratio HA:PE(from Functionalized PE):PE(from PE-*g*-MA). The 85:10:5 material was expected to behave similarly to CopolyGel 85:15 but with additional strength from the small amount of PE-*g*-MA; in other words, the crystalline character of PE-*g*-MA would serve to strengthen the hydrogel. The 70:15:15 material was designed such that the Functionalized PE would act as a compatibilizer,

functionalizing the PE-*g*-MA so that it would be more reactive.

As expected from the final product ratios, 70:15:15 displayed greater mechanical strength than 85:10:5, although both products held together extremely well and swelled significantly in PBS (96.72% for 85:10:5, 94.67% for 70:15:15). The properties of 85:10:5 resembled those of the nucleus pulposus: it was flexible, elastic, durable, and slippery. Meanwhile, 70:15:15 was more reminiscent of cartilage, tough and sturdy with a lubricated outer surface. Unlike the CopolyGel materials, which tended to break apart under stress and gradually lose some of its viscous surface, the TripolymerGel materials withstood both pressure and agitation and did not appear to lose any material even after several days.

HMDI-Crosslinked TripolymerGel

Although the TripolymerGels behaved extremely well in PBS, they were HMDI crosslinked to further improve networking. In keeping with the results from CopolyGel crosslinking, the 85:10:5 network did not swell at all in HMDI/DMSO, while 70:15:15 did slightly. Swell tests yielded expected results (94.66% for 85:10:5 crosslinked, 84.36% for 70:15:15 crosslinked). The crosslinked 70:15:15 was noticeably stiffer than the uncrosslinked version, although 85:10:5 felt only marginally tougher after crosslinking. As discussed in CopolyGel crosslinking, better crosslinking and swell results may be achieved with a different solvent, a less concentrated HMDI solution, or a shorter reaction time.

Conclusion

Of the many approaches described in this paper, crosslinked CopolyGel and the assortment of TripolymerGel materials are the most promising and applicable to a wide range of orthopedic functions. Further work will explore and improve the biocompatibility, swelling and mechanical properties of these hydrogels.

Acknowledgements

This project was funded by the National Science Foundation Research Experiences for Undergraduates and hosted by the Colorado State University Department of Chemistry during the summer of 2009. Susan Yonemura, Professor Sue James, and the other members of the James Group provided invaluble guidance and expertise during the course of this research.

References

[1]Kurkowski, R; James, SP (2008). *Copolymer synthesized from modified glycosaminoglycan, GAG, and an anhydride functionalized hydrophobic polymer.* U.S. Patent No. PCT/US09/05054. Colorado State University, Fort Collins, CO, USA.

[2]Butler, MF; Ng, Y; Pudney, PD. Mechanism and kinetics of the crosslinking reaction between biopolymers containing primary amine groups and genipin. *J Poly Sci* 2003. **41**, 3941-3953.

[3]Baran, ET; Mano, JF; Reis, RL. Starch-chitosan hydrogels prepared by reductive alkylation cross-linking. *J Mater Sci* 2004. **15**, 759-765.

[4]Pourjavadi, A; Aghajani, V; Ghasemzadeh, H. Synthesis, characterization and swelling behavior of chitosan-sucrose as a novel full-polysaccharide superabsorbant hydrogel. *J Appl Poly Sci* 2008. **109**, 2648-2655.

[5]Stern, R; Kogan, G; Jedrzejas, MJ; Soltes, L. The many ways to cleave hyaluronan. *Biotech Advances* 2007. **25**, 537-557.

[6]Tokita, Y; Okamoto, A. Hydrolytic degradation of hyaluronic acid. *Polymer Degradation and Stability* 1995. **48**, 269-273.

[7]Gu, L; Zhu, S; Hrymak, AN. Acidic and basic hydrolysis of poly(N-vinylformamide). *J Appl Poly Sci* 2002. **86**, 3412-3419.

APPENDIX E: DEMINERALIZED BONE MATRIX-REINFORCED GELS

Initial attempts at strengthening the HA-*co*-PEMA hydrogels focused upon the use of demineralized bone matrix (DBM) as a particulate reinforcing agent. DBM is a readily-available allogenic graft material with a long history of use in orthopaedic applications. With the mineral phase removed, DBM consists primarily of collagen and other bone proteins, including growth factors. These endogenous growth factors can elicit a regenerative healing response, thus the DBM was expected to play both a reinforcing role and a bioactive role. DBM has been shown to attract chondrocytes and NP cells and to be chondrogenic rather than osteogenic when used in avascular synovial environments [1-3].

Materials and Methods

Gel Synthesis

DBM-reinforced gels were cast by methods similar to those described in Specific Aim 2 of the dissertation research chapter. Briefly, concentrated solutions of HA-CTA in DMSO and PEMA in DMSO were prepared. DBM generously donated from Allosource (Centennial, CO) was ground using a cryogrinder and sieved to isolate particles in the size range between 100 μm and 250 μm. An unreinforced and two DBM-reinforced hydrogel formulations were synthesized; constituents for the gel formulations are

Table E1: DBM-reinforced gel formulations

Formulation	HA-CTA (g)	PEMA (g)	DBM (g)
Unreinforced	0.4	0.06	n/a
5:1 HA:DBM	0.4	0.06	0.05
3:1 HA:DBM	0.4	0.06	0.08

summarized in Table E1. The DBM and the concentrated solutions were combined and thoroughly mixed in 70x50 mm crystallizing dishes, then were placed in a vacuum oven to cure overnight.

Following curing, cast gels were soaked in acetone for four hours. Solvents were drained, then the gels were divided in half; one half was crosslinked using a 1% v/v solution of hexamethylene diisocyanate (HMDI) in DMSO, cured at room temperature for 24 hours. Crosslinked gels were soaked in several changes of acetone to remove excess HMDI. All gels were then hydrolyzed in a 0.2M NaCl aqueous solution with gentle agitation at room temperature. Hydrolyzed gels were vacuum dried, then were characterized by swell testing as described previously.

Rheometry

In preparation for mechanical testing, gels were swollen to equilibrium in deionized water (DI). Test samples (n=5 per group) were punched using an 8 mm biopsy punch and were maintained in DI until testing. Instrument setup and test methods used were as described in Specific Aim 2 for all 8 mm samples. For gels that were too compliant to reliably register torque within the detection range of the instrument using the 8 mm setup, a 25 mm serrated plate geometry was used if sufficient samples were available for the larger geometry. Unreinforced and 3:1 HA:DBM gels fell into this latter category. Crosslinked gels were also at the lower detection limit of the instrument, but there was insufficient gel available for 25 mm samples.

Results

Gel Synthesis

Figure E1: DBM-reinforced gels. DBM in the gel at left has denatured due to curing under an uncontrolled temperature profile. At right, a gel cured at 45°C for 12 hours.

During the initial attempts to cast DBM-reinforced gels, difficulty was encountered in controlling the temperature of the vacuum ovens used for curing. Gels were subjected to an unknown temperature profile, resulting in the denaturing of the DBM as evidenced by a change in color from white to golden-brown. A 3:1 DBM-reinforced gel was re-cast with a modified cure process; the crystallizing dishes into which the gels had been cast were sealed in N_2-charged vacuum bags and were placed into oil baths maintained at 45°C for 12 hours. The DBM in gels cast using this modified curing process did not exhibit signs of denaturation. Figure E1 compares a gel subjected to an uncontrolled temperature cycle to one maintained at a steady 45°C.

Swell Testing

Swell testing was performed using both DI and PBS as swelling media for gels produced during this experimental series, including crosslinked and denatured samples (n=2 per group). Figure E2 shows the difference in swelling behavior of un-

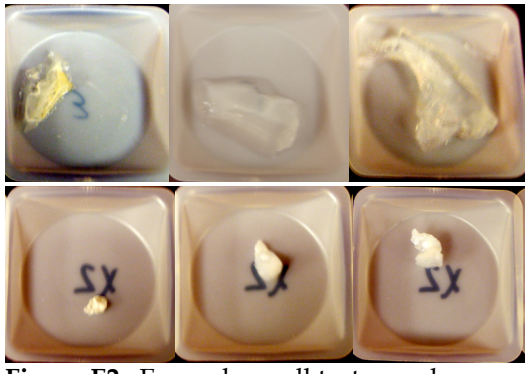

Figure E2: Example swell test samples. Unreinforced (top row) and crosslinked (bottom row) gels in a dry state (left column), swollen in PBS (middle column), and swollen in DI (right column).

crosslinked and crosslinked gels. Percent hydration (H) and swell ratio (Q) parameters were calculated based upon equilibrium measurements and are presented in Table E2 below.

Table E2: Swell test parameters for DBM-reinforced gels

	H (DI)	Q (DI)	H (PBS)	Q (PBS)
Unreinforced	99.4%	175.3 ± 43.2	97.9%	46.7 ± 4.2
3:1 Native	98.3%	59.8 ± 13.5	95.6%	22.1 ± 3.6
Unreinforced-XL	85.3%	6.1 ± 1.5	95.4%	21.6 ± 3.9
5:1Denatured	88.1%	7.5 ± 0.5	96.0%	24.3 ± 1.4
3:1 Denatured	73.4%	2.9 ± 0.8	92.8%	13.0 ± 1.5
5:1 Denatured XL	99.0%	95.9 ± 12.2	97.0%	29.1 ± 3.5
3:1 Denatured XL	97.0%	32.7 ± 1.2	94.8%	18.3 ± 0.1

Rheometry

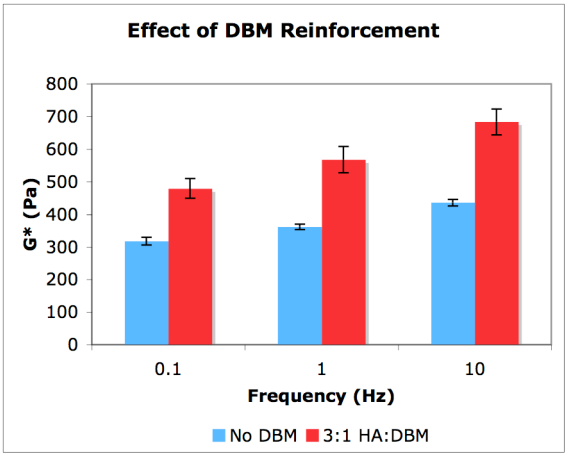

Figure E3: Effect of particulate reinforcement with native DBM. Reinforcement with a 3:1 w/w ratio of HA to DBM resulted in roughly a 50% increase in G*.

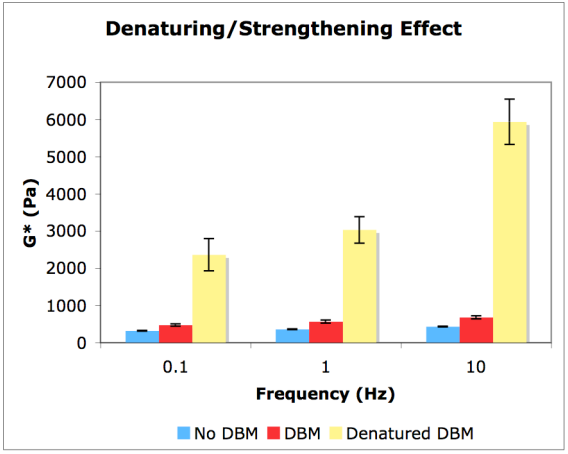

Figure E4: Strengthening effect of denatured DBM. G* increased by an order of magnitude when comparing unreinforced gels to gels reinforced with denatured DBM.

The effect of particulate reinforcement with DBM alone is illustrated in Figure E3, in which unreinforced gels are compared to gels reinforced with a 3:1 w/w ratio of HA to native DBM (n=3 per group). The addition of DBM to the gel resulted in a modest 50% increase in the complex shear modulus. A much more profound

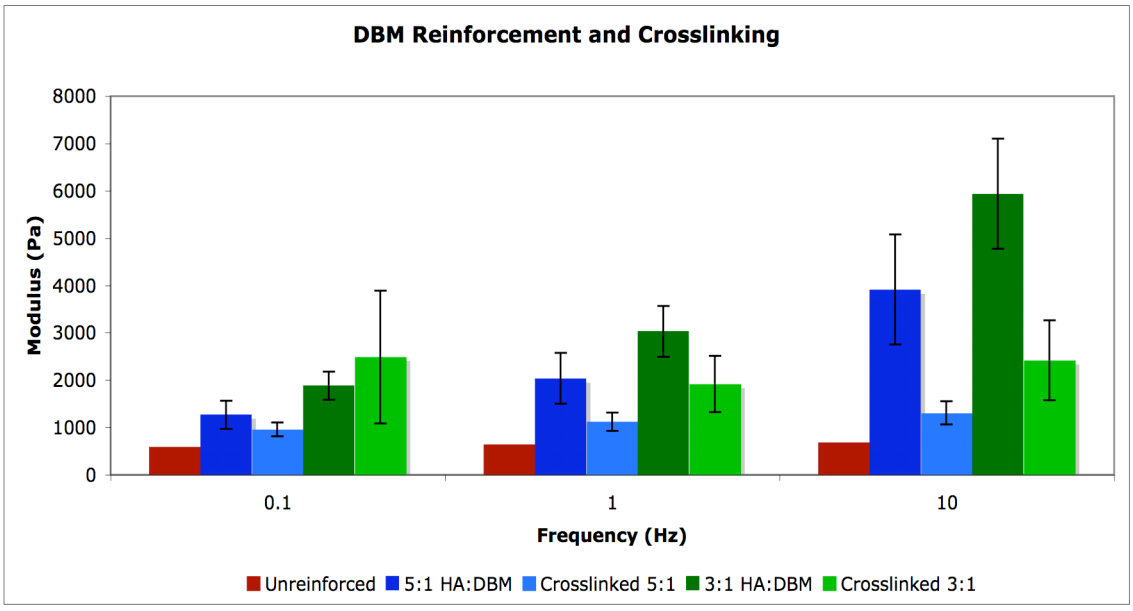

Figure E5: DBM reinforcement combined with HMDI crosslinking. Although HMDI crosslinking increases G* relative to unreinforced gels, it does not make a significant difference compared to the denatured DBM reinforcement at 0.1 Hz and reduces the reinforcing effect at 1 and 10 Hz.

strengthening effect was achieved through the inadvertent denaturing of the DBM; G* increases ten-fold, as seen in Figure E4. The possibility of synergistic strengthening effects were investigated by crosslinking the denatured gels with HMDI. The resulting complex shear modulus measurements are compared in Figure E5.

Discussion

The reinforcing effect of DBM on the hydrogels developed in this dissertation research was briefly investigated in this set of experiments. Reinforcement with a 3:1 HA to DBM ratio (w/w) has provided a modest level of strengthening, with G* increasing by 50% compared to unreinforced gels. This is consistent with swell test results, where a modest reduction in hydration was associated with the DBM reinforcement. Qualitatively, the DBM does not appear well-integrated with the gel matrix. Grains of DBM were released from the gel during the sonication step of the

hydrolysis process, and grains at the edge of cut samples are easily dislodged. Further, while mechanical properties have improved, the 500-700 Pa range for G* falls well short of the 7-20 KPa G* values reported in the literature for human NP tissue [4, 5].

Gel mechanical properties approached the appropriate order of magnitude when the DBM reinforcement was inadvertently denatured. Denaturing produced a ten-fold improvement in G* and a correspondingly large drop in hydration level measured during swell testing. Qualitatively, the denatured DBM turned the entire gel a golden-brown color while the DBM grains themselves turned dark brown. Individual DBM grains were well-integrated with the gel matrix, suggesting some physical or chemical association between the two phases. The unfolding of proteins during denaturing can expose hydrophobic domains or regions amenable to hydrogen bonding, possibly allowing for adsorption to the gel matrix. The "tanning" of the DBM is also suggestive of the quinone crosslinking of collagen and other proteins seen in various natural materials [6]. Quinones and maleic anhydrides are both ring structures with two carbonyl groups, so it seems plausible that with high enough temperature or with catalysis of metal contaminants in the vacuum oven [7] that the maleic acids could have participated in a quinone-like crosslinking reaction with the collagen component of the DBM.

Gels were crosslinked with HMDI to see if the mechanical properties could be further improved. While swell tests on unreinforced gels after crosslinking suggested an improvement in properties as suggested by a drop in hydration level, the opposite was seen when denatured gels were crosslinked. Rheometry confirmed a reduction in shear modulus of crosslinked denatured gels. The strengthening mechanisms provided by denaturing and chemical crosslinking are not synergistic; the covalent bonding via HMDI

crosslinking appears to disrupt whatever strengthening mechanism is at play in the denatured gel.

While and the reinforcing effect of denaturing is far greater than that of crosslinking, the exact mechanism of reinforcement is not understood and has not been reproduced. Further, the impression a denatured protein would make in a clinical setting is uncertain, making further development of this material as a therapeutic agent impractical.

References

1. Dahlberg, L. and Kreicbergs, A., *Demineralized Allogeneic Bone-Matrix For Cartilage Repair.* Journal Of Orthopaedic Research, 1991. **9**(1): p. 11-19.
2. Li, X.D., et al., *Demineralized bone matrix gelatin as scaffold for osteochondral tissue engineering.* Biomaterials, 2006. **27**(11): p. 2426-2433.
3. van Osch, G., et al., *The role of trabecular demineralized bone in combination with perichondrium in the generation of cartilage grafts.* Biomaterials, 1999. **20**(3): p. 233-240.
4. Iatridis, J.C., et al., *The viscoelastic behavior of the non-degenerate human lumbar nucleus pulposus in shear.* Journal Of Biomechanics, 1997. **30**(10): p. 1005-1013.
5. Iatridis, J.C., et al., *Is the nucleus pulposus a solid or a fluid? Mechanical behaviors of the nucleus pulposus of the human intervertebral disc.* Spine, 1996. **21**(10): p. 1174-1184.
6. Wainwright, S.A., et al., *Mechanical Design in Organisms*. 1976, Princeton, NJ: Princeton University Press.
7. Yamauchi, A., et al., *Enzyme-free quinone crosslinking reaction for proteins: a macromolecular characterization study using gelatin.* Macromolecular Bioscience, 2009. **2009**(9): p. 875-883.

APPENDIX F: RHEOMETRY METHOD VALIDATION

Numerous research groups have reported on the rheometric testing of soft tissues and hydrogels, but there is tremendous variation in reported parameters for similar materials. For example, reported shear moduli for nucleus pulposus tissue have ranged from as low as 300 Pa (G' @ 1 Hz) for porcine NP [1] to as high as 7.4 ± 11.6 kPa (G* at 1 rad/s or 6.28 Hz) for non-degenerate human NP [2]. Likewise, for hyaluronan-based hydrogels reported shear moduli have ranged from as low as 105 Pa for a type of dermal filler [3] to approximately 4 KPa for a thiol-modified HA heavily crosslinked with poly(ethylene glycol) diacrylate (PEGDA) [4]. While some of the differences could be due to true differences in the material properties, the authors employed different methods that likely had a greater effect on the variability of measurements. Rheometry experiments were designed such that the gels developed in this research would be directly compared to NP tissue tested by the same methodology; however, pilot experiments were undertaken to ensure a valid testing methodology.

Agarose was selected as the model system to validate rheometry test methodology. Recent publications have similarly used agarose to validate soft tissue shear measurements by magnetic resonance elastography [5, 6]. MRE measurements were compared to dynamic mechanical analysis (DMA) measurements made in "shear sandwich" mode. These authors found good agreement between the two methods of shear measurements, providing confidence in the DMA methods employed.

Furthermore, these papers provide a dataset that can be used for comparison to torsional shear measurements obtained via rheometry (Figure F1).

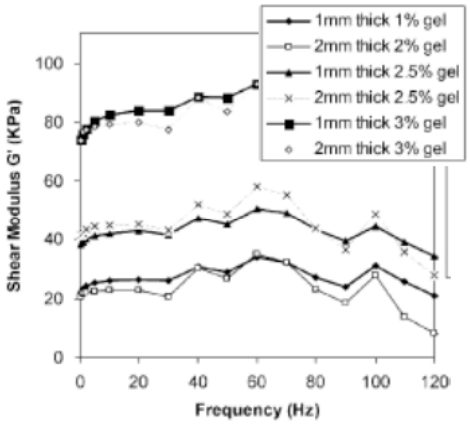

Figure F1: Agarose shear modulus results figure. Reused with permission from Chen, Q., et al., *Identification of the testing parameters in high frequency dynamic shear measurement on agarose gels.* Journal of Biomechanics, 2005.

For the rheometric test method validation experiments, agarose gels of 1.5% and 2.5% (w/v) were prepared by dissolving BioRad Molecular Biology Grade agarose in near-boiling deionized water and casting into a Petri dish to a thickness of approximately 2mm. Petri dishes were covered and the gels were allowed to set overnight. 8mm test samples were cored with a biopsy punch immediately prior to testing.

Test conditions as described in the MRE validation papers were duplicated to the extent possible. Sandpaper was adhered to the DMA fixture to improve grip. A 10% compressive preload was applied to the samples, and a 0.5% strain amplitude was applied. The MRE experiments examined a wider frequency range than was possible on the rheometer, but there was overlap in the 0.1 – 10 Hz range. Temperature was maintained at 27°C, and a humidified environment was maintained. The main differences in test set-up included the application of torsional shear rather than lateral shear and the sample dimensions.

One of the first questions addressed was the importance of sample grip. A cleated bottom plate was available for use with the rheometer, but only a polished platen was available in an 8 mm geometry for the top plate. Agarose gel samples were tested both with the polished platen and with an 8 mm disc of 150 grit sandpaper adhered to to the

platen. The top platen was lowered until approximately 10 grams force registered on the axial load cell, and the gap read was taken to be the sample height. A 10% compressive preload was applied, then a strain sweep covering the range from 0.005 to 20% strain amplitude was run to confirm the linear viscoelastic region (LVR). The 0.5% strain used in the MRE experiments was in the LVR, so a frequency sweep was run and measured parameters were compared to those reported in the literature.

Figure F2 illustrates G* measured with and without sandpaper (n=3 per group). Modulus values measured with sandpaper were in better agreement, though somewhat higher than the values reported in the literature (Table F1). The methods described in the MRE papers did not discuss the effect of stress relaxation after sample loading, so the effect of allowing for a relaxation delay before the initiation of testing was investigated (Figure F3). Frequency sweeps

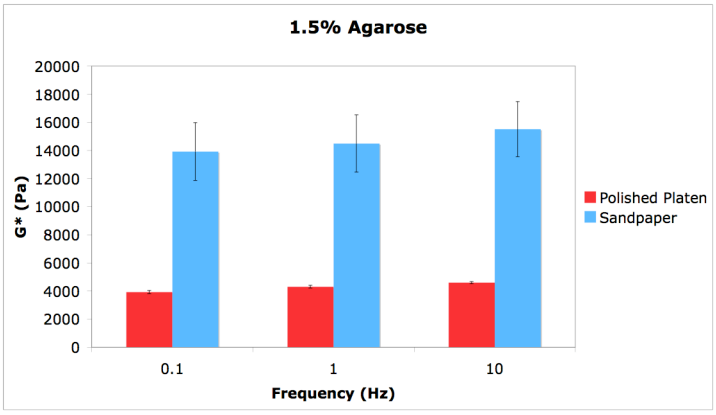

Figure F2: Comparison of complex shear modulus (G*) measured with and without sandpaper to aid in gripping the test specimen.

Table F1: Comparison of measured G* to values reported in the literature

Agarose Conc.	G* (Pa ± SEM)		
	0.1 Hz	1 Hz	10 Hz
1.5%	18289.6 ±1820.5	19662.8 ±1965.0	20910.5 ±2102.0
	14280±1340*		
2.5%	55245.0 ±7827.8	58950.9 ±8083.1	64918.0 ±8311.1
	49260±1380*		

*Ringleb, S.I., et al.

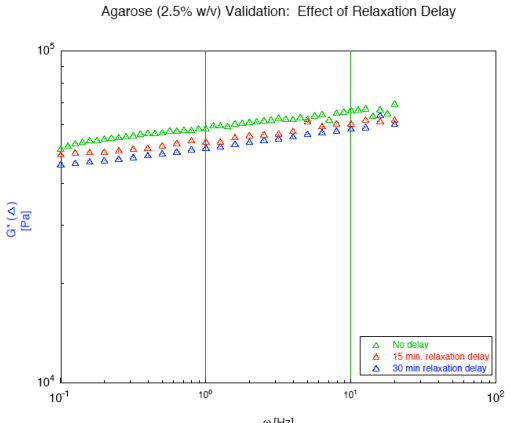

Figure F3: Effect of axial stress relaxation on measured G* values

were run immediately upon loading the sample, after a 15 minute delay, and after a 30 minute delay. Axial force readings were monitored, and no further relaxation after 30 minutes could be reliably observed as the axial force dropped below the specified sensitivity of the axial load cell. While allowing for axial stress relaxation to stabilize did bring measurements into line with the literature, waiting 30 minutes would add significantly to the overall test time and other factors, e.g. maintaining hydration, could become a concern. To reduce the required delay for relaxation the loading protocol was modified to lower the platen until ~1 gram force was read. With this loading condition results similar to those reported by Ringleb et. al. were achieved without need for a relaxation delay, so this loading protocol was adopted.

One final question to be addressed was whether any pre-conditioning cycles were required for stable measurements. 10 consecutive frequency sweeps were run and the consistency of the data was monitored (Figure F4). Over this cohort, measurements were seen to be quite stable through the first 7-8 frequency sweeps. Measured modulus values begin to noticeably drop at the 9th cycle and drop even further in cycle 10. These late changes are likely due to loss of grip rather than to a pre-conditioning effect. Since measurements were stable over the first 7 cycles no need for pre-conditioning was seen.

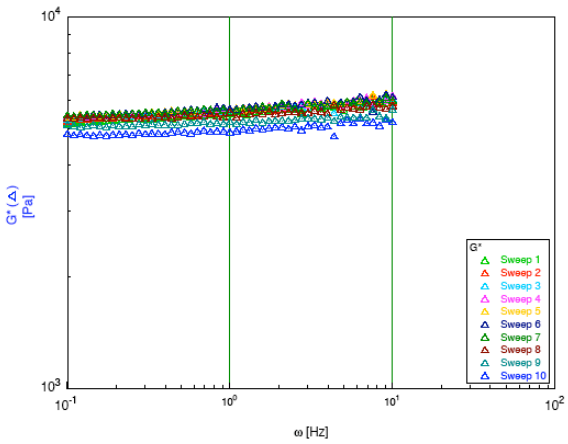

Figure F4: Repeatability of measurements over 10 identical frequency sweep cycles.

Experimental conditions employed for the rheometric testing of NP tissue and the hydrogels synthesized in this work were based upon the learnings from these validation experiments. Sample grip is a key factor, so gluing a disc of sandpaper to the 8mm top platen was added to the testing protocol. It was also determined that over-compression of the sample can lead to over-reporting of modulus values; this can be overcome either by allowing for or minimizing axial stress relaxation effects. Finally, no need for pre-conditioning was observed.

References

1. Causa, F., et al., *Spatial and structural dependence of mechanical properties of porcine intervertebral disc.* Journal Of Materials Science-Materials In Medicine, 2002. **13**(12): p. 1277-1280.

2. Iatridis, J.C., et al., *The viscoelastic behavior of the non-degenerate human lumbar nucleus pulposus in shear.* Journal Of Biomechanics, 1997. **30**(10): p. 1005-1013.

3. Kablik, J., et al., *Comparative Physical Properties of Hyaluronic Acid Dermal Fillers.* Dermatologic Surgery, 2009. **35**(1): p. 302-312.

4. Ghosh, K., et al., *Rheological characterization of in situ cross-linkable hyaluronan hydrogels.* Biomacromolecules, 2005. **6**(5): p. 2857-2865.

5. Chen, Q., et al., *Identification of the testing parameters in high frequency dynamic shear measurement on agarose gels.* Journal of Biomechanics, 2005. **38**: p. 959-963.

6. Ringleb, S.I., et al., *Quantitative shear wave magnetic resonance elastography: comparison to a dynamic shear material test.* Magnetic Resonance In Medicine, 2005. **53**: p. 1197-1201.

APPENDIX G: REINFORCEMENT LEVEL AND AIR-FREE CHEMISTRY

The anhydride esterification chemistry employed for the synthesis of HA-*co*-PEMA hydrogels is known to be sensitive to water. As such, exposure to air at any point during the reaction represents a source of variability, in that changes in humidity from day to day is an uncontrollable factor. Despite this known issue, the initial reinforced gels were briefly exposed to air during the casting process. The reactive maleic anhydride moieties were available in sufficient excess that gels could still form, and reinforced gels bracketing the properties of ovine nucleus pulposus tissue when tested in shear were successfully produced. Comparing swell test results for unreinforced, air-exposed cast gels to the initial gels produced in air-free glassware confirmed a less complete reaction in the presence of air.

We speculated that controlling the air exposure would allow for further tuning of the mechanical properties of the reinforced gels. In particular, it was expected that lower levels of particulate reinforcement entrapped in a more densely crosslinked gel matrix could duplicate the elastic properties of the air-cast gels while improving the dissipative properties of the composite since the compliant gel matrix would play a larger role in the mechanical response. In a follow-on experiment to test this hypothesis, two gels were cast in a commercial glove box under an inert argon gas environment.

As in Specific Aim 2, concentrated solutions of HA-CTA in DMSO (2.5% w/v) and PEMA in DMSO were prepared using air-free chemistry techniques. Reactants were

vacuum dried and glassware was stored at 100°C for a minimum of 24 hours prior to use. Reactants were measured into 3-necked flasks and the two outer necks were sealed with serum stoppers secured by copper wire. The third neck was connected to a condenser circulating chilled water. Sealed flasks were charged and vented with N_2 gas three times, then the appropriate measured volume of DMSO was transferred to the flask via cannula under dry N_2 flow. Flasks were lowered into oil baths and heated to 80°C with magnetic stirring until the reactants were fully dissolved. Flasks were again vented with N_2 while being removed from the condenser and were sealed with a slight positive pressure of N_2 in the flask.

In preparation for gel casting in the glove box, all reactants and casting materials were gathered and placed in the glove box antechamber. The antechamber was vacuum-evacuated and charged with argon gas three times prior to moving materials into the glove box. A slight vacuum was pulled on the antechamber to ensure that the glove box remained sealed for the duration of work.

Table G1: Comparison of gel formulations for in-air and air-free casting

Formulation	HA-CTA (g)	PEMA (g)	TS-720 (g)
720-R (cast in air)	0.4	0.06	0.8
AF-MR	0.4	0.06	0.4
AF-LR	0.4	0.06	0.2

The composition of the gels was identical to that of the 720-R gel described in Specific Aim 2, with the exception that the amount of silica added to the gel was reduced by 50% (AF-MR) and 75% (AF-LR). Gel constituents are summarized in Table G2. As in Specific Aim 2, gel constituents were mixed by hand in 70x50 mm crystallizing dishes. The crystallizing dishes were sealed in vacuum bags prior to removal from the glove box, then were placed in a 75°C oven to cure for 12 hours overnight.

Following curing, gels were removed from their vacuum bags and were further processed by sequential sonication cycles in acetone, 0.2M NaCl aqueous solution, a 0.1M NaCl aqueous solution, deionized water, and ethanol with 2-3 cycles in each solvent. The acetone cycle was intended to remove DMSO and unreacted PEMA from the gel. Ion exchange in the NaCl solutions hydrolyzes the gel, while lowering the concentration of the salt solution provides increasingly larger osmotic driving forces to clear the CTA^+ from the gel. The final ethanol cycles start to dehydrate the gel. Once drained of ethanol, the gels were placed in a vacuum until completely dry.

Gels were re-swollen to equilibrium in PBS in preparation for rheometry. Test samples were prepared with an 8 mm biopsy punch and were loaded for testing as described previously in Specific Aim 2. A dynamic strain sweep was run on one sample to confirm that test parameters used previously were in the linear viscoelastic region for the air-free cast gels. Once the LVR was verified, dynamic frequency sweeps were run from 0.1 Hz $\leq f \leq$ 10 Hz at 2% strain. A total of 5 samples from each gel (AF-LD and AF-MD) were tested and data was compared to ovine NP tissue results collected previously.

Dynamic shear parameters at 0.1 Hz, 1 Hz, and 10 Hz are compared among the two air-free cast gels and ovine NP tissue in Figure G1. Statistical comparisons were made between the cast gels and the NP tissue using the Holm-Sidak method for multiple comparisons versus a control group. No significant differences were detected between NP tissue and either gel formulation for G' and G*. Loss modulus for AF-MR was statistically higher than NP at 0.1 Hz ($p=0.014$) and at 1 Hz ($p=0.021$). The loss factor tanδ for both cast gels was significantly different from NP (AF-LR < NP, $p=0.018$;

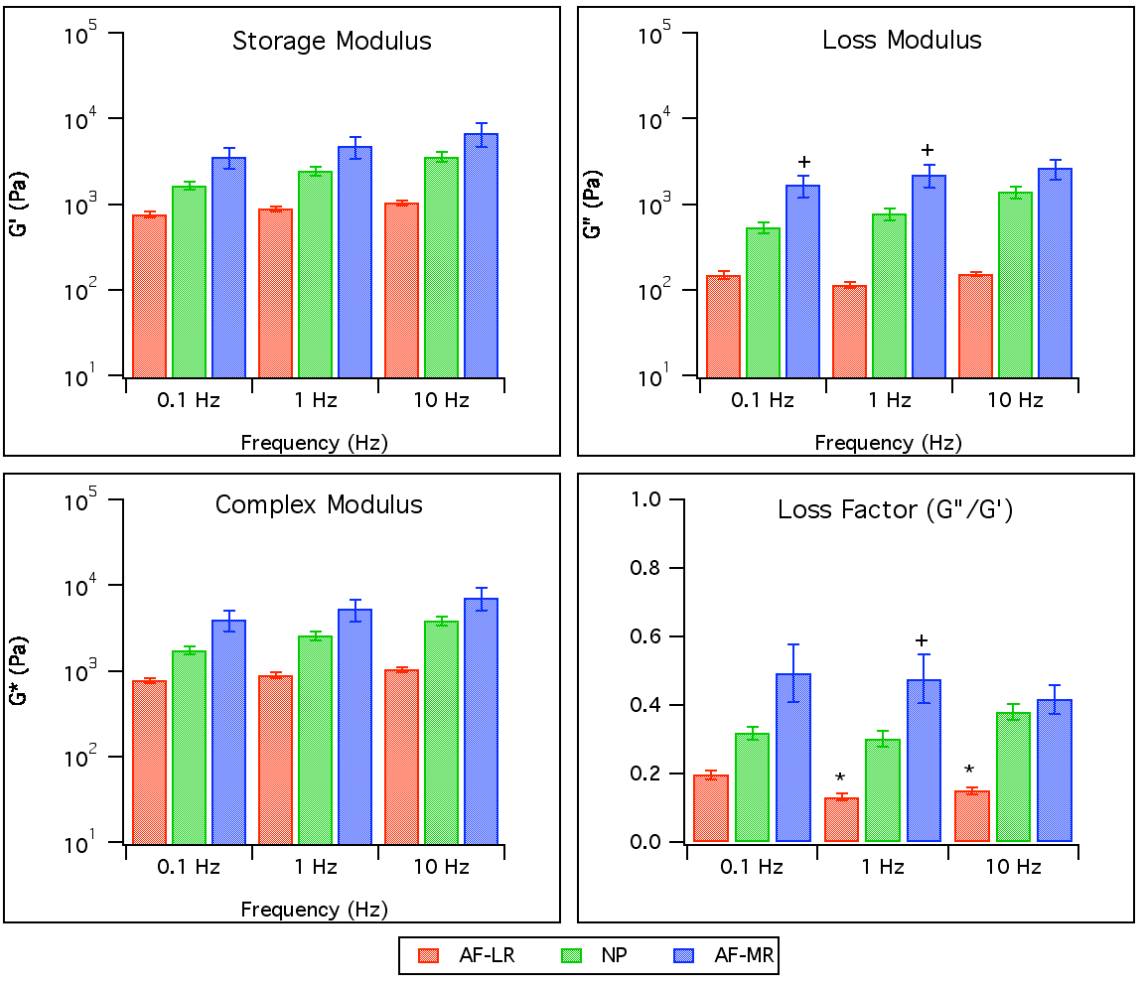

Figure G1: Comparison of dynamic shear properties between air-free cast gels and ovine NP tissue. The two reinforcement levels effectively bracket the NP properties for all parameters.

AF-MR > NP, p=0.015) at 1 Hz but no differences were detected at 0.1 Hz and only AF-LR was significantly different from NP at 10 Hz ($p<0.001$).

This experiment demonstrates that when synthesized under a controlled environment, the mechanical properties of silica-reinforced HA-*co*-PEMA hydrogels can be tuned by varying the proportion of particulate reinforcement. Our chosen AF-LR and AF-MR reinforcement levels bracketed the properties previously measured for ovine NP, with AF-MR being a closer match. G' and tanδ differed from results seen previously, in that the more reinforced gel exhibited the largest values for these parameters. Typically,

the loss factor is interpreted as a measure of "solid-like" versus "liquid-like" behavior, and the range seen for the AF-MR gel (0.49 ± 0.08 at 0.1 Hz, 0.47 ± 0.07 at 1 Hz, and 0.41 ± 0.04 at 10 Hz) is typically interpreted as the transition from solid-like to liquid-like behavior. The simplest interpretation of this result, that the AF-MR gel has a higher volume fraction of water, is not borne out by preliminary swell test data (Table G-2).

Table G2: Swell test parameters after 72 hours in PBS

Formulation	Q	H
AF-LR	26.3 ± 4.9	96.0% ± 0.8%
AF-MR	6.6 ± 0.3	86.8% ± 0.6%

The higher loss modulus of the AF-MR gel can be better rationalized based upon the movement of water rather than the overall water content. With the higher fraction of hydrophobic filler, water is not as tightly bound in the AF-MR gel as in the AF-LR gel. Thus, when subjected to dynamic loading, the water is more mobile in the AF-MR gel allowing for more dissipation of energy and a correspondingly higher G'. Differences in the water binding properties of various gel formulations can be better quantified through transient tests such as creep or stress relaxation.

The heterogeneous nature of the reinforced gel system further belies the simple explanation of its dynamic mechanical behavior. In basic polymer characterization studies, dynamic mechanical analysis is used to identify changes in phase behavior. Over a large frequency span, the behavior of dilute polymer solutions transitions from liquid to rubbery to glassy as frequency increases. Similarly, these transitions in behavior are mirrored when temperature is varied, going from glassy to rubbery to liquid as temperature increases. A peak in the loss modulus as a function of temperature is an indication of the glass transition temperature (T_g), a secondary phase transition that is a key specification in choosing a polymer for a specific application; T_g should lie

significantly above intended operating temperatures for any application where the polymer is intended to behave as a solid, or significantly below temperatures where it is intended as a liquid [1]. In the reinforced gel systems we are combining elements with very different T_g behavior, so it is difficult to make predictions about where we lie in the spectrum of behavior. The air-free hydrogels are even more networked than those cast in the presence of air – the high degree of networking and the reinforcement likely broadens, flattens, and shifts the tanδ peak (i.e., glass transition) to higher frequencies. It is possible that the test frequencies used were below the glass transition. Fully characterizing this behavior would require frequency sweeps over a much broader range of frequencies or temperature sweeps over a significant temperature span.

While there are a slew of further experiments that could be performed to more fully characterize the reinforced hydrogel system, the focus here was to describe the behavior over a physiologically-relevant range. We confirmed that the dynamic shear properties could be altered based upon the level of particulate reinforcement introduced into the composite gel system, and that when synthesized in a controlled environment gels bracketing the properties of ovine nucleus pulposus tissue could be produced with modest fractions of silica reinforcement.

Reference

1. Hiemenz, P.Z. and Lodge, T.P., *Polymer Chemistry*. Second ed. 2007, Boca Raton, FL: CRC Press.

APPENDIX H: STATISTICAL ANALYSES

Data analysis was conducted using the statistics tools built into the SigmaPlot® 11.2 software package (Systat Software Incorporated, San Jose CA). Generally continuous data was collected, but in cases where the equal variance and/or normality assumptions did not hold the data was treated as categorical. Pair-wise comparisons were analyzed with t-tests, and one-way Analysis of Variance (ANOVA) with multiple-group adjustments were used for experiments with more than two groups. Statistical significance was based upon α=0.05.

Specific Aim 1: Swell Test Parameters for LD and HD Gel Formulations

Swell Ratio (Q)

t-test
Normality Test: Passed (P = 0.834)
Equal Variance Test: Passed (P = 0.080)

Group Name	N	Missing	Mean	Std Dev	SEM
LD	3	0	168.369	38.867	22.440
HD	3	0	21.673	9.464	5.464

Difference 146.695

t = 6.352 with 4 degrees of freedom. (P = 0.003)

95 percent confidence interval for difference of means: 82.571 to 210.819

The difference in the mean values of the two groups is greater than would be expected by chance; there is a statistically significant difference between the input groups (P = 0.003).

Power of performed test with alpha = 0.050: 0.995

Percent Hydration (H)

t-test
Normality Test: Passed (P = 0.709)
Equal Variance Test: Passed (P = 0.431)

Group Name	N	Missing	Mean	Std Dev	SEM

LD	3	0	0.982	0.0136	0.00784
HD	3	0	0.951	0.0182	0.0105

Difference 0.0314

t = 2.394 with 4 degrees of freedom. (P = 0.075)

95 percent confidence interval for difference of means: -0.00502 to 0.0679

The difference in the mean values of the two groups is not great enough to reject the possibility that the difference is due to random sampling variability. There is not a statistically significant difference between the input groups (P = 0.075).

Power of performed test with alpha = 0.050: 0.380

The power of the performed test (0.380) is below the desired power of 0.800.
Less than desired power indicates you are less likely to detect a difference when one actually exists. Negative results should be interpreted cautiously.

Specific Aim 2: Reinforced Gel Characterization

Swell Testing: Q in Deionized Water (DI)

One Way Analysis of Variance

Group Name	N	Missing	Mean	Std Dev	SEM
HD-GC	3	0	175.250	74.478	43.000
620-R	3	0	22.750	2.667	1.540
720-R	3	0	25.590	23.452	13.540

Source of Variation	DF	SS	MS	F	P
Between Groups	2	45662.431	22831.216	11.221	0.009
Residual	6	12208.219	2034.703		
Total	8	57870.650			

The differences in the mean values among the treatment groups are greater than would be expected by chance; there is a statistically significant difference (P = 0.009).

Power of performed test with alpha = 0.050: 0.881

All Pairwise Multiple Comparison Procedures (Holm-Sidak method):
Overall significance level = 0.05

Comparisons for factor:

Comparison	Diff of Means	t	Unadjusted P	Critical Level	Significant?
HD-GC vs. 620-R	152.500	4.141	0.006	0.017	Yes
HD-GC vs. 720-R	149.660	4.064	0.007	0.025	Yes
720-R vs. 620-R	2.840	0.0771	0.941	0.050	No

Swell Testing: Q in Phosphate-Buffered Saline (PBS)

One Way Analysis of Variance

Group Name	N	Missing	Mean	Std Dev	SEM
HD-GC	3	0	46.770	7.327	4.230
620-R	3	0	6.920	1.247	0.720
720-R	3	0	4.440	1.091	0.630

Source of Variation	DF	SS	MS	F	P
Between Groups	2	3386.002	1693.001	90.014	<0.001
Residual	6	112.849	18.808		
Total	8	3498.851			

The differences in the mean values among the treatment groups are greater than would be expected by chance; there is a statistically significant difference (P = <0.001).

Power of performed test with alpha = 0.050: 1.000

All Pairwise Multiple Comparison Procedures (Holm-Sidak method):
Overall significance level = 0.05

Comparisons for factor:

Comparison	Diff of Means	t	Unadjusted P	Critical Level	Significant?
HD-GC vs. 720-R	42.330	11.954	<0.001	0.017	Yes
HD-GC vs. 620-R	39.850	11.254	<0.001	0.025	Yes
620-R vs. 720-R	2.480	0.700	0.510	0.050	No

Swell Testing: H in DI

One Way Analysis of Variance

Group Name	N	Missing	Mean	Std Dev	SEM
HD-GC	3	0	99.400	0.260	0.150
620-R	3	0	95.780	0.450	0.260
720-R	3	0	95.100	6.824	3.940

Source of Variation	DF	SS	MS	F	P
Between Groups	2	32.057	16.028	1.027	0.414
Residual	6	93.682	15.614		
Total	8	125.739			

The differences in the mean values among the treatment groups are not great enough to exclude the possibility that the difference is due to random sampling variability; there is not a statistically significant difference (P = 0.414).

Power of performed test with alpha = 0.050: 0.053

The power of the performed test (0.053) is below the desired power of 0.800.
Less than desired power indicates you are less likely to detect a difference when one actually exists. Negative results should be interpreted cautiously.

Swell Testing: H in PBS

One Way Analysis of Variance

Group Name	N	Missing	Mean	Std Dev	SEM
HD-GC	3	0	97.890	0.329	0.190
620-R	3	0	87.310	2.338	1.350
720-R	3	0	81.470	4.417	2.550

Source of Variation	DF	SS	MS	F	P
Between Groups	2	415.658	207.829	24.857	0.001
Residual	6	50.167	8.361		
Total	8	465.825			

The differences in the mean values among the treatment groups are greater than would be expected by chance; there is a statistically significant difference (P = 0.001).

Power of performed test with alpha = 0.050: 0.998

All Pairwise Multiple Comparison Procedures (Holm-Sidak method):
Overall significance level = 0.05

Comparisons for factor:

Comparison	Diff of Means	t	Unadjusted P	Critical Level	Significant?
HD-GC vs. 720-R	16.420	6.955	<0.001	0.017	Yes
HD-GC vs. 620-R	10.580	4.481	0.004	0.025	Yes
620-R vs. 720-R	5.840	2.474	0.048	0.050	Yes

Rheometry: Complex Modulus (G) at 0.1 Hz*

One Way Analysis of Variance
Normality Test: Passed (P = 0.157)
Equal Variance Test: Failed (P < 0.050)

Test execution ended by user request, ANOVA on Ranks begun

Kruskal-Wallis One Way Analysis of Variance on Ranks

Group	N	Missing	Median	25%	75%
C620	6	0	2243.900	1876.470	2299.960
C720	6	0	4403.990	3959.430	5579.410
CNP	5	0	1903.870	1722.400	2093.390

H = 12.165 with 2 degrees of freedom. (P = 0.002)

The differences in the median values among the treatment groups are greater than would be expected by chance; there is a statistically significant difference (P = 0.002)

To isolate the group or groups that differ from the others use a multiple comparison procedure.

Multiple Comparisons versus Control Group (Dunn's Method) :

Comparison	Diff of Ranks	Q	P<0.05
C720 vs CNP	10.300	3.368	Yes
C620 vs CNP	3.300	1.079	No

Note: The multiple comparisons on ranks do not include an adjustment for ties.

Rheometry: G at 1 Hz*

One Way Analysis of Variance
Normality Test: Passed (P = 0.707)
Equal Variance Test: Passed (P = 0.116)

Group Name	N	Missing	Mean	Std Dev	SEM
C620	6	0	2192.222	611.536	249.658
C720	6	0	5540.698	1037.245	423.454
CNP	5	0	2875.220	271.339	121.346

Source of Variation	DF	SS	MS	F	P
Between Groups	2	37104735.271	18552367.635	34.430	<0.001
Residual	14	7543767.458	538840.533		
Total	16	44648502.729			

The differences in the mean values among the treatment groups are greater than would be expected by chance; there is a statistically significant difference (P = <0.001).

Power of performed test with alpha = 0.050: 1.000

Multiple Comparisons versus Control Group (Holm-Sidak method):
Overall significance level = 0.05

Comparisons for factor:

Comparison	Diff of Means	t	Unadjusted P	Crit. Level	Significant?
CNP vs. C720	2665.478	5.997	<0.001	0.025	Yes
CNP vs. C620	682.998	1.537	0.147	0.050	No

Rheometry: G at 10 Hz*

One Way Analysis of Variance
Normality Test: Passed (P = 0.506)
Equal Variance Test: Passed (P = 0.247)

Group Name	N	Missing	Mean	Std Dev	SEM
C620	6	0	2543.067	702.751	286.897
C720	6	0	6548.505	1157.850	472.690
CNP	5	0	4287.782	633.673	283.387

Source of Variation	DF	SS	MS	F	P
Between Groups	2	48365547.472	24182773.736	31.410	<0.001
Residual	14	10778543.791	769895.985		
Total	16	59144091.263			

The differences in the mean values among the treatment groups are greater than would be expected by chance; there is a statistically significant difference (P = <0.001).

Power of performed test with alpha = 0.050: 1.000

Multiple Comparisons versus Control Group (Holm-Sidak method):
Overall significance level = 0.05

Comparisons for factor:

Comparison	Diff of Means	t	Unadjusted P	Critical Level	Significant?
CNP vs. C720	2260.723	4.255	<0.001	0.025	Yes
CNP vs. C620	1744.715	3.284	0.005	0.050	Yes

Rheometry: Storage Modulus (G') at 0.1 Hz

One Way Analysis of Variance
Normality Test: Passed (P = 0.148)
Equal Variance Test: Failed (P < 0.050)

Test execution ended by user request, ANOVA on Ranks begun

Kruskal-Wallis One Way Analysis of Variance on Ranks

Group	N	Missing	Median	25%	75%
S620	6	0	2229.360	1868.170	2283.450
S720	6	0	4372.735	3936.040	5538.910
SNP	5	0	1803.140	1643.073	1973.063

H = 12.740 with 2 degrees of freedom. (P = 0.002)

The differences in the median values among the treatment groups are greater than would be expected by chance; there is a statistically significant difference (P = 0.002)

To isolate the group or groups that differ from the others use a multiple comparison procedure.

Multiple Comparisons versus Control Group (Dunn's Method) :

Comparison	Diff of Ranks	Q	P<0.05
S720 vs SNP	10.700	3.499	Yes
S620 vs SNP	4.033	1.319	No

Note: The multiple comparisons on ranks do not include an adjustment for ties.

Rheometry: G' at 1 Hz

One Way Analysis of Variance
Normality Test: Passed (P = 0.640)
Equal Variance Test: Passed (P = 0.111)

Group Name	N	Missing	Mean	Std Dev	SEM
S620	6	0	2178.412	605.320	247.121
S720	6	0	5493.200	1033.231	421.815
SNP	5	0	2736.312	251.071	112.282

Source of Variation	DF	SS	MS	F	P
Between Groups	2	37230123.989	18615061.994	35.113	<0.001
Residual	14	7422034.245	530145.303		
Total	16	44652158.233			

The differences in the mean values among the treatment groups are greater than would be expected by chance; there is a statistically significant difference (P = <0.001).

Power of performed test with alpha = 0.050: 1.000

Multiple Comparisons versus Control Group (Holm-Sidak method):
Overall significance level = 0.05

Comparisons for factor:

Comparison	Diff of Means	t	Unadjusted P	Critical Level	Significant?
SNP vs. S720	2756.888	6.253	<0.001	0.025	Yes
SNP vs. S620	557.900	1.265	0.226	0.050	No

Rheometry: G' at 10 Hz

One Way Analysis of Variance
Normality Test: Passed (P = 0.664)
Equal Variance Test: Passed (P = 0.215)

Group Name	N	Missing	Mean	Std Dev	SEM
S620	6	0	2527.002	697.108	284.593
S720	6	0	6479.703	1147.203	468.344
SNP	5	0	3982.474	555.743	248.536

Source of Variation	DF	SS	MS	F	P
Between Groups	2	47829131.674	23914565.837	32.678	<0.001
Residual	14	10245569.291	731826.378		
Total	16	58074700.964			

The differences in the mean values among the treatment groups are greater than would be expected by chance; there is a statistically significant difference (P = <0.001).

Power of performed test with alpha = 0.050: 1.000

Multiple Comparisons versus Control Group (Holm-Sidak method):

Overall significance level = 0.05

Comparisons for factor:

Comparison	Diff of Means	t	Unadjusted P	Critical Level	Significant?
SNP vs. S720	2497.229	4.821	<0.001	0.025	Yes
SNP vs. S620	1455.472	2.810	0.014	0.050	Yes

Rheometry: Loss Modulus (G") at 0.1 Hz

One Way Analysis of Variance
Normality Test: Passed (P = 0.112)
Equal Variance Test: Passed (P = 0.255)

Group Name	N	Missing	Mean	Std Dev	SEM
L620	6	0	236.629	47.502	19.393
L720	6	0	579.380	122.101	49.848
LNP	5	0	598.649	120.392	53.841

Source of Variation	DF	SS	MS	F	P
Between Groups	2	480714.150	240357.075	23.400	<0.001
Residual	14	143802.104	10271.579		
Total	16	624516.254			

The differences in the mean values among the treatment groups are greater than would be expected by chance; there is a statistically significant difference (P = <0.001).

Power of performed test with alpha = 0.050: 1.000

Multiple Comparisons versus Control Group (Holm-Sidak method):
Overall significance level = 0.05

Comparisons for factor:

Comparison	Diff of Means	t	Unadjusted P	Critical Level	Significant?
LNP vs. L620	362.020	5.899	<0.001	0.025	Yes
LNP vs. L720	19.268	0.314	0.758	0.050	No

Rheometry: G" at 1 Hz

One Way Analysis of Variance
Normality Test: Passed (P = 0.083)
Equal Variance Test: Passed (P = 0.490)

Group Name	N	Missing	Mean	Std Dev	SEM
L620	6	0	243.524	93.905	38.336
L720	6	0	710.716	176.348	71.994
LNP	5	0	877.428	150.325	67.228

Source of Variation	DF	SS	MS	F	P
Between Groups	2	1220377.910	610188.955	29.460	<0.001
Residual	14	289973.941	20712.424		
Total	16	1510351.852			

The differences in the mean values among the treatment groups are greater than would be expected by chance; there is a statistically significant difference (P = <0.001).

Power of performed test with alpha = 0.050: 1.000

Multiple Comparisons versus Control Group (Holm-Sidak method):
Overall significance level = 0.05

Comparisons for factor:

Comparison	Diff of Means	t	Unadjusted P	Critical Level	Significant?
LNP vs. L620	633.903	7.274	<0.001	0.025	Yes
LNP vs. L720	166.712	1.913	0.076	0.050	No

Rheometry: G" at 10 Hz

One Way Analysis of Variance
Normality Test: Passed (P = 0.120)
Equal Variance Test: Passed (P = 0.187)

Group Name	N	Missing	Mean	Std Dev	SEM
L620	6	0	284.134	93.505	38.173
L720	6	0	933.602	232.843	95.058
LNP	5	0	1581.398	350.564	156.777

Source of Variation	DF	SS	MS	F	P
Between Groups	2	4603597.672	2301798.836	39.963	<0.001
Residual	14	806376.312	57598.308		
Total	16	5409973.984			

The differences in the mean values among the treatment groups are greater than would be expected by chance; there is a statistically significant difference (P = <0.001).

Power of performed test with alpha = 0.050: 1.000

Multiple Comparisons versus Control Group (Holm-Sidak method):
Overall significance level = 0.05

Comparisons for factor:

Comparison	Diff of Means	t	Unadjusted P	Critical Level	Significant?
LNP vs. L620	1297.264	8.927	<0.001	0.025	Yes
LNP vs. L720	647.796	4.458	<0.001	0.050	Yes

Rheometry: Loss Factor (G"/G') at 0.1 Hz

One Way Analysis of Variance
Normality Test: Passed (P = 0.493)
Equal Variance Test: Passed (P = 0.320)

Group Name	N	Missing	Mean	Std Dev	SEM
T620	6	0	0.109	0.0128	0.00523
T720	6	0	0.125	0.0272	0.0111
CNP	5	0	0.330	0.0383	0.0171

Source of Variation	DF	SS	MS	F	P
Between Groups	2	0.160	0.0802	108.267	<0.001
Residual	14	0.0104	0.000741		
Total	16	0.171			

The differences in the mean values among the treatment groups are greater than would be expected by chance; there is a statistically significant difference (P = <0.001).

Power of performed test with alpha = 0.050: 1.000

Multiple Comparisons versus Control Group (Holm-Sidak method):
Overall significance level = 0.05

Comparisons for factor:

Comparison	Diff of Means	t	Unadjusted P	Critical Level	Significant?
CNP vs. T620	0.220	13.373	<0.001	0.025	Yes
CNP vs. T720	0.205	12.440	<0.001	0.050	Yes

Rheometry: G"/G' at 1 Hz

One Way Analysis of Variance
Normality Test: Passed (P = 0.927)
Equal Variance Test: Passed (P = 0.352)

Group Name	N	Missing	Mean	Std Dev	SEM
T620	6	0	0.108	0.0189	0.00773
T720	6	0	0.130	0.0290	0.0118
TNP	5	0	0.320	0.0424	0.0190

Source of Variation	DF	SS	MS	F	P
Between Groups	2	0.144	0.0722	76.603	<0.001
Residual	14	0.0132	0.000942		
Total	16	0.158			

The differences in the mean values among the treatment groups are greater than would be expected by chance; there is a statistically significant difference (P = <0.001).

Power of performed test with alpha = 0.050: 1.000

Multiple Comparisons versus Control Group (Holm-Sidak method):
Overall significance level = 0.05

Comparisons for factor:

Comparison	Diff of Means	t	Unadjusted P	Critical Level	Significant?
TNP vs. T620	0.212	11.418	<0.001	0.025	Yes
TNP vs. T720	0.190	10.233	<0.001	0.050	Yes

Rheometry: G"/G' at 10 Hz

One Way Analysis of Variance
Normality Test: Passed (P = 0.331)
Equal Variance Test: Failed (P < 0.050)

Test execution ended by user request, ANOVA on Ranks begun

Kruskal-Wallis One Way Analysis of Variance on Ranks

GroupN	Missing	Median	25%	75%	
T620	6	0	0.110	0.101	0.114
T720	6	0	0.144	0.122	0.164
TNP	5	0	0.401	0.365	0.433

H = 12.209 with 2 degrees of freedom. (P = 0.002)

The differences in the median values among the treatment groups are greater than would be expected by chance; there is a statistically significant difference (P = 0.002)

To isolate the group or groups that differ from the others use a multiple comparison procedure.

Multiple Comparisons versus Control Group (Dunn's Method) :

Comparison	Diff of Ranks	Q	P<0.05
T620 vs TNP	10.667	3.488	Yes
T720 vs TNP	6.333	2.071	No

Note: The multiple comparisons on ranks do not include an adjustment for ties.

Swell Testing: Q for Air-Cast and Air-Free Cast Gels

One Way Analysis of Variance

Group Name	N	Missing	Mean	Std Dev	SEM
HD	3	0	21.670	9.457	5.460
HD-GC	3	0	46.770	7.327	4.230
620-R	3	0	6.920	1.247	0.720
720-R	3	0	4.440	1.091	0.630
AF-HD-GC	3	0	22.550	1.143	0.660
AF-620-R	3	0	3.570	0.277	0.160

Source of Variation	DF	SS	MS	F	P
Between Groups	5	4128.084	825.617	33.643	<0.001
Residual	12	294.486	24.540		
Total	17	4422.570			

The differences in the mean values among the treatment groups are greater than would be expected by chance; there is a statistically significant difference (P = <0.001).

Power of performed test with alpha = 0.050: 1.000

All Pairwise Multiple Comparison Procedures (Holm-Sidak method):
Overall significance level = 0.05

Comparisons for factor:

Comparison	Diff of Means	t	Unadjusted P	Critical Level	Significant?
HD-GC vs. AF-620-R	43.200	10.680	<0.001	0.003	Yes
HD-GC vs. 720-R	42.330	10.465	<0.001	0.004	Yes
HD-GC vs. 620-R	39.850	9.852	<0.001	0.004	Yes
HD-GC vs. HD	25.100	6.206	<0.001	0.004	Yes
HD-GC vs. AF-HD-GC	24.220	5.988	<0.001	0.005	Yes
AF-HD-GC vs. AF-620-R	18.980	4.692	<0.001	0.005	Yes
AF-HD-GC vs. 720-R	18.110	4.477	<0.001	0.006	Yes
HD vs. AF-620-R	18.100	4.475	<0.001	0.006	Yes
HD vs. 720-R	17.230	4.260	0.001	0.007	Yes
AF-HD-GC vs. 620-R	15.630	3.864	0.002	0.009	Yes
HD vs. 620-R	14.750	3.647	0.003	0.010	Yes
620-R vs. AF-620-R	3.350	0.828	0.424	0.013	No
620-R vs. 720-R	2.480	0.613	0.551	0.017	No
AF-HD-GC vs. HD	0.880	0.218	0.831	0.025	No
720-R vs. AF-620-R	0.870	0.215	0.833	0.050	No

Rheometry: Air-Cast vs. Air-Free Cast 620-R Gel

t-test (0.1 Hz)

Group Name	N	Missing	Mean	Std Dev	SEM
AF-620-R	3	0	7410.190	4099.123	2366.630
620-R	7	0	1798.320	547.057	206.768

Difference 5611.870

t = 3.866 with 8 degrees of freedom. (P = 0.005)

95 percent confidence interval for difference of means: 2264.415 to 8959.325

The difference in the mean values of the two groups is greater than would be expected by chance; there is a

statistically significant difference between the input groups (P = 0.005).

Power of performed test with alpha = 0.050: 0.914

t-test (1 Hz)

Group Name	N	Missing	Mean	Std Dev	SEM
AF-620-R	3	0	10224.900	3063.825	1768.900
620-R	7	0	2062.730	655.006	247.569

Difference 8162.170

t = 7.241 with 8 degrees of freedom. (P = <0.001)

95 percent confidence interval for difference of means: 5562.690 to 10761.650

The difference in the mean values of the two groups is greater than would be expected by chance; there is a statistically significant difference between the input groups (P = <0.001).

Power of performed test with alpha = 0.050: 1.000

t-test (10 Hz)

Group Name	N	Missing	Mean	Std Dev	SEM
AF-620-R	3	0	14760.500	9762.064	5636.130
620-R	7	0	2380.650	772.139	291.841

Difference 12379.850

t = 3.641 with 8 degrees of freedom. (P = 0.007)

95 percent confidence interval for difference of means: 4540.143 to 20219.557

The difference in the mean values of the two groups is greater than would be expected by chance; there is a statistically significant difference between the input groups (P = 0.007).

Power of performed test with alpha = 0.050: 0.875

Specific Aim 3: Cytotoxicity

Cytotoxicity Elution Assay

Box Plot:

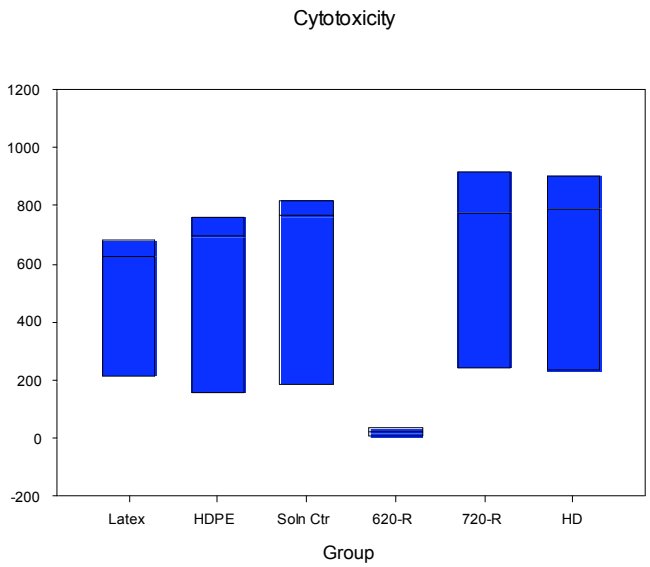

Studentized Residuals:

Sol'n Ctr	Residual	SEM	Stdnt-Residual	620-R	Residual	SEM	Stdnt-Residual
173.364	-417.3	129.095	-3.23251	23.916	2.7685	10.664	0.259612
826.528	235.8637	129.095	1.827055	63.584	42.4365	10.664	3.979417
814.888	224.2237	129.095	1.736889	-17.333	-38.4805	10.664	-3.60845
746.773	156.1087	129.095	1.209254	27.322	6.1745	10.664	0.579004
787.668	197.0037	129.095	1.526037	15.511	-5.6365	10.664	-0.52855
194.765	-395.899	129.095	-3.06673	13.885	-7.2625	10.664	-0.68103
Latex				720-R			
280.281	-213.659	114.538	-1.86539	301.818	-346.382	157.907	-2.19358
628.901	134.9615	114.538	1.178312	733.561	85.3615	157.907	0.540581
745.64	251.7005	114.538	2.197528	819.86	171.6605	157.907	1.087099
657.978	164.0385	114.538	1.432175	853.39	205.1905	157.907	1.299439
627.616	133.6765	114.538	1.167093	1111.097	462.8975	157.907	2.931456
23.221	-470.719	114.538	-4.10971	69.471	-578.729	157.907	-3.665
HDPE				HD-GC			
192.589	-337.985	130.258	-2.59473	251.939	-388.675	136.117	-2.85544
718.345	187.7715	130.258	1.441535	841.728	201.1145	136.117	1.477512
784.744	254.1705	130.258	1.951285	742.29	101.6765	136.117	0.746979
756.503	225.9295	130.258	1.734477	895.744	255.1305	136.117	1.874347
673.412	142.8385	130.258	1.096581	926.506	285.8925	136.117	2.100344
57.848	-472.726	130.258	-3.62915	185.474	-455.14	136.117	-3.34374

One Way Analysis of Variance

Normality Test: Failed (P < 0.050)

Test execution ended by user request, ANOVA on Ranks begun

Kruskal-Wallis One Way Analysis of Variance on Ranks

Group	N	Missing	Median	25%	75%
Soln Ctr	6	0	767.221	194.765	814.888
Latex	6	1	628.901	540.782	679.893
HDPE	6	1	718.345	553.206	763.563
620-R	6	2	19.714	14.698	25.619
720-R	6	0	776.711	301.818	853.390
HD-GC	6	0	792.009	251.939	895.744

H = 11.744 with 5 degrees of freedom. (P = 0.038)

The differences in the median values among the treatment groups are greater than would be expected by chance; there is a statistically significant difference (P = 0.038)

To isolate the group or groups that differ from the others use a multiple comparison procedure.

Multiple Comparisons versus Control Group (Dunn's Method) :

Comparison	Diff of Ranks	Q	P<0.05
620-R vs Soln Ctr	16.167	2.670	Yes
Latex vs Soln Ctr	4.067	0.716	No
HD-GC vs Soln Ctr	2.167	0.400	Do Not Test
720-R vs Soln Ctr	1.667	0.308	Do Not Test
HDPE vs Soln Ctr	1.467	0.258	Do Not Test

Note: The multiple comparisons on ranks do not include an adjustment for ties.

One Way Analysis of Variance – Fluorescence, comparisons vs. control

Normality Test: Passed (P = 0.051)

Equal Variance Test: Passed (P = 0.415)

Group Name	N	Missing	Mean	Std Dev	SEM
Soln Ctr	6	2	793.964	35.425	17.713
Latex	6	2	665.034	55.536	27.768
HDPE	6	2	733.251	48.288	24.144
620-R	6	2	22.271	33.399	16.699
720-R	6	2	879.477	162.454	81.227
HD-GC	6	2	851.567	80.841	40.420

Source of Variation	DF	SS	MS	F	P
Between Groups	5	2059476.325	411895.265	60.702	<0.001
Residual	18	122138.954	6785.497		
Total	23	2181615.280			

The differences in the mean values among the treatment groups are greater than would be expected by chance; there is a statistically significant difference (P = <0.001).

Power of performed test with alpha = 0.050: 1.000

Multiple Comparisons versus Control Group (Holm-Sidak method):
Overall significance level = 0.05

Comparisons for factor:

Comparison	Diff of Means	t	Unadjusted P	Critical Level	Significant?
Soln Ctr vs. 620-R	771.693	13.249	<0.001	0.010	Yes
Soln Ctr vs. Latex	128.931	2.214	0.040	0.013	No
Soln Ctr vs. 720-R	85.513	1.468	0.159	0.017	No
Soln Ctr vs. HDPE	60.713	1.042	0.311	0.025	No
Soln Ctr vs. HD-GC	57.603	0.989	0.336	0.050	No

One Way Analysis of Variance – normalized to cell count, all pair-wise comparisons
Normality Test: Passed (P = 0.051)
Equal Variance Test: Passed (P = 0.415)

Group Name	N	Missing	Mean	Std Dev	SEM
Latex	4	0	26.987	2.765	1.382
HDPE	4	0	30.383	2.404	1.202
Ctr	4	0	33.406	1.764	0.882

620-R	4	0	-5.013	1.663	0.831
720-R	4	0	37.663	8.088	4.044
HD	4	0	36.273	4.024	2.012

Source of Variation	**DF**	**SS**	**MS**	**F**	**P**
Between Groups	5	5104.302	1020.860	60.700	<0.001
Residual	18	302.725	16.818		
Total	23	5407.027			

The differences in the mean values among the treatment groups are greater than would be expected by chance; there is a statistically significant difference (P = <0.001).

Power of performed test with alpha = 0.050: 1.000

All Pairwise Multiple Comparison Procedures (Holm-Sidak method):
Overall significance level = 0.05

Comparisons for factor:

Comparison	**Diff of Means**	**t**	**Unadjusted P**	**Critical Level**	**Significant?**
720-R vs. 620-R	42.675	14.716	<0.001	0.003	Yes
HD vs. 620-R	41.285	14.237	<0.001	0.004	Yes
Ctr vs. 620-R	38.418	13.248	<0.001	0.004	Yes
HDPE vs. 620-R	35.395	12.206	<0.001	0.004	Yes
Latex vs. 620-R	31.999	11.035	<0.001	0.005	Yes
720-R vs. Latex	10.676	3.682	0.002	0.005	Yes
HD vs. Latex	9.286	3.202	0.005	0.006	Yes
720-R vs. HDPE	7.280	2.510	0.022	0.006	No
Ctr vs. Latex	6.419	2.213	0.040	0.007	No
HD vs. HDPE	5.890	2.031	0.057	0.009	No
720-R vs. Ctr	4.257	1.468	0.159	0.010	No
HDPE vs. Latex	3.396	1.171	0.257	0.013	No
Ctr vs. HDPE	3.023	1.042	0.311	0.017	No
HD vs. Ctr	2.867	0.989	0.336	0.025	No
720-R vs. HD	1.390	0.479	0.638	0.050	No

Cytotoxicity Titration Assay

Box Plot

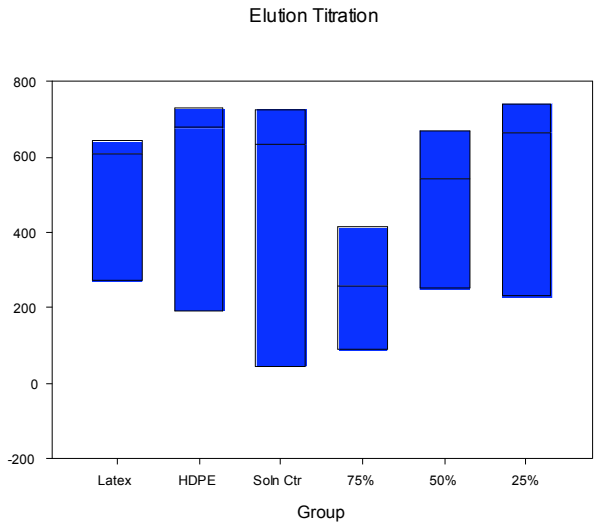

Studentized Residuals

Soln Ctr	Residual	SEM	St. Resid.	75%	Residual	SEM	St. Resid.
-1.11	-468.075	139.528	-3.3547	200.232	-43.16	70.068	-0.61597
626.517	159.5522	139.528	1.143514	416.969	173.577	70.068	2.477265

755.98	289.0152	139.528	2.071378	320.823	77.431	70.068	1.105084
641.73	174.7652	139.528	1.252546	412.312	168.92	70.068	2.410801
715.96	248.9952	139.528	1.784554	124.968	-118.424	70.068	-1.69013
62.712	-404.253	139.528	-2.89729	-14.952	-258.344	70.068	-3.68705
Latex				50%			
367.725	-109.023	106.601	-1.02272	340.343	-124.322	110.766	-1.12238
648.64	171.8925	106.601	1.612485	496.392	31.7273	110.766	0.286435
639.1	162.3525	106.601	1.522992	590.295	125.6303	110.766	1.134196
583.265	106.5175	106.601	0.999217	727.755	263.0903	110.766	2.37519
632.398	155.6505	106.601	1.460122	650.341	185.6763	110.766	1.676293
-10.643	-487.391	106.601	-4.5721	-17.138	-481.803	110.766	-4.34973
HDPE				25%			
255.848	-259.105	125.419	-2.06591	312.032	-206.613	125.908	-1.64098
719.984	205.0312	125.419	1.63477	712.163	193.5182	125.908	1.536981
666.337	151.3842	125.419	1.207028	615.011	96.3662	125.908	0.76537
689.822	174.8692	125.419	1.39428	751.426	232.7812	125.908	1.84882
747.773	232.8202	125.419	1.856339	736.136	217.4912	125.908	1.727382
9.953	-505	125.419	-4.0265	-14.899	-533.544	125.908	-4.23757

One Way Analysis of Variance
Normality Test: Failed (P < 0.050)
Test execution ended by user request, ANOVA on Ranks begun

Kruskal-Wallis One Way Analysis of Variance on Ranks

Group	N	Missing	Median	25%	75%
Sol Ctr	6	1	641.730	485.566	725.965
Latex	6	1	632.398	529.380	641.485
HDPE	6	1	689.822	502.241	726.931
75%	6	1	320.823	181.416	413.476
50%	6	1	590.295	457.380	669.695
25%	6	1	712.163	539.266	739.958

H = 7.828 with 5 degrees of freedom. (P = 0.166)

The differences in the median values among the treatment groups are not great enough to exclude the possibility that the difference is due to random sampling variability; there is not a statistically significant difference (P = 0.166)

One Way Analysis of Variance – Fluorescence, Comparisons vs. Control

Normality Test: Passed (P = 0.270)

Equal Variance Test: Passed (P = 0.295)

Group	Name	N	Missing	Mean	Std Dev	SEM
Sol Ctr	6	2	685.047	61.344	30.672	
Latex	6	2	625.851	29.162	14.581	
HDPE	6	2	705.979	35.475	17.737	
75%	6	2	318.768	136.573	68.287	
50%	6	2	616.196	97.699	48.849	
25%	6	2	703.684	61.284	30.642	

Source of Variation	DF	SS	MS	F	P
Between Groups	5	434892.191	86978.438	13.797	<0.001
Residual	18	113474.904	6304.161		
Total	23	548367.095			

The differences in the mean values among the treatment groups are greater than would be expected by chance; there is a statistically significant difference (P = <0.001).

Power of performed test with alpha = 0.050: 1.000

Multiple Comparisons versus Control Group (Holm-Sidak method):
Overall significance level = 0.05

Comparisons for factor:

Comparison	Diff of Means	t	Unadjusted P	Critical Level	Significant?
Sol Ctr vs. 75%	366.279	6.524	<0.001	0.010	Yes
Sol Ctr vs. 50%	68.851	1.226	0.236	0.013	No
Sol Ctr vs. Latex	59.196	1.054	0.306	0.017	No
Sol Ctr vs. HDPE	20.932	0.373	0.714	0.025	No
Sol Ctr vs. 25%	18.637	0.332	0.744	0.050	No

One Way Analysis of Variance – Normalized to Cell Count, All 2-Way Comparisons
Normality Test: Passed (P = 0.664)
Equal Variance Test: Passed (P = 0.396)

Group Name	N	Missing	Mean	Std Dev	SEM
Latex	4	0	22.335	1.430	0.715
HDPE	4	0	26.263	1.739	0.870
Ctr	4	0	25.236	3.007	1.504
75%	3	0	10.447	2.658	1.535
50%	4	0	21.861	4.789	2.395
25%	4	0	26.150	3.004	1.502

Source of Variation	DF	SS	MS	F	P
Between Groups	5	577.361	115.472	12.884	<0.001
Residual	17	152.366	8.963		
Total	22	729.726			

The differences in the mean values among the treatment groups are greater than would be expected by chance; there is a statistically significant difference (P = <0.001).

Power of performed test with alpha = 0.050: 1.000

All Pairwise Multiple Comparison Procedures (Holm-Sidak method):
Overall significance level = 0.05

Comparisons for factor:

Comparison	Diff of Means	t	Unadjusted P	Critical Level	Significant?
HDPE vs. 75%	15.815	6.917	<0.001	0.003	Yes
25% vs. 75%	15.703	6.868	<0.001	0.004	Yes
Ctr vs. 75%	14.789	6.468	<0.001	0.004	Yes
Latex vs. 75%	11.887	5.199	<0.001	0.004	Yes
50% vs. 75%	11.414	4.992	<0.001	0.005	Yes
HDPE vs. 50%	4.402	2.079	0.053	0.005	No
25% vs. 50%	4.289	2.026	0.059	0.006	No
HDPE vs. Latex	3.928	1.856	0.081	0.006	No
25% vs. Latex	3.816	1.802	0.089	0.007	No
Ctr vs. 50%	3.375	1.594	0.129	0.009	No
Ctr vs. Latex	2.902	1.371	0.188	0.010	No
HDPE vs. Ctr	1.026	0.485	0.634	0.013	No
25% vs. Ctr	0.914	0.432	0.671	0.017	No
Latex vs. 50%	0.474	0.224	0.826	0.025	No
HDPE vs. 25%	0.113	0.0531	0.958	0.050	No

APPENDIX I: PATENT APPLICATION

Electronic Acknowledgement Receipt

EFS ID:	8735188
Application Number:	
International Application Number:	PCT/US10/54745
Confirmation Number:	8622
Title of Invention:	POLYMERIC MATERIALS INCLUDING A GLYCOSAMINOGLYCAN NETWORKED WITH A POLYOLEFIN-CONTAINING POLYMER
First Named Inventor/Applicant Name:	COLORADO STATE UNIVERSITY RESEARCH FOUNDATION
Customer Number:	23405
Correspondence Address:	Heslin Rothenberg Farley & Mesiti Andrew K. Gonsalves 5 Columbia Circle - Albany NY 12203 US 518-452-5600 hesroth@hrfmlaw.com
Filer:	Andrew K. Gonsalves
Filer Authorized By:	
Attorney Docket Number:	3124.010AWO
Receipt Date:	29-OCT-2010
Filing Date:	
Time Stamp:	16:42:01
Application Type:	International Application for filing in the US receiving office

Payment information:

Submitted with Payment	yes

Payment Type	Deposit Account
Payment was successfully received in RAM	$2761
RAM confirmation Number	3505
Deposit Account	081935
Authorized User	

The Director of the USPTO is hereby authorized to charge indicated fees and credit any overpayment as follows:

Charge any Additional Fees required under 37 CFR 1.445 (International application filing, processing and search fees)

Charge any Additional Fees required under 37 CFR 1.17(t) (Acceptance of an unintentionally delayed claim for priority)

File Listing:

Document Number	Document Description	File Name	File Size(Bytes)/ Message Digest	Multi Part /.zip	Pages (if appl.)
1	ZIP	3124010AWO.zip	50977	yes	

Multipart Description/PDF files in .zip description		
Document Description	Start	End
fees.pdf	1	2
pct101.pdf	1	4

Warnings:

Information:

2		3124010AWO_APPLICATION_Filed_2010-10-29.pdf	1022633	yes	51

Multipart Description/PDF files in .zip description		
Document Description	Start	End
Specification	1	39
Claims	40	50
Abstract	51	51

Warnings:

Information:

3	Drawings-other than black and white line drawings	3124010AWO_DRAWINGS_Filed_2010-10-29.pdf	1484827	no	10

Warnings:

Information:

4	RO/101 - Request form for new IA - PCT EASY Format	3124010AWO_Request_SIGNED.pdf	97250	no	4

Warnings:					
Information:					
5	RO/101 - Annex (fee calculation sheet)	3124010AWO_Annex-SIGNED.pdf	55449	no	4
Warnings:					
Information:					
6	Fee Worksheet (PTO-875)	fee-info.pdf	36623	no	2
Warnings:					
Information:					
		Total Files Size (in bytes):	2767996		

This Acknowledgement Receipt evidences receipt on the noted date by the USPTO of the indicated documents, characterized by the applicant, and including page counts, where applicable. It serves as evidence of receipt similar to a Post Card, as described in MPEP 503.

New Applications Under 35 U.S.C. 111
If a new application is being filed and the application includes the necessary components for a filing date (see 37 CFR 1.53(b)-(d) and MPEP 506), a Filing Receipt (37 CFR 1.54) will be issued in due course and the date shown on this Acknowledgement Receipt will establish the filing date of the application.

National Stage of an International Application under 35 U.S.C. 371
If a timely submission to enter the national stage of an international application is compliant with the conditions of 35 U.S.C. 371 and other applicable requirements a Form PCT/DO/EO/903 indicating acceptance of the application as a national stage submission under 35 U.S.C. 371 will be issued in addition to the Filing Receipt, in due course.

New International Application Filed with the USPTO as a Receiving Office
If a new international application is being filed and the international application includes the necessary components for an international filing date (see PCT Article 11 and MPEP 1810), a Notification of the International Application Number and of the International Filing Date (Form PCT/RO/105) will be issued in due course, subject to prescriptions concerning national security, and the date shown on this Acknowledgement Receipt will establish the international filing date of the application.

3124010AWO

PCT (ANNEX - FEE CALCULATION SHEET)

Original (for SUBMISSION)

(This sheet is not part of and does not count as a sheet of the international application)

0	For receiving Office use only	
0-1	International Application No.	
0-2	Date stamp of the receiving Office	

0-4 0-4-1	Form PCT/RO/101 (Annex) PCT Fee Calculation Sheet Prepared Using	PCT-SAFE [EASY mode] Version 3.51.047.223 MT/FOP 20101001/0.20.5.18
6-9	Applicant's or agent's file reference	3124010AWO
2	Applicant	COLORADO STATE UNIVERSITY RESEARCH FOUNDATION

12	Calculation of prescribed fees		Fee amount/multiplier		Total amounts (USD)	
12-1	Transmittal fee	T	⇨		240	
12-2-1	Search fee	S	⇨		1092	
12-2-2	International search to be carried out by		KR			
12-3	International filing fee (first 30 sheets)	I1		1147		
12-4	Remaining sheets		35			
12-5	Additional amount	(K)	13			
12-6	Total additional amount	I2		455		
12-7	I1 + I2 =	I		1602		
12-12	EASY Filing reduction	R		-86		
12-13	Total international filing fee (I-R)	I	⇨		1516	
12-14	Fee for priority document Number of priority documents requested		1			
12-15	Fee per document	(K)	0			
12-16	Total priority document fee	P	⇨			
12-17	Fee for restoration of priority rights Number of requests for restoration of priority rights	RP	0			
	Total amount of fees for restoration of priority rights					
12-19	TOTAL FEES PAYABLE (T+S+I+P+RP)		⇨		2848	

3124610AWO

PCT (ANNEX - FEE CALCULATION SHEET)

Original (for **SUBMISSION**)

(This sheet is not part of and does not count as a sheet of the international application)

12-21	Mode of payment	Authorization to charge current account
12-22	Current account instructions The receiving Office	United States Patent and Trademark Office (USPTO) (RO/US)
12-22-1	Authorization to charge the total fees indicated above	✓
12-22-2	Authorization to charge any deficiency or credit any overpayment in the total fees indicated above	✓
12-22-3	Authorization to charge the fee for priority document	✓
12-23	Current account No.	081935
12-24	Date	29 October 2010 (29.10.2010)
12-25	Name and signature	GONSALVES, Andrew K., Reg. No. 48,145 /Andrew K. Gonsalves/

PCT

13-2-3	Validation messages Names	Green? Applicant 1:Telephone No. missing
	Validation messages Names	Green? Applicant 1:Facsimile No. missing
	Validation messages Names	Green? Applicant 1: no e-mail address has been indicated. Please verify.
13-2-7	Validation messages Contents	Green? A power of attorney or a copy of a general power of attorney may be required by the receiving Office unless at least one of the applicants signs the request form. Please contact the receiving Office for further information.

The present invention relates to polymeric materials including a glycosaminoglycan networked with a polyolefin-containing polymer. The present invention also relates to hydrogels containing the polymeric materials. The present invention further relates to methods of synthesizing the polymeric materials and hydrogels of the present invention.

Electronic Patent Application Fee Transmittal	
Application Number:	
Filing Date:	
Title of Invention:	POLYMERIC MATERIALS INCLUDING A GLYCOSAMINOGLYCAN NETWORKED WITH A POLYOLEFIN-CONTAINING POLYMER
First Named Inventor/Applicant Name:	COLORADO STATE UNIVERSITY RESEARCH FOUNDATION
Filer:	Andrew K. Gonsalves
Attorney Docket Number:	3124.010AWO

International Application for filing in the US receiving office Filing Fees

Description	Fee Code	Quantity	Amount	Sub-Total in USD($)
Basic Filing:				
Transmittal fee	1601	1	240	240
Suppl. Intl Filing Fee (each page > 30)	1703	35	13	455
International Search (KIPO)	1709	1	1092	1092
Int'l Filing Fee (1st-30 Pgs.) EFS Web	1710	1	974	974
Pages:				
Claims:				
Miscellaneous-Filing:				
Petition:				

Description	Fee Code	Quantity	Amount	Sub-Total in USD($)
Patent-Appeals-and-Interference:				
Post-Allowance-and-Post-Issuance:				
Extension-of-Time:				
Miscellaneous:				
			Total in USD ($)	2761

PCT REQUEST

Original (for SUBMISSION)

0	For receiving Office use only	
0-1	International Application No.	
0-2	International Filing Date	
0-3	Name of receiving Office and "PCT International Application"	
0-4	Form PCT/RO/101 PCT Request	
0-4-1	Prepared Using	PCT-SAFE [EASY mode] Version 3.51.047.223 MT/FOP 20101001/0.20.5.18
0-5	Petition The undersigned requests that the present international application be processed according to the Patent Cooperation Treaty	
0-6	Receiving Office (specified by the applicant)	United States Patent and Trademark Office (USPTO) (RO/US)
0-7	Applicant's or agent's file reference	3124010AWO
I	Title of invention	POLYMERIC MATERIALS INCLUDING A GLYCOSAMINOGLYCAN NETWORKED WITH A POLYOLEFIN-CONTAINING POLYMER
II	Applicant	
II-1	This person is	Applicant only
II-2	Applicant for	All designated States except US
II-4	Name	COLORADO STATE UNIVERSITY RESEARCH FOUNDATION
II-5	Address	P.O. Box 483 Fort Collins, Colorado 80522 United States of America
II-6	State of nationality	US
II-7	State of residence	US
III-1	Applicant and/or Inventor	
III-1-1	This person is	Applicant and inventor
III-1-2	Applicant for	US only
III-1-4	Name (LAST, First)	JAMES, Susan P.
III-1-5	Address	46 Split Stone Lane Bellvue, Colorado 80512 United States of America
III-1-6	State of nationality	US
III-1-7	State of residence	US

PCT REQUEST

Original (for SUBMISSION)

II-2	Applicant and/or inventor	
II-2-1	This person is	Applicant and inventor
II-2-2	Applicant for	US only
II-2-4	Name (LAST, First)	YONEMURA, Susan S.
II-2-5	Address	2926 Bassick Street Fort Collins, Colorado 80526 United States of America
II-2-6	State of nationality	US
II-2-7	State of residence	US
II-3	Applicant and/or inventor	
II-3-1	This person is	Applicant and inventor
II-3-2	Applicant for	US only
II-3-4	Name (LAST, First)	VARTANIAN, Ariane
II-3-5	Address	116 Arcadia Avenue Santa Clara, California 95051 United States of America
II-3-6	State of nationality	US
II-3-7	State of residence	US
IV-1	Agent or common representative; or address for correspondence The person identified below is hereby/ has been appointed to act on behalf of the applicant(s) before the competent International Authorities as:	Agent
IV-1-1	Name (LAST, First)	GONSALVES, Andrew K.
IV-1-2	Address	Heslin Rothenberg Farley & Mesiti 5 Columbia Circle Albany, New York 12203 United States of America
IV-1-3	Telephone No.	518-452-5600
IV-1-4	Facsimile No.	518-452-5579
IV-1-5	e-mail	hesroth@hrfmlaw.com
IV-1-5(a)	E-mail authorization The receiving Office, the International Searching Authority, the International Bureau and the International Preliminary Examining Authority are authorized to use this e-mail address, if the Office or Authority so wishes, to send notifications issued in respect of this international application:	as advance copies followed by notifications
IV-1-6	Agent's registration No.	48145
V	DESIGNATIONS	
V-1	The filing of this request constitutes under Rule 4.9(a), the designation of all Contracting States bound by the PCT on the international filing date, for the grant of every kind of protection available and, where applicable, for the grant of both regional and national patents.	

PCT REQUEST

Original (for SUBMISSION)

VI-1	Priority claim of earlier national application		
VI-1-1	Filing date	29 October 2009 (29.10.2009)	
VI-1-2	Number	61/256,275	
VI-1-3	Country	US	
VI-2	Priority document request The receiving Office is requested to prepare and transmit to the International Bureau a certified copy of the earlier application(s) identified above as item(s):	VI-1	
VI-3	Incorporation by reference : where an element of the international application referred to in Article 11(1)(iii)(d) or (e) or a part of the description, claims or drawings referred to in Rule 20.5(a) is not otherwise contained in this international application but is completely contained in an earlier application whose priority is claimed on the date on which one or more elements referred to in Article 11(1)(iii) were first received by the receiving Office, that element or part is, subject to confirmation under Rule 20.6, incorporated by reference in this international application for the purposes of Rule 20.5.		
VII-1	International Searching Authority Chosen	Korean Intellectual Property Office (ISA/KR)	
VIII	Declarations	Number of declarations	
VIII-1	Declaration as to the identity of the inventor	-	
VIII-2	Declaration as to the applicant's entitlement, as at the international filing date, to apply for and be granted a patent	-	
VIII-3	Declaration as to the applicant's entitlement, as at the international filing date, to claim the priority of the earlier application	-	
VIII-4	Declaration of inventorship (only for the purposes of the designation of the United States of America)	-	
VIII-5	Declaration as to non-prejudicial disclosures or exceptions to lack of novelty	-	
IX	Check list	Number of sheets	Electronic file(s) attached
IX-1	Request (including declaration sheets)	4	✓
IX-2	Description	39	-
IX-3	Claims	11	-
IX-4	Abstract	1	✓
IX-5	Drawings	10	-
IX-7	TOTAL	65	

PCT REQUEST

Original (for SUBMISSION)

	Accompanying Items	Paper document(s) attached	Electronic file(s) attached
IX-8	Fee calculation sheet	✓	-
IX-18	PCT-SAFE physical media	-	✓
IX-20	Figure of the drawings which should accompany the abstract	1	
IX-21	Language of filing of the international application	English	
X-1	Signature of applicant, agent or common representative	/Andrew K. Gonsalves/ Reg. No. 48,145	
X-1-1	Name (LAST, First)	GONSALVES, Andrew K.	
X-1-2	Name of signatory		
X-1-3	Capacity		

FOR RECEIVING OFFICE USE ONLY

10-1	Date of actual receipt of the purported international application	
10-2	Drawings:	
10-2-1	Received	
10-2-2	Not received	
10-3	Corrected date of actual receipt due to later but timely received papers or drawings completing the purported international application	
10-4	Date of timely receipt of the required corrections under PCT Article 11(2)	
10-5	International Searching Authority	ISA/KR
10-6	Transmittal of search copy delayed until search fee is paid	-

FOR INTERNATIONAL BUREAU USE ONLY

11-1	Date of receipt of the record copy by the International Bureau	

POLYMERIC MATERIALS INCLUDING A GLYCOSAMINOGLYCAN NETWORKED WITH A POLYOLEFIN-CONTAINING POLYMER

CROSS-REFERENCE TO RELATED APPLICATIONS

[0001] This application claims priority benefit of U.S. Provisional Patent Application Serial No. 61/256,275, filed October 29, 2009, which is hereby incorporated by reference herein in its entirety.

GOVERNMENT RIGHTS STATEMENT

[0002] The present invention was made with U.S. Government support under National Science Foundation (NSF) Grant No. CHE0649263. The U.S. Government has certain rights in the invention.

FIELD OF THE INVENTION

[0003] The present invention relates to polymeric materials including a glycosaminoglycan networked with a polyolefin-containing polymer. The present invention also relates to hydrogels containing the polymeric materials. The present invention further relates to methods of synthesizing the polymeric materials and hydrogels of the present invention.

BACKGROUND OF THE INVENTION

[0004] Hyaluronan (HA) is a ubiquitous, highly conserved macromolecule found in numerous species and present in almost every tissue in the body. HA has a long-standing history of use in numerous commercial applications including cosmetics, wound repair, drug delivery, and select biomedical engineering applications (e.g., cell-seeded hydrogels and scaffolds, osteochondral defect repairs). While its biocompatibility and bioactive properties make it an attractive biomaterial, its mechanical properties are insufficient for load-bearing applications. Attempts to improve mechanical properties have included various crosslinking methodologies, but commercially-available crosslinked HA hydrogels are still orders of magnitude weaker than required for many load-bearing biomedical applications. Therefore, there is a need for hydrogels that have suitable mechanical, biocompatibility, and bioactive properties.

[0005] The present invention is directed to overcoming these and other deficiencies in the art.

SUMMARY OF THE INVENTION

[0006] In one aspect, the present invention relates to a polymeric material including a glycosaminoglycan ("GAG") networked with a polyolefin-containing polymer. In one embodiment, the glycosaminoglycan networked with a polyolefin-containing polymer is synthesized by reacting a glycosaminoglycan constituent with a polyolefin constituent, where the glycosaminoglycan constituent includes a modified glycosaminoglycan, and where the polyolefin constituent includes an alternating copolymer of a polyolefin with an acid anhydride. Therefore, the polymeric material of the present invention includes a glycosaminoglycan covalently bound to a polyolefin-containing polymer.

[0007] In another aspect, the present invention relates to a method of synthesizing a polymeric material including a glycosaminoglycan networked with a polyolefin-containing polymer. This method involves reacting a glycosaminoglycan constituent with a polyolefin constituent under conditions effective to yield the polymeric material including a glycosaminoglycan networked with a polyolefin-containing polymer. The glycosaminoglycan constituent used in this method can be one or more modified glycosaminoglycans. The polyolefin constituent used in this method can be an alternating copolymer of a polyolefin with an acid anhydride. This method is effective to yield a polymeric material including a glycosaminoglycan networked with a polyolefin-containing polymer, where the glycosaminoglycan is covalently bound to the polyolefin–containing polymer. In a particular embodiment, the polymeric material synthesized by this method includes hyaluronan and poly(ethylene-*alt*-maleic anhydride) ("PEMA") covalently bound to one another.

[0008] In another aspect, the present invention relates to a polymeric material that includes a tripolymer glycosaminoglycan-polyolefin network, where the tripolymer glycosaminoglycan-polyolefin network is synthesized by reacting a first constituent, a second constituent, and a third constituent with one another, thereby yielding the tripolymer glycosaminoglycan-polyolefin network. The first constituent used to synthesize the tripolymer glycosaminoglycan-polyolefin network can include one or more modified glycosaminoglycans. The second constituent used to synthesize the tripolymer glycosaminoglycan-polyolefin network is an alternating copolymer of a polyolefin with an acid anhydride. The third constituent used to synthesize the tripolymer glycosaminoglycan-polyolefin network is a graft copolymer having a polyolefin backbone functionalized/grafted with an acid anhydride. The first constituent, the second constituent, and the third constituent react to form covalent bonds in the polymeric material.

[0009] In another aspect, the present invention relates to a method of synthesizing a polymeric material that includes a tripolymer glycosaminoglycan-polyolefin network. This method involves providing the following constituents: (i) a first constituent including one or more modified glycosaminoglycans; (ii) a second constituent including an alternating copolymer of a polyolefin with an acid anhydride; and (iii) a third constituent including a graft copolymer having a polyolefin backbone functionalized/grafted with an acid anhydride. The first constituent, the second constituent, and the third constituent are reacted under conditions effective to yield a tripolymer glycosaminoglycan-polyolefin network. The first constituent, the second constituent, and the third constituent react to form covalent bonds in the polymeric material. Suitable first, second, and third constituents for use in this method can include, without limitation, those as described herein above.

[0010] In another aspect, the present invention relates to a polymeric material including a glycosaminoglycan networked with a polyolefin-containing polymer, where the glycosaminoglycan networked with a polyolefin-containing polymer includes glycosaminoglycan covalently bound to a polyolefin-containing polymer. In a particular embodiment, the glycosaminoglycan is hyaluranon and the polyolefin-containing polymer is PEMA.

[0011] In another aspect, the present invention relates to hydrogels that include the polymeric materials of the present invention.

[0012] Hydrogels of the polymeric materials (including, for example, copolymers and tripolymers) of the present invention can be used for various purposes. For example, the hydrogels of the present invention can be used for orthopedic and other medical applications, including, without limitation, the following: (1) intervertebral disc repair, reconstruction, and regeneration; (2) cartilage repair, reconstruction, and regeneration; (3) meniscus repair, reconstruction, and regeneration; (4) soft tissue augmentation, repair, reconstruction, regeneration. Other possible uses and applications for the hydrogels of the present invention can include, without limitation, adhesion barriers; drug delivery vehicles; contact lenses; plant-florist shop flower gels; cooling bands, cooling mats, temperature and hydration control/regulation where biocompatibility is important; diapers; fire suppression; plastic surgery (e.g., facial augmentation, wrinkle injections, cosmetics, breast implants/augmentation); and water absorbing applications (e.g., super water absorbency).

[0013] The GAG-based hydrogels of the present invention are capable of absorbing many times their dry weight in water or saline and still maintain their mechanical integrity with swelling and have mechanical properties amenable to use in orthopedic implants (e.g.,

cartilage repair, meniscal repair, IVD repair). The GAG (e.g., HA) should make the hydrogel biocompatible and bioactive. Crosslinking the copolymer after synthesis improves network characteristics (e.g., mechanical integrity) and exhibits slightly decreased water absorption (swelling).

[0014] Reference is made to International Application No. PCT/US2008/005054, filed April 18, 2008, which published as WO 2008/130647 on October 30, 2008, and which claims benefit of priority to U.S. Provisional Patent Application Serial No. 60/925,452, filed April 19, 2007, the entire disclosures of which are hereby incorporated by reference in their entirety. The present application has at least one inventor in common with PCT/US2008/005054. The polymeric materials (including copolymers and tripolymers) of the present invention are distinct from the graft copolymer described in PCT/US2008/005054, but have some general similarities. For example, certain of the polymeric materials (including copolymers and tripolymers) of the present invention and the copolymers of PCT/US2008/005054 are similar in that they have –OH groups on GAG that react with maleic anhydride (MAH or MA) on maleated polyethylene (PE).

[0015] However, the polymeric materials (including copolymers and tripolymers) of the present invention are distinguishable from the copolymers of PCT/US2008/005054 in a number of important ways. For example, the polymeric materials (including copolymers and tripolymers) of the present invention are effective in producing hydrophilic hydrogels (i.e., a crosslinked network that maintains shape and mechanical integrity when swollen in aqueous solvents like water and absorbs many times its own weight in water). By way of contrast, the polymeric material made of the copolymer of PCT/US2008/005054 is an amphiphilic material.

[0016] Another distinction between the polymeric materials (including copolymers and tripolymers) of the present invention and the copolymers of PCT/US2008/005054 is with regard to the starting reactant. The copolymers of PCT/US2008/005054 used grafted MAH-PE as the starting reactant. By way of contrast, the polymeric materials (including copolymers and tripolymers) of the present invention uses an alternating MAH-PE (PEMA) copolymer as a starting reactant. Therefore, unlike the copolymer of PCT/US2008/005054, the reactive MAH groups of the polymeric materials (including copolymers and tripolymers) of the present invention are in the PE backbone (not grafted). In addition, compared to the copolymers of PCT/US2008/005054, the polymeric materials (including copolymers and tripolymers) of the present invention have significantly more MAH groups available for reaction.

[0017] Another distinction between the polymeric materials (including copolymers and tripolymers) of the present invention and the copolymers of PCT/US2008/005054 relates to the copolymerization reaction. Synthesis of the copolymers of PCT/US2008/005054 required a 2-phase reaction or emulsion reaction. By way of contrast, the polymeric materials (including copolymers and tripolymers) of the present invention only require a copolymerization reaction done in a single phase (e.g., DMSO). In one embodiment, the tripolymers of the present invention are synthesized using copolymers of both the present invention and of PCT/US2008/005054, except that 1,2,4-trichlorobenzene (TCB) is used in place of xylenes. DMSO is miscible with benzene but immiscible with xylene.

[0018] Another distinction between the polymeric materials (including copolymers and tripolymers) of the present invention and the copolymers of PCT/US2008/005054 relates to hydrogel characteristics. For example, the hydrogels made from the polymeric materials (including copolymers and tripolymers) of the present invention form an infinite network and are more gel-like than the copolymers of PCT/US2008/005054. In addition, in some cases the hydrogels of the present invention have physical crosslinks that do not last and more permanent chemical crosslinks with subsequent HMDI crosslinking.

BRIEF DESCRIPTION OF THE DRAWINGS

[0019] For the purpose of illustrating the invention, there are depicted in the drawings certain embodiments of the invention. However, the invention is not limited to the precise arrangements and instrumentalities of the embodiments depicted in the drawings.

[0020] Figure 1 is a photograph of three samples of crosslinked HA-*co*-PEMA stained gels suspended in deionized water. The gels were stained with toluidine blue O to highlight hyaluronan content. From left-to-right, the gels were crosslinked with 1%, 2.5%, and 5% v/v crosslinking solutions.

[0021] Figures 2A-2H are photographs of variations in copolymer formulation, shown swollen in phosphate-buffered saline (PBS), as follows: (A) 85:15 CoPEMA; (B) crosslinked 85:15 CoPEMA; (C) 70:30 CoPEMA; (D) crosslinked 70:30 CoPEMA; (E) 85:10:5 tripolymer gel; (F) 85:10:5 crosslinked tripolymer gel; (G) 70:15:15 tripolymer gel; and (H) 70:15:15 crosslinked tripolymer gel. The samples shown in FIG. 2F and FIG. 2H have been stained with toluidine blue O.

[0022] Figure 3 is a graph showing swell test results for three batches of a "95:5 CoPEMA" formulation (7:1 HA-CTA:PEMA weight ratio). No significant difference is seen among mean equilibrium swell ratios for the three batches (n=3 per group).

[0023] Figure 4 is a graph showing complex shear moduli for silica-reinforced 95:5 CoPEMA gels (TS-620 and TS-720, n=6 per group) and ovine nucleus pulposus (NP, n=5); properties appropriate for NP in a physiological frequency range can be achieved via particulate reinforcement of the gel.

[0024] Figure 5 is a graph showing representative storage (G') and loss (G'') shear moduli for silica-reinforced 95:5 CoPEMA gels (TS-620 and TS-720) and ovine nucleus pulposus (NP) over the frequency range 0.05 Hz $< f <$ 20 Hz.

[0025] Figure 6 is a graph showing the effect of reinforcement level with swell ratio of silica-reinforced 95:5 CoPEMA gels (TS-620 and TS-720). As silica content increases swell ratio decreases.

[0026] Figure 7 is a graph showing the effect of crosslinking and solution on swell ratio. Swell ratio for untreated gels significantly increases in deionized water vs. phosphate buffered saline due to repulsive forces among negatively-charged hyaluronan molecules; charges are masked by cations in the PBS. No difference is seen in crosslinked gels.

[0027] Figure 8 is a graph showing an FTIR spectrum identifying 95:5 CoPEMA gel.

[0028] Figure 9 is a graph showing FTIR spectra for CoPEMA gel vs. a control blend of HA and PEMA. The difference spectra (subtraction of control blend spectra from CoPEMA spectra) shows the development of an ester peak along with a decrease in anhydride moieties.

[0029] Figure 10 is a graph showing an FTIR spectrum identifying 85:15:15 tripoly gel.

DETAILED DESCRIPTION OF THE INVENTION

[0030] The present invention generally relates to a polymeric material that includes a glycosaminoglycan networked with a polyolefin-containing polymer having a glycosaminoglycan covalently bound to a polyolefin-containing polymer. As described in more detail herein, one aspect of the present invention relates to an embodiment of the polymeric material that is synthesized from the combination of a modified glycosaminoglycan with an alternating copolymer of a polyolefin with an acid anhydride. The polymeric material of the present invention can be used in numerous applications, including, for example, in the preparation of hydrogels for use in medical devices.

[0031] Prior to discussing the present invention in detail, provided below are definitions of certain terms used to describe the present invention or aspects thereof. In general, the terms are used within their accepted meanings. The definitions provided herein

below are meant to clarify, but not limit, the terms defined. Throughout this specification, the terms and substituents retain their definitions, unless otherwise stated.

[0032] A "polymer" is a substance composed of macromolecules, the structure of which essentially comprises the multiple repetition of units derived from molecules of low relative molecular mass.

[0033] A "monomer" that is polymerized along with one or more other monomers creates a "copolymer."

[0034] A "polyolefin" (also referred to in the relevant art as a "polyalkene") is a polymer produced from olefin, or alkene, as the monomer. For example, "polyethylene" is the polyolefin produced by polymerizing the olefin, ethylene. Polyethylene is a well-accepted engineering plastic with high toughness and good load bearing properties. Introducing polyethylene into HA hydrogels allows for improved mechanical integrity while retaining the hydrophilicity and bioactivity of HA. The mechanical properties can be tuned by varying constituent ratios and/or chemically crosslinking gels produced via the reactions described herein. "Polypropylene" is the name given to the polyolefin which is made from propylene.

[0035] "Synthetic polymers" encompass a large number of polymers, including, for example, polyethylene, polypropylene, polystyrene (a polymer made from the monomer styrene), etc.

[0036] A "copolymer" is a polymer derived from a mixture of two or more starting compounds, or monomers; a copolymer exists in many forms in which the monomers are arranged to form different types, or structures. The properties of a polymer depends both on the type of monomers that make up the molecule, and how those monomers are arranged. For example, a linear chain polymer may be soluble or insoluble in water depending on whether it is composed of polar monomers or nonpolar monomers, and also on the ratio of the former to the latter.

[0037] As used herein, a "tripolymer" is a polymer derived from a mixture of three or more starting compounds, monomers, polymers, or copolymers.

[0038] A "graft copolymer" can be synthesized by grafting one polymer onto a second polymer (i.e., rather than starting with monomers, synthesis starts with pre-polymerized polymers that are then grafted together). As used herein, graft copolymers can be identified by using the letter "*g*" or the word "*graft*" between the different polymers of a particular graft copolymer (e.g., polyethylene-*graft*-maleic anhydride).

[0039] An "alternating copolymer" refers to a copolymer having alternating monomers, as opposed to one polymer making up the backbone and the other polymer being grafted onto the backbone. As used herein, alternating copolymers can be identified by using the abbreviation "*alt*" or the word "*alternating*" between the different polymers of a particular alternating copolymer (e.g., poly(ethylene-*alt*-maleic anhydride)).

[0040] The terminology that has developed to describe polymers refers to both the nature of the monomers as well as their relative arrangement within the polymer structure. The most simple form of polymer molecule is a "linear" or "straight chain" polymer, composed of a single, linear backbone with pendant groups.

[0041] A "branched polymer molecule" is composed of a main chain, or "backbone," with one or more constituent side chains or branches (for example, branched polymers include star polymers, comb polymers, and brush polymers). If the polymer contains a side chain that has a different composition or configuration than the main chain, the polymer is considered a "graft" or "grafted polymer." Anhydride graft polyethylene is an example of a polyolefin that has been grafted with anhydride functional groups.

[0042] A "crosslink" suggests a branch point from which one polymer chain is covalently bound to another polymer chain, or a part of itself. A polymer molecule with a high degree of crosslinking is often referred to as a "polymer network" or an "elastomer." If there is a very high graft rate of a smaller (side chain) polymer molecule onto a larger (backbone) polymer molecule and there is a high graft rate and one side chain is grafted to more than one backbone molecule at a time, then the graft copolymer can form a polymer network.

[0043] As used herein, the terms "network" or "networked" or "polymer network" are used to describe a polymeric material in which the polymeric molecules are covalently bound to each other, resulting in a gel which will swell in a good solvent for the constituent polymers, but will not dissolve.

[0044] As used herein, the term "hydrogel" is meant to include a networked polymeric material in an aqueous solvent.

[0045] "Melt-processable" refers to those thermoplastic polymers that have a distinct thermodynamic, first order phase transition melting point that is below the degradation point of the polymer. Such a polymer will melt when heated, making it easier to form into different shapes, and when cooled down will recrystallize. Only the crystalline portion of the material actually melts, the amorphous regions do not. For most thermoplastic polymers,

melting of the crystalline regions will make the polymer flow and thus make it thermally formable, if the melting point is well below the degradation point of the material.

[0046] "Glycosaminoglycan" (abbreviated as "GAG"), as used herein, is intended to include, without limitation, hyaluronan, chondroitin sulfate, dermatan sulfate, keratan sulfate, heparan sulfate, and heparin; these are generally considered to be biodegradable molecules. A glycosaminoglycan is composed of a repeating disaccharide; that is, it has the structure -A-B-A-B-A-, where A and B represent two different sugars.

[0047] As used herein, "poly(ethylene-*alt*-maleic anhydride)" (abbreviated as "PEMA") is an alternating copolymer of polyethylene with maleic anhydride. Because PEMA is water-soluble, a polymeric material containing PEMA can be distinguished from other polymeric materials not containing PEMA (e.g., HA-*g*-HDPE) with higher swelling ratios and lower elastic/shear modulus. Using Fourier transform infrared (FTIR) spectroscopy, the polyolefin peaks are broader and less distinct.

[0048] PEMA can be described structurally as follows:

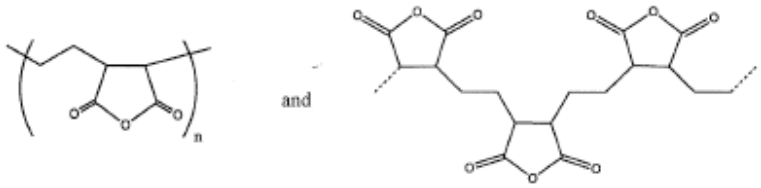

Poly(ethylene-*alt*-maleic anhydride) (PEMA)

[0049] In one aspect, the present invention relates to a polymeric material including a glycosaminoglycan networked with a polyolefin-containing polymer. In one embodiment, the glycosaminoglycan networked with a polyolefin-containing polymer is synthesized by reacting a glycosaminoglycan constituent with a polyolefin constituent, where the glycosaminoglycan constituent includes one or more modified glycosaminoglycans, and where the polyolefin constituent includes an alternating copolymer of a polyolefin with an acid anhydride. Therefore, the polymeric material of the present invention includes a glycosaminoglycan networked with a polyolefin-containing polymer where the glycosaminoglycan is covalently bound to a polyolefin-containing polymer.

[0050] As used herein, suitable glycosaminoglycans can include, without limitation, hyaluronan, chondroitin sulfates, dermatan sulfates, keratan sulfates, heparan sulfates, and

heparin. Further, more than one type of glycosaminoglycan or modified glycosaminoglycan may be used or contained in the polymeric materials of the present invention. The glycosaminoglycan constituent can be a glycosaminoglycan modified with a paraffin ammonium cation dissociated from a salt, including, without limitation, alkyltrimethylammonium chloride, alkylamine hydrochloride, alkylpyridinium chloride, alkyldimethylbenzyl ammonium chloride, alkyltrimethylammonium bromide, alkylamine hydrobromide, alkylpyridinium bromide, and alkyldimethylbenzyl ammonium bromide. In a particular embodiment, the alkyltrimethylammonium bromide can be cetyl alkyltrimethylammonium bromide (CTAB).

[0051] As used herein, a suitable polyolefin can included, without limitation, polyethylene.

[0052] As used herein, a suitable acid anhydride can include, without limitation, maleic anhydride.

[0053] As used herein, the term polyolefin-containing polymer can include a polymer having an alternating copolymer of an olefin with maleic anhydride (e.g., PEMA).

[0054] In one embodiment, the polyolefin constituent can be an alternating copolymer of polyethylene with maleic anhydride, including, for example, poly(ethylene-*alt*-maleic anhydride) (PEMA) as described herein.

[0055] In another embodiment, the polyolefin constituent can include, without limitation, poly(ethylene-*alt*-maleic anhydride), poly(styrene-*alt*-maleic anhydride), poly(isobutylene-*alt*-maleic anhydride), poly(maleic anhydride-*alt*-1-octadecene), poly(methyl vinyl ether-*alt*-maleic anhydride), and derivatives thereof.

[0056] In another embodiment, the polyolefin-containing polymer can include, without limitation, poly(ethylene-*alt*-maleic anhydride), poly(styrene-*alt*-maleic anhydride), poly(isobutylene-*alt*-maleic anhydride), poly(maleic anhydride-*alt*-1-octadecene), poly(methyl vinyl ether-*alt*-maleic anhydride), and derivatives thereof.

[0057] A structural representation of one embodiment of the polymeric material of the present invention (CoPEMA) is provided below:

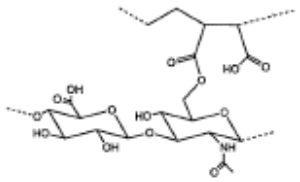

[0058] In another embodiment, the polymeric material can further include a reinforcing agent. The reinforcing agent can be an inorganic reinforcing agent, an organic reinforcing agent, or a mixture thereof. Suitable examples of inorganic reinforcing agents can include, without limitation, inorganic agents such as silica, alumina, zirconia, calcium phosphates, and hydroxyapatite, as well as compositions containing these inorganic agents. Suitable examples of organic reinforcing agents can include, without limitation, carbon nanotubes, carbon nanofibers, chitosan nanofibers, demineralized bone matrix (DBM), collagen, silk, and cellulose. Further, the inorganic reinforcing agents and the organic reinforcing agents can be modified to provide additional desired characteristics to the polymeric material. For example, the reinforcing agent can be surface-modified. In one embodiment, the inorganic reinforcing agent can be silica modified with polydimethylsiloxane to make it hydrophobic. Suitable reinforcing agents can also include synthetic polymers well known in the art and readily available. For example, suitable synthetic polymers for use as reinforcing agents can include, without limitation, DACRON®, TEFLON®, KEVLAR®, and the like. Other reinforcing agents can include, without limitation, any non-water soluble agent (e.g., fiber, particulate) that provides reinforcement to the polymeric material, and that does not interfere with synthesis of the polymeric material. One of ordinary skill in the art can readily determine various reinforcing agents suitable for use in the present invention, as well as suitable modifications to the reinforcing agents.

[0059] The present invention also relates to a method of synthesizing a polymeric material including a glycosaminoglycan networked with a polyolefin-containing polymer. This method involves reacting a glycosaminoglycan constituent with a polyolefin constituent under conditions effective to yield the polymeric material including a glycosaminoglycan networked with a polyolefin-containing polymer. The glycosaminoglycan constituent used in this method can be one or more modified glycosaminoglycans. The polyolefin constituent used in this method can be an alternating copolymer of a polyolefin with an acid anhydride. This method is effective to yield a polymeric material including a glycosaminoglycan networked with a polyolefin-containing polymer, where the glycosaminoglycan is covalently bound to the polyolefin-containing polymer. In a particular embodiment, the polymeric material synthesized by this method includes hyaluronan and PEMA covalently bound to one another.

[0060] In one embodiment, the reacting step of the above method of synthesizing the polymeric material is an esterification reaction between the glycosaminoglycan constituent

and the polyolefin constituent. The various glycosaminoglycan constituents and polyolefin constituents suitable for use in this method are as described herein.

[0061] Set forth for illustration purposes is a synthetic scheme (**Scheme 1**) that generally depicts one embodiment of the synthesis of the polymeric material of the present invention, as follows:

Scheme 1

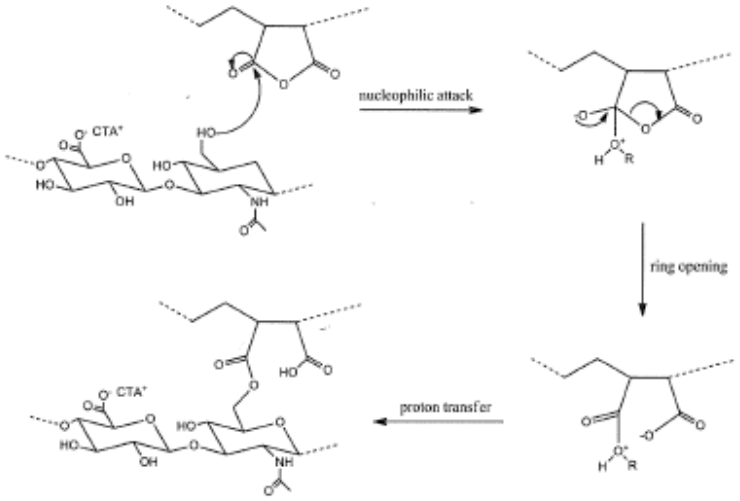

[0062] In view of **Scheme 1**, one of ordinary skill in the art can see that in the final hydrolyzed form, the glycosaminoglycan (i.e., hyaluronan (HA)) is no longer a "modified" glycosaminoglycan as it is when the reaction is occurring. As shown in this scheme, the modified glycosaminoglycan can be HA-CTA (HA complexed with cetyltrimethyl ammonium salt). Further, the polyolefin-containing polymer (i.e., PEMA) maintains the PE-*alt*-MA structure, but the MA (maleic anhydride) ring has opened up and reacted (bonded) to the HA, or has remained open in acid form.

[0063] In another embodiment, the above method of synthesizing the polymeric material can further include incubating the glycosaminoglycan constituent and the polyolefin constituent in a crosslinker constituent. Suitable crosslinker constituents can include any molecule or composition that is effective to crosslink with an alcohol group of the

glycosaminoglycan constituent. For example, suitable crosslinker constituents can include, without limitation, diisocyanates, polyisocyanates, hexamethylenediisocyanate (HMDI), methylene diphenyl diisocyanate, toluene diisocyanate, isophorone diisocyanate, divinyl sulphone, poly(ethylene glycol) diglycidyl ether, phosphoryl chloride, glutaraldehyde, dialdehyde via Passerini reaction, diamine via Ugi reaction, and carbodiimide.

[0064] In another embodiment, the above method of synthesizing the polymeric material can further include combining the glycosaminoglycan constituent and the polyolefin constituent with a reinforcing agent. Suitable reinforcing agents are as described herein. In view of the present specification and the teachings in the relevant art, one of ordinary skill would readily discern the types of reinforcing agents that can be used in the present invention, as well as the concentrations and protocols.

[0065] The present invention further relates to a polymeric material that includes a tripolymer glycosaminoglycan-polyolefin network, where the tripolymer glycosaminoglycan-polyolefin network is synthesized by reacting a first constituent, a second constituent, and a third constituent with one another, thereby yielding the tripolymer glycosaminoglycan-polyolefin network. The first constituent used to synthesize the tripolymer glycosaminoglycan-polyolefin network can include one or more a modified glycosaminoglycans. The second constituent used to synthesize the tripolymer glycosaminoglycan-polyolefin network is an alternating copolymer of a polyolefin with an acid anhydride. The third constituent used to synthesize the tripolymer glycosaminoglycan-polyolefin network is a graft copolymer having a polyolefin backbone functionalized/grafted with an acid anhydride. The first constituent, the second constituent, and the third constituent react to form covalent bonds in the polymeric material.

[0066] Suitable first and second constituents of the tripolymer glycosaminoglycan-polyolefin network are those as described herein above as the modified glycosaminglycan and the alternating copolymer of a polyolefin with an acid anhydride. Further, a suitable third constituent of this tripolymer glycosaminoglycan-polyolefin network can include, without limitation, maleic anhydride-*graft*-polyethylene, maleic anhydride-*graft*-polypropylene, maleic anhydride-*graft*-polystyrene, polystyrene-*graft*-maleic anhydride, polyisoprene-*graft*-maleic anhydride, and polypropylene-*graft*-maleic anhydride.

[0067] In one embodiment, the tripolymer glycosaminoglycan-polyolefin network includes hyaluron as the first constituent, poly(ethylene-*alt*-maleic anhydride) as the second constituent, and maleic anhydride-*graft*-polyethylene as the third constituent.

[0068] Structural representations of poly(ethylene-*alt*-maleic anhydride) (also referred to as PE-*alt*-MA and PEMA) is provided above.

[0069] Structural representations of a maleic anhydride-*graft*-polyethylene (also referred to as PE-*g*-MA) is provided below:

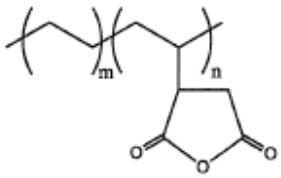

PE-*g*-MA

[0070] In another embodiment, the tripolymer glycosaminoglycan-polyolefin network can further include a reinforcing agent as described herein, a crosslinker constituent as described herein, or both.

[0071] The present invention also relates to a method of synthesizing a polymeric material that includes a tripolymer glycosaminoglycan-polyolefin network. This method involves providing the following constituents: (i) a first constituent including one or more modified glycosaminoglycans; (ii) a second constituent including an alternating copolymer of a polyolefin with an acid anhydride; and (iii) a third constituent including a graft copolymer having a polyolefin backbone functionalized/grafted with an acid anhydride. The first constituent, the second constituent, and the third constituent are reacted under conditions effective to yield a tripolymer glycosaminoglycan-polyolefin network. The first constituent, the second constituent, and the third constituent react to form covalent bonds in the polymeric material. Suitable first, second, and third constituents for use in this method can include, without limitation, those as described herein above.

[0072] In one embodiment, the reacting step of the above method of synthesizing the polymeric material (i.e., that includes a tripolymer glycosaminoglycan-polyolefin network) is an esterification reaction between the first constituent and the second and third constituents. The various constituents suitable for use in this method are as described herein.

[0073] In another embodiment, the above method of synthesizing the polymeric material (i.e., that includes a tripolymer glycosaminoglycan-polyolefin network) can further include incubating the first, second, and third constituents in a crosslinker constituent. Suitable crosslinker constituents are as described herein.

[0074] In another embodiment, the above method of synthesizing the polymeric material (i.e., that includes a tripolymer glycosaminoglycan-polyolefin network) can further

include combining the first, second, and third constituents with a reinforcing agent. Suitable reinforcing agents are as described herein.

[0075] In another aspect, the present invention relates to a polymeric material including a glycosaminoglycan networked with a polyolefin-containing polymer, where the glycosaminoglycan networked with a polyolefin-containing polymer includes glycosaminoglycan covalently bound to a polyolefin–containing polymer. In a particular embodiment, the glycosaminoglycan is hyaluranon and the polyolefin-containing polymer is PEMA.

[0076] In another aspect, the present invention relates to hydrogels that include the polymeric materials of the present invention. One of ordinary skill, in view of the teachings provided herein, can readily determine how to prepare a hydrogel that includes a polymeric material of the present invention.

[0077] The polymeric materials and hydrogels of the present invention can be distinguished from other polymeric materials and hydrogels using various techniques well known in the art. For example, Fourier transform infrared (FTIR) spectroscopy can be used to determine covalent bonding in the polymeric material/hydrogel by analyzing the formation of ester bonds between the constituents. Swelling properties can also be analyzed, where certain embodiments of the polymeric materials/hydrogels of the present invention exhibit swelling, but not dissolving, in an aqueous medium. Additionally, mechanical properties of the polymeric materials/hydrogels of the present invention can be used to distinguish them from other polymeric materials and hydrogels.

Description of PCT/US2008/005054

[0078] As discussed herein above, the polymeric material, copolymers, and tripolymers of the present invention are distinguishable from the copolymers disclosed in International Application No. PCT/US2008/005054, filed April 18, 2008, which published as WO 2008/130647 on October 30, 2008, and which claims benefit of priority to U.S. Provisional Patent Application Serial No. 60/925,452, filed April 19, 2007. The present application shares at least one inventor in common with PCT/US2008/005054.

[0079] One embodiment of a particular copolymer of PCT/US2008/005054 involved glycosaminoglycan covalently bound to polyethylene-*graft*-maleic anhydride. The tripolymer of the present invention includes as one of three constituents the polyethylene-*graft*-maleic anhydride.

[0080] Therefore, included below are portions of the disclosure of PCT/US2008/005054, substantially as set forth in PCT/US2008/005054.

A. Abstract of PCT/US2008/005054

[0081] A new copolymer synthesized from a glycosaminoglycan (GAG) such as hyaluronan/ hyaluronic acid (HA), chondroitin sulfates, dermatan sulfates, keratin sulfates, heparin sulfate, and heparin, and an anhydride functionalized hydrophobic polymer, i.e., any polyolefin which has been 'functionalized' (grafted onto the backbone or incorporated into the backbone) with anhydride functional groups, such as maleic anhydride-graft-polyethylene, (or, maleated polyethylene), maleic anhydride-graft-polystyrene, maleic anhydride-graft-polypropylene, etc. The functionalized polyolefin may be a polyolefin backbone to which the anhydride functional groups have been grafted, or otherwise incorporated with the backbone. Also, a unique synthesis technique combines a modified GAG with a graft polyolefin, resulting in a unique copolymer with its constituents by-and-large covalently bound to each other.

B. Technical Field of PCT/US2008/005054

[0082] In general, the invention relates to polymers and polymeric systems, as well as associated techniques for synthesizing polymers. More particularly, one aspect is directed to a new copolymer synthesized from a glycosaminoglycan (or simply, GAG) such as hyaluronan/ hyaluronic acid (HA), chondroitin sulfates, dermatan sulfates, keratin sulfates, heparin sulfate, and heparin, and an anhydride functionalized hydrophobic polymer, i.e., any polyolefin which has been 'functionalized' (grafted onto the backbone or incorporated into the backbone) with anhydride functional groups, such as maleic anhydride-graft-polyethylene, (known, also, as maleated polyethylene), maleic anhydride-graft-polystyrene, maleic anhydride-graft-polypropylene, and so on. The unique synthesis technique also disclosed, to combine a modified GAG with a graft polyolefin, results in a unique copolymer with its constituents by-and-large covalently bound to each other. While GAG's such as hyaluronan, or hyaluronic acid, are generally non-melt-processable and biodegradable, hydrophobic polymers such as polyolefins to which anhydride functional groups have been grafted, e.g., maleic anhydride-graft-polyethylene/ maleated polyethylene, are usually melt-processable and non-biodegradable.

[0083] Depending on the ratio and molecular weight of reactants (i.e., main constituents of copolymer), and graft percent of maleic anhydride onto the polyolefin, one

aspect of the novel copolymer is an amphiphilic, biphasic construct consisting of a glycosaminoglycan (GAG) backbone and synthetic polymeric side chains; a second aspect comprises a synthetic polymer backbone with GAG side chains; and a third aspect comprises a continuous network of GAG and synthetic polymer, in which the synthetic polymer acts as crosslinks between different GAG chains or vice versa. The synthesis and characterization of the various identified aspects of the novel copolymer will be appreciated in connection with the technical discussion set forth, herein.

[0084] The anhydride functional groups grafted to the polyethylene chain are highly reactive compared to the hydrolyzed form of anhydrides, dicarboxylic acid. Hydrolysis occurs in the presence of water; for this reason, the reactions (details of which are included in the discussion identified as **Example 1**) were performed in an inert atmosphere (e.g. dry medical grade nitrogen gas) and in non-aqueous solvents. Hyaluronan/hyaluronic acid (HA) is immiscible with non-polar (i.e. nonaqueous) solvents. Here, the glycosaminoglycan was first modified with, by way of example, an ammonium salt to decrease the polarity of the molecule ("modified glycosaminoglycan"); such a uniquely modified glycosaminoglycan was miscible with non-polar solvents (e.g. dimethyl sulfoxide). Other modified GAG's are contemplated; for example, the GAG may be modified with other paraffin ammonium cations dissociated from a salt selected from the group consisting of alkyltrimethylammonium chloride, alkylamine hydrochloride, alkylpyridinium chloride, alkyldimethylbenzyl ammonium chloride, alkyltrimethylammonium bromide, alkylamine hydrobromide, alkylpyridinium bromide, and alkyldimethylbenzyl ammonium bromide.

[0085] The anhydride graft polyethylene is miscible with xylenes at 135°C. The novel amphiphilic copolymer was washed and the modified glycosaminoglycan portion of the copolymer was reverted back to its unmodified chemical structure through hydrolysis.

[0086] ***Applicant's earlier work in synthesizing hydrophobic- hydrophilic polymers.*** The assignee hereof also owns U.S. Pat. App. No. 10/283,760 filed 29-Oct-02, James et al., entitled "Outer Layer having Entanglement of Hydrophobic Polymer Host and Hydrophilic Polymer Guest," Pub. No. US 2003/0083433 on 0l-May-03 describing earlier design and research efforts of at least one applicant-inventor hereof, and is fully incorporated herein by reference to the extent it provides supportive technological information of the unique copolymer, and its synthesis, and is consistent with this technical discussion. The assignee hereof also owns PCT International App. No. PCT/ US2004/ 030666 filed 20-Sept-04, James et al., entitled "Hyaluronan (HA) Esterification via Acylation Technique for Moldable

Devices," international pub. No. WO 2005/028632 A2 describing other earlier related research and development efforts of at least one applicant-inventor hereof.

C. Summary Disclosure of PCT/US2008/005054

[0087] One will appreciate the many distinguishable features of copolymer described herein from conventional products. Certain of the unique features of the invention, and further unique combinations of features — as supported and contemplated herein— provide a variety of advantages.

[0088] Briefly described, once again, the invention is directed to a novel copolymer synthesized from a glycosaminoglycan (e.g. hyaluronan, chondroitin sulfate, dermatan sulfate, keratan sulfate, heparan sulfate, heparin), and an anhydride functionalized hydrophobic polymer (such as any melt-processable polyolefin which has been grafted, or otherwise incorporated, with anhydride functional groups, e.g. anhydride graft polyethylene). The copolymer includes an amphiphilic, biphasic construct composed of a glycosaminoglycan (GAG) and a synthetic polymer. Also characterized is an associated novel process for synthesizing the copolymer.

[0089] One aspect of the invention is directed to a new copolymer synthesized from a glycosaminoglycan (GAG) such as hyaluronan, or hyaluronic acid (HA), chondroitin sulfates, dermatan sulfates, keratan sulfates, heparan sulfate, and heparin, and an anhydride functionalized hydrophobic polymer, i.e., any polyolefin which has been 'functionalized' (grafted onto the backbone or incorporated into the backbone) with anhydride functional groups; many such functionalized hydrophobic polymers are contemplated, such as maleic anhydride-graft- polyethylene (or simply, maleated polyethylene), maleic anhydride-graft-polystyrene, maleic anhydride-graft-polypropylene, and so on. The unique synthesis technique described herein to combine a modified GAG with an anhydride functionalized hydrophobic polymer, such as a graft poly olefin, results in a unique copolymer with its constituents by-and-large covalently bound to each other. One aspect of the novel copolymer is an amphiphilic, biphasic construct consisting of a glycosaminoglycan (GAG) backbone and synthetic polymeric side chains; a second aspect comprises a synthetic polymer backbone with GAG side chains; and a third aspect comprises a continuous network of GAG and synthetic polymer.

D. Description Detailing Features of PCT/US2008/005054

[0090] By viewing the figures depicting representative embodiments — further details included and labeled **Example 1**— of the unique copolymer and process to synthesize same, one can further appreciate the unique nature of core as well as additional and alternative features that are within the spirit and scope of this technical discussion. Reference has been made to various features — those depicted in the figures and diagrams (including those incorporated within an Example) — by way of back-and-forth reference and association.

[0091] Turning, first, to Figure 6 of PCT/US2008/005054: the copolymer synthesis technique represented at 20 joins a modified glycosaminoglycan dissolved in non-aqueous solvent 22A, e.g., hyaluronan complexed with ammonium salt (HA-CTA), with an anhydride graft polyethylene also having been dissolved in a non-aqueous solvent 22B, e.g., maleic anhydride graft polyethylene (MA-*g*-HDPE). The anhydride functional groups grafted to the polyethylene chain are highly reactive compared to the hydrolyzed form of anhydrides, dicarboxylic acid. Since hydrolysis occurs in the presence of water, the copolymer reaction must be performed in an inert atmosphere (e.g. dry industrial nitrogen or argon gas) and in non-aqueous solvents; see, also Figure 2 of PCT/US2008/005054. A covalent bond forms between the modified glycosaminoglycan and the anhydride graft polyethylene (24) forming the structure HA-CTA-*co*-HDPE (see, Figure 7 of PCT/US2008/005054 at 30).

[0092] Once the copolymer reaction is complete, hydrolysis is purposely performed converting the modified glycosaminoglycan portion of the copolymer back to 'unmodified' glycosaminoglycan resulting in the GAG-poly olefin copolymer (in this specific example, HA-co-HDPE, box 26). Due to hyaluronan's immiscibility with non-polar (i.e. non-aqueous) solvents, the glycosaminoglycan was first modified with an ammonium salt to decrease the polarity of the molecule (i.e. modified glycosaminoglycan) 22A; once this was achieved the modified glycosaminoglycan was miscible with non-polar solvents (e.g. dimethyl sulfoxide). The anhydride graft polyethylene is miscible with xylenes at above approximately 100°C. As mentioned, the novel amphiphilic copolymer was washed and the modified glycosaminoglycan was reverted back to its unmodified chemical structure through hydrolysis (box 26, Figure 6 of PCT/US2008/005054; see also Figure 7 of PCT/US2008/005054). The glycosaminoglycan or polyolefin portions of the graft copolymer are now available for further processing (box 28), e.g, may be crosslinked. This may be performed 'individually' as is suggested at 28: crosslink HA portion with poly(diisocyanate) to form XLHA-g- HDPE; and crosslink HDPE portion with dicumyl peroxide.

[0093] A wide range of applications of the new copolymer are contemplated, to include a variety of devices and procedures, including but not limited to: total joint arthroplasty (as part or all of implant), hemi-arthroplasty, partial hemi-arthroplasty, scaffold for tissue engineering (specifically articular cartilage), meniscus replacement, catheters, condoms, cosmetics, wound dressing, ear tubes for chronic ear infections, carrier for drugs, demineralized bone matrix and bone morphogenetic proteins, bone defect filler, cosmetic surgery, maxio-facial reconstructions, non fouling coating for catheters, tissue engineering scaffold, anti adhesive film or coating, soft tissue augmentation - meniscus, cartilage, spinal disc, temporomandibular disc replacement, low friction coating on instruments/ devices, wound covering (nonstick bandage, etc), viscosupplementation, eye surgery lubricant, etc.

EXAMPLES

[0094] The following examples are intended to illustrate particular embodiments of the present invention, but are by no means intended to limit the scope of the present invention.

Example 1

Synthesis of HA-CTA-*co*-HDPE and its Hydrolysis to Yield HA-*co*-HDPE

[0095] This example corresponds to Example 1 of PCT/US2008/005054 (discussed herein above). This example discusses the synthesis of HA-CTA-*co*-HDPE and its hydrolysis to yield HA-*co*-HDPE (reaction conditions given for 98 and 85% HA HA-CTA-*co*-HDPE with HA molecular weight of 1.5 MDa, and 0.3% MA (graft percent) MA-*g*-HDPE wherein the HDPE has a molecular weight of 121.5 kg/mol).

[0096] Complexation methods for sodium HA with CTAB are known. See, by way of further example: Zhang,M. and James,S.P.: Novel Hyaluronan Esters for Biomedical Applications, *Rocky Mountain Bioengineering Symposium, Biomedical Sciences Instrumentation* 238, 2004; Zhang,M. and James,S.P.: Silylation of hyaluronan to improve hydrophobicity and reactivity for improved processing and derivatization, Polymer 46:3639, 2005; and Zhang,M. and James,S.P.: Synthesis and properties of melt-processable hyaluronan esters, *Journal of Materials Science: Materials in Medicine* 16:587 (2005).

[0097] In U.S. Pat. App. No 10/283,760, James et al., "Outer Layer having Entanglement of Hydrophobic Polymer Host and Hydrophilic Polymer Guest," U.S. Patent

Application Publication No. US 2003/0083433 (mentioned above) on May 1, 2003, such complexes of HA were discussed:

-- Begin QUOTED text --

EXAMPLE 2

> **(1)** Reaction of HA with long-chain aliphatic quaternan ammonium salts (QN^+). Polyanions, such as HA. combined with certain organic cations, such as paraffin chain ammonium (QN^+) ions, produces a precipitable complex. The complex is a true salt of the polyand and quaternary base. HA was modified with long-chain aliphatic ammonium salts, to improve its solubility in organic solvents. Combination of QN+ with polyannions occurs in those pH ranges in which the polyannions are negatively charged. The reaction between HA and ammonium cations in water can be expressed:
>
> $$HA^-Na^+ + QN^+A^- \rightarrow HA^- QN^+ \downarrow + Na^+ A^-$$
>
> where HA^-Na^+ is the sodium salt of hyaluronic acid; HA^-QN^+ is the precipitable complex between HA carboxylic polyanion and long chain paraffin ammonium cations. HA^-QN^+ (HA-CPC / HA-CTAB) complexes were used. The complexes (HA^-QN^+) precipitated from HA aqueous solution are soluble in concentrated salt solutions, so HA can be recovered from its insoluble complexes. Ammonium salts used were: cetyltrimethylammonium bromide monohydrale (MW: 358.01) (CTAB) and cetylpyridinum chloride (M.W. 364.46) (CPC).

-- End QUOTED text --

[0098] Briefly, for this **Example 1**, aqueous solutions of 0.2% (w/ v) sodium HA and 1.0% (w/ v) CTAB were mixed at room temperature to precipitate the HA-CTA. The precipitate was centrifuged, washed with H_2O several times to remove Na^+Br^- salt, and vacuum dried at room temperature for 72 hours (or until no change in weight was observed). The molecular weight of HA-CTA was determined to be 2.48 x 10^6 Da. HA-CTA and MA-*g*-HDPE, are the two constituents of the graft copolymer HA-co-HDPE, and their structures are shown below; however, the MA-*g*-HDPE used in this study was HDPE with MA grafted (0.36 weight%) randomly along the HDPE backbone, unlike the structure shown below (bottom chemical structure), where it appears such that the MA is grafted at the 'tail-end' of the HDPE chains:

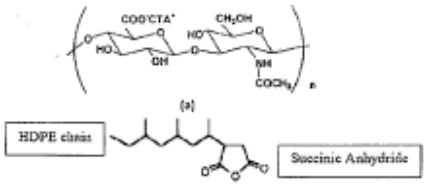

Chemical structures: top structure is of HA-CTA; and bottom is of MA-*g*-HDPE.

[0099] A 0.1 % (w/ v) solution of MA-g-HDPE in xylenes was refluxed for two hours at 135°C under a dry N_2 atmosphere ensuring all of the MA-g-HDPE had gone into solution. HA-CTA was dissolved in DMSO at 80°C (a 0.5% (w/ v) solution). The MA-*g*-HDPE solution was added to the HA-CTA solution via a heated cannula (Fig 2 of PCT/US2008/005054) under dry N_2 flow (see chemical structures diagrammed immediately below):

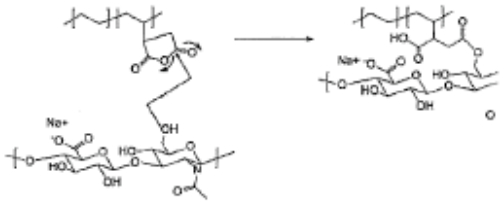

Chemical structures of: (left-side) HA-CTA; and (right-side) MA-*g*-HDPE.

[00100] After 24 hours the viscous gel product and supernatant were vacuum dried at 50°C for 72 hours; due to the complexity of evaporating off DMSO, only the xylenes portion of the supernatant was removed via vacuum drying. The DMSO was removed through hydrolysis process since it is miscible with both H_2O and ethanol.

[00101] The amount (g) of HA-CTA and MA-g-HDPE used in the reaction, as determined by amount of the 0.1% (w/v) solution of MA-g-HDPE in xylenes and 0.5% (w/v) solution of HA-CTA in DMSO used in the reaction, can be adjusted to synthesize copolymer products with different theoretical weight percentages of HA and HDPE. The glycosaminoglycan weight percentage of the copolymer was calculated prior to the reaction assuming 100% reaction between constituents and complete substitution of the CTA+ with Na+ during hydrolysis, which determined the required amount of MA-*g*-HDPE and HA-CTA

to be used in the reaction (see, also, **Example 2** of Prov. App. Ne 60/925,452, section 3.2.2 for general reference).

[00102] Using techniques similar to those described above, multiple theoretical weight percentages (40-98%) of the glycosaminoglycan to polyolefin, in the novel amphiphilic copolymer, were fabricated in order to observe the effects of different weight percentages of the glycosaminoglycan. The copolymer was also fabricated from glycosaminoglycans with various molecular weights (640 kDa and 1.5 Da) and functionalized polyolefins with various anhydride graft (i.e., weight) percentages (0.3 and 3.0%) and various molecular weights (15 kg/mol and 121.5 kg/mol). Chemical crosslinking of the glycosaminoglycan portion of the graft copolymer (see, also, Figure 6 of PCT/US2008/005054 at 28) was accomplished via a poly(hexamethylene diisocyanate) crosslinker after hydrolysis.

[00103] To determine if the graft copolymer and the crosslinked graft copolymer powders could be compression molded, powder was placed in a stainless steel mold (such molds are commonplace, and can be shaped with a cylindrical inner cavity for molding the material in compression). The compression molding cycles for both the graft copolymer and the crosslinked (XL) graft copolymer were identical; refer to Figure 3(b) of PCT/US2008/005054, also labeled in **Example 2** of Prov. App. N° 60/925,452 as Figure 3.4: "Compression molding cycle for HA-*co*-HDPE and XL HA-*co*-HDPE specimens (85 and 98 weight % HA)" depicting how temp and pressure varied over time. The melt soak temperature was approximately 10-15°C above the average melt temperature of the graft copolymer, which was deduced from differential scanning calorimetry results.

[00104] The reaction between the modified glycosaminoglycan and the anhydride graft polyethylene was carried out in an inert atmosphere, forming the novel graft copolymer. Figure 2 of PCT/US2008/005054 depicts a reaction test set-up configuration for **Example 1** graft copolymer synthesis. The reaction yields were approximately 95%. The resulting product was a swollen gel network (encapsulating the non-aqueous solvents) for higher weight percents of HA and was a melt-processable powder for lower weight percents of HA. A white, fluffy, porous powder was generated via hydrolysis, in which modified glycosaminoglycan graft copolymer converted to an unmodified glycosaminoglycan graft copolymer. Figure 3 of PCT/US2008/005054 is a scanning electron microscopy (SEM) image of the converted graft copolymer in powder form (Figure 6 of PCT/US2008/005054, box 26).

[00105] Upon hydration with water, the graft copolymer behaved like a hydrogel; the liquid prevented the polymer network (i.e. physically and chemically crosslinked mesh made up of polymer chains) from collapsing into a compact mass, and .the network retained the

liquid. The non-crosslinked graft copolymer was completely dispersed, but not dissolved, in water at room temperature after several hours; the crosslinked graft copolymer behaved qualitatively similar to the non-crosslinked graft copolymer. The graft copolymers both dispersed, but did not dissolve, in either or xylenes at room temperature. The insolubility of the copolymer indicates that a reaction did take place to form covalent bonds between the water soluble HA and xylenes soluble HDPE. The insoluble nature of the unique copolymer poses a challenge when attempting to characterize the graft copolymer and crosslinked graft copolymer using standard, conventional analytical techniques. Both a graft copolymer that is unmodified and a crosslinked graft copolymer are not soluble in any typical organic solvent, which hinders the use of solution dependent polymer characterization methods. The lack of solubility precludes the measurement of molecular weight, for example.

[00106] Figure 4(a) of PCT/US2008/005054 graphically depicts results from a differential scanning calorimetric scan overlay of anhydride graft polyethylene (refluxed MA-*g*-HDPE; 0.3% MA, 121.5 kg/mol), the glycosaminoglycan (HA; 1.5 MDa), and various graft copolymers with specific glycosaminoglycan weight percentages (10 molar = 85% HA, 1 molar = 98% HA). Figure 4(b) of PCT/US2008/005054 graphically depicts results from a differential scanning calorimetric scan of HA-co-HDPE fabricated from MA-*g*-HDPE with a molecular weight of 15 kg/ mole (50% HA). The introduction of HA lowered the melt temperature (peak temperature value) and percent crystallinity (peak area) of the anyhydride graft polyethylene. The changes in the peak values and areas, representing changes in the crystalline domains of the copolymer compared to the two constituents indicate covalent bonding between the HA to MA-*g*-HDPE (i.e., indicate copolymer formation). As described above, the melt temperature of the different graft copolymers was used to develop the compression molding cycle for the graft copolymers.

[00107] Thermogravimetric analysis scans were also analyzed and the degradation temperature of each polymer was determined: Figure 5 of PCT/US2008/005054 graphically depicts results from a thermal gravimetric analysis scan of the graft copolymer, a blend of the anhydride graft polyethylene and glycosaminoglycan (MA-*g*-HDPE and HA), and its constituents. The TGA scans show that the esterification reaction between HA and HDPE affects the degradation profiles of the two constituent polymers, verifying covalent bond formation between HA and MA-*g*-HDPE in the copolymer. From the thermogravimetric analysis data, the experimental weight percentages of the constituents can be compared to theoretical weight percentage calculations performed prior to the reaction taking place. **Table 1** compares the values for theoretical and experimental weight percentages.

Table 1

Comparison Between Theoretical Constituent Weight Ratios and the Weight Ratios Calculated from TGA Data for HA-*co*-HDPE

Theoretical HA:HDPE	TGA HA:HDPE
30:70	*42:53*
40:60	*37:50*
50:50 (HA, $1.4x10^6$ Da)	*33:67*
50:50 (HA, $6.4x10^5$ Da)	*35:65*
60:40 (HA, $1.4x10^6$ Da)	*56:44*

[00108] To further verify that the resultant copolymer was the product of the anhydride graft polyethylene and the HA-CTA, two negative control (also referred to as 'sham') reactions were performed. The first sham/control reaction was run, exactly as described above, but with plain high density polyethylene (HDPE) in the place of the anhydride graft polyethylene. In other words, in the absence of air and water, plain HDPE was refluxed in xylenes at ~145°C and then added to the HA- CTA in DMSO at ~80°C.

[00109] A second sham/ control reaction was carried out between anhydride graft polyethylene in xylenes and DMSO with no HA-CTA.

[00110] Neither sham/ control reaction formed a copolymer. The sham reactions did not form a gel product as occurs with the anhydride polyethylene/ HA-CTA reaction according to the processes depicted in Figures 6 and 7 of PCT/US2008/005054. When the solvents were evaporated, two distinct phase-separated powders remained from the first sham reaction and a single powder (anhydride graft polyethylene) remained from the second sham reaction. In other words, no copolymer was formed.

[00111] The non-degradable hydrophobic portion of the novel copolymer may also be chemically crosslinked via irradiation (gamma or e-beam), silane or peroxides (e.g. dicumyl peroxide [(bis(l-methyl-l-phenylethyl) peroxide], and benzyl peroxide [2,5- Dimethyl-2,5-di-(tert-butyl-peroxy) hexyne-3 peroxide], 2,5-dimethyl-2,5-bis(tert- butylperoxy)-3-hexyne), which would serve to increase the mechanical properties of the graft copolymer and alter the physical (rheological) properties of the graft copolymer.

Example 2

HA-*co*-PEMA Hydrogel Synthesis

[00112] One embodiment of the HA-*co*-PEMA hydrogel of the present invention was synthesized according to the protocol presented below.

[00113] Determine the dry weight of reactants (HA-CTA and PEMA) for the desired formulation based upon the reactant weight ratio (*see* **Table 2**).

Table 2

Copolymer Formulation Weight Ratios

Internal Nomenclature	Reactant Weight Ratio HA-CTA:PEMA
99:1 CoPEMA	36:1
95:5 CoPEMA	7:1
85:15 CoPEMA	2:1
70:30 CoPEMA	4:5
5:95 CoPEMA	1:20

[00114] For example, approximately 1 g of a 95:5 gel formulation (unhydrolyzed) will require 7/8 g HA-CTA and 1/8 g PEMA.

[00115] Weigh a slight excess of reactants (to allow for weight loss due to the evaporation of water) and place into separate labeled containers. Vacuum dry reactants at 50°C and -25 inches Hg for a minimum of 24 hours. Place glassware to be used for the reaction in a 100°C oven. Note: Exposure to water will hydrolyze the maleic anhydride and reduce the reactivity of the PEMA. Vacuum drying will close the anhydride rings and reactivate the MA functional groups.

[00116] ***Copolymerization Reaction:*** Place HA-CTA in 500 ml RBF along with an appropriate stir bar. Spread vacuum grease on two rubber serum stoppers and place stoppers in side necks of the flask. Secure stoppers with copper wire and parafilm. Attach condenser to middle neck of RBF, using vacuum grease or teflon sleeve to seal. Wrap connection with parafilm and secure with Keck clip. Add DMSO via cannula under dry N_2 flow, forming ~0.5% w/v solution (for 1.6 MDa HA; higher concentrations can be used for smaller HA). Continue to flush the system for a few minutes after the appropriate volume of DMSO has been added, closing off the system with a slight positive pressure of dry N_2. Heat to 80°C in an oil bath and stir vigorously for four hours to dissolve all HA-CTA. Place PEMA and appropriate stir bar in 250 ml RBF. Seal flask and add DMSO as described above for HA-

CTA to form a 0.1% w/v concentration. Heat to 80°C under vigorous stirring in an oil bath until PEMA goes into solution, approximately two hours. Once the HA-CTA and PEMA have gone into solution, raise the temperature for the HA-CTA/DMSO flask to 90°C. Transfer the PEMA-DMSO solution to the 500 ml RBF via cannula under N_2 flow. Mix the two solutions, stirring vigorously, for 12 hours at 90°C.

[00117] ***Copolymer Processing:*** Process reaction product per a CoPEMA Crosslinking protocol (*see* Example 4) or a Copolymer Washing protocol (*see* Example 5).

Example 3

Tripolymer Hydrogel Synthesis

[00118] Calculate the dry weight of reactants (HA-CTA, PEMA, and PE-*g*-MA) for the desired formulation based upon the reactant weight ratio (*see* **Table 3**):

Table 3

Copolymer Formulation Variations

Internal Nomenclature	Reactant Weight Ratio HA-CTA:PEMA
85:10:5 Tripoly	27.2:8.7:1*
70:15:15 Tripoly	7.5:4.4:1*

[00119] Weigh a slight excess of reactants (to allow for weight loss due to the evaporation of water) and place into separate labeled containers. Vacuum dry reactants at 50°C and -25 inches Hg for a minimum of 24 hours. Place glassware to be used for the reaction in a 100°C oven. Note: Exposure to water will hydrolyze the maleic anhydride and reduce the reactivity of the PEMA. Vacuum drying will close the anhydride rings and reactivate the MA functional groups.

[00120] ***Copolymerization Reaction:*** Place HA-CTA in 500 ml RBF along with an appropriate stir bar. Spread vacuum grease on two rubber serum stoppers and place stoppers in side necks of the flask. Secure stoppers with copper wire and parafilm. Attach condenser to middle neck of RBF, using vacuum grease or teflon sleeve to seal. Wrap connection with parafilm and secure with Keck clip. Add DMSO via cannula under dry N_2 flow, forming ~0.5% w/v solution (for 1.6 MDa HA; higher concentrations can be used for smaller HA). Continue to flush the system for a few minutes after the appropriate volume of DMSO has

been added, closing off the system with a slight positive pressure of dry N_2. Heat to 80°C in an oil bath and stir vigorously for four hours to dissolve all HA-CTA.

[00121] While HA-CTA is stirring, prepare PE solution: Place PEMA and appropriate stir bar in 250 ml RBF. Seal flask and add DMSO as described above for HA-CTA to form a 0.1% w/v concentration. Heat to 80°C under vigorous stirring in an oil bath. Place PE-*g*-MA and an appropriate volume of TCB to form a 0.1% w/v concentration in a 250 ml RBF. Add stir bar and seal flask as described above. Attach to condenser and flush with dry N_2 for a few minutes. Heat to 80°C under vigorous stirring in an oil bath. Once both PE mixtures have gone into solution (approximately two hours), transfer the PEMA solution to the PE-*g*-MA flask. Allow to mix vigorously for two hours. Once the HA-CTA has gone into solution and the PE mixture is well entangled, raise the temperature for the HA-CTA/DMSO flask to 90°C. Transfer the PEMA-DMSO solution to the 500 ml RBF via cannula under N_2 flow. Mix the two solutions, stirring vigorously, for 12 hours at 90°C.

[00122] ***Copolymer Processing:*** Process reaction product per a CoPEMA Crosslinking protocol (*see* Example 4) or a Copolymer Washing protocol (*see* Example 5).

Example 4

CoPEMA Crosslinking

[00123] Combine the coPEMA reaction product and an excess volume (3-4x) of a non-solvent (e.g., acetone, xylenes) in a large beaker to form a "gel" precipitate. Acetone can be used for high HA content; xylenes for mid to high PEMA content. Cover and soak for a minimum of 4 hours. Filter solvents from the gel using a Büchner funnel and vacuum flask. Wash and filter gel precipitate with acetone three times (may be increased). Resuspend the copolymer in a small volume of DMSO; mix vigorously using a vortexer. Add HMDI for a final concentration of up to 5% v/v with the DMSO and cast the suspension into a vial or petri dish as appropriate for desired shape. Allow the suspension to cure at room temperature for a minimum of 24 hours. Soak the crosslinked gel in several changes of acetone to remove excess HMDI. Prepare a 0.2M NaCl aqueous hydrolyzing solution. Immerse the crosslinked gel in the hydrolyzing solution and gently agitate (e.g. in shaker oven) at room temperature overnight.

Example 5

Washing Protocol

[00124] Prepare a 0.2M NaCl aqueous hydrolyzing solution (volume greater than the reaction volume) in a large beaker or flask. Add the copolymer suspension (HA-*co*-HDPE, HA-*co*-PEMA, tripolymer) to the hydrolyzing solution and mix at room temperature overnight. Add an excess of chilled EtOH and mix for a minimum of four hours to precipitate the copolymer. Allow to stand at room temperature; copolymer will begin to settle at the bottom of the beaker/flask. Centrifuge for 10 minutes to begin separating precipitate from supernatant. Filter supernatant using a ceramic filter and vacuum flask; soak precipitate pellets in isopropyl alcohol. Wash and filter precipitate with isopropyl alcohol three times (may be increased). Resuspend the copolymer in a small volume of distilled H_2O; mix at room temperature for four hours. Re-precipitate with an excess of isopropyl alcohol, mixing again at room temperature for four hours. Allow the solution to stand at room temperature; filter and wash as described above. Vacuum dry the HA-*co*-PEMA at ~25 inches Hg overnight or until there is no change in weight.

Example 6

Preliminary Swell Tests for Crosslinked HA-*co*-PEMA Hydrogels in Deionized Water

[00125] Swell tests were conducted for various crosslinked HA-*co*-PEMA hydrogels in deionized water. HA-co-PEMA gels were crosslinked with 1% (Hydrogel #1), 2.5% (Hydrogel #2), and 5% (Hydrogel #3) v/v crosslinking solutions. The results of these tests are shown below in **Table 4**:

Table 4

Preliminary Swell Test Results for Crosslinked HA-*co*-PEMA Hydrogels in Deionized Water

	Hydrogel #1	Hydrogel #2	Hydrogel #3
% HMDI (v/v)	1%	2.5%	5%
Swell ratio (Q) (wet weight/dry weight)	152.6	57.1	33.3
% water content ((wet – dry)/wet)	99.3%	98.2%	96.9%

HMDI = hexamethylene diisocyanate, a chemical crosslinker

[00126] **Figure 1** illustrates the stained gels suspended in deionized water, with the vials from left-to-right corresponding to gels crosslinked with 1% (Hydrogel #1), 2.5% (Hydrogel #2), and 5% (Hydrogel #3) v/v crosslinking solutions. The gels were stained with toluidine blue to indicate HA content.

Example 7

HA-*co*-PEMA Cast Gel Synthesis

[00127] One embodiment of the HA-*co*-PEMA hydrogel of the present invention was synthesized according to the protocol presented below.

[00128] ***Materials & Equipment:*** The following is a list of materials and equipment that were used to synthesize one embodiment of the polymeric material and hydrogel of the present invention: Hyaluronan-cetyl trimethylammonium complex (HA-CTA); Poly(ethylene-*alt*-maleic anhydride) (PEMA); Dimethyl sulfoxide (DMSO); Qty. 2 two-necked round-bottomed flasks (RBF); Serum stoppers; Copper wire; Keck clips; Condensers; N_2 (dry) gas; Oil bath; Weigh boat(s); Analytical scale; Magnetic stir bar(s); Stir plate(s); 70x50 crystallizing dish; Reinforcing agents (optional) (e.g., Particulate reinforcement: Cab-o-Sil fumed silica, TS-620/TS-720 (Cabot, Boston, MA)) (e.g., Fibrous reinforcement: Carbon nanotubes (nanotubes or nanofibers), Chitosan nanofibers); Disposable pipettes, 25 ml and 1 ml; Forceps; Pipette aid or bulb pipette; Vacuum bags and sealer; Disposable glove box (Sigma Aldrich); Temperature-controlled oven, e.g. Shake 'n Bake Hybridization Oven; Ultrasonic bath; Acetone; NaCl; Deionized water; Ethanol (EtOH); and Vacuum oven.

[00129] ***Procedure:*** The following are procedures that were used to synthesize one embodiment of the polymeric material and hydrogel of the present invention:

[00130] Stock Solutions: Note: Allow a minimum of 1 day prior to gel casting for preparation of stock solutions. Precautions for air/water-sensitive chemistry should be observed, i.e. HA-CTA and PEMA powders should be vacuum dried a minimum of 24 hours prior to use, glassware should be stored at 100°C to ensure it is completely dry, stir bars should be rinsed with acetone before use.

[00131] Prepare a concentrated solution of HA-CTA in DMSO, aiming for a viscosity similar to honey. A 2.5% w/v concentration is appropriate for HA-CTA prepared from HA in the 450-500 kDa size range. The procedure is as follows: Weigh HA-CTA and place along with stir bar in an appropriately-sized RBF. Seal side neck of RBF with a serum stopper secured with copper wire. Attach RBF to condenser with a Keck clip, lower into oil bath, set

temperature to 80°C and begin stirring. Insert vent needle and transfer canula into rubber serum stopper. Transfer appropriate volume of DMSO (100 ml for every 2.5g HA-CTA) into flask via canula under N_2 flow. Flush flask with N_2 by plugging vent, allowing slight positive pressure to build, and releasing plug a total of 3 times; plug vent and remove along with canula, leaving slight positive pressure of N_2 in the flask. When HA-CTA is fully dissolved (can take 12+ hours) remove from heat and allow to come to room temperature.

[00132] Prepare a 10% w/v concentrated solution of PEMA in DMSO, following procedure described above for HA-CTA solution. The PEMA will go into solution much more readily than the HA-CTA and thus will not need to be on heat for as long.

[00133] Gel Casting: Note: This reaction is air/water sensitive. If available, work inside a glove box filled w/ dry nitrogen, sealing the cast gel into a vacuum bag prior to removal from the glove box. If a glove box is not available, air/water contact can be minimized by working with sealed vacuum bags as described below.

[00134] Base formulation: 16.5 ml 2.5% (w/v) HA-CTA in DMSO; 0.6 ml 10% (w/v) PEMA in DMSO.

[00135] Reinforcement (optional): 0.8g treated silica (Cabot TS-620 or TS-720) max or fibrous reinforcement (e.g. carbon nanotubes, chitosan nanofibers).

[00136] Measure PEMA solution into a vial and seal with a serum stopper and copper wire. Flush vial with N_2 gas.

[00137] Measure HA-CTA solution into 70x50 crystallizing dish using 25 ml serological pipette. If reinforcement is to be used, add and stir by hand at this time. Place appropriately-sized stir bar into dish, then place dish and a pair of forceps into a large vacuum bag modified with a serum-stopper "port"; remove air with vacuum and flush with N_2 gas three times. Omit vacuum bag if working in glove box.

[00138] Place crystallizing dish on stir plate; turn-on stir plate to start mixing. Slowly add PEMA solution to the stirring HA-CTA solution via canula and low N_2 flow (if using vacuum bag) or dropwise using a pipette (if working in a glove box). The HA-CTA and PEMA solutions should complex, becoming more viscous. This may necessitate moving the dish around on the plate and adjusting the stir plate r.p.m. to get good mixing.

[00139] Remove the stir bar from the dish using the forceps. If working in a glove box, place the cast gel into a vacuum bag and seal immediately upon removal from glove box. Otherwise, push the forceps and stir bar to one end of the vacuum bag and re-seal the vacuum bag around the forceps and stir bar; cut bag to remove.

[00140] Place sealed dish into 75°C oven to cure for 24 hours.

[00141] After curing, remove excess PEMA by sonication with acetone for 30 minutes. Flip gel and repeat.

[00142] Prepare a 0.2M NaCl aqueous hydrolyzing solution in a large beaker or flask. Add the hydrolyzing solution to the crystallizing dish and sonicate for 30 minutes.

[00143] Replace hydrolyzing solution with deionized water and repeat sonication for 30 minutes. The gel will swell to a greater extent in deionized water, allowing trapped NaCTA to be removed. Repeat the sonication if the solution appears to be "soapy."

[00144] Dehydrate gel by soaking in ethanol a few hours or overnight; drain ethanol and completely dry in a vacuum oven at equipped with a solvent trap at -25 inches Hg until there is negligible change in weight.

Example 8

Synthesis of a Hyaluronan-Polyethylene Copolymer Hydrogel for Orthopedic Repair

[00145] **Abstract:** Hyaluronan-high density polyethylene graft copolymer (HA-*co*-HDPE, or Copoly) has previously been synthesized from hyaluronan (HA), a glycosaminoglycan, and high density polyethylene (HDPE), a synthetic plastic. HA-*co*-HDPE combines the mechanical properties of polyethylene with the lubricating benefits of hyaluronan; due to its biocompatibility, it may be a promising material for meniscal cartilage replacement or injectable nucleus pulposus repair. The following study attempts to improve upon the chemistry of the original reaction in order to synthesize a hyaluronan-polyethylene copolymer that behaves as a true hydrogel.

[00146] **Introduction:** Biocompatible hydrogels serve as practical materials in orthopedic medicine. A true hydrogel network will swell and preserve structural integrity in a water or saline environment, which are advantageous properties for materials used in orthopedic replacements or repair. An ideal hydrogel for such applications would feature both the mechanical strength of polyethylene (PE), a plastic used in artificial joints, and the lubricating character of hyaluronan (HA), the "gooey" or viscous glycosaminoglycan found throughout the body, including in synovial fluid and around articular cartilage. Previous studies[1] synthesized an HA-PE copolymer (HA-*co*-PE) from ammonium cation-complexed HA and maleated PE, via esterification reactions between the primary hydroxyls of the HA chain and maleic anhydride (MA) groups grafted onto the polyethylene backbone. However, this original HA-*co*-PE lacked mechanical integrity when swollen in water. The objective of

this research was to synthesize a hyaluronanpolyethylene copolymer that behaves as a true hydrogel.

[00147] Hyaluronan is a hydrophilic glycosaminoglycan found in synovial fluid and coating articular cartilage, known for its lubricating properties. The structure of hyaluronan is well known.

[00148] Polyethylene is a hydrophobic durable thermoplastic often used in artificial joints. The structure of polyethylene is well known.

[00149] Several approaches are described here. The original copolymer reaction was repeated, replacing 1,2,4-trichlorobenzene for xylenes as a more DMSO-miscible solvent in order to increase the reactive interface. An HA amide reduction experiment was also conducted in an attempt to functionalize HA with crosslinker-compatible primary amine reactive groups. Finally and most promisingly, a collection of copolymers with varying ratios of PE-*g*-MA, PE-*alt*-MA, and HA-CIA, were synthesized, crosslinked, and characterized by swell tests and FTIR.

CopolyGel: PE-alt-MA and HA-CTA

[00150] The maleic anhydride to hydroxyl (MA:OH) reactive ratio of the Copoly reaction is 1:185; that is, the hydroxyl is in extreme excess. In order to optimize the molar ratio, a polyethylene incorporating more maleic anhydride groups is ideal. For this purpose poly(ethylene-*alternating*-maleic anhydride), comprised of 78% maleic anhydride by weight, was chosen to replace polyethylene-*graft*-maleic anhydride, which featured only 3% maleic anhydride by weight, leaving OH in great excess and limiting the number ester linkages. In the case of an 85:15 HA:PE final product ratio, this shifts the reactive ratio to 1:1.58, in favor of MA (the "perfect" ratio is 1:4, since HA contains four hydroxyl groups, only one of which is primary and thus reactive).

[00151] The esterification reaction between maleated polyethylene and HA-CTA is as shown in **Scheme 1** (provided above).

[00152] PE-*alt*-MA, unlike PE-*g*-MA, is actually a copolymer with an alternating ethylene-MA-ethylene-MA structure. Without a polyethylene backbone, PE-*alt*-MA may not behave like true polyethylene. In fact, PE-*alt*-MA is water-soluble, while polyethylene and PE-*g*-MA are hydrophobic; PE-*alt*-MA is also soluble in DMSO. This allows the copolymer esterification reaction to occur in only DMSO, eliminating the need for a second solvent (xylenes or TCB) and expanding the reaction interface to the entire volume of solution. However, the dissimilarity of its physical properties also suggests that PE-*alt*-MA may not

provide the strength or durability of polyethylene, since it cannot form the random crystalline segments that provide polyethylene its characteristic strength, and any network it forms with HA could potentially lack necessary mechanical integrity.

[00153] The structures of (a) a polyethylene backbone with grafted maleic anhydride groups and (b) an alternating ethylene-maleic anhydride copolymer are provided hereinabove.

[00154] CopolyGel was synthesized in two formulations, a 85:15 or 70:30 HA:PE final product ratio, so that it could be compared to Copoly materials of similar product composition. PE-*alt*-MA and HA-CTA were dissolved in DMSO separately, then reacted together at 90°C for 12 hours. (A single solvent flask reaction yielded similar results, but separate solvent flasks are recommended to ensure homogeneity.) Hydrolysis, precipitation, washing, hydration, and drying steps were followed as according to the Copoly protocol, although isopropanol replaced ethanol as a washing agent but *not* as a precipitating agent as salt solutions are insoluble in isopropanol.

[00155] Both CopolyGel products behaved as hydrogels. 70:30 was stronger than 85:15 as expected by the relative amount of modified polyethylene present, but both swelled significantly in PBS, a saline solution that mimics physiological salt concentration (95.08% water after one hour for 70:30, 93.53% for 85:15) without falling apart. Still, they lacked the desired mechanical strength; the lubricated outer surface easily separated from the rest of the network, and too much agitation or pressure could cause the network to break apart entirely.

HMDI-Crosslinked CopolyGel

[00156] The diisocyanate crosslinker HMDI was explored as a potential avenue for increasing networking in CopolyGel. HMDI, or hexamethylenediisocyanate, crosslinks via an alcohol group on hyaluronan, so it can link together stray chains of HA that disrupt the mechanical integrity of the network. It is less toxic than the commonly used HA crosslinker gluteraldehyde, but due to its water sensitivity it cannot be used as an injectable *in vivo* crosslinker and requires toxic non-aqueous solvents. An ideal crosslinked gel strikes a balance between strength and swelling ability; a more crosslinked network will hold together tightly but may not be able to absorb much water.

[00157] Dry CopolyGel networks were soaked in excess 5% (v/v) HMDI/DMSO solution for approximately 20 hours under nitrogen. The samples were transferred to the vacuum oven at 50-70°C for 2 hours in order to cure the crosslinker, then washed with acetone and dried. The 70:30 CopolyGel swelled significantly in the HMDI solution, while

85:15 did not swell at all; this may be attributable to the possible excess of PE-*alt*-MA in 70:30. It is likely that the crosslinking solution could not saturate the network and access loose HA strands, which is reflected in the swell tests (85.39% for 70:30 crosslinked, but 95.31% for 85:15 crosslinked, an increase). However, both crosslinked CopolyGels appeared qualitatively more resistant to stress; 70:30 was hardly lubricious and held together incredibly well in PBS. In order to improve crosslinking, a different CopolyGeland HMDI-soluble solvent should be tested, and to optimize swelling ability, future work can use a more dilute HMDI solution and shorten the reaction time. This study utilized aggressive conditions to test the effectiveness of crosslinking.

TripolymerGel: PE-alt-MA, PE-g-MA, and HA-CTA

[00158] While CopolyGel swelled significantly and maintained a network in water, it lacked mechanical strength and cohesion, breaking apart fairly easily under stress. Meanwhile, Copoly featured the might of polyethylene but never successfully behaved as a hydrogel. Thus a new polymer material, TripolymerGel, was synthesized to unite both features and create a sturdy, resilient hydrogel. PE-*alt*-MA in DMSO and PE-*g*-MA in TCB were tangled together, effectively functionalizing the graft polyethylene with an abundance of maleic anhydride groups and creating a reactive polyethylene backbone. This new functionalized polyethylene was reacted with HA-CTA; subsequent steps adhered to the Copoly protocol.

[00159] Two TripolymerGel compositions (85:10:5 and 70:15:15) were synthesized according to the amount of final HA to PE provided by each reactant, in the ratio HA:PE(from PE-*alt*-MA):PE(from PE-*g*-MA). The 85:10:5 material was expected to behave similarly to CopolyGel 85:15 but with additional strength from the small amount of PE-*g*-MA; in other words, the PE-*g*-MA would serve to strengthen the hydrogel. The 70:15:15 material was designed such that the PE-*alt*-MA would act as a compatibilizer, functionalizing the PE-*g*-MA so that it would be more reactive.

[00160] As expected from the final product ratios, 70:15:15 displayed greater mechanical strength than 85:10:5, although both products held together extremely well and swelled significantly in PBS (96.72% for 85:10:5, 94.67% for 70:15:15). The properties of 85:10:5 resembled those of the nucleus pulposus: it was flexible, elastic, durable, and slippery. Meanwhile, 70:15:15 was more reminiscent of cartilage, tough and sturdy with a lubricated outer surface. Unlike the CopolyGel materials, which tended to break apart under

stress and gradually lose some of its viscous surface, the TripolymerGel materials withstood both pressure and agitation and did not appear to lose any material.

HMDI-Crosslinked TripolymerGel

[00161] Although the TripolymerGels behaved extremely well in PBS, they were HMDI crosslinked to further improve networking. In keeping with the results from CopolyGel crosslinking, the 85:10:5 network did not swell at all in HMDI/DMSO, while 70:15:15 did slightly. Swell tests yielded expected results (94.66% for 85:10:5 crosslinked, 84.36% for 70:15:15 crosslinked). The crosslinked 70:15:15 was noticeably stiffer than the uncrosslinked version, although 85:10:5 felt only marginally tougher after crosslinking. As discussed in CopolyGel crosslinking, better crosslinking and swell results may be achieved with a different solvent, a less concentrated HMDI solution, or a shorter reaction time.

[00162] **Conclusion:** Of the many approaches described in this paper, crosslinked CopolyGel and the assortment of TripolymerGel materials are the most promising and applicable to a wide range of orthopedic functions. Further work will explore and improve the biocompatibility, swelling and mechanical properties of these hydrogels.

[00163] **References:** [1]Kurkowski, R; James, SP (2008). *Copolymer synthesized from modified glycosaminoglycan, GAG, and an anhydride functionalized hydrophobic polymer*. U.S. Patent No. PCT/US09/05054. Colorado State University, Fort Collins, CO, USA. [2]Butler, MF; Ng, Y; Pudney, PD. Mechanism and kinetics of the crosslinking reaction between biopolymers containing primary amine groups and genipin. *J Poly Sci* 2003. 41, 3941-3953. [3]Baran, ET; Mano, JF; Reis, RL. Starch-chitosan hydrogels prepared by reductive alkylation cross-linking. *J Mater Sci* 2004. 15, 759-765. [4]Pourjavadi, A; Aghajani, V; Ghasemzadeh, H. Synthesis, characterization and swelling behavior of chitosan-sucrose as a novel full-polysaccharide superabsorbant hydrogel. *J Appl Poly Sci* 2008. 109, 2648-2655. [5]Stern, R; Kogan, G; Jedrzejas, MJ; Soltes, L. The many ways to cleave hyaluronan. *Biotech Advances* 2007. 25, 537-557. [6]Tokita, Y; Okamoto, A. Hydrolytic degradation of hyaluronic acid. *Polymer Degradation and Stability* 1995. 48, 269-273. [7]Gu, L; Zhu, S; Hrymak, AN. Acidic and basic hydrolysis of poly(N-vinylformamide). *J Appl Poly Sci* 2002. 86, 3412-3419.

Example 9

Copolymer Formulation Variations

[00164] Provided below is a table showing various copolymer formulation variations of the present invention.

Table 5

Copolymer Formulation Variations

Internal Nomenclature	Reactant Weight Ratio HA-CTA:PEMA	Reinforcement Level HA-CTA:other	Comments
99:1 CoPEMA	36:1	-	
95:5 CoPEMA	7:1	-	
95:5 XL	7:1	-	Crosslinked with HMDI (hexamethylene diisocyanate)
620-reinforced	7:1	1:2 1:1 5:1	TS-620 fumed silica (Cabot Corp.); high, med, low reinforcement
720-reinforced	7:1	1:2 1:1 5:1	TS-720 fumed silica (Cabot Corp.); high, med, low reinforcement
CN-low	7:1	40:1	Carbon nanotubes, low level of reinforcement
CN-high	7:1	4:1	Carbon nanotubes
Chi-reinforced	7:1	40:1	Chitosan nanofibers
85:15 CoPEMA	2:1	-	
85:15 XL	2:1	-	Crosslinked with HMDI
70:30 CoPEMA	4:5	-	
70:30 XL	4:5	-	Crosslinked with HMDI
85:10:5 Tripoly	27.2:8.7:1*	-	* MA-*g*-HDPE used as 3rd reactant
85:10:5 XL	27.2:8.7:1*	-	* MA-*g*-HDPE used as 3rd reactant; crosslinked with HMDI
70:15:15 Tripoly	7.5:4.4:1*	-	* MA-*g*-HDPE used as 3rd reactant
70:15:15 XL	7.5:4.4:1*	-	* MA-*g*-HDPE used as 3rd reactant; crosslinked with HMDI
5:95 CoPEMA	1:20	-	Brittle/crumbly texture

Example 10

Swell Test Results

[00165] Provided below is a table showing swell test results of various copolymer formulation variations of the present invention.

FIG.	Polymer (HA:PE Product Ratio)	Swell Test Water %	Qualitative Properties
FIG. 2A	CopolyGel 85:15	93.53	Viscous, breaks apart with mild agitation or pressure
FIG. 2B	CopolyGel 85:15 crosslinked	95.31	Viscous, breaks apart with moderate agitation or pressure
FIG. 2C	CopolyGel 70:30	95.08	Thick, breaks apart with vigorous agitation
FIG. 2D	CopolyGel 70:30 crosslinked	85.39	Rubbery, elastic, not lubricious, holds together extremely well
FIG. 2E	Tripolymer Gel 85:10:5	96.72	Sturdy, flexible, lubricated surface, like nucleus pulposus
FIG. 2F	Tripolymer Gel 85:10:5 crosslinked	94.66	Sturdy, flexible, durable, somewhat lubricated surface
FIG. 2G	Tripolymer Gel 70:15:15	94.67	Tough, durable, lubricated surface, like cartilage
FIG. 2H	Tripolymer Gel 70:15:15 crosslinked	84.36	Extremely tough, lubricated surface, holds together well

[00166] As referenced in the above table, **FIG. 2A** through **FIG. 2H** are photographs of each polymer hydrogel in PBS solution. Blue gels have been stained with toluidine blue.

Example 11

FTIR Results

[00167] FTIR scans were produced for various embodiments of the polymeric material and hydrogels of the present invention, as shown in **FIG. 8** through **FIG. 10**.

[00168] As shown in the figures, the FTIR scans indicate the appearance of an ester bond peak (i.e., the covalent bond between the HA and PEMA). In the figures, peaks relating to the ester bond , the base constituents, and the reactive groups have been identified.

[00169] Based on the FTIR data, the following conclusions were made with respect to the Tripolymer Gel: (i) strong CH_2-OH peak (indicative of HA content); (ii) moderate, sharp C-H_2 peaks (indicative of PE content); (iii) indications of desired reaction, including (a) OH peak diminished compared to HA, (b) characteristic peaks for maleic anhydride (C=O, cyclic C-O-C) gone, (c) appearance of moderate –COOH peak, unreacted maleic anhydride hydrolized to maleic acid, and (d) appearance of an ester peak.

[00170] Based on the FTIR data, the following conclusions were made with respect to the Co-PEMA:(i) strong OH peak (indicative of HA content); (ii) moderate, broad C-H_2 peaks indicative of the small ethylene units in hydrolyzed PEMA; (iii) indications of desired reaction, including (a) OH peak broadened compared to HA, (b) characteristic peaks for maleic anhydride (C=O, cyclic C-O-C) gone, (c) appearance of –COOH peak, unreacted maleic anhydride hydrolized to maleic acid, and (d) appearance of ester peak.

[00171] While certain representative embodiments and certain details have been shown for the purpose of illustrating the invention, those skilled in the art will appreciate that various modifications, whether specifically or expressly identified herein, may be made to these representative embodiments without departing from the novel core teachings or scope of this technical disclosure. Accordingly, all such modifications are intended to be included within the scope of the claims. Whether the commonly employed phrase "comprising the steps of" may be used in a method claim, the applicant(s) does not intend to invoke any law in a manner that unduly limits rights to its innovation. Furthermore, in any claim that is filed herewith or hereafter, any means-plus-function clauses used, or later found to be present, are intended to cover at least all structure(s) described herein as performing the recited function and not only structural equivalents but also equivalent structures.

WHAT IS CLAIMED IS:

1. A polymeric material comprising a glycosaminoglycan networked with a polyolefin-containing polymer, wherein said glycosaminoglycan networked with a polyolefin-containing polymer is synthesized by reacting a glycosaminoglycan constituent with a polyolefin constituent,

wherein said glycosaminoglycan constituent comprises a modified glycosaminoglycan, and

wherein said polyolefin constituent comprises an alternating copolymer of a polyolefin with an acid anhydride.

2. The polymeric material according to claim 1, wherein the glycosaminoglycan is selected from the group consisting of hyaluronan, chondroitin sulfates, dermatan sulfates, keratan sulfates, heparan sulfates, and heparin.

3. The polymeric material according to claim 1, wherein the polyolefin is polyethylene.

4. The polymeric material according to claim 1, wherein the acid anhydride is maleic anhydride.

5. The polymeric material according to claim 1, wherein the polyolefin constituent comprises an alternating copolymer of polyethylene with maleic anhydride.

6. The polymeric material according to claim 1, wherein the polyolefin constituent is selected from the group consisting of poly(ethylene-*alt*-maleic anhydride), poly(styrene-*alt*-maleic anhydride), poly(isobutylene-*alt*-maleic anhydride), poly(maleic anhydride-*alt*-1-octadecene), poly(methyl vinyl ether-*alt*-maleic anhydride), and derivatives thereof.

7. The polymeric material according to claim 1, wherein the polyolefin-containing polymer is selected from the group consisting of poly(ethylene-*alt*-maleic anhydride), poly(styrene-*alt*-maleic anhydride), poly(isobutylene-*alt*-maleic anhydride),

poly(maleic anhydride-*alt*-1-octadecene), poly(methyl vinyl ether-*alt*-maleic anhydride), and derivatives thereof.

8. The polymeric material according claim 1, wherein the glycosaminoglycan constituent comprises a glycosaminoglycan modified with a paraffin ammonium cation dissociated from a salt selected from the group consisting of alkyltrimethylammonium chloride, alkylamine hydrochloride, alkylpyridinium chloride, alkyldimethylbenzyl ammonium chloride, alkyltrimethylammonium bromide, alkylamine hydrobromide, alkylpyridinium bromide, and alkyldimethylbenzyl ammonium bromide.

9. The polymeric material according to claim 1, wherein said polymeric material comprises a structure as follows:

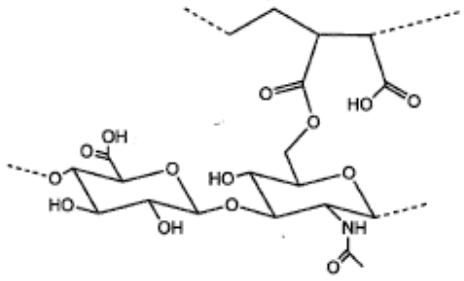

10. The polymeric material according to claim 1 further comprising:

a reinforcing agent selected from the group consisting of an inorganic reinforcing agent and an organic reinforcing agent.

11. The polymeric material according to claim 10, wherein the inorganic reinforcing agent comprises silica.

12. The polymeric material according to claim 10, wherein the organic reinforcing agent is selected from the group consisting of carbon nanotubes, carbon nanofibers, chitosan nanofibers, demineralized bone matrix (DBM), collagen, silk, and cellulose.

13. A hydrogel comprising the polymeric material according to claim 1.

14. A method of synthesizing a polymeric material comprising a glycosaminoglycan networked with a polyolefin-containing polymer, said method comprising:

reacting a glycosaminoglycan constituent with a polyolefin constituent under conditions effective to yield a polymeric material comprising a glycosaminoglycan networked with a polyolefin-containing polymer,

wherein said glycosaminoglycan constituent comprises one or more modified glycosaminoglycans, and

wherein said polyolefin constituent comprises an alternating copolymer of a polyolefin with an acid anhydride.

15. The method according to claim 14, wherein said reacting step comprises an esterification reaction between the glycosaminoglycan constituent and the polyolefin constituent.

16. The method according to claim 14, wherein the glycosaminoglycan is selected from the group consisting of hyaluronan, chondroitin sulfates, dermatan sulfates, keratan sulfates, heparan sulfates, and heparin.

17. The method according to claim 14, wherein the polyolefin is polyethylene.

18. The method according to claim 14, wherein the acid anhydride is maleic anhydride.

19. The method according to claim 14, wherein the polyolefin constituent comprises an alternating copolymer of polyethylene with maleic anhydride.

20. The method according to claim 14, wherein the polyolefin constituent is selected from the group consisting of poly(ethylene-*alt*-maleic anhydride), poly(styrene-

alt-maleic anhydride), poly(isobutylene-*alt*-maleic anhydride), poly(maleic anhydride-*alt*-1-octadecene), poly(methyl vinyl ether-*alt*-maleic anhydride), and derivatives thereof.

21. The method according to claim 14, wherein the polyolefin-containing polymer is selected from the group consisting of poly(ethylene-*alt*-maleic anhydride), poly(styrene-*alt*-maleic anhydride), poly(isobutylene-*alt*-maleic anhydride), poly(maleic anhydride-*alt*-1-octadecene), poly(methyl vinyl ether-*alt*-maleic anhydride), and derivatives thereof.

22. The method according to claim 14, wherein the glycosaminoglycan constituent comprises a glycosaminoglycan modified with a paraffin ammonium cation dissociated from a salt selected from the group consisting of alkyltrimethylammonium chloride, alkylamine hydrochloride, alkylpyridinium chloride, alkyldimethylbenzyl ammonium chloride, alkyltrimethylammonium bromide, alkylamine hydrobromide, alkylpyridinium bromide, and alkyldimethylbenzyl ammonium bromide.

23. The method according to claim 14, wherein said polymeric material comprises the glycosaminoglycan and the polyolefin-containing polymer covalently bound to one another.

24. The method according to claim 14, wherein said polymeric material comprises a structure as follows:

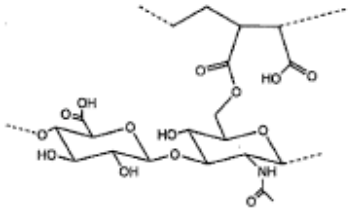

25. The method according to claim 14 further comprising:

incubating the glycosaminoglycan constituent and the polyolefin constituent in a crosslinker constituent.

26. The method according to claim 25, wherein said crosslinker constituent is effective to crosslink with an alcohol group of the glycosaminoglycan constituent.

27. The method according to claim 26, wherein said crosslinker constituent is selected from the group consisting of diisocyanates, polyisocyanates, hexamethylenediisocyanate (HMDI), methylene diphenyl diisocyanate, toluene diisocyanate, isophorone diisocyanate, divinyl sulphone, poly(ethylene glycol) diglycidyl ether, phosphoryl chloride, glutaraldehyde, dialdehyde via Passerini reaction, diamine via Ugi reaction, and carbodiimide.

28. The method according to claim 14 further comprising:

combining the glycosaminoglycan constituent and the polyolefin constituent with a reinforcing agent.

29. The method according to claim 28, wherein the reinforcing agent is selected from the group consisting of an inorganic reinforcing agent and an organic reinforcing agent.

30. The method according to claim 29, wherein the inorganic reinforcing agent comprises an inorganic agent selected from the group consisting of silica, alumina, zirconia, calcium phosphates, and hydroxyapatite.

31. The method according to claim 29, wherein the organic reinforcing agent is selected from the group consisting of carbon nanotubes, carbon nanofibers, chitosan nanofibers, demineralized bone matrix (DBM), collagen, silk, and cellulose.

32. The method according to claim 14, wherein said glycosaminoglycan constituent comprises a modified hyaluranon, wherein said polyolefin constituent comprises poly(ethylene-*alt*-maleic anhydride), and wherein said reacting step comprises a synthetic scheme as follows:

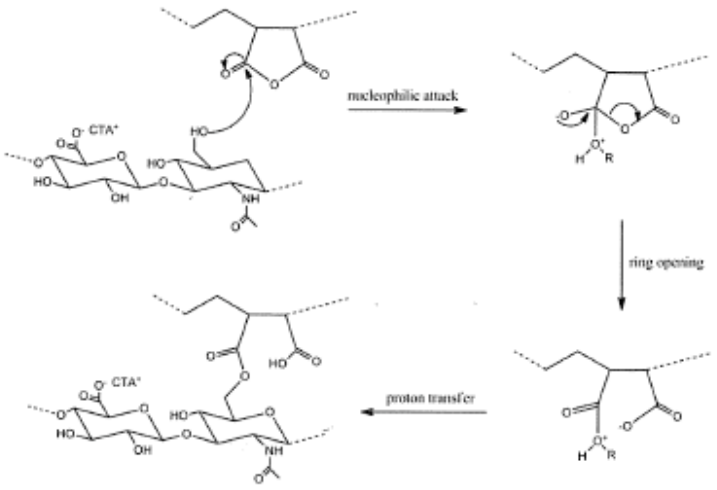

33. A hydrogel comprising the polymeric material produced according to the method of claim 14.

34. A polymeric material comprising a tripolymer glycosaminoglycan-polyolefin network, wherein said tripolymer glycosaminoglycan-polyolefin network is synthesized by reacting a first constituent, a second constituent, and a third constituent with one another,

wherein said first constituent comprises a modified glycosaminoglycan,

wherein said second constituent comprises an alternating copolymer of a polyolefin with an acid anhydride,

wherein said third constituent comprises a graft copolymer having a polyolefin backbone functionalized/grafted with an acid anhydride, and

wherein the first constituent, the second constituent, and the third constituent react to form covalent bonds.

35. The polymeric material according to claim 34, wherein the glycosaminoglycan is selected from the group consisting of hyaluronan, chondroitin sulfates, dermatan sulfates, keratan sulfates, heparan sulfates, and heparin.

36. The polymeric material according to claim 34, wherein the polyolefin is polyethylene.

37. The polymeric material according to claim 34, wherein the acid anhydride is maleic anhydride.

38. The polymeric material according claim 34, wherein the first constituent comprises a glycosaminoglycan modified with a paraffin ammonium cation dissociated from a salt selected from the group consisting of alkyltrimethylammonium chloride, alkylamine hydrochloride, alkylpyridinium chloride, alkyldimethylbenzyl ammonium chloride, alkyltrimethylammonium bromide, alkylamine hydrobromide, alkylpyridinium bromide, and alkyldimethylbenzyl ammonium bromide.

39. The polymeric material according to claim 34, wherein the second constituent comprises an alternating copolymer of polyethylene with maleic anhydride.

40. The polymeric material according to claim 34, wherein the second constituent is selected from the group consisting of poly(ethylene-*alt*-maleic anhydride), poly(styrene-*alt*-maleic anhydride), poly(isobutylene-*alt*-maleic anhydride), poly(maleic anhydride-*alt*-1-octadecene), poly(methyl vinyl ether-*alt*-maleic anhydride), and derivatives thereof.

41. The polymeric material according to claim 34, wherein the third constituent is selected from the group consisting of maleic anhydride-*graft*-polyethylene, maleic anhydride-*graft*-polypropylene, maleic anhydride-*graft*-polystyrene, polystyrene-*graft*-maleic anhydride, polyisoprene-*graft*-maleic anhydride, and polypropylene-*graft*-maleic anhydride.

42. The polymeric material according to claim 34, wherein the first constituent is hyaluranon, the second constituent is poly(ethylene-*alt*-maleic anhydride), and the third constituent is maleic anhydride-*graft*-polyethylene.

43. The polymeric material according to claim 34 further comprising:

a reinforcing agent selected from the group consisting of an inorganic reinforcing agent and an organic reinforcing agent.

44. The polymeric material according to claim 43, wherein the inorganic reinforcing agent comprises an inorganic agent selected from the group consisting of silica, alumina, zirconia, calcium phosphates, and hydroxyapatite.

45. The polymeric material according to claim 43, wherein the organic reinforcing agent is selected from the group consisting of carbon nanotubes, carbon nanofibers, chitosan nanofibers, demineralized bone matrix (DBM), collagen, silk, and cellulose.

46. A hydrogel comprising the polymeric material according to claim 34.

47. A method of synthesizing a polymeric material comprising a tripolymer glycosaminoglycan-polyolefin network, said method comprising:

providing the following constituents:

(i) a first constituent comprising a modified glycosaminoglycan;

(ii) a second constituent comprising an alternating copolymer of a polyolefin with an acid anhydride; and

(iii) a third constituent comprising a graft copolymer having a polyolefin backbone functionalized/grafted with an acid anhydride; and

reacting the first constituent, the second constituent, and the third constituent under conditions effective to yield a tripolymer glycosaminoglycan-polyolefin network,

wherein said tripolymer glycosaminoglycan-polyolefin network comprises the first constituent, the second constituent, and the third constituent covalently bound to one another.

48. The method according to claim 47, wherein the glycosaminoglycan is selected from the group consisting of hyaluronan, chondroitin sulfates, dermatan sulfates, keratan sulfates, heparan sulfates, and heparin.

49. The method according to claim 47, wherein the polyolefin is polyethylene.

50. The method according to claim 47, wherein the acid anhydride is maleic anhydride.

51. The method according to claim 47, wherein the second constituent comprises an alternating copolymer of polyethylene with maleic anhydride.

52. The method according to claim 47, wherein the second constituent is selected from the group consisting of poly(ethylene-*alt*-maleic anhydride), poly(styrene-*alt*-maleic anhydride), poly(isobutylene-*alt*-maleic anhydride), poly(maleic anhydride-*alt*-1-octadecene), poly(methyl vinyl ether-*alt*-maleic anhydride), and derivatives thereof.

53. The method according to claim 47, wherein the first constituent comprises a glycosaminoglycan modified with a paraffin ammonium cation dissociated from a salt selected from the group consisting of alkyltrimethylammonium chloride, alkylamine hydrochloride, alkylpyridinium chloride, alkyldimethylbenzyl ammonium chloride, alkyltrimethylammonium bromide, alkylamine hydrobromide, alkylpyridinium bromide, and alkyldimethylbenzyl ammonium bromide.

54. The method according to claim 47, wherein the wherein the third constituent is selected from the group consisting of maleic anhydride-*graft*-polyethylene, maleic anhydride-*graft*-polypropylene, maleic anhydride-*graft*-polystyrene, polystyrene-*graft*-maleic anhydride, polyisoprene-*graft*-maleic anhydride, and polypropylene-*graft*-maleic anhydride.

55. The method according to claim 47, wherein the first constituent is hyaluron, the second constituent is poly(ethylene-*alt*-maleic anhydride), and the third constituent is maleic anhydride-*graft*-polyethylene.

56. The method according to claim 47 further comprising:

incubating the first constituent, second constituent, and third constituent in a crosslinker constituent.

57. The method according to claim 56, wherein said crosslinker constituent is effective to crosslink with an alcohol group of the first constituent.

58. The method according to claim 57, wherein said crosslinker constituent is selected from the group consisting of diisocyanates, polyisocyanates, hexamethylenediisocyanate (HMDI), methylene diphenyl diisocyanate, toluene diisocyanate, isophorone diisocyanate, divinyl sulphone, poly(ethylene glycol) diglycidyl ether, phosphoryl chloride, glutaraldehyde, dialdehyde via Passerini reaction, diamine via Ugi reaction, and carbodiimide

59. The method according to claim 47 further comprising:

combining the first constituent, second constituent, and third constituent with a reinforcing agent.

60. The method according to claim 59, wherein the reinforcing agent is selected from the group consisting of an inorganic reinforcing agent and an organic reinforcing agent.

61. The method according to claim 59, wherein the inorganic reinforcing agent comprises an inorganic agent selected from the group consisting of silica, alumina, zirconia, calcium phosphates, and hydroxyapatite.

62. The method according to claim 59, wherein the organic reinforcing agent is selected from the group consisting of carbon nanotubes, carbon nanofibers, chitosan nanofibers, demineralized bone matrix (DBM), collagen, silk, and cellulose.

63. A hydrogel comprising the polymeric material produced according to the method of claim 47.

64. A polymeric material comprising a glycosaminoglycan networked with a polyolefin-containing polymer, wherein said glycosaminoglycan networked with a polyolefin-containing polymer comprises glycosaminoglycan covalently bound to a polyolefin-containing polymer.

65. The polymeric material according to claim 64, wherein said glycosaminoglycan is hyaluranon and said polyolefin-containing polymer is poly(ethylene-*alt*-maleic anhydride).

66. The polymeric material according to claim 64, wherein said polymeric material comprises a structure as follows:

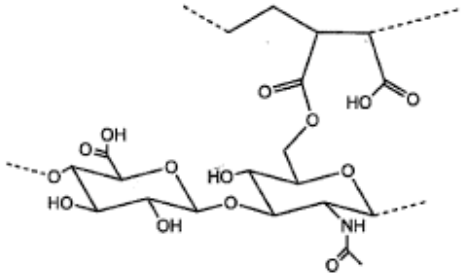

67. A hydrogel comprising the polymeric material according to claim 64.

ABSTRACT OF THE DISCLOSURE

The present invention relates to polymeric materials including a glycosaminoglycan networked with a polyolefin-containing polymer. The present invention also relates to hydrogels containing the polymeric materials. The present invention further relates to methods of synthesizing the polymeric materials and hydrogels of the present invention.

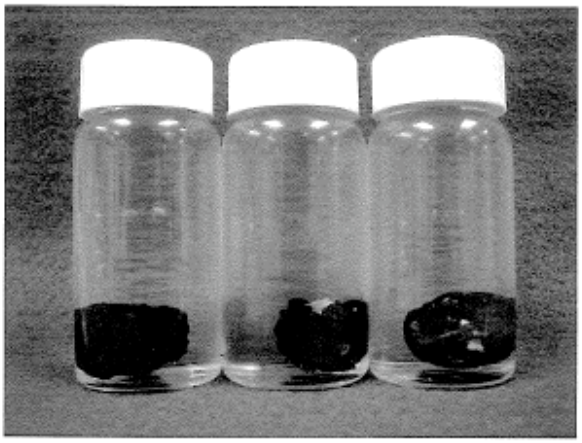

FIG. 1

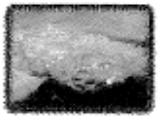

FIG. 2A

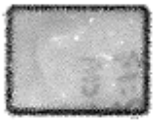

FIG. 2B

FIG. 2C

FIG. 2D

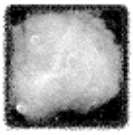

FIG. 2E

FIG. 2F

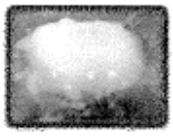

FIG. 2G

FIG. 2H

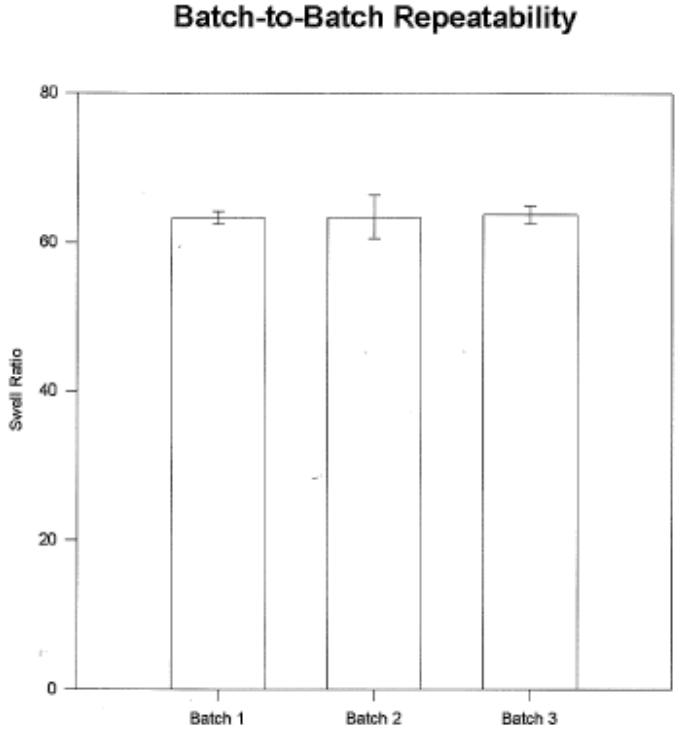
Batch-to-Batch Repeatability
Swell Ratio
80
60
40
20
0
Batch 1
Batch 2
Batch 3

FIG. 3

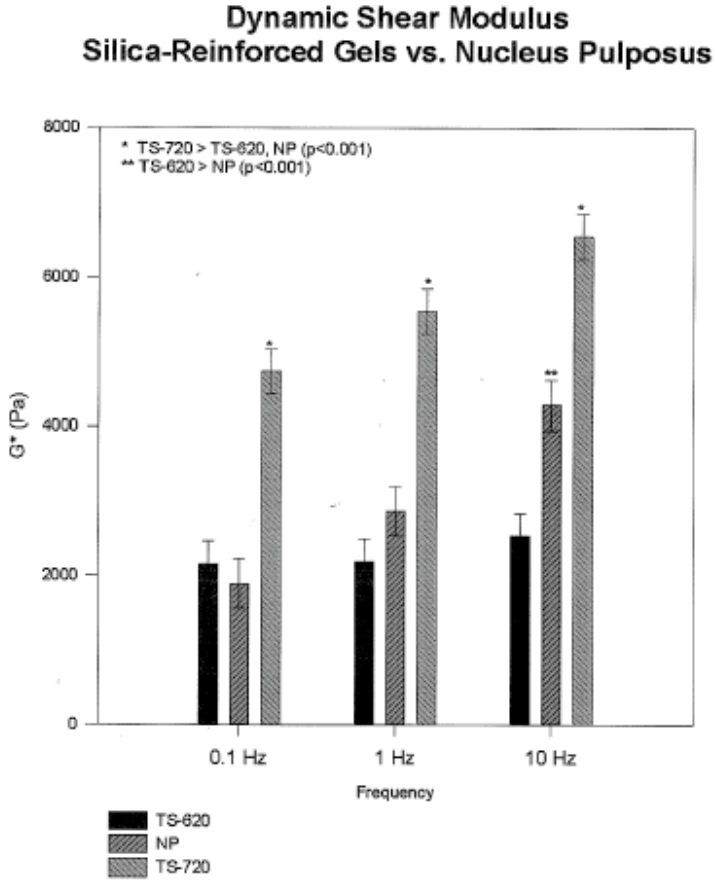
Dynamic Shear Modulus
Silica-Reinforced Gels vs. Nucleus Pulposus
* TS-720 > TS-620, NP (p<0.001)
** TS-620 > NP (p<0.001)
8000
6000
4000
2000
0
G* (Pa)
0.1 Hz
1 Hz
10 Hz
Frequency
TS-620
NP
TS-720

FIG. 4

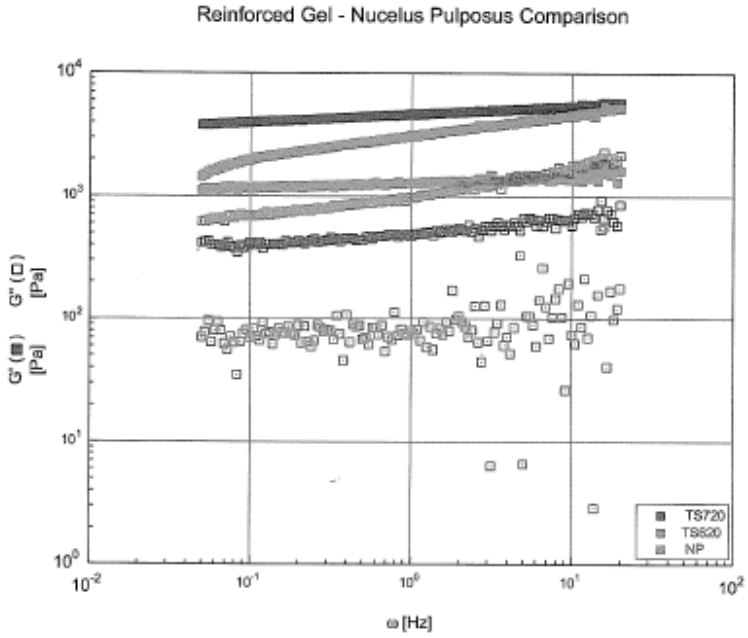
Reinforced Gel - Nucelus Pulposus Comparison
G' (■) [Pa]
G'' (□) [Pa]
ω [Hz]
TS720
TS620
NP

FIG. 5

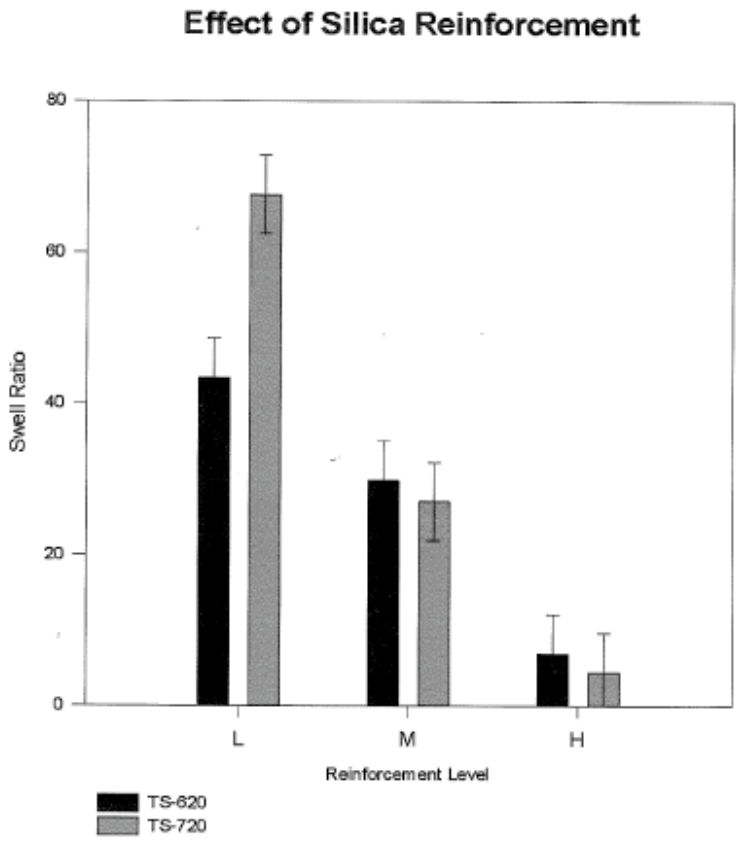
Effect of Silica Reinforcement
80
60
40
20
0
Swell Ratio
L
M
H
Reinforcement Level
TS-620
TS-720

FIG. 6

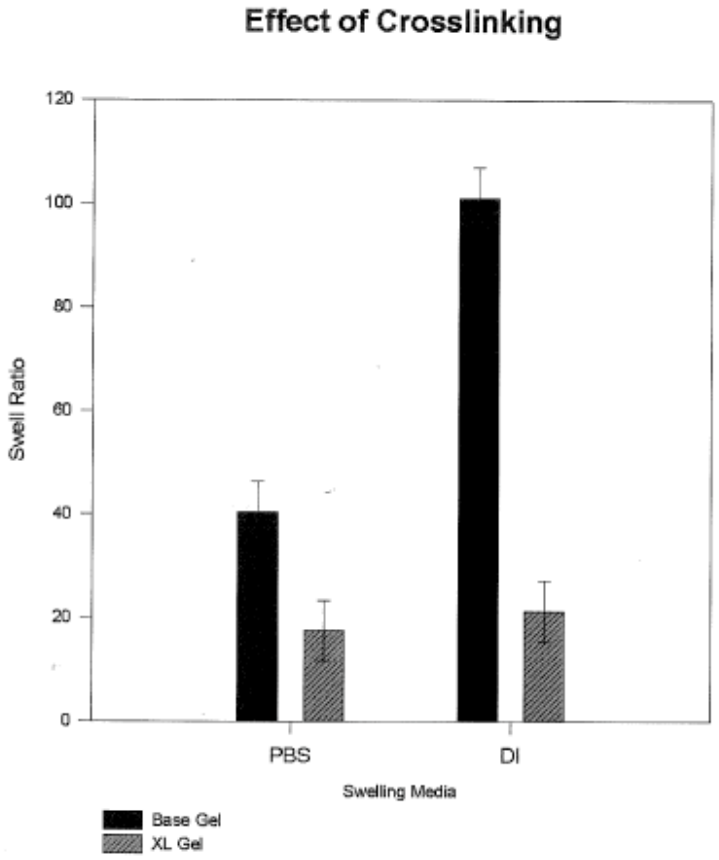
Effect of Crosslinking
120
100
80
60
40
20
0
Swell Ratio
PBS
DI
Swelling Media
Base Gel
XL Gel

FIG. 7

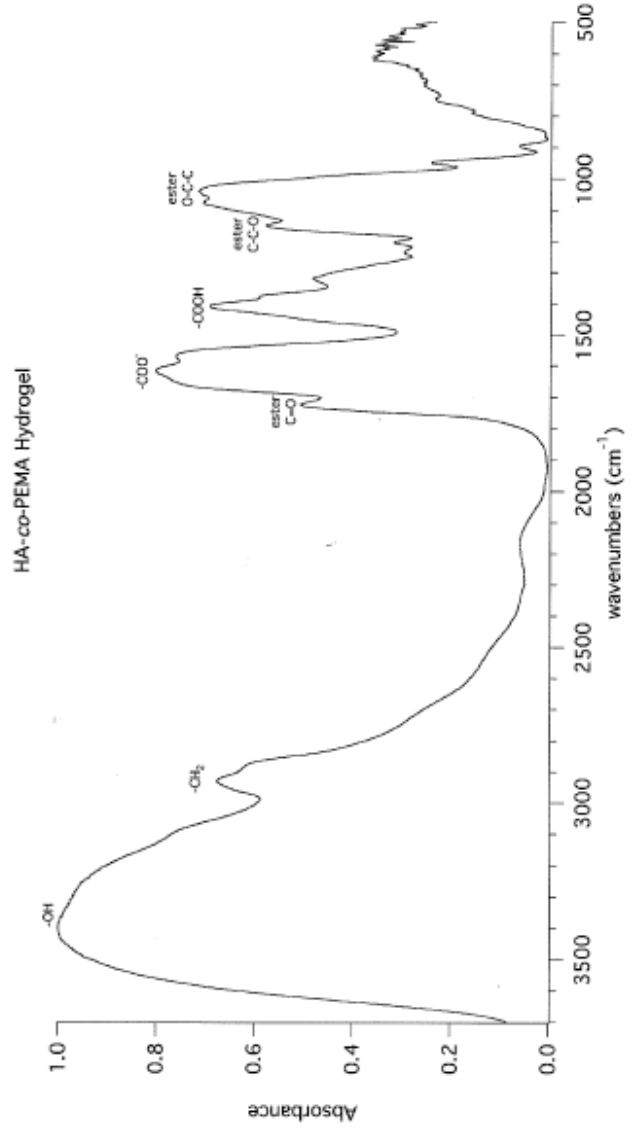
HA-co-PEMA Hydrogel
Absorbance
1.0
0.8
0.6
0.4
0.2
0.0
3500
3000
2500
2000
1500
1000
500
wavenumbers (cm-1)
-OH
-CH2
ester C=O
-COO-
-COOH
ester C-C-O
ester O-C-C

FIG. 8

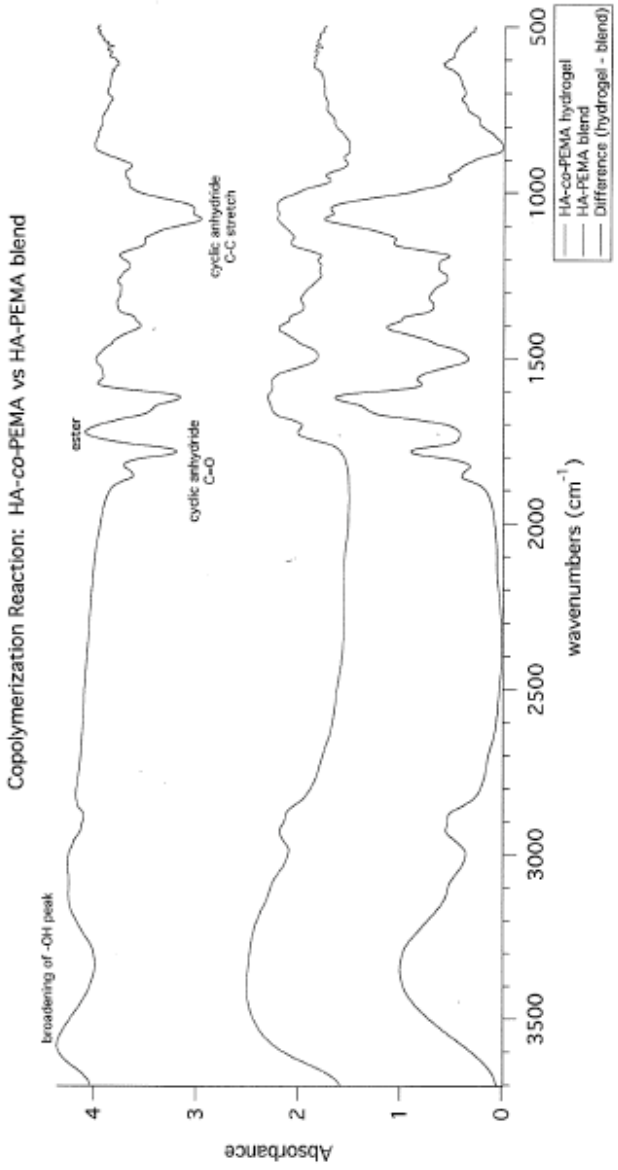
Copolymerization Reaction: HA-co-PEMA vs HA-PEMA blend
broadening of -OH peak
ester
cyclic anhydride C=O
cyclic anhydride C-C stretch
Absorbance
wavenumbers (cm-1)
HA-co-PEMA hydrogel
HA-PEMA blend
Difference (hydrogel - blend)

FIG. 9

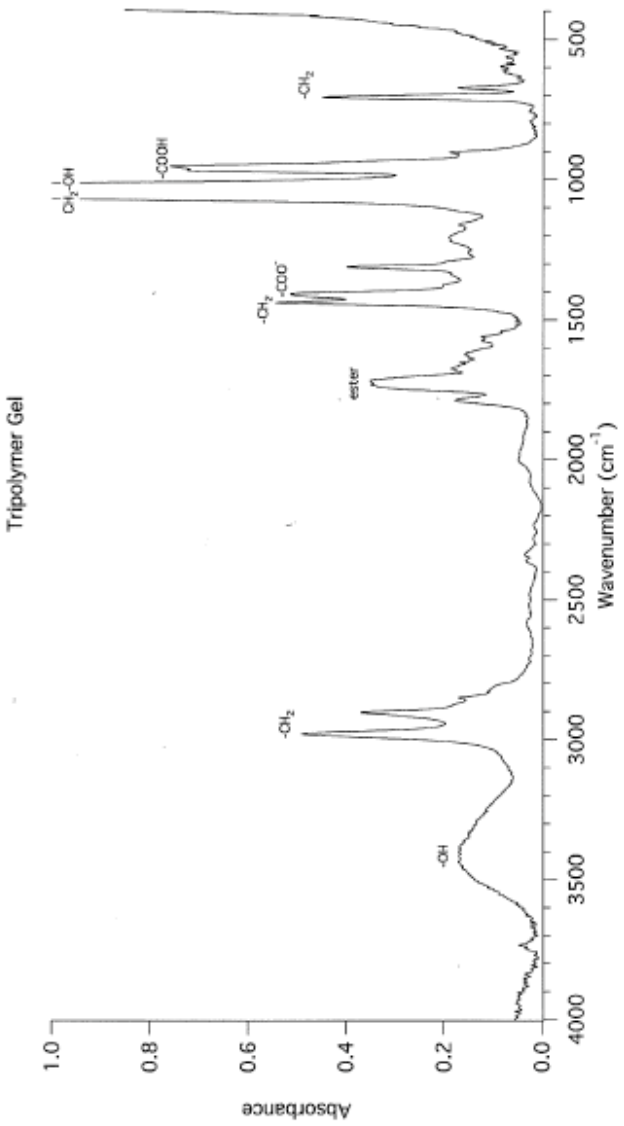
Tripolymer Gel
Absorbance
1.0
0.8
0.6
0.4
0.2
0.0
4000
3500
3000
2500
2000
1500
1000
500
Wavenumber (cm-1)
-OH
-CH2
-CH2-OH
-COOH
-CH2
-COO-
ester
-CH2

FIG. 10